Assessing the Status and Trends of Spring Chinook Habitat in the Upper Grande Ronde River and Catherine Creek: Annual Report 2018

publication date: April 30, 2019

Authors: Seth White, Casey Justice, Lauren Burns, David Graves, Denise Kelsey, and Matthew Kaylor

Technical Report 19-04

Columbia River Inter-Tribal Fish Commission

700 NE Multnomah St, Ste 1200, Portland OR 97232 · (503)238-0667 · www.critfc.org

Funding for this work came from the Columbia Basin Fish Accords (2008-2018), a ten-year tribal/federal partnership between the Bonneville Power Administration, Bureau of Reclamation, Columbia River Inter-Tribal Fish Commission, The Confederated Tribes of the Umatilla Indian Reservation, The Confederated Tribes of the Warm Springs Reservation of Oregon, US Army Corps of Engineers, and The Confederated Tribes and Bands of the Yakama Nation.

Assessing the Status and Trends of Spring Chinook Habitat in the Upper Grande Ronde River and Catherine Creek

BPA Project # 2009-004-00

Report covers work performed under BPA contract #(s) 75586, 73354 REL 2

Report was completed under BPA contract #(s) 73354 REL 2

Report covers work performed from:

January – December 2018

Seth White[1,2], Casey Justice[1], Lauren Burns[1], David Graves[1], Denise Kelsey[1], and Matthew Kaylor[2]

[1]Columbia River Inter-Tribal Fish Commission, Portland, OR 97232

[2]Department of Fisheries & Wildlife, Oregon State University, Corvallis, OR 97331

April 2019

This report was funded by the Bonneville Power Administration (BPA), U.S. Department of Energy, as part of BPA's program to protect, mitigate, and enhance fish and wildlife affected by the development and operation of hydroelectric facilities on the Columbia River and its tributaries. The views in this report are the author's and do not necessarily represent the views of BPA.

Table of Contents

Executive Summary

Background and Objectives

The Columbia River Inter-Tribal Fish Commission is conducting a research, monitoring, and evaluation study designed to determine the effectiveness of aggregate restoration actions in improving freshwater habitat conditions and viability of ESA-listed spring Chinook Salmon populations. A critical uncertainty for fisheries managers in the Columbia Basin is whether freshwater habitat restoration actions will improve basin-wide habitat quantity/quality and thereby salmon productivity to a level sufficient to offset human-caused survival impairments elsewhere in the life cycle. Geographically, this project is focused on the upper Grande Ronde River and Catherine Creek basins (tributaries of the Snake River in the Columbia River basin), but with applications and testing of models also occurring in other Columbia River tributaries.

The objectives of this project are to: 1) Assess current status and trends in fish habitat characteristics considered to be key ecological concerns for viability of spring Chinook Salmon populations; 2) Evaluate effectiveness of aggregate stream restoration actions aimed at improving key ecological concerns; and 3) Develop a life cycle model to link biotic responses of spring Chinook populations to projected changes in stream habitat conditions.

We have categorized our work towards these objectives into the following project components:

- Component 1: Habitat and biotic assessments,
- Component 2: Riverscape analyses, and
- Component 3: Fish-habitat modeling.

These individual components are linked together conceptually in an overall cycle of research, monitoring, and evaluation, with analyses feeding into an adaptive management framework (Figure 1).

Figure 1. CRITFC's cycle of research, monitoring, and evaluation providing the basis for decision-making in an adaptive management framework.

Progress and Key Findings

Component 1: Habitat and Biotic Assessments

Evaluation of Habitat Protocol Using Remote Sensing

- With the goal of reducing the time, cost, and limited spatial extent of ground-based habitat surveys, we tested the use of an unmanned aerial vehicle (UAV) for remotely-sensed data collection during the 2018 field season.

- We conducted ground based and remotely-sensed UAV surveys at 13 sites in the Grande Ronde River and Catherine Creek basins and computed channel unit and site level metrics that are relevant to fish in a similar manner as the Columbia Habitat Monitoring Program (CHaMP).

- Metrics generated from each of the two survey techniques (ground-based and UAV) related to large wood, habitat area, and pool frequency and depth largely agreed, but we found instream and riparian obstructions (vegetation, overhanging banks, large wood) increased the observed variation for metrics.

- These results are so far preliminary, as they are based on the analysis of a single site. The forthcoming analysis of the remaining 12 sites will provide a better understanding of the variability in metrics generated using both techniques. Ultimately, this project seeks to identify cost-effective, repeatable approaches to collecting stream habitat metrics over larger spatial extents.

Development of Stream Temperature Database

- We compiled and error-checked all hourly water temperature measurements collected by various natural resource organizations in the Grande Ronde River basin upstream of and including the Wallowa River from 1993 to 2017 and imported this data into an SQL database.

- From these data we computed a total of 22 water temperature metrics representing the magnitude, variability, and frequency of the thermal regime that is biologically relevant to cold-water fishes.

- This comprehensive water temperature database will be used for development of a water temperature model capable of predicting how water temperatures would change in response to stream and riparian restoration as well as climate change across the entire salmon-bearing portion of the stream network. These data will also be useful for more general habitat assessments, restoration planning and effectiveness monitoring.

Updates to Food Web and Carcass Addition Studies

- Recovery of salmonid populations within the Columbia Basin may require an integrated approach involving management actions that consider food webs in addition to physical habitat availability. This report summarizes findings of three draft manuscripts related to studies of food webs relevant to juvenile Chinook salmon, *O. mykiss*, and other resident stream fish.

- In the first study, we link spatial patterns of stream nutrient concentrations, stream metabolism, and juvenile salmonids throughout the upper Grande Ronde and Catherine Creek river network. Although we found strong patterns of nutrient limitation and primary production, the distribution of salmonids appeared to be driven by non-food web factors (e.g., water temperature).

- Based on the results of the above study, we first identified areas with abundant juvenile salmonids and oligotrophic conditions and next quantified juvenile salmonid growth, body condition, mean size, and diets in response to experimental carcass additions. Most notably, salmonid growth rates substantially increased in treatment reaches relative to controls primarily through direct consumption of carcasses and eggs.

- The third study focuses on the response of the fish assemblage to the experimental carcass additions described above. Assimilation patterns of non-salmonids (as measured using stable isotopes) and a lack of eggs and carcass tissue in diets suggests non-salmonids obtained carcass-derived nitrogen through bottom-up pathways. Our results suggest salmon subsidies have the potential to broadly impact stream food webs in this region, but that species able to directly consume eggs and carcass material clearly benefit more from these subsidies.

Component 2: Riverscape Analyses

Effect of Riparian Vegetation and Channel Width on Stream Shade

- With the objective of developing accurate predictive models for shade and thermal loading to streams in the upper Grande Ronde River basin, we analyzed the relationship between shade measured in streams and remotely-sensed estimates of riparian tree height and basal area as well as ground-based measurements of channel width.

- The best fitting model for shade included basal area and bankfull width as additive explanatory variables, explaining approximately 47% of the total variation in shade. Shade was positively related to basal area and negatively related to bankfull width, with both variables being highly significant.

- The observed relationship between shade in streams and tree basal area and bankfull channel width may help improve the accuracy of landscape scale models such as NetMap or NorWeST which are commonly used to evaluate alternative land management or climate scenarios and their impact on aquatic habitats.

Climate and Land Use Drivers of Salmonid Food Web Indicators

- Using macroinvertebrate collections from the upper Grande Ronde River, Catherine Creek, and Minam River from 2011-2017, we evaluated climate and land use drivers of salmonid food web indicators. Our analysis focused on an aquatic species composition score (ASC_{Rel}), with abundance of drift traits at each site expressed on a relative scale.

- This metric was poorly correlated with invertebrate drift biomass, but cluster analysis revealed that most invertebrate taxa had high fidelity to groups of low, medium, and high drift frequency. The metric was associated with the uppermost limit of juvenile Chinook salmon and *O. mykiss* abundance at monitoring sites as indicated by the 98^{th} quantile regression, lending evidence that food availability may be a limiting factor.

- The ASC_{Rel} metric appeared to be driven by climate and land use. Cattle grazing and number of winter flooding events had negative impacts on ASC_{Rel}, but climate had an additional direct negative effect and therefore its relative magnitude of influence was

much larger. Climate change projections indicate that winter flooding will increase substantially in the 2040s and 2080s time periods, likely decreasing food availability to salmonids based on our model.

Component 3: Fish-Habitat Modeling

Updates to Life Cycle Model

- We worked in collaboration with Eco Logical Research to update a life cycle model for upper Grande Ronde River and Catherine Creek spring Chinook Salmon populations and evaluate potential future population responses to a suite of climate and restoration scenarios.

- Overall, our modelling results indicated minimal potential increases in adult Chinook Salmon abundance and low to moderate improvements in extinction risk from basin-wide restoration of riparian vegetation and channel narrowing, owing largely to the overriding negative influence of climate change. For example, median natural spawner abundance in the upper Grande Ronde River was projected to increase from approximately 48 under current climate and stream habitat conditions to only 89 for a 2080's future scenario (i.e., '*ClimVegWid'*) that included restored riparian and channel width conditions in combination with climate change. Similarly, Catherine Creek natural spawners were projected to increase from 265 under the current scenario to 346 under the *ClimVegWid* scenario. These projected increases in natural spawner abundance fall well below the minimum abundance target of 1000 identified in NOAA's NE Oregon Snake River recovery plan as necessary for long term persistence of these populations.

- Quasi extinction risk for the UGR population was predicted to decrease from 0.97 under current population conditions (i.e., '*Curr*') to roughly 0.78 under the most aggressive restoration scenario (i.e., '*ClimVegWid*'). Catherine Creek has a relatively low extinction risk 0.032 under current conditions that we predict could be reduced to less than 0.01 with basin-wide riparian and channel restoration.

- The relatively low projected population responses to habitat restoration actions in the face of climate change are in part related to the limited set of restoration actions and life stages evaluated in the model, and work is in progress to expand model functionality to include additional factors such as temperature effects on pre-spawn mortality and juvenile growth.

- Sensitivity analysis indicated that our LCM was more sensitive to changes in productivity parameters than capacity and was most sensitive to changes in smolt-to-adult survival rates overall. Survival at other life-stage transitions, such as spawning grounds survival

and winter survival of rearing presmolt also appeared to significantly impact the viability of each population over the range of values considered.

- While we do not attempt to make broad management recommendations here, the hope is that these model outcomes can be used to optimize future investment in restoration and hatchery supplementation programs that support viable natural populations in these systems.

Introduction

The Columbia River Inter-Tribal Fish Commission is conducting a research, monitoring, and evaluation study designed to determine the effectiveness of aggregate restoration actions in improving freshwater habitat conditions and viability of ESA-listed spring Chinook Salmon populations. A critical uncertainty for fisheries managers in the Columbia Basin is whether freshwater habitat restoration actions will improve basin-wide habitat quantity/quality and thereby salmon productivity to a level sufficient to offset human-caused survival impairments elsewhere in the life cycle. Geographically, this project is focused on the upper Grande Ronde River and Catherine Creek basins (tributaries of the Snake River in the Columbia River basin), but with applications and testing of models occurring in other Columbia River tributaries.

Many studies in recent years have examined the current condition of fish habitat in Columbia River subbasins. Some of the most common impediments to survival of salmon include high water temperatures, increased concentrations of fine sediment in spawning gravel, loss of riparian vegetation, channelization and diminished floodplain complexity, loss of large woody debris in the channel, loss of large pools for adult fish holding and juvenile rearing, and summertime depletion of streamflows in the channel. We refer to these as *ecological concerns* (formerly known as *limiting factors*). More recent studies have additionally identified food webs (e.g., nutrient limitation, primary productivity, or prey availability) as ecological concerns for salmonids. Climate change is becoming an emerging issue, as it can lead to changes in the timing of runoff from snowmelt, increased summer air temperatures, and change in the seasonal distribution of precipitation.

Habitat restoration in the upper Grande Ronde River and Catherine Creek basins is being conducted by agencies such as the U.S. Forest Service, the Confederated Tribes of the Umatilla Indian Reservation (CTUIR), the Oregon Department of Fish and Wildlife (ODFW), Union County Soil and Water Conservation District, and the Grande Ronde Model Watershed. The U.S. Bureau of Reclamation is also conducting studies of water use and availability in Catherine Creek watershed and may implement projects based on their findings. However, it remains unclear how these collective restoration actions affect tributary salmon habitat quality and quantity in the freshwater tributary life stages, let alone accounting for the complete salmon life cycle. Fish habitat relationships are inherently complex as they are influenced by interactions among intrinsic watershed factors (e.g., geology, valley form, flood regime) and anthropogenic factors (e.g., land use, climate change, restoration). These in turn affect ecological concerns and ultimately drive changes in fish abundance and productivity. This project incorporates several of these interacting factors in a holistic analytical framework.

The objectives of this project are to: 1) Assess current status and trends in fish habitat characteristics considered to be key ecological concerns for viability of spring Chinook Salmon populations; 2) Evaluate effectiveness of aggregate stream restoration actions aimed at

improving these ecological concerns; and 3) Develop a life cycle model to link biotic responses of spring Chinook populations to projected changes in stream habitat conditions.

We have categorized our work towards these objectives into the following project components:

- Component 1: Habitat and biotic assessments,
- Component 2: Riverscape analyses, and
- Component 3: Fish-habitat modeling.

These individual components are linked together conceptually in an overall sequence of research, monitoring, and evaluation, with analyses feeding into an adaptive management framework (Figure 2).

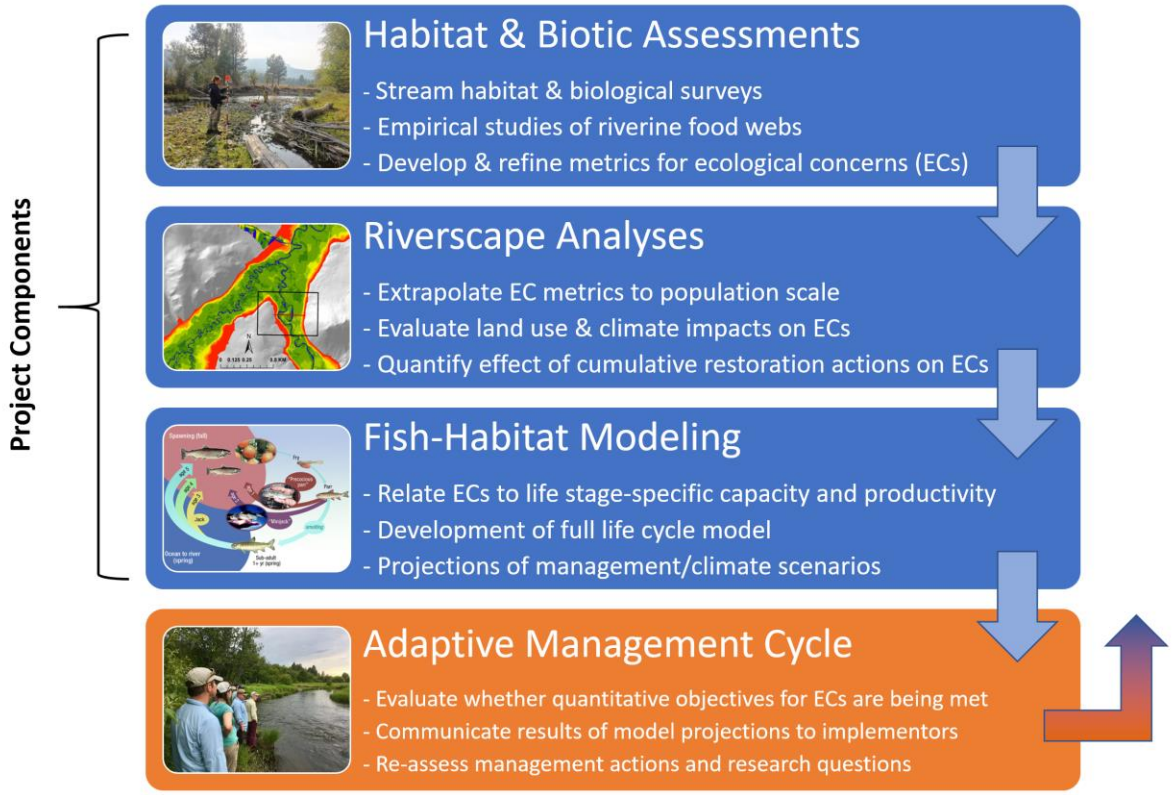

Figure 2. CRITFC's cycle of research, monitoring, and evaluation providing the basis for decision-making in an adaptive management framework.

Component 1: Habitat and biotic assessments—This component of our work involves collecting raw data from field surveys and remote sensing required to develop metrics for ecological concerns including habitat quality and quantity, site-specific estimates of fish capacity and productivity, and condition of terrestrial and aquatic macroinvertebrates. Since 2010 CRITFC has monitored fish habitat conditions in the upper Grande Ronde River and Catherine Creek (impacted basins) and the Minam River (wilderness reference system). In 2010 we initiated our

own habitat protocol, but in 2011 we were encouraged by Bonneville Power Administration (BPA) staff to adopt the Columbia Habitat Monitoring Program (CHaMP) stream habitat assessment survey. Data collected under these programs provided the basis for describing status and trends of key ecological concerns for Chinook salmon in the study basins. In 2017, BPA commissioned a review of CHaMP which revealed several potential problems concerning both the collection of measurements and extrapolation of metrics. In response, our project initiated a revised habitat protocol in 2018 that includes a pared-down list of metrics identified as having minimal observer bias, and is intended to provide comparison with metrics collected using emerging technologies, including unmanned aerial vehicles (UAVs) in collaboration with Bureau of Indian Affairs (BIA). Measurements of physical habitat are paired with snorkel estimates of fish abundance and collection of drift and benthic macroinvertebrates. Additional work includes development and maintenance of an inter-agency stream temperature database in the upper Grande Ronde River basin. An emerging concern in the Columbia River basin and elsewhere is the ability for food webs to support salmonids and other aquatic life in freshwater tributaries. This prompted an experimental carcass addition study in 2017 to evaluate the role of nutrient limitation and food availability on juvenile salmonid growth.

Component 2: Riverscape analyses—This component of our work involves extrapolating metrics for ecological concerns across stream networks and to the watershed/population scale using advanced statistical approaches (e.g., GRTS-based averages or spatial statistical network [SSN] models). Additionally, we evaluate linkages among habitat conditions, land use, and climate conditions to understand ridgetop-to-ridgetop processes affecting spatial and temporal trends in ecological concerns and an understanding of which management or policy scenarios will have the greatest impact. Quantifying the effects of cumulative restoration efforts in the subbasins is another aspect of this work, and includes developing a comprehensive restoration database for generating standardized metrics of restoration intensity. In 2018 we continued development of stream habitat condition metrics from remote sensing (LiDAR) and a digital stream layer. We additionally analyzed relationships among food web indicators derived from benthic macroinvertebrates, land use, climate conditions, and instream habitat conditions. The above endeavors work towards assessing current patterns and trends of habitat quality and quantity that can be measured against historical or reference baselines.

Component 3: Fish-habitat modeling—This component draws from the above data and analyses to relate ecological concerns to life stage-specific capacity or productivity, develop and apply a full life cycle model, and project the outcomes of alternative management and climate change scenarios. Life stage-specific models have thus far emphasized relationships between water temperature, instream habitat conditions, and abundance of rearing fish (parr); these models are then used to project anticipated changes to habitat capacity based on alternative riparian management and climate change. The life cycle model (Figure 3) is a tool to simulate fish population trends in relation to projected habitat conditions, and to examine the relative benefits

of habitat improvements on fish population recovery potential accounting for out-of-basin impacts such as survival of out-migrating smolts at dams or mortality in the ocean phase. The fundamental basis of the model is that intrinsic watershed factors (such as geology, climate, or valley morphology) interact with human actions (such as forest harvest, cattle grazing, or stream restoration) to affect processes that drive known ecological concerns (e.g., flow, temperature, pool area, etc.), and therefore fish survival via both density-dependent and density-independent processes.

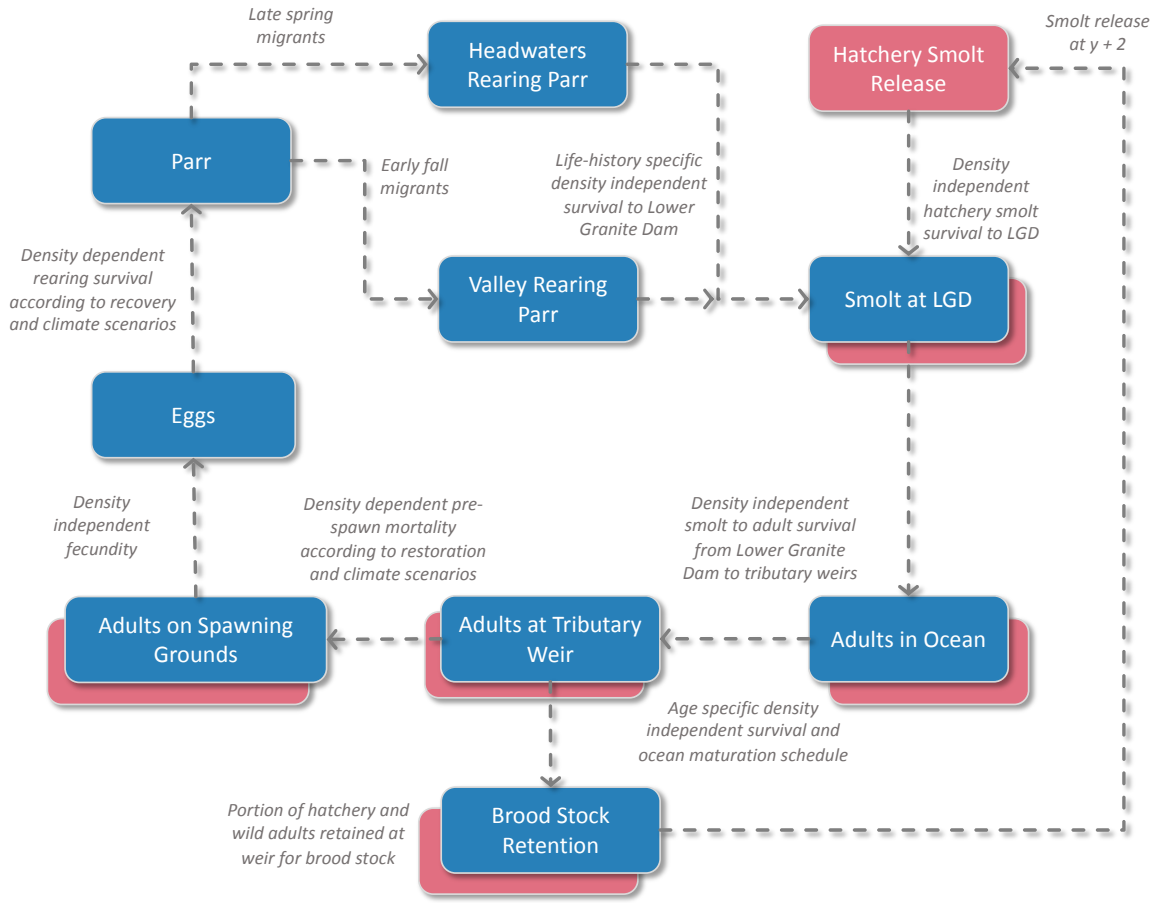

Figure 3. Conceptual diagram of the CRITFC life cycle model (LCM) structure. Stacked boxes represent stages in which the model tracks natural and hatchery origin Chinook. All naturally spawned Chinook are considered of natural origin.

Adaptive management framework—CRITFC plays an important but limited role in the adaptive management framework for the Grande Ronde subbasin. Our project is involved in collection of data, development of models, and hypothesis testing regarding the types of cumulative management activities likely to be most effective for restoring fish populations. Local agencies (e.g., CTUIR, ODFW, USFS) play a larger role in implementing restoration projects and conducting site-scale action effectiveness monitoring of individual restoration projects. CRITFC communicates results of model projections to local managers who re-assess the efficacy of management actions. CRITFC is currently working towards a clarified vision of adaptive management with Grande Ronde Model Watershed and its cooperating agencies.

Study Area

This study is being conducted in the Grande Ronde River and its tributaries, which originates in the Blue Mountains of NE Oregon and flows 334 km to its confluence with Snake River near the town of Rogersburg, Washington (Figure 4). Focal watersheds include the upper Grande Ronde River above the town of La Grande, Catherine Creek, and to a lesser extent, the Minam River, which drain areas of approximately 1,896, 1,051, and 618 km^2 respectively.

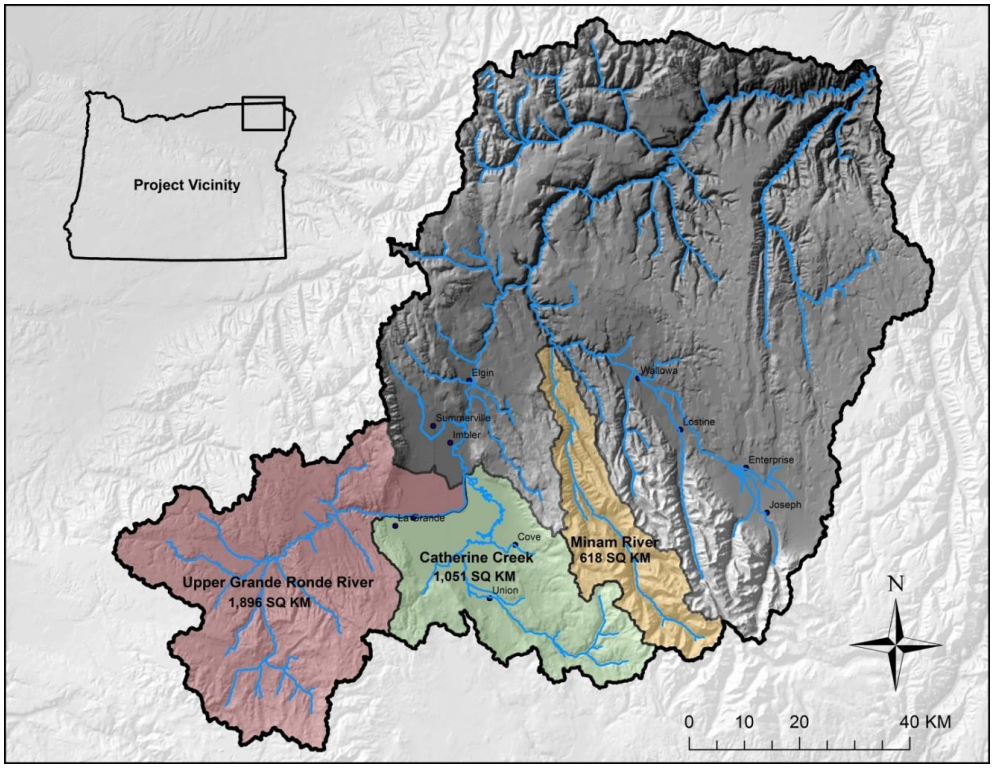

Figure 4. Study area in the Grande Ronde River basin, NE Oregon. Focal watersheds include the upper Grande Ronde River, Catherine Creek, and Minam River. The upper Grande Ronde and Catherine Creek are the basins with significantly damaged habitat that is undergoing restoration in various locations. The Minam River basin is the local reference basin that has far less current evidence of human impact.

The topography of the upper portion of the subbasin (i.e., upstream of the Wallowa River confluence) is characterized by rugged mountains in the headwater areas and a broad, low gradient valley between the Blue and Wallowa Mountains. Peaks in the Wallowa Mountains reach a maximum elevation of 2,999 m, and provide the source of many of the Grande Ronde's tributaries including Catherine Creek and the Wallowa River. The Blue Mountains reach elevations of 2,347 m and are the source of the Grande Ronde River, Wenaha River, and other tributaries. Due to the lower elevation of the Blue Mountains, snow melt generally occurs earlier in these tributaries, often resulting in very low flows during summer.

Surface geology of the Grande Ronde subbasin is dominated by rocks of the Columbia River Basalt group, with some older granitic intrusives and volcanics with associated sedimentary deposits present in the headwater areas of the upper Grande Ronde and Catherine Creek. The climate is characterized by cold, moist winters and warm, dry summers with mean daily air temperatures near La Grande averaging -0.42°C in January and 21°C in July. Average annual precipitation ranges from 36 cm in the valleys to 152 cm in the mountains, with most of the precipitation in the mountains falling as winter snow.

The vegetation community at lower elevations is dominated by grasslands consisting of Idaho fescue/bluebunch wheatgrass (Festuca idahoensis-Agropyron spicatum) and bluebunch wheatgrass-Sandberg's bluegrass (Agropyron spicatum-Poa sandbergii) (Nowak 2004). As elevation increases, the grasslands transition to shrub/scrub plants, and eventually to coniferous forests in the mountains. Forest species consist of low elevation Ponderosa pine (Pinus ponderosa) and lodgepole pine (Pinus contorta) associations grading into Douglas-fir (Pseudotsuga menziesii), grand fir (Abies grandis), subalpine fir (Abies lasiocarpa), and mountain hemlock (Tsuga mertensiana) associations at higher elevations. Riparian vegetation is dominated by black cottonwood (Populus trichocarpa) and willow (Salix spp.), black hawthorn (Crataegus douglasii), mountain alder (Alnus incana), and mountain maple (Acer glabrum).

Approximately 49% of the land in the Grande Ronde basin is publicly owned, of which about 97% is managed by the US Forest Service. The remaining public land is managed by the Bureau of Land Management and the States of Oregon and Washington. Excepting the Eagle Cap and Wenaha-Tucannon Wilderness Areas, the National Forests are managed for multiple use including timber production, livestock grazing, and recreation. Private property comprises 51% of the land in the basin and is located primarily in lower elevation valleys and along rivers. A large proportion of the private property is used for agriculture including crop production, livestock grazing, and forestry. Only 0.1% of the land in the Grande Ronde Basin is currently owned by the tribes, although the tribes retain fishing and hunting access rights at all usual and accustomed locations as afforded under the treaties of 1855 and 1863.

Spring Chinook populations in these basins were listed as threatened under the Endangered Species Act in 1992. Population declines over the past century were due in part to severely

degraded habitat conditions resulting from intensive anthropogenic disturbances including timber harvest, cattle grazing, levee and road construction, and stream diversions for irrigation. Specifically, stream temperature, streamflow, fine sediment, habitat diversity, and quantity of key habitats such as large pools, have been identified as key ecological concerns for recovery of Chinook populations in these basins.

Project Components

Habitat and Biotic Assessments

Evaluation of Habitat Protocol Using Remote Sensing

Introduction

Advances in the development of high-resolution surveying technologies have substantially increased the ability to map riverine topography with high accuracy and precision. Compared to historic "stick and tape" measurement techniques that can be expensive and labor intensive, remotely-sensed techniques have become the new standard for bathymetric, floodplain topography, and more recently of fish habitat surveys (Tamminga et al., 2015). Ranging in application from air based (e.g., airborne laser scanning (ALS), Structure from Motion using UAVs), to boat (e.g., single and multibeam SONAR), and ground-based surveys (e.g., terrestrial laser scanning (TLS), total station (TS), and real-time kinematic global positioning system (rtkGPS), Bangen et al., 2014), these advances in technology have led to the ability to map sub-centimeter level resolution of topography. These emerging technologies provide opportunities to improve the accuracy and precision of fish habitat metrics at larger spatial extents.

Unmanned aerial vehicles (UAVs) represent one solution capable of quantifying habitat at resolutions relevant to fish (mesohabitat; 1 km) and over continuous spatial scales (Tamminga et al., 2015). Here we assess the performance and capabilities of UAVs for stream habitat surveys by comparing measurements derived from UAV imagery to those from ground-based surveys in the Grande Ronde River and Catherine Creek basins in Northeast Oregon. While many studies have demonstrated the capabilities of UAVs and post-processing methods to obtain bathymetry and characterize in-stream habitat, no other studies to our knowledge have examined their application across varying canopy and stream reach types.

Methods

Site selection

Thirteen study reaches were selected from prior locations associated with the Columbia Habitat Monitoring Program (CHaMP, 2016), a protocol that used a spatially-balanced probabilistic survey design for evaluating spatial and temporal trends in fish habitat conditions in tributaries of the Columbia River basin. To evaluate how a UAV would perform in a variety of settings, we selected sites that represented the greatest diversity of geomorphic and riparian conditions encountered by salmonids in the study area (Table 2). Sampling locations were chosen based on four criteria: 1) watershed size (i.e., small or large), 2) the combination of river confinement and gradient (i.e., constrained or unconstrained), 3) riparian canopy density (i.e., sparse, medium, or dense) and 4) occurrence on public land (e.g., USFS); excepting one location where a suitable

location for our “large, dense, unconstrained” classification was not found on public land (CBW05583-430250). The first two selection criteria are based on the stream classification methodology developed by White et al. (2011). On a digital stream layer generated from a 10-m digital elevation model, reaches of length 20 times the bankfull channel width were categorized as “small” or “large” based on a multivariate analysis of watershed characteristics (watershed area, elevation, stream order, and accumulated mean precipitation). Reaches designated as “small” were further delineated as “response” (gradient ≤ 3 %) or “transport” (gradient > 3 %). Finally, all reaches were designated as “constrained” or “unconstrained” based on potential for lateral channel migration. Unconstrained reaches were those with ≤ 10% of the stream channel abutting bedrock or terrace features (Brierley and Fryirs, 2005) as determined from aerial photographs and 10-m digital elevation models. The third criterion, density of the canopy layer (vegetation taller than 1.5 m), was evaluated using LiDAR collected in 2009 and classified by height strata by Wells et al. (2015). To account for the expected natural differences in canopy cover in unconstrained versus constrained reaches, thresholds for canopy density were classified using quartile values of vegetation density specific to stream channel constraint (Table 1). The fourth criterion, access to public land, was desirable during this initial study because of uncertainty regarding public perceptions of UAVs, ease of land access (acquiring permits), and the benefits of increased safety and security measures of established USFS reporting and communication procedures.

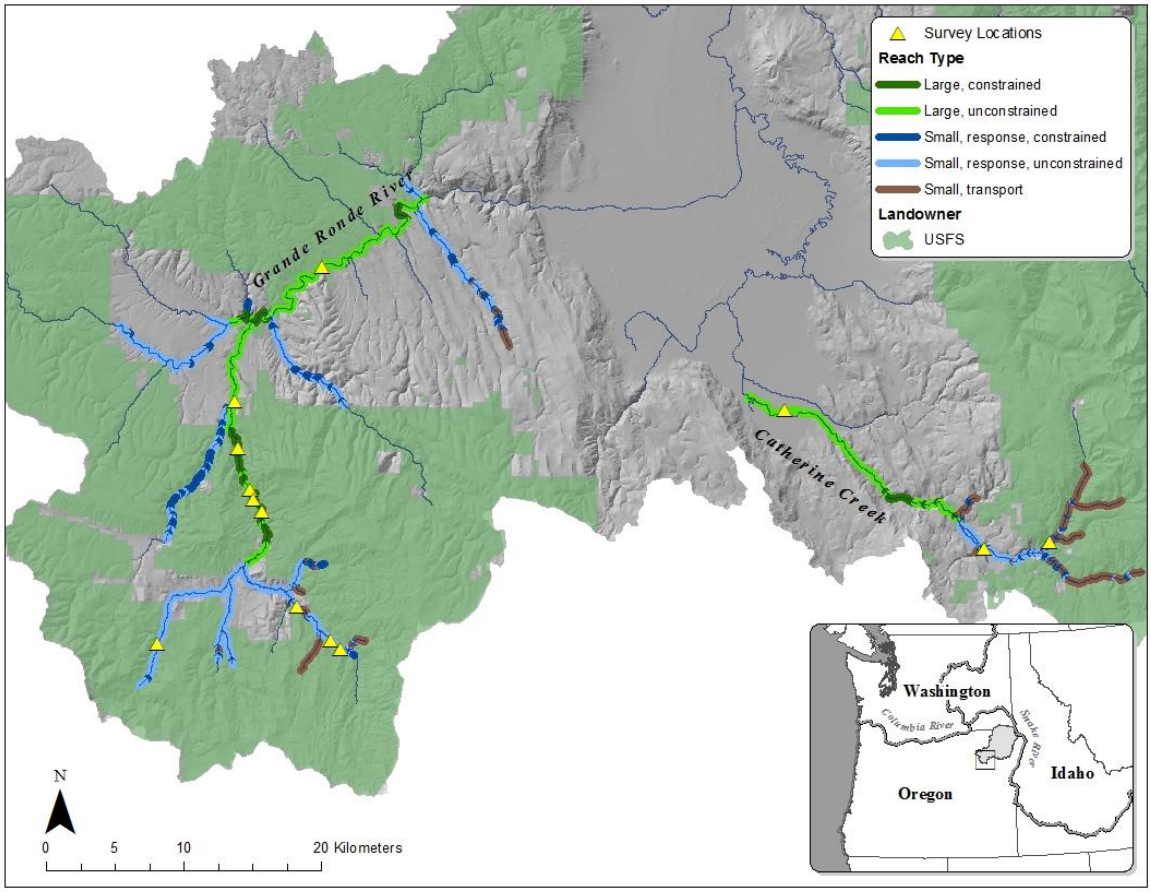

Figure 5. Sampling locations (n=13) with their associated stream reach classifications within the upper Grande Ronde River and Catherine Creek basins in Eastern Oregon.

Table 1. Thresholds of canopy density by stream channel constraint type.

	Canopy density values (%)		
Reach type	**Sparse** *	**Medium** †	**Dense** +
Constrained	15.8 – 30.4	35.9 – 42.8	44.9 – 53.1
Unconstrained	9.6 – 22.4	25.7 – 38.5	45.8 – 65.7
Quartiles:	* 5th-25th	† 35th-65th	+ 75th-95th

Small, response, constrained

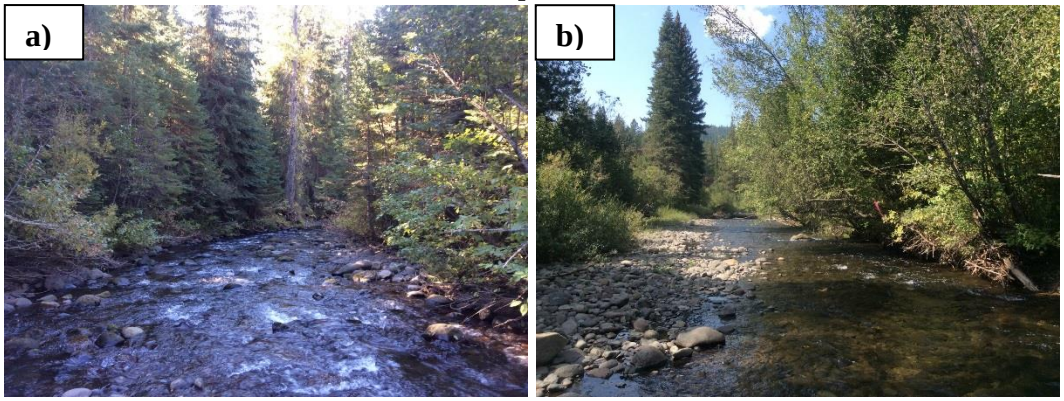

Small, response, unconstrained

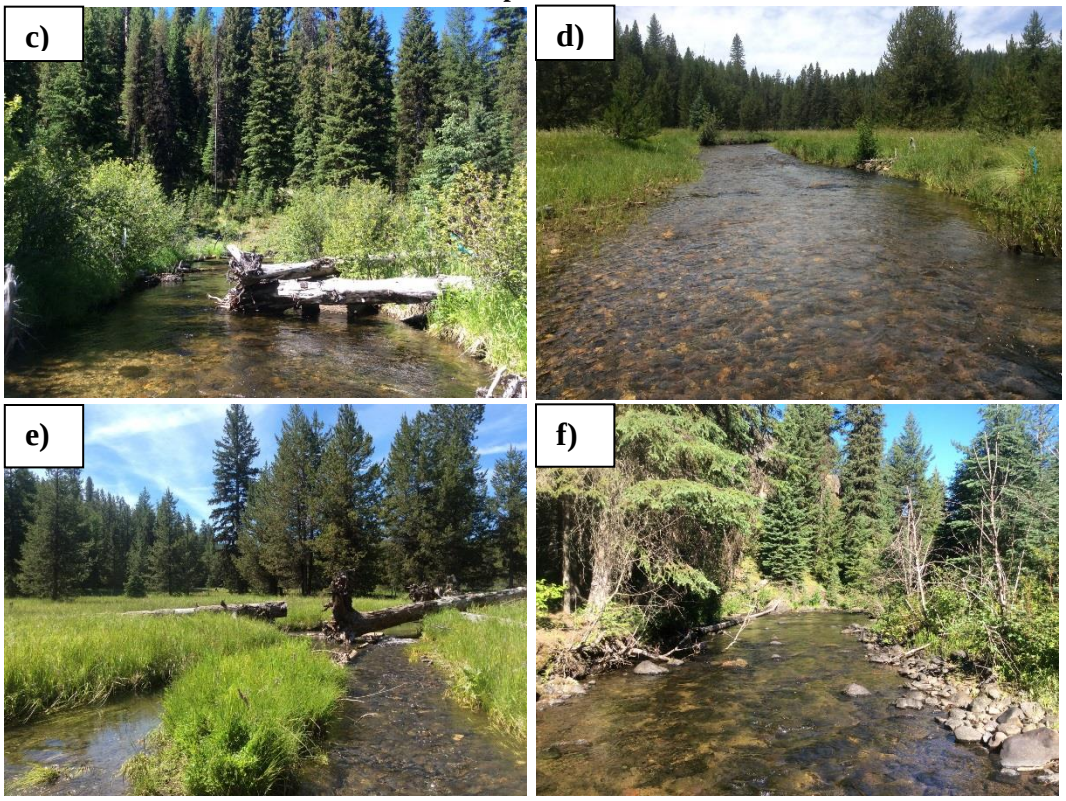

Large, constrained

g)

h)

i)

Large, unconstrained

j)

k)

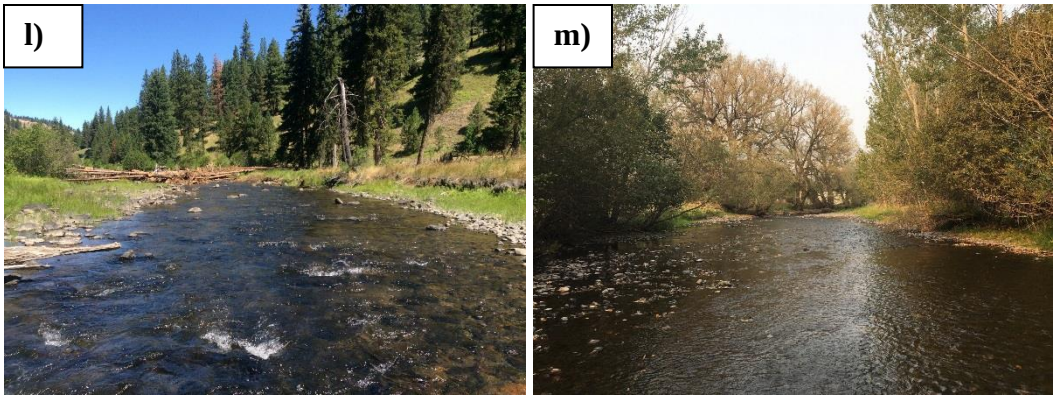

Figure 6. Example site photos for each stream classification.

Table 2. Sampling locations (n=13) and associated characteristics within the upper Grande Ronde and Catherine Creek Watersheds in Eastern Oregon.

	Site	Classification	Canopy Density	Elev. (m)	Grad. (%)	Latitude	Longitude
a	CBW05583-138666	Small, response, constrained	Dense	1178	2.66	45.12718962	-117.6361884
b	CBW05583-456106	Small, response, constrained	Medium	1044	1.11	45.12275127	-117.6966604
c	CBW05583-099818	Small, response, unconstrained	Medium	1359	0.58	45.05123037	-118.2901869
d	CBW05583-280042	Small, response, unconstrained	Sparse	1372	0.62	45.05725543	-118.299575
e	CBW05583-335162	Small, response, unconstrained	Sparse	1334	0.86	45.05285634	-118.4599315
f	CBW05583-468458	Small, response, unconstrained	Dense	1306	2.49	45.07913711	-118.3316825
g	CBW05583-321338	Large, constrained	Sparse	1169	2.82	45.14067676	-118.3647973
h	CBW05583-370490	Large, constrained	Medium	1189	0.85	45.14882726	-118.372891
i	CBW05583-486202	Large, constrained	Dense	1303	1.71	45.18258685	-118.3883779
j	CBW05583-031546	Large, unconstrained	Medium	1077	0.74	45.21293119	-118.3927931
k	CBW05583-071770	Large, unconstrained	Sparse	942	0.44	45.30198127	-118.312525
l	CBW05583-235322	Large, unconstrained	Sparse	1154	0.92	45.15516505	-118.3763865
m	CBW05583-430250	Large, unconstrained	Dense	847	0.69	45.21194527	-117.8830458

Field methods - Overview

Stream habitat surveys typically collect a large number of habitat variables, and of particular importance to this work are those which are both quantifiable and have been found to be key ecological concerns for salmonids (e.g., stream temperature, biological production, and channel dynamics and morphology (CHaMP, 2016)). Using the Columbia Habitat Monitoring Program methodology as a basis for comparison, we identified a select number of variables which we expected could be obtained from a UAV survey to produce habitat metrics with similar, if not greater, resolution and accuracy as compared to methods using high precision (subcentimeter) professional surveying equipment (e.g., Total Station). We present comparisons here on a subset of these metrics which can be subdivided into four categories: 1) important but cannot be measured using a drone, 2) used for validation of data collected by the drone, and 3) used to supplement the drone data. Supplemental data may be necessary to fill in areas not well covered by the drone (e.g., dense or channel-overhanging canopy cover) or in deep water areas where

imagery cannot visualize the channel bed. In-stream habitat and UAV imagery for this study were collected from late July through October of 2018 coinciding with low flow conditions in the basin. Conducting sampling during this period increased the likelihood of obtaining bathymetry from a shallower water column and decreased potential error associated with changing water levels between in-stream habitat and topography surveys and UAV surveys. The summer low-flow period has also been identified has a critical temperature and space limiting bottleneck for juvenile salmonids (e.g., Justice et al., 2017; White et al., 2017), and therefore represents a biological critical time period.

Field methods - Stream habitat data collection

During the summer of 2018, we conducted field surveys to characterize physical habitat conditions. Logistical constraints resulted in a difference in timing between the two survey techniques. However, in agreement with Roper et al. (2010), sampling during low flow conditions when these systems were reaching their hydrograph minima reduced the likelihood of in-stream substrate and large wood movement that would affect measurements between the two sampling techniques.

In-stream habitat types (channel units) were identified at the reach scale for each of 13 sampling locations. Using a modified two-tiered hierarchal classification scheme modified from Hawkins et al. (1993), channel units were used as the basis for determining where additional habitat data were collected (Figure 7). Within each Tier 2 channel unit type, we counted large woody debris within or overhanging any portion of the active channel and meeting a minimum size criteria of 15 cm diameter and 3 m in length. Substrate size distribution was measured at Tier 2 fast water turbulent, fast water non-turbulent, and slow water pool habitats following the Wolman pebble count procedure until 100 particles were measured within each (Wolman 1954). Though not included in analyses here, site level data were also collected for solar access, discharge, conductivity, land use, and restoration actions. A detailed explanation of which variables and how they were collected is provided in the draft sampling protocol in *Appendix A*.

Following the methods in White et al. (2012), late summer snorkel surveys were also conducted to quantify juvenile chinook and steelhead abundance and size. Site level count data were corrected for fish not observed using paired mark-recapture population estimates. Additionally, benthic macroinvertebrate samples were collected concurrently with snorkel surveys to assess food availability.

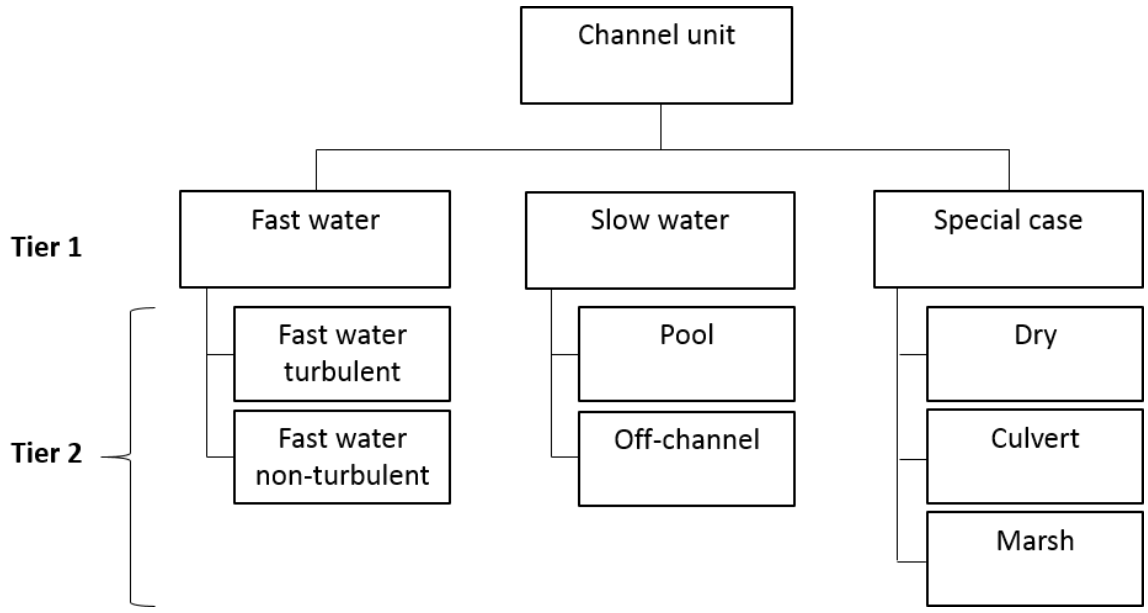

Figure 7. Hierarchical channel unit classification scheme modified from Hawkins et al. (1993).

Field methods – Ground control points and topographic surveys

A control network consisting of 10 ground control points (GCPs) was established at each of the 13 sampling locations using a Topcon rtkGPS or Total Station. The locations of each GCP were dependent on the topographic complexity and riparian canopy density at each site. Where possible we attempted to evenly distribute the GCPs throughout the sampling area where they would be both visible in imagery from overhead and represent the topographic variability throughout the site.

Data were collected using a Topcon Total Station following a modified version of the procedures outlined in the CHaMP protocol (See *Appendix A*). Topographic surveys were conducted both in the active channel and surrounding floodplain using coded points and lines to reflect changes in topography (e.g., inflection points), where higher complexity areas such as concave pools within the active channel resulted in higher point densities compared to uniform planar features (e.g., riffles; Bangen et al., 2014). Additional data were also collected at transects spaced every 2 times the site bankfull width to enhance the resolution of the topographic models, supplement the UAV data, and serve as fixed locations for site level measurements (e.g., solar access, bankfull width and depth).

Field methods – Unmanned aerial vehicle flights

Two imagery sets were obtained for each site using a 15 mm Zenmuse X5 visible spectrum camera (equipped with a circular polarizing filter) and a Micasense Rededge-M five band multispectral camera mounted on a commercial hexarotor UAV (DJI Matrice 600 Pro; Figure 8). Prior to each UAV flight mission, 1.524 m x 1.524 m iron cross targets (Figure 9) were laid out

over the 10 surveyed GCPs. Flight missions were planned using DJI Ground Station Pro at altitudes of 80-or-120 m and average ground sampling distances (GSD) of 4.9 and 7 cm/pixel for the Zemuse X5 and Micasense Rededge-M cameras, respectively. Flights were limited between 10:00 and 14:00 to maximize solar noon lighting and reduce shadows from riparian vegetation. Due to software and gimbal restrictions at the time of survey, independent flight plans were created for each of the two imagery sets that accounted for time of survey, obstructing vegetation, stream orientation, and incident solar angle creating sun glint on the water surface. Resulting flight lines for visible imagery occurred at nadir and off-nadir camera angles (90 and ≤ 26.5 degrees for nadir and off-nadir) with an 80 % forward and 70 % side overlap and at an average speed ≤ 6 m/s. To ensure high image quality and reduce potential image blur, imagery for this dataset were collected while the UAV was hovering (i.e., stop-and-go shooting).

Figure 8. Matrice 600 Pro hexarotor UAV used to collect imagery; 1.524 m landing pad for scale.

Figure 9. Example imagery showing aerial targets used for identifying ground control points (GCPs) from imagery during flight from 120 m above ground level (AGL); inset figure showing a 1.524 x 1.524 m target secured with stakes.

Processing and analysis - Topographic data

Topographic data, collected following the CHaMP protocol (CHaMP, 2016a) at each of the 13 sampling locations, were processed using the CHaMP Topo Toolbar ArcMap add-in (http://champtools.northarrowresearch.com/). Metrics were generated by North Arrow Research, Inc. for each of the sampling locations accounting for our modified survey design. Though the number of metrics generated is dependent on the site complexity (e.g., presence of multiple channels), the computed metrics from the CHaMP typically result in > 100 metrics related to site level and channel unit level attributes.

Processing and analysis – Unmanned aerial vehicle imagery

The resulting photosets from each sampling location were processed in three stages: 1) image pre-processing in Agisoft Metashape, 2) post-processing in ArcMap and CloudCompare, and 3) data product corrections and error assessment in Python. Pre-processing in Agisoft Metashape (previously Agisoft Photoscan Pro; version 1.4) was performed following a modified version of the USGS UAS Data Post-Processing workflow (Section 1 and 2 of USGS, 2017). The resulting

high resolution orthophoto reconstructions of each sampling location were exported from Agisoft and used for feature classification in ArcMap 10.6.

Because many of the metrics produced from the CHaMP relate to features within the wetted channel (e.g., wetted depths, volumes, and areas), a method to subsample and extract these features from the larger dense point cloud (DPC) was necessary. Using the Image Classification tool, a Maximum Likelihood Supervised Classification was performed to identify and extract pixels corresponding to water in the active channel. Only pixels corresponding to water were retained, allowing us to exclude large wood, bare substrate, and vegetation features that would negatively influence the subsequent depth corrections. The wetted perimeter identified from the orthoimagery in ArcMap was then imported into CloudCompare (free and open software; version 2.10.2). For each of the points falling within this wetted perimeter, depth corrections were performed following the multi-camera refraction correction for SfM point clouds outlined by Dietrich (2017). Metrics were then computed using the corrected water depths and elevations.

Results and Discussion

There exists a wide range of applications for UAVs in fisheries related to topography, habitat assessments, and even population surveys (Tyler et al., 2017). However, to date studies examining the accuracy and precision of UAV derived data products have been limited and without replication. We collected stream habitat data and topographic data to examine the agreement of common stream metrics relevant to fish. Data presented here are limited to site CBW05583-280042 on the Grande Ronde River; a complete analysis including all 13 locations is forthcoming.

Stream habitat data

We identified eight distinct channel units at site CBW05583-280042 during our low-flow stream habitat surveys. Figure 10 shows the frequency and distribution of Tier 2 channel unit types at site CBW05583-280042. Of the total 847 m^2 wetted area, slow water accounted for 40%, fast water turbulent areas 43% and fast water non-turbulent areas 17%.

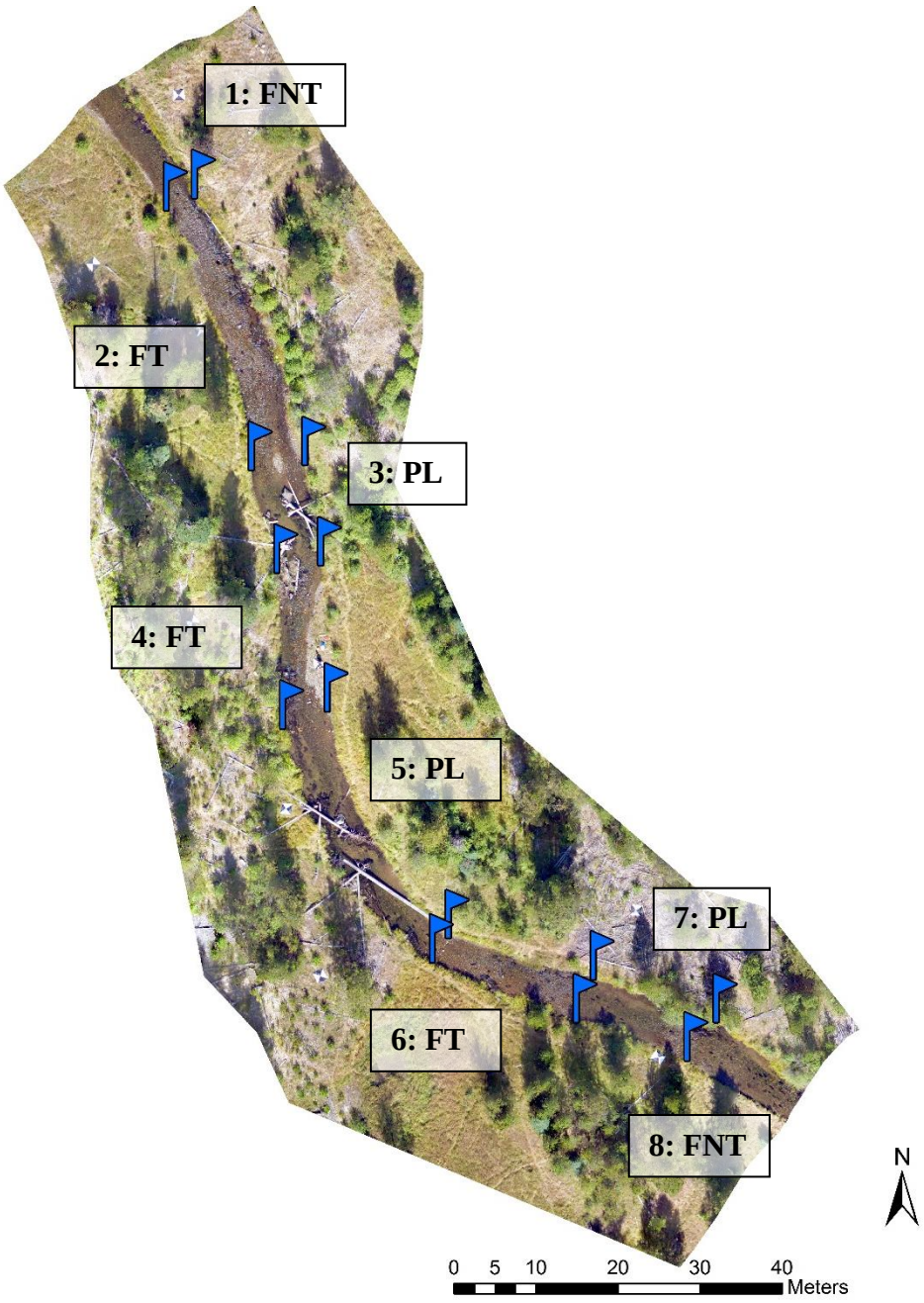

Figure 10. Orthoimage for site CBW05583-280042 showing in-stream Tier 2 channel unit delineations.

Substrate

Substrate measurements taken with the revised protocol largely agreed with those data collected prior (2011-2017) using the CHaMP protocol and have remained fairly stable at each of the 13 sampling locations throughout monitoring years (Figure 11.b). Using Wentworth substrate size classifications, the median substrate diameter within each Tier 1 unit type at the 13 sampling locations were predominantly gravel and cobble. Larger substrate sizes (cobbles) were more

commonly associated with fast water turbulent channel units, while smaller sizes (gravels) in fast water non-turbulent units and slow water areas (Figure 11.a). Future sampling will test the use of UAVs to obtain accurate substrate data using UAV derived products such as image texture (Tamminga et al., 2015; Carbonneau et al., 2004) and spectral composition (Legleiter et al., 2016).

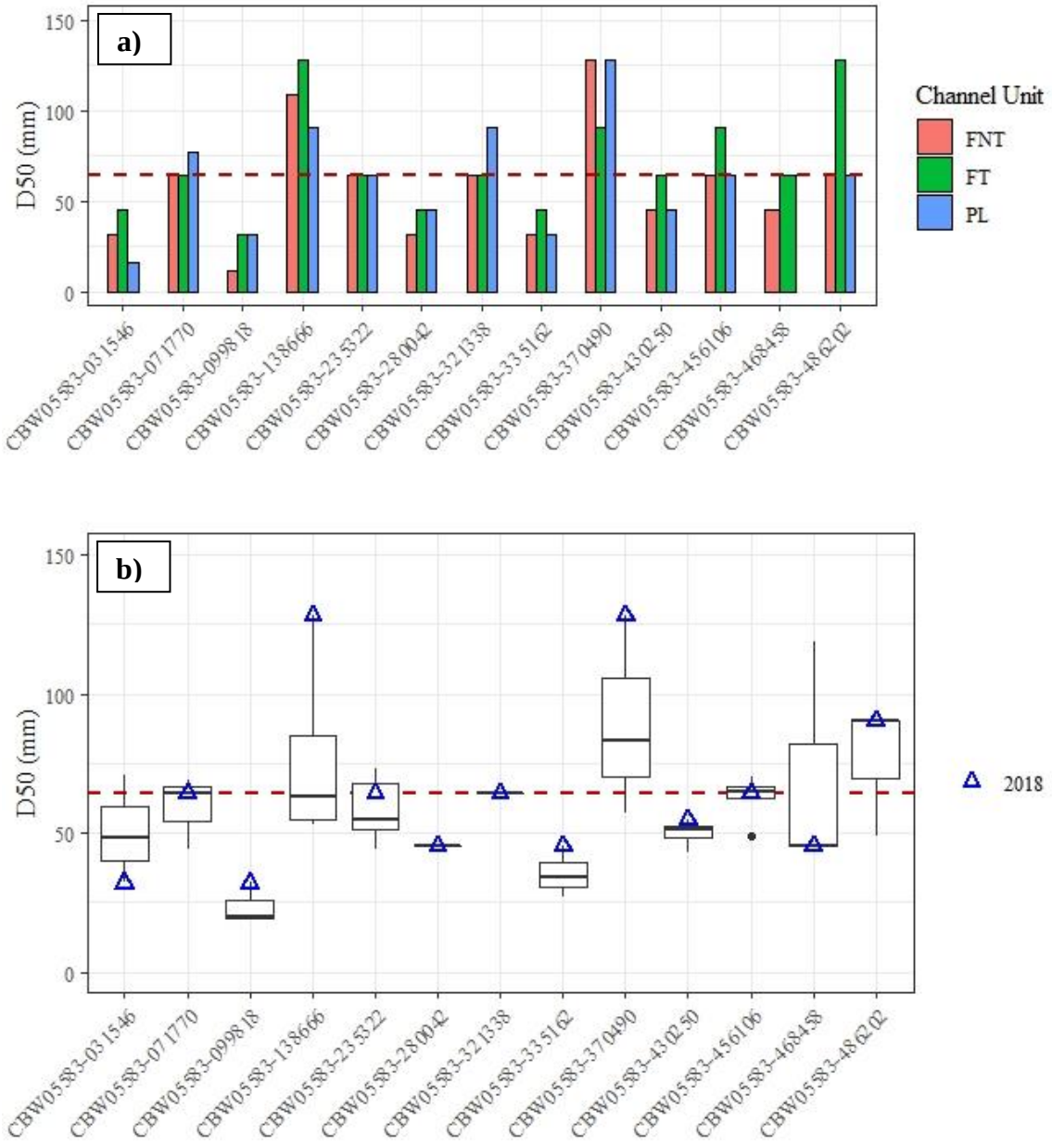

Figure 11. Calculated D50 particle size for a) Tier 2 channel unit types in 2018, and b) distribution of D50 measurements from 2011 – 2018 at each the 13 sampled sites. Blue triangles represent the 2018 measurements and the red dashed line is the cutoff between gravel and cobble size classes (64 mm). Boxplots showing 25th, 50th, and 75th percentiles with the median as the black bold line and whiskers extending 1.5*IQR.

Large woody debris

The location and number of pieces of large woody debris (LWD) are important measurements that influence stream morphology and biological productivity. Studies of large wood within streams are typically performed through surveys of wood distribution (ground based or aerial counts), dating (residence time), and tracking (tagging) movement and accumulation (MacVicar et al., 2009). However, where LWD is abundant, measuring and geotagging each piece can be very time consuming. This work focused on the level of agreement of large wood counts between our two measurement techniques (ground-based vs. UAV imagery). Where not obstructed by vegetation, banks, or additional overlapping pieces, large wood meeting our size criteria were straightforward to identity from the UAV reconstructed orthoimagery using image classification schemes, and visually from orthophotos.

From our surveys of wood distribution, we found a difference in the two techniques, with fewer wood pieces counted using the UAV approach (Figure 14; Table 4). Though we failed to detect any qualifying pieces of large wood in imagery that were counted by crews in units six through eight (6:FT, 7:PL, 8:FNT), the largest observed difference between methods was measured in channel unit five (5: PL). In this unit, four fewer pieces were identified in imagery.

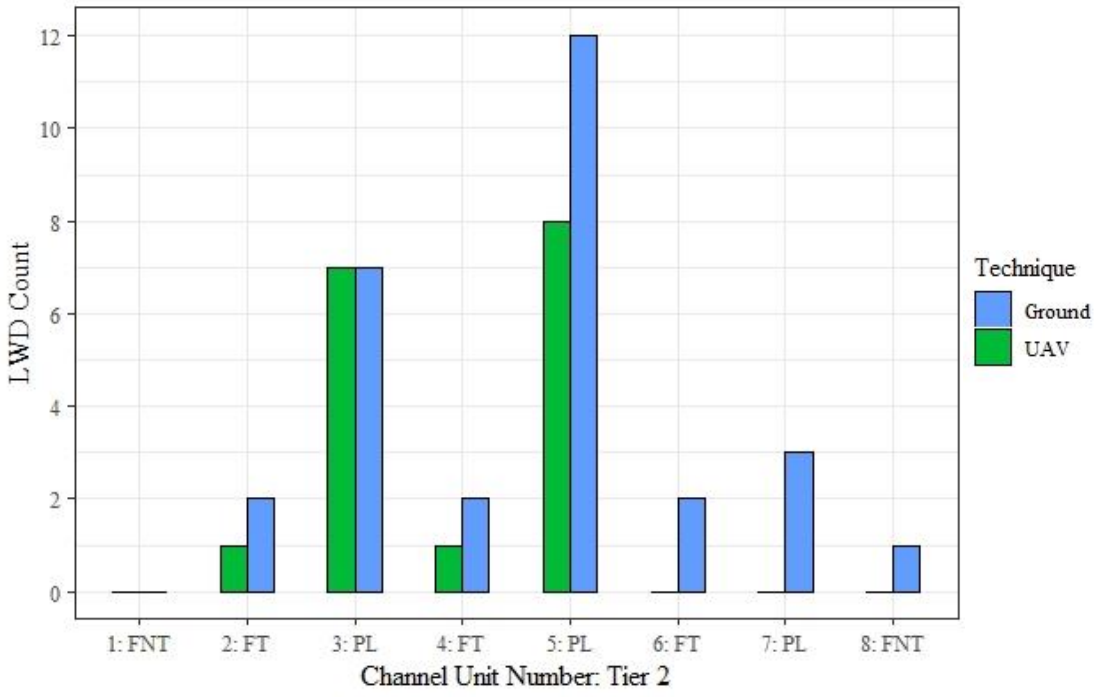

Figure 12. Comparison of ground-based counts compared to those from resulting UAV orthoimagery of large woody debris by channel unit Tier 2 type for site CBW05583-280042.

This observed discrepancy may partially be attributed to large wood structures spanning the channel that were both overlapping and partially sunken (e.g., into the bank, bedform, or underwater), which restricted our ability to identify qualifying pieces meeting our length and diameter requirements. Additionally, across the entire site, we found water surface roughness/turbulence, shadows, overlapping sections, and riparian vegetation (grasses, trees) to impair our ability to identify all pieces counted on the ground. To a smaller degree, some of the variability in measurements between the two techniques may be attributable to crew observer error. Crews were trained to count pieces meeting our minimum criteria, but were not required to measure each piece. This methodology may have resulted in over or undercounting pieces.

We identified counts of large wood debris directly within or overhanging the active channel, as the simplest quantifiable survey technique to obtain large wood distributions by unit type for a given stream reach. However, a hybridized approach using both ground-based count data coupled with UAV imagery could considerably enhance what we know about large wood movement, residence times, and volumes within streams. Though increasingly difficult to measure in complex channels (e.g., braided) or where obstructions are abundant, volumetric measures of large wood from imagery are possible. We found our average image resolution (4.9 cm/pixel) from our UAV surveys at 80-or-120 meters to be sufficient in visually identifying and measuring large wood for validation. Furthermore, though we did not explicitly measure the length and diameter of each piece, Comiti et al. (2008b) found measurement errors from aerial imagery were greatly reduced (15%) when image resolution was at most twice that of the minimum large wood diameter. Continued work assessing the comparability between sampling locations with higher canopy and riparian densities will be important in determining the feasibility of coupling UAV surveys with ground-based surveys of large wood.

Biological data

Fish densities in the upper Grand Ronde River were typically lower than other populations and have substantially decreased since 2011. Though highly variable, average densities for both Catherine Creek and the upper Grande Ronde River continued to increase in 2018. Juvenile salmon densities in the Minam River Wilderness area tended to be as high or higher than Catherine Creek during the three years of sampling there, with the final year of sampling (2015) exhibiting the largest difference from other populations. These trends should be interpreted with caution as they do not account for annual differences in site selection inherent to the Generalized Random Tessellation Stratified (GRTS) sampling design. We plan to extrapolate these data to the population scale using a spatial statistical network model (SSN) approach (Isaak et al. 2017).

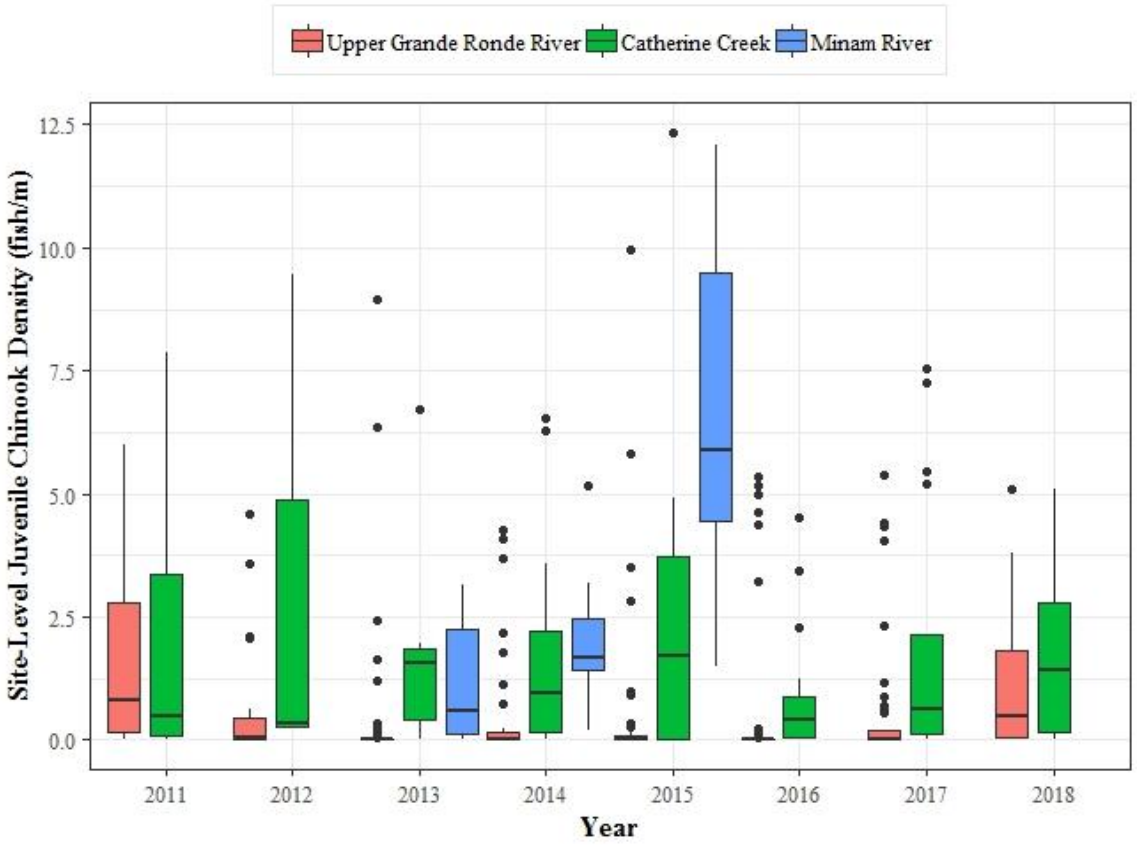

Figure 13. Juvenile spring Chinook Salmon density (fish/m) by ICTRT population from 2011-2018 in the upper Grande Ronde River and Catherine Creek, and from 2013-2015 in the Minam River for Julian days 200-260.

Topographic metrics

Using commonly computed stream habitat metrics that are relevant to fish, we found UAV based remote sensing methods overall showed good agreement in comparison to traditional ground-based total station surveys of topography. However, notable differences between the survey techniques revealed obstructions (overhanging vegetation, channel spanning large wood) to play a large role in decreasing the wetted area and therefore wetted volume across the entire site **(**Table 3) and within individual channel units (Table 4; Figure 14). More specifically, UAV derived measurements of total wetted area only accounted for 78% of the area mapped using ground-based topographic surveying.

Table 3. Computed site level metrics for location CBW05583-280042.

	Measurement Technique	
Metric	**Ground**	**UAV**
Average Thalweg Depth (m)	0.24	0.22
Average Pool Residual Depth (m)	0.32	0.33
Gradient (%)	0.62	0.63
Wetted Length (m)	163.73	163.01
Slow Water Area (m^2)	338.45	253.66
Fast Water Turbulent Area (m^2)	362.51	286.19
Fast Water Non-turbulent Area (m^2)	146.47	119.39
Slow Water Volume (m^3)	74.69	35.00
Fast Water Turbulent Volume (m^3)	33.20	38.58
Fast Water Non-turbulent Volume (m^3)	21.44	18.71

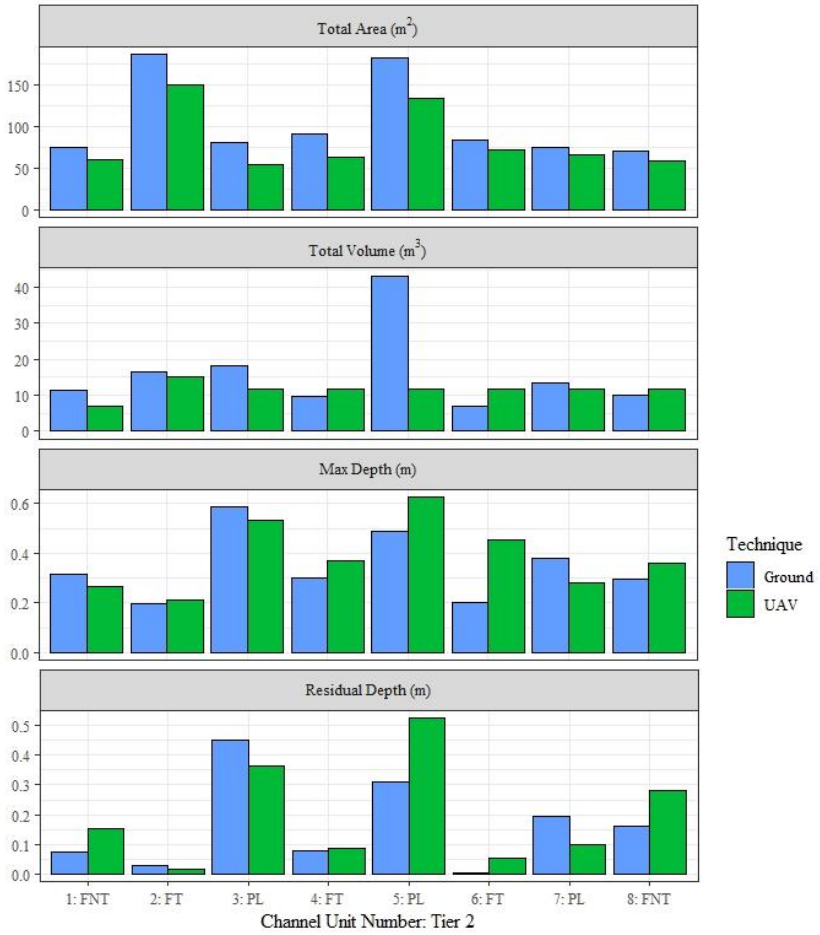

Figure 14. Comparison of computed metrics by Tier 2 channel unit classification for each survey technique at site CBW05583-280042.

We attribute this discrepancy in area measured mainly to overhanging vegetation and to a minimal extent, large wood and boulders. While the metrics from the UAV survey fail to characterize the total wetted area, the resolution of data is much finer in comparison to the sparse point density surveyed in-situ by crews and should therefore provide a more precise representation of bathymetry at the channel unit scale. Continued work refining the post-processing methodology to remove the effects of obstructions from generated surfaces (e.g., digital elevation model (DEM)) should further improve the agreement between metrics.

Table 4. Comparison of computed metrics by Tier 2 channel unit classification for each survey technique at site CBW05583-280042.

	Channel Unit		LWD Count		Max Depth (m)		Residual Depth (m)		Total Area (m^2)		Total Volume (m^3)	
	Tier 1	**Tier 2**	**Ground**	**UAV**	**Ground**	**UAV**	**Ground**	**UAV**	**Ground**	**UAV**	**Ground**	**UAV**
1	Fast Water	FNT	0	0	0.32	0.27	NA	NA	75.41	60.65	11.36	7.04
2	Fast Water	FT	2	1	0.20	0.21	NA	NA	187.01	151.00	16.60	15.24
3	Slow Water	PL	7	7	0.59	0.53	0.45	0.37	80.64	54.35	18.17	11.67
4	Fast Water	FT	2	1	0.30	0.37	NA	NA	91.10	62.77	9.74	11.67
5	Slow Water	PL	12	8	0.49	0.62	0.31	0.52	182.68	133.91	43.23	11.67
6	Fast Water	FT	2	0	0.20	0.45	NA	NA	84.41	72.41	6.87	11.67
7	Slow Water	PL	3	0	0.38	0.28	0.19	0.10	75.13	65.39	13.29	11.67
8	Fast Water	FNT	1	0	0.30	0.36	NA	NA	71.06	58.74	10.09	11.67

Interestingly, there has been much disagreement and skepticism regarding the capabilities of UAV especially with regard to obtaining accurate bathymetry data. At the reach scale, we found the difference between techniques varied ≤ 2 cm for thalweg and pool residual depths (Table 3) and on average ≤ 9 cm for max and residual depth measurements within each of the eight channel units at site CBW05583-280042 (Figure 14; Table 4). In the context of previous studies assessing the accuracy of topographic surveys from ground and remotely sensed surveys, vertical error has been recorded ranging from as low as 4-6 cm for terrestrial laser scanning (Williams et al., 2013; Schürchet al., 2011), 15 – 40 cm for LiDAR (Notebaert et al., 2009), and 4.5 cm – 1.1 m between terrestrial and aerial photogrammetry (Tamminga et al., 2015; Chandler et al., 2002; Lejot et al., 2007).

While the comparisons between UAV and ground-based surveys presented here are limited to a single site with relatively low vegetation density, these preliminary results are promising and suggest that UAV surveys coupled with limited ground-based measurements may be an accurate and cost-effective method for monitoring fish habitat conditions. This approach represents a feasible option to aid CRITFC and other regional partners in continuing to evaluate status and trends of fish habitat quantity and quality while improving efficiency and data accuracy.

References

Bangen, S. G., Wheaton, J. M., Bouwes, N., Bouwes, B., Jordan, C. 2014. A methodological intercomparison of topographic survey techniques for characterizing wadeable streams and rivers. Geomorphology, 206, 343–361. https://doi.org/10.1016/j.geomorph.2013.10.010

Brierley, G. J, and K. A Fryirs. 2005. Geomorphology and River Management: Applications of the River Styles Framework. Blackwell Oxford.

Carbonneau, P.E., Lane, S.N. and Bergeron, N.E., 2004. Catchment-scale mapping of surface grain size in gravel bed rivers using airborne digital imagery. Water resources research, 40(7).

CHaMP (Columbia Habitat Monitoring Program). 2016a. Scientific protocol for salmonid habitat surveys within the Columbia Habitat Monitoring Program.

Comiti F, Pecorari E, Mao L, Picco L. Rigon E, Lenzi MA. 2008b. New methods for determining wood storage and mobility in large gravel–bed rivers EPIC FORCE project Deliverable D20bis https://research.ncl.ac.uk/epicforce/assets/D20bis.pdf.

Dietrich, J. T. 2017. Bathymetric Structure-from-Motion: extracting shallow stream bathymetry from multi-view stereo photogrammetry. Earth Surface Processes and Landforms, 42(2), 355–364. https://doi.org/10.1002/esp.4060

Hawkins, C. P., J. L. Kershner, P. A. Bisson, M. D. Bryant, L. M. Decker, S. V. Gregory, D. A. McCullough, C. K. Overton, G. H. Reeves, R. J. Steedman, and M. K. Young. 1993. A hierarchical approach to classifying stream habitat features. Fisheries 18(6):3–12.

Isaak, D. J., J. M. Ver Hoef, E. E. Peterson, D. L. Horan, and D. E. Nagel. 2017. Scalable population estimates using spatial-stream-network (SSN) models, fish density surveys, and national geospatial database frameworks for streams. Canadian Journal of Fisheries and Aquatic Sciences 74(2):147–156.

Legleiter, C.J., Stegman, T.K. and Overstreet, B.T., 2016. Spectrally based mapping of riverbed composition. Geomorphology, 264, pp.61-79.

MacVicar, B.J., Piégay, H., Henderson, A., Comiti, F., Oberlin, C. and Pecorari, E., 2009. Quantifying the temporal dynamics of wood in large rivers: field trials of wood surveying, dating, tracking, and monitoring techniques. Earth Surface Processes and Landforms, 34(15), pp.2031-2046.

Nowak, M.C. 2004. Grande Ronde Subbasin Plan. Prepared for Northwest Power and Conservation

Council. 491 p.Roper, B. B., Buffington, J. M., Bennett, S., Lanigan, S. H., Archer, E., Downie, S. T., … Pleus, A. (2010). A Comparison of the Performance and Compatibility of Protocols Used by Seven Monitoring Groups to Measure Stream Habitat in the Pacific Northwest. North American Journal of Fisheries Management, 30(2), 565–587. https://doi.org/10.1577/M09-061.1

Tamminga A, Hugenholtz C, Eaton B, Lapointe M. 2015. Hyperspatial remote sensing of channel reach morphology and hydraulic fish habitat using an unmanned aerial vehicle (UAV): a first assessment in the context of river research and management. River Res Appl, 31:379–391. https://doi.org/10.1002/rra.2743.

Tyler, S., Jensen, O. P., Hogan, Z., Chandra, S., Galland, L. M., Simmons, J., & 2017 Taimen Research Team. (2018). Perspectives on the Application of Unmanned Aircraft for Freshwater Fisheries Census. Fisheries, 43(11), 510-516.

U.S. Geological Survey, 2017.Unmanned Aircraft Systems Data Post-Processing: Structure-from-Motion Photogrammetry. Section 1 - Digital Single-Lens Reflex (DSLR) Imagery. USGS National UAS Project Office.

U.S. Geological Survey, 2017.Unmanned Aircraft Systems Data Post-Processing: Structure-from-Motion Photogrammetry. Section 2 – MicaSense 5-band Multispectral Imagery. USGS National UAS Project Office.

White, S.M., C. Justice, L. Burns, D. Kelsey, and D. Graves, M.J. Kaylor. 2017. Assessing the status and Trends of Spring Chinook Habitat in the Upper Grande Ronde River and Catherine Creek. Annual Report to Bonneville Power Administration. Portland, OR: Columbia River Inter-Tribal Fish Commission.

White, S.M, C. Justice, D. McCullough. 2012. Protocol for snorkel surveys of fish densities. A component of BPA Project 2009-004-00: Monitoring Recovery Trends in Key Spring Chinook Habitat Variables and Validation of Population Viability Indicators. 15 p. https://www.monitoringmethods.org/Protocol/Details/499.

White S. M., McCullough D. A., Justice C., Kelsey D. 2011. Conceptual Framework, Methods, and Field Test of a Stream Classification in the Grande Ronde River Basin. A Component of Monitoring Recovery Trends in Key Spring Chinook Habitat Variables and Validation of Population Viability Indicators. Portland, OR: Columbia River Inter-Tribal Fish Commission

Wells, A.F., E. Crowe, and R. Blaha. 2015. Riparian vegetation mapping in the Grande Ronde watershed, Oregon: monitoring and validation of spring Chinook habitat recovery and population viability. ABR, Inc.-Environmental Research & Services, Anchorage, AK. 183 pp.

Wolman, M. G. 1954. A method of sampling coarse river-bed material. Transaction of the American Geophysical Union 35:951–956.

Development of Stream Temperature Database

During 2018, we compiled all hourly water temperature measurements collected by various natural resource organizations in the Grande Ronde River basin upstream of and including the Wallowa River from 1993 to 2017 and imported this data into an SQL database. The objective of this work was to provide input data necessary for development of a spatial statistical network (SSN) model of water temperature with the capacity to predict how water temperatures would change in response to stream and riparian restoration. These data will also be useful for more general habitat assessments, restoration planning and restoration effectiveness monitoring. We are currently working to finalize this database and make the data accessible through the Central Database Management System (CDMS) developed by the Confederated Tribes of the Umatilla Indian Reservation (CTUIR).

Water temperature data were provided by ten organizations or data sources including the Columbia Habitat Monitoring Program (CHaMP), Columbia River Inter-Tribal Fish Commission (CRITFC), CTUIR, Oregon Department of Environmental Quality (DEQ), Grande Ronde Model Watershed (GRMW), the Nez Perce Tribe, Oregon Department of Fish and Wildlife (ODFW), Oregon Water Resources Department (OWRD), U.S. Forest Service (USFS), and U.S. Geological Survey (USGS). A total of 605 unique water temperature sites were originally compiled from all data sources. However, many of these sites included incomplete, duplicate or erroneous data and were therefore removed from the final site list. The final dataset (excluding incomplete, duplicate, or erroneous data) included 457 unique sites and 2237 unique site/year combinations (Figure 15).

We applied an extensive Quality Assurance/Quality Control (QA/QC) process to flag potential errors prior to calculating water temperature metrics. Most data supplied by outside agencies did not include any information regarding the QA status of each temperature measurement except for data from DEQ and USGS. Although some other organizations such as CHaMP and CTUIR did provide records indicating which temperature measurements had passed a QA check, a cursory examination of these records indicated that some of these data were likely erroneous. In the interest of producing the most accurate and conservative set of water temperature metrics possible, we applied a standard set of QA/QC criteria to all data consistent with procedures used by Isaak et al. (2017). Specifically, hourly temperature measurements greater than 30 °C or less than -1 °C and any sequential hourly measurements with a temperature difference greater than 3 °C were flagged as potential errors. Measurements flagged as potential errors were excluded from metric calculations but were retained in the database to allow for future changes to QA status. Finally, we only computed temperature metrics for a given site and time period (i.e., day, week, month, season) if the number of valid temperature records was at least 90 % of the total number of records possible (Table 5). For example, since the total number of days in August is 31, the number of daily average water temperature measurements required to compute average August water temperature is 0.90 * 31, or 28.

We computed a total of 22 water temperature metrics for each site/year combination including four daily metrics, one weekly metric, one monthly metric, and 16 seasonal metrics (i.e., spring,

summer, and spring/summer; Table 6). Metrics were selected based partly on the recommendations of Heck et al. (2018) and were intended to capture the magnitude, variability, and frequency of the thermal regime relevant to cold-water fishes. For example, temperature thresholds of 16, 18, and 20 °C are commonly associated with thermal tolerance limits for various life stages of cold-water fish species (USEPA 2003).

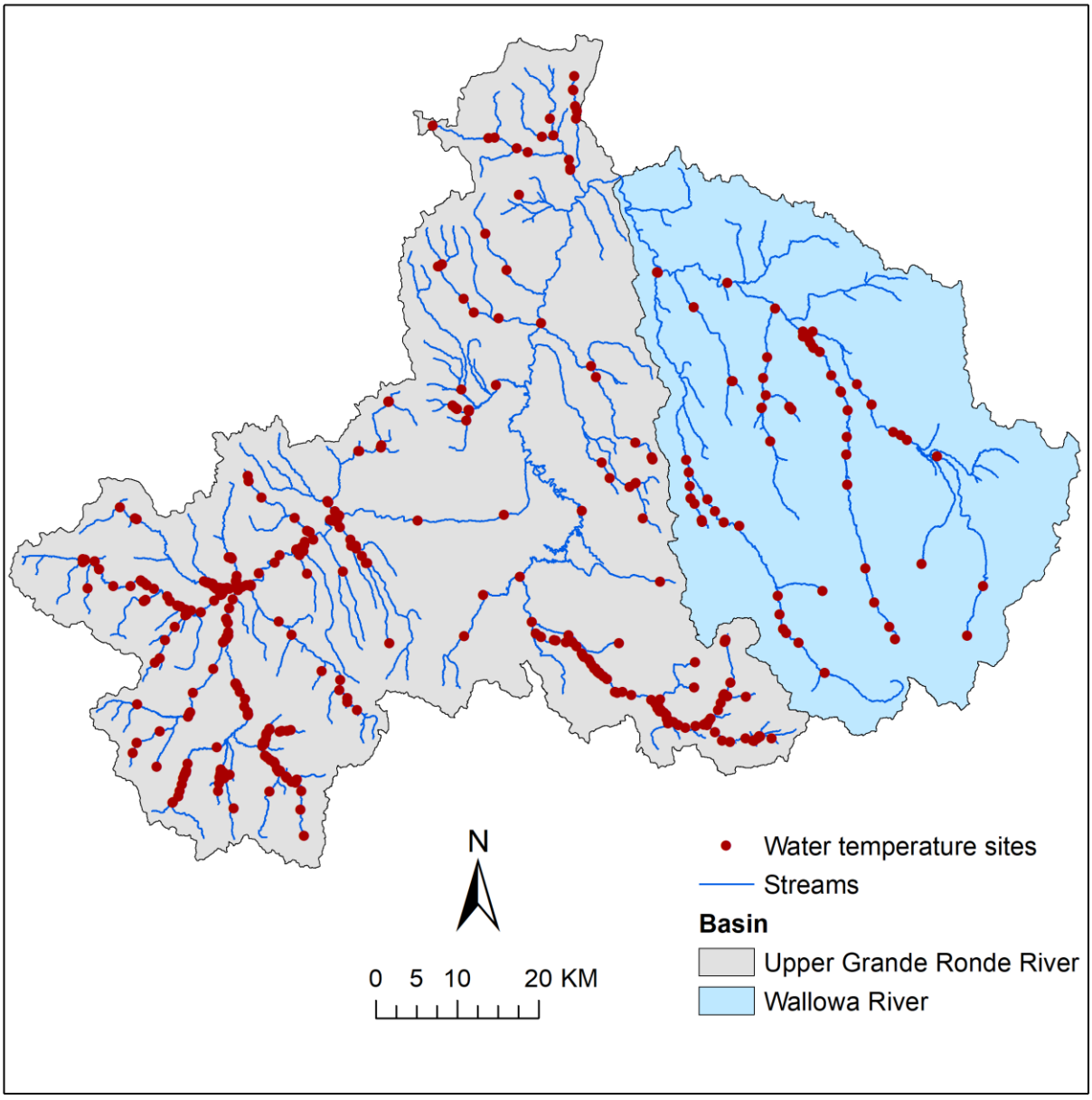

Figure 15. Water temperature observation sites in the upper Grande Ronde River and Wallowa River from 1993 to 2017.

Table 5. Minimum number of records required for metric calculation for each time period of interest. Minimum records were based on 90 % of the total number of possible records rounded to the nearest whole number.

Time period	Total records	Minimum records	Units
Daily	24	22	hours
Weekly	7	6	days
Monthly (August)	31	28	days
Spring (April 1 - June 30)	91	82	days
Summer (July 1 - September 15)	77	69	days
Spring/Summer (April 1 - September 15)	168	151	days

Table 6. Water temperature metric definitions.

Time period	Metric	Definition
Daily	*DayMinT*	Minimum hourly water temperature (°C) in a given day
Daily	*DayAvgT*	Average hourly water temperature (°C) in a given day
Daily	*DayMaxT*	Maximum hourly water temperature (°C) in a given day
Daily	*DayTVar*	Variance of all hourly water temperatures in a given day
Weekly	*WMT*	Weekly maximum water temperature (°C) for day *n* is the 7-day moving average of daily maximum water temperatures (*DayMaxT)* from day *n*-3 through day *n*+3
Spring	*AvgSprT*	Average of daily average water temperatures (°C) during Spring (April 1- June 30)
Spring	*SprDegD*	Sum of daily average water temperatures above 0 °C during Spring
Summer	*AvgSumT*	Average of daily average water temperatures (°C) during Summer (July 1 - September 15)
Summer	*SumDegD*	Sum of daily average water temperatures above 0 °C during Summer
Spring/Summer	*AvgSpSuT*	Average of daily average water temperatures (°C) during Spring and Summer (April 1 - September 15)
Spring/Summer	*SpSuDegD*	Sum of daily average water temperatures above 0 °C during Spring and Summer
Monthly (August)	*AvgAugT*	Average of daily average water temperatures (°C) during August
Summer	*MWMT*	Maximum weekly maximum water temperature (maximum *WMT*) during Summer
Summer	*DWMTA16*	Number of days with weekly maximum water temperatures (*WMT)* above 16 °C during Summer
Summer	*DWMTA18*	Number of days with weekly maximum water temperatures (*WMT)* above 18 °C during Summer
Summer	*DWMTA20*	Number of days with weekly maximum water temperatures (*WMT)* above 20 °C during Summer

Time period	Metric	Definition
Spring	*VDATSp*	Variance of daily average water temperatures (*DayAvgT*) during Spring; a measure of seasonal variability in water temperature
Spring	*ADTVSp*	Average of daily water temperature variance (*DayTVar)* during Spring; a measure of daily variability in water temperature
Summer	*VDATSu*	Variance of daily average water temperatures (*DayAvgT)* during Summer
Summer	*ADTVSu*	Average of daily water temperature variance (*DayTVar*) during Summer
Spring/Summer	*VDATSpSu*	Variance of daily average water temperatures (*DayAvgT*) during Spring and Summer
Spring/Summer	*ADTVSpSu*	Average of daily water temperature variance (*DayTVar*) during Spring and Summer

Most water temperature metrics were highly correlated, particularly those related to the magnitude of the thermal regime (e.g., average summer temperature, maximum weekly maximum water temperature, average August temperature; Table 7). This suggests that the choice of temperature metric to use in development of water temperature models or fish habitat relationships will not substantially influence model fit and therefore, it makes sense to focus on one or two metrics that are most readily available with demonstrated relevance to aquatic organisms such as fish and invertebrates. Average August water temperature may be the best option for analysis purposes because of the short time window required for computation and because August is a month of low flows and easier access to temperature monitoring sites. On the other hand, temperature metrics related to variability in the temperature regime (e.g., variance of daily average water temperatures and average of daily water temperature variance) tended to be less correlated to the other temperature metrics and may therefore provide unique information relevant to biotic response to habitat conditions (Table 7).

During the next contract year, we intend to perform a detailed analysis to compare the relative explanatory power of these temperature metrics in relation to benthic macroinvertebrate abundance/richness and juvenile salmonid density/growth. In addition, we plan to develop a spatial statistical network (SSN) model from these data to evaluate how restoration actions and climate change could impact water temperatures at various spatial scales and for specific areas of interest (e.g., biologically significant reaches). Although the NorWeST model (Isaak et al. 2017), a currently available SSN water temperature model for the Northwest region, provides a very useful predictive tool for climate impacts on water temperature, it doesn't currently provide the ability to evaluate stream or riparian restoration actions on water temperature.

Table 7. Pearson correlation matrix for seasonal water temperature metrics. Color shading denotes higher correlations in red and weaker correlation in blue.

Metric	Time period	n	AvgSprT	SprDegD	AvgSumT	SumDegD	AvgSpSuT	SpSuDegD	AvgAugT	MWMT	DWMTA16	DWMTA18	DWMTA20	VDATSp	ADTVSp	VDATSu	ADTVSu	VDATSpSu	ADTVSpSu
AvgSprT	Spring	736	**1.00**	1.00	0.81	0.80	0.95	0.95	0.74	0.83	0.68	0.71	0.72	0.72	0.68	0.46	0.50	0.39	0.67
SprDegD	Spring	736		**1.00**	0.81	0.80	0.95	0.95	0.74	0.83	0.68	0.71	0.72	0.74	0.68	0.46	0.50	0.39	0.67
AvgSumT	Summer	1676			**1.00**	0.99	0.94	0.94	0.98	0.94	0.90	0.92	0.89	0.68	0.57	0.52	0.66	0.80	0.65
SumDegD	Summer	1676				**1.00**	0.94	0.94	0.98	0.94	0.90	0.92	0.89	0.67	0.57	0.52	0.65	0.79	0.64
AvgSpSuT	Spring/Summer	654					**1.00**	0.99	0.89	0.91	0.80	0.84	0.84	0.77	0.69	0.46	0.56	0.58	0.68
SpSuDegD	Spring/Summer	654						**1.00**	0.90	0.91	0.81	0.85	0.85	0.77	0.68	0.46	0.56	0.60	0.67
AvgAugT	Monthly (August)	2104							**1.00**	0.91	0.89	0.90	0.87	0.59	0.51	0.53	0.63	0.80	0.60
MWMT	Summer	1606								**1.00**	0.90	0.92	0.90	0.76	0.71	0.65	0.80	0.73	0.83
DWMTA16	Summer	1606									**1.00**	0.92	0.80	0.54	0.53	0.48	0.71	0.69	0.68
DWMTA18	Summer	1606										**1.00**	0.94	0.60	0.58	0.51	0.76	0.75	0.74
DWMTA20	Summer	1606											**1.00**	0.67	0.61	0.53	0.79	0.77	0.77
VDATSp	Spring	736												**1.00**	0.66	0.44	0.59	0.56	0.70
ADTVSp	Spring	728													**1.00**	0.48	0.61	0.31	0.86
VDATSu	Summer	1676														**1.00**	0.49	0.39	0.50
ADTVSu	Summer	1669															**1.00**	0.56	0.93
VDATSpSu	Spring/Summer	654																**1.00**	0.49
ADTVSpSu	Spring/Summer	648																	**1.00**

References

Heck, M. P., L. D. Schultz, D. Hockman-Wert, E. C. Dinger, and J. B. Dunham. 2018. Monitoring stream temperatures—A guide for non-specialists. Page 76 U.S. Geological Survey Techniques and Methods, book 3, chapter A25.

Isaak, D. J., S. J. Wenger, E. E. Peterson, J. M. Ver Hoef, D. E. Nagel, C. H. Luce, S. W. Hostetler, J. B. Dunham, B. B. Roper, S. P. Wollrab, G. L. Chandler, D. L. Horan, and S. Parkes-Payne. 2017. The NorWeST Summer Stream Temperature Model and Scenarios for the Western U.S.: A Crowd-Sourced Database and New Geospatial Tools Foster a User Community and Predict Broad Climate Warming of Rivers and Streams: STREAM CLIMATES IN THE WESTERN U.S. Water Resources Research 53(11):9181–9205.

U.S. Environmental Protection Agency. 2003. EPA region 10 guidance for Pacific Northwest state and tribal temperature water quality standards. Page 49. U.S. Environmental Protection Agency, EPA 910-B-03-002, Region 10 Office of Water, Seattle, Washington.

Updates to Food Web and Carcass Addition Studies

Introduction

Recovery of salmonid populations within the Columbia Basin may require an integrated approach involving management actions that consider food webs in addition to physical habitat availability (Naiman et al. 2012). The abundance and productivity of fish populations are constrained by the availability of habitat but also the availability of prey within these habitats that sustain population densities and growth rates. Determining factors that may be limiting prey production and energy flow to the food web is therefore important to understanding potential constraints on fish production. Between the summers of 2016 and 2017, we conducted three related studies to improve understanding of food webs in two tributaries of the Grande Ronde River in NE Oregon where Spring Chinook (*Oncorhynchus tshawytscha*) and steelhead (*O. mykiss*) are imperiled. Increased understanding of aquatic food webs in this region and how food web productivity may limit juvenile salmonid productivity has the potential to guide management efforts focused on salmon and steelhead recovery.

Collectively, these research efforts have resulted in three draft manuscripts that will be submitted to journals in 2019. Below we outline these three manuscripts in greater detail and highlight some of the key findings.

Manuscript 1: Linking spatial patterns of stream nutrient concentrations, stream metabolism, and juvenile salmonids in a river network.

Authors: MJ Kaylor (Oregon State University); SM White (CRITFC); WC Saunders (USDA Forest Service); and DR Warren (Oregon State University)

Target Journal: *Ecosphere* – to be submitted in spring 2019

Primary production is a key energy source at the base of the food web that can limit productivity of higher trophic levels including juvenile salmonids. Variability in primary production throughout a stream network may therefore elucidate spatial patterns of energy flow to the food web and thus the productivity of juvenile salmonids. For example, Saunders et al. (2018) found that juvenile salmonid density was positively correlated with gross primary production in a NE Oregon basin, suggesting energy produced at the base of the food web may be constraining juvenile salmonid production. Building upon these ideas, we implemented a network-scale study in 2016 where we quantified spatial patterns of stream metabolism (gross primary production (GPP) and ecosystem respiration (ER)), and juvenile salmonid densities at 50 sites distributed across the upper Grande Ronde River and Catherine Creek of NE Oregon. To gain understanding of the potential drivers of spatial variability in GPP across these sub-

basins, we additionally quantified abiotic variables expected to influence GPP. Sites were associated with the Columbia Habitat Monitoring Program (CHaMP 2016), and thus we were able to leverage data collection efforts conducted by CRITFC and the Oregon Department of Fish and Wildlife (ODFW).

We found that nutrient concentrations (nitrate and phosphate) were extremely low across both basins (typically below 25 μg L^{-1} Nitrate-N and Phosphorous-P), suggesting low rates of nutrient input and high stream biological demand for nutrients. A complementary nutrient limitation experiment confirmed these results and demonstrated that biofilms in UGR were limited by both inorganic nitrogen and phosphorous, while biofilms in CC were only limited by nitrogen. Across these stream networks, we were able to explain 70% of the variation in GPP using a mixed-effects modeling approach that incorporated light availability, temperature, and nutrients as explanatory variables but also included spatial autocorrelation among sites. GPP was generally very low in headwaters and increased with distance downstream. In contrast to Saunders et al. (2018), we found that juvenile salmonids were most abundant in headwaters where nutrient concentrations and rates of primary production were very low and therefore there was a negative relationship between GPP and juvenile salmonid density. In these sub-basins, temperature has been shown to limit the distribution of juvenile salmonids (Justice et al. 2017) and our data suggests that the greatest abundance of juveniles occur in cool, oligotrophic areas where low rates of primary production may be limiting energy flow to the food web and ultimately juvenile salmonid productivity.

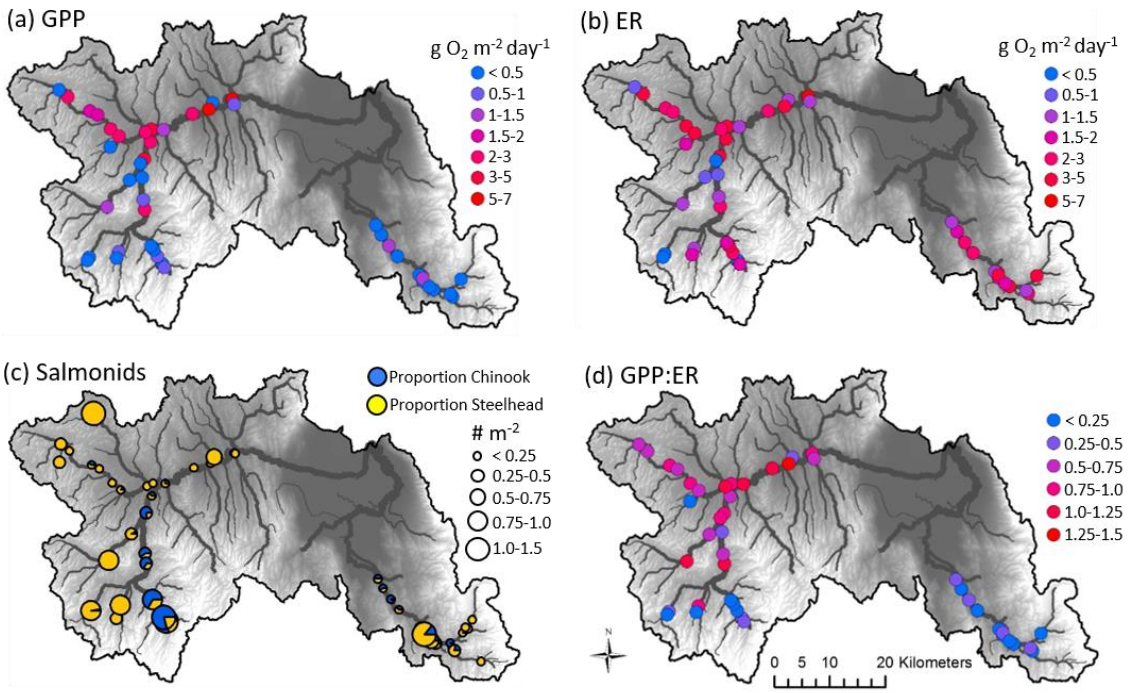

Figure 16: Spatial patterns of gross primary production (a; GPP), ecosystem respiration (b; ER), salmonid density (c), and the ratio of GPP to ER (d) in the upper Grande Ronde River (left basin) and Catherine Creek (right basin). Salmonids densities are greatest in areas where GPP rates are very low.

Manuscript 2: Juvenile salmonid responses to carcass additions along a thermal and species assemblage gradient

Authors: MJ Kaylor (Oregon State University); SM White (CRITFC); ER Sedell (Oregon Department of Fish and Wildlife); and DR Warren (Oregon State University)

Target Journal: *Fisheries* – to be submitted in spring 2019

The study conducted in 2016 demonstrated that juvenile salmonids were most abundant in areas of the stream network where nutrient concentrations and rates of GPP were very low. A potential explanation for oligotrophic conditions in these sections may be the drastic reduction of returning adult salmon to these basins. Adult salmon and steelhead transport large amounts of carbon and nutrients from the ocean to headwaters, and these subsidies can fuel stream food webs by promoting algal growth (Verspoor et al. 2011) and enhancing invertebrate (Minakawa et al. 2002) and fish production (Bilby et al. 1998; Bentley et al. 2012; Collins et al. 2016). With fewer spawning adults and reduced nutrient subsidies, the growth rates and production of juvenile salmonids may be much lower now than historically. To evaluate this hypothesis, we added steelhead carcasses to three locations in the upper Grande Ronde River (UGR) and quantified juvenile salmonid growth, body condition, and mean size. We additionally quantified juvenile salmonid diets to determine whether any potential growth responses were attributed to increased consumption of invertebrate prey or alternatively, consumption of eggs and carcass tissue. Each of the carcass addition sites were paired with a control site (Figure 17) and both control and treatment sites were sampled before and after the addition of carcasses.

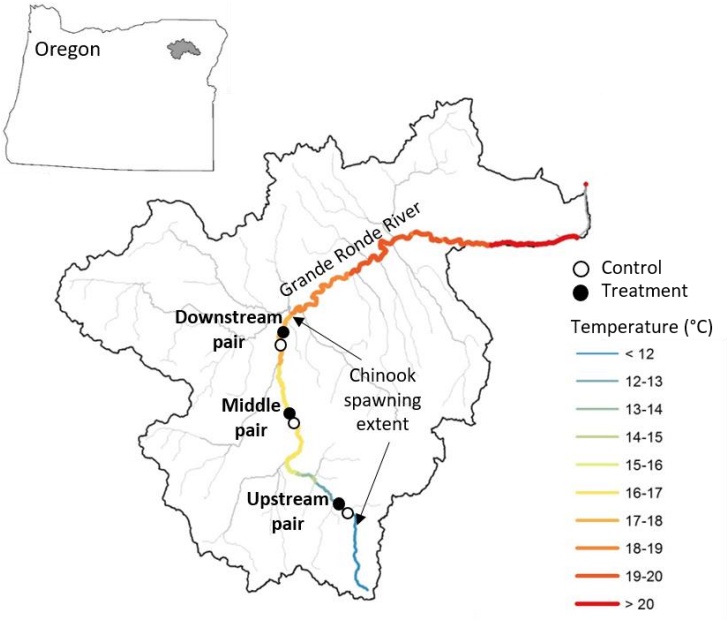

Figure 17: Map of the three study pairs each with an upstream control (open circles) and downstream treatment reach (filled circles) where carcasses were added.

After the addition of carcasses in August, juvenile chinook and steelhead growth rates substantially increased in treatment reaches relative to controls. Growth rates were often close to zero for steelhead in control reaches and, consequently, short-term effect sizes in treatment reaches were large. From one to three weeks after carcass addition, steelhead growth rates were 23, 22 and 6 times greater in the treatment reach compared to the control reach of the upstream, middle, and downstream pairs, respectively (Figure 18A). However, from three to eight weeks after carcass additions, steelhead growth rates were similar between control and treatment reaches. Steelhead body condition also increased in response to carcass addition, especially in the middle and downstream pair (Figure 18B). Chinook growth rates were only quantified in the upstream and middle pair due to inadequate numbers in the downstream pair. Chinook growth rates were only quantified after the addition of carcasses due to small size early in the summer that prohibited tagging. In the upstream pair, growth rates were slightly greater in the treatment reach one to three weeks after carcass additions. The effect of carcasses on Chinook growth rates was more pronounced in the middle pair where growth rates were five times greater in the treatment reach compared to the control between one and three weeks after carcass additions (Figure 19A). In this pair, Chinook body condition was significantly greater and Chinook were 33% larger (by weight) in the treatment reach eight weeks after carcass addition (Figure 19). Diet analysis clearly demonstrated that steelhead and Chinook were consuming an abundance of eggs and carcass tissue and that this drastically increased energy intake (data not shown).

Growth responses demonstrate clear food limitation and that growth potential in these stream reaches in summer is far greater than observed in the absence of subsidies. Results also indicate that the effect of carcass additions on growth occurred primarily through the consumption of eggs and carcass material rather than through increases in primary production and invertebrate production. The addition of carcasses to Grande Ronde tributaries could be an effective way to increase juvenile salmonid production within the reaches carcasses are added. When adding carcasses to stream reaches, eggs should be retained within carcasses to yield the greatest effects on juvenile salmonid growth and body condition.

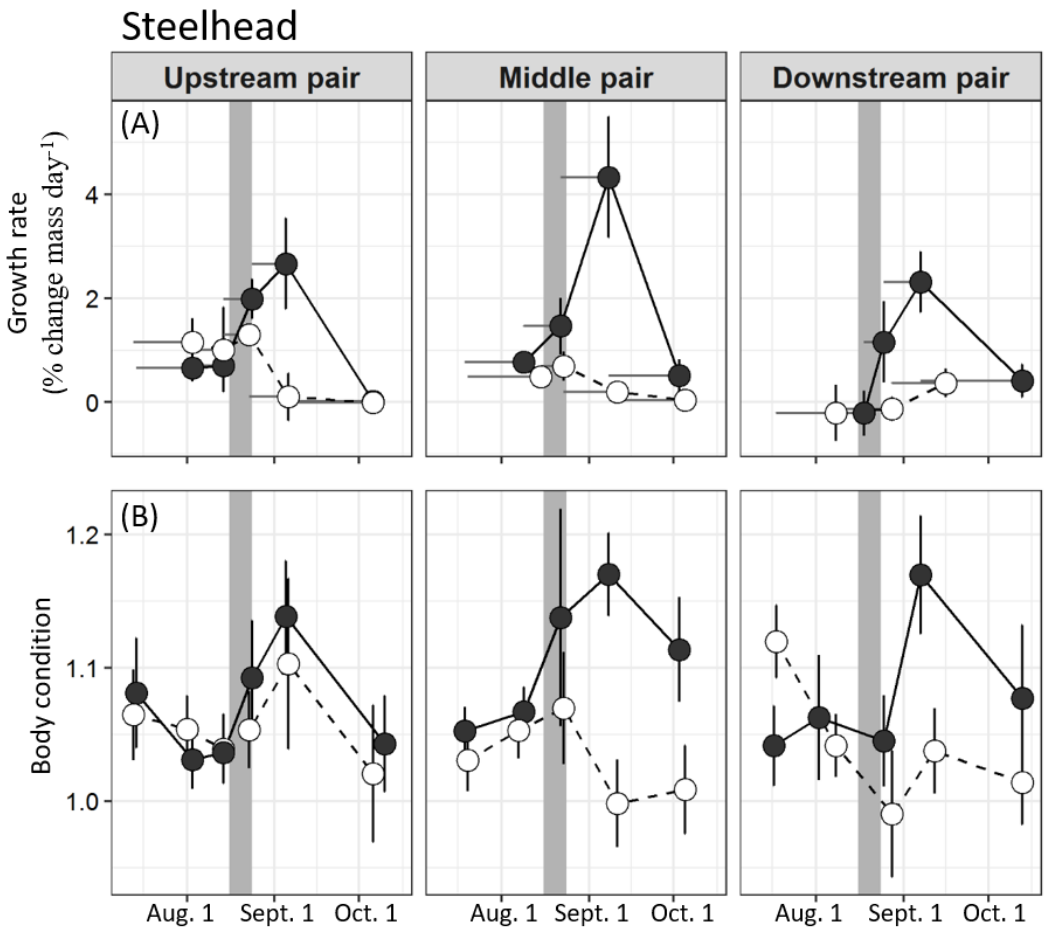

Figure 18: Juvenile O. mykiss mean instantaneous growth rate (A; % change mass/day) and mean body condition (B) over time. The shaded box indicates approximately when carcasses were added to streams. Vertical error bars indicate 95% confidence intervals. Horizontal error bars for growth indicate the duration growth rates were calculated for with the point representing the date of recapture for that interval.

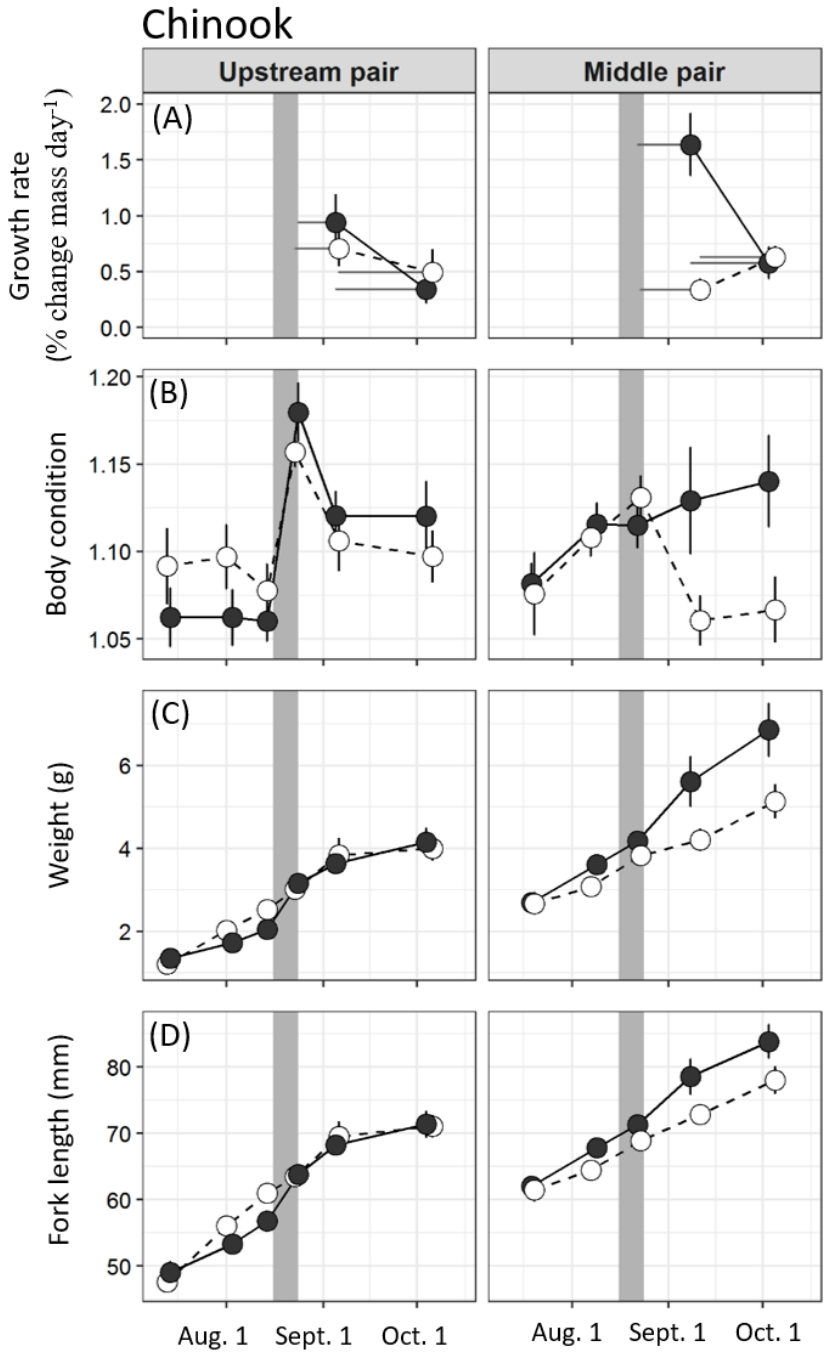

Figure 19: Juvenile Chinook mean instantaneous growth rate (A), condition (B), weight (C) and fork length (D) over time. See Figure 18 for details.

Manuscript 3: Carcass additions influence food webs through bottom-up and direct consumption pathways along a NE Oregon stream with varying fish species assemblages

Authors: MJ Kaylor (Oregon State University); SM White (CRITFC); ER Sedell (Oregon Department of Fish and Wildlife); AM Sanders (Oregon State University); and DR Warren (Oregon State University).

Target Journal: *Freshwater Biology* – to be submitted in spring 2019

The loss of subsidies delivered by adult salmon to streams may have broad impacts to stream food webs beyond juvenile salmonids (discussed above). In this study, we evaluate responses of the broader food web including organisms at the base of the food web, invertebrates, salmonids, and non-salmonid fish. The upstream pair was dominated by juvenile Chinook and steelhead while the downstream pair was dominated by native non-salmonids (See Figure 17 for map). The goals of this study were to 1) estimate the degree to which taxa assimilated nutrients from carcasses, and 2) to evaluate the pathways in which taxa assimilated nutrients.

Stable isotope analysis provides a tool to trace carcass nutrients through the food web. In particular, it provides a way to estimate the percent of a taxa's nitrogen that is derived from carcasses. Patterns of food web assimilation of carcass nitrogen can further be used to infer whether nutrients were assimilated through bottom-up pathways (i.e. dissolved nutrients are assimilated at the base of the food web and then transferred to higher trophic levels) or through the direct consumption of eggs and carcass tissue (Bilby et al. 1998; Kiffney et al. 2018). We sampled taxa during three events; before carcass addition, 3-4 weeks after addition, and 7-8 weeks after addition. The proportion of nitrogen obtained from carcasses was assessed using changes in the ratio of ^{15}N:^{14}N ($\delta^{15}N$) in treatment reaches relative to control reaches for each taxa and each sampling event using a Bayesian model framework. In addition, we evaluated diets of salmonids and non-salmonids to assess direct consumption of eggs and carcass tissue.

Periphyton and most invertebrate taxa assimilated carcass-derived nitrogen (~5-12% of taxa nitrogen was carcass-derived) in the middle and downstream pairs (Figure 20), indicating that nutrients were being assimilated at the base of the food web and transferred to higher trophic levels. This was not observed in the upstream pair where bears removed the majority of carcasses before they were able to decompose. Non-salmonids in the middle and downstream pair also assimilated carcass-derived nitrogen with 5-10% of their nitrogen being carcass-derived. Assimilation patterns of non-salmonids and a lack of eggs and carcass tissue in diets suggests non-salmonids obtained carcass-derived nitrogen through bottom-up pathways. Across all three pairs, salmonids

exhibited the greatest assimilation of carcass-derived nitrogen; Chinook and steelhead obtained up to 25% and 57% of their nitrogen from carcasses, respectively. In contrast to non-salmonids, diet analysis and stable isotope patterns indicated that assimilation occurred primarily through direct consumption of eggs and carcass tissue. Our results suggest salmon subsidies have the potential to broadly impact stream food webs in this region, but that species able to directly consume eggs and carcass material clearly benefit more from these subsidies.

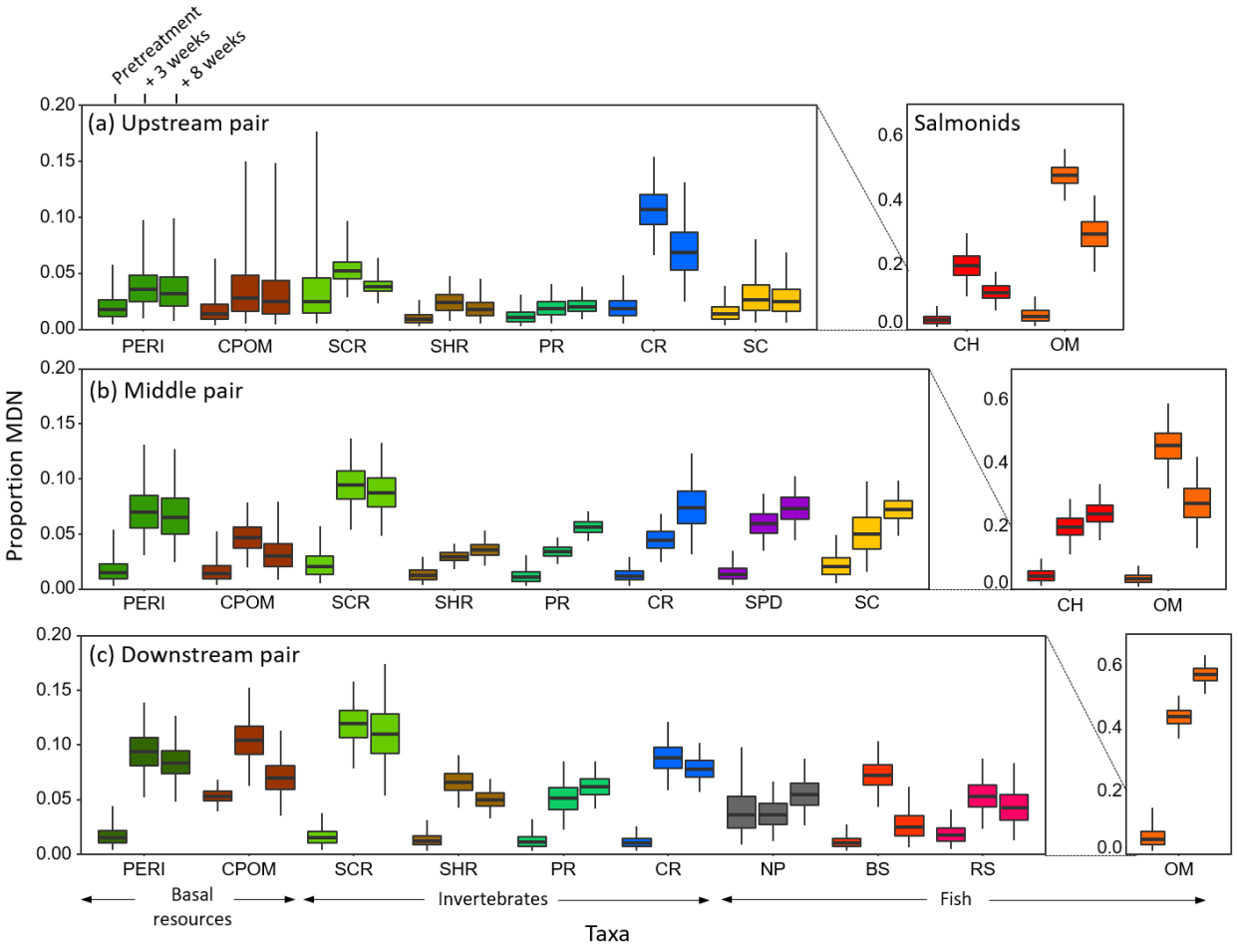

Figure 20: The estimated proportion of a taxa's nitrogen that was derived from carcasses (marine derived nutrients; MDN) during three sampling periods (pretreatment; + 3 weeks after carcass addition; + 8 weeks after carcass addition). PERI = periphyton (algae); CPOM = coarse particulate organic matter (alder leaves); SCR = invertebrate scrapers (Elmidae and Heptigeniidae); invertebrate shredders (Pteronarcyidae); PR = invertebrate predators (Perlidae); CR = crayfish; SC = sculpin (Cottus spp.); SD = speckled dace (Rhinichthys osculus); NP= northern pikeminnow (Ptychocheilus oregonensis); RS = redside shiner (Richardsonius balteatus); BS = bridgelip sucker (Catostomus columbianus); CH = Chinook; OM = steelhead.

References

Bentley, K. T., D. E. Schindler, J. B. Armstrong, R. Zhang, C. P. Ruff, and P. J. Lisi. 2012. Foraging and growth responses of stream-dwelling fishes to inter-annual variation in a pulsed resource subsidy. Ecosphere 3(12):113.

Bilby, R. E., B. R. Fransen, P. A. Bisson, and J. K. Walter. 1998. Response of juvenile coho salmon (Oncorhynchus kisutch) and steelhead (Oncorhynchus mykiss) to the addition of salmon carcasses to two streams in southwestern Washington, U.S.A. Canadian Journal of Fisheries and Aquatic Sciences 55:1909–1918.

CHaMP, (Columbia Habitat Monitoring Program). 2016. Scientific protocol for salmonid habitat surveys within the Columbia Habitat Monitoring Program.

Collins, S. F., C. V. Baxter, A. M. Marcarelli, and M. S. Wipfli. 2016. Effects of experimentally added salmon subsidies on resident fishes via direct and indirect pathways. Ecosphere 7(3):1–18.

Justice, C., S. M. White, D. A. McCullough, D. S. Graves, and M. R. Blanchard. 2017. Can stream and riparian restoration offset climate change impacts to salmon populations? Journal of Environmental Management 188:212–227.

Kiffney, P. M., S. M. Naman, J. M. Cram, M. Liermann, and D. G. Burrows. 2018. Multiple pathways of C and N incorporation by consumers across an experimental gradient of salmon carcasses. Ecosphere 9(4):e02197.

Minakawa, N., R. I. Gara, and J. M. Honea. 2002. Increased individual growth rate and community biomass of stream insects associated with salmon carcasses. Journal of the North American Benthological Society 21(4):651–659.

Naiman, R. J., J. R. Alldredge, D. A. Beauchamp, P. A. Bisson, J. Congleton, C. J. Henny, N. Huntly, R. Lamberson, C. Levings, E. N. Merrill, W. G. Pearcy, B. E. Rieman, G. T. Ruggerone, D. Scarnecchia, P. E. Smouse, and C. C. Wood. 2012. Developing a broader scientific foundation for river restoration: Columbia River food webs. Proceedings of the National Academy of Sciences of the United States of America 109(52):21201–7.

Saunders, W. C., N. Bouwes, P. McHugh, and C. E. Jordan. 2018. A network model for primary production highlights linkages between salmonid populations and autochthonous resources. Ecosphere 9(3):e02131.

Verspoor, J. J., D. C. Braun, M. M. Stubbs, and J. D. Reynolds. 2011. Persistent ecological effects of a salmon-derived nutrient pulse on stream invertebrate communities. Ecosphere 2(February):1–17.

Riverscape Analyses

Effect of riparian vegetation and channel width on stream shade in the upper Grande Ronde River basin

Introduction

Understanding the influence of riparian vegetation on stream shade and water temperature is an important objective of the Columbia River Inter-Tribal Fish Commission's (CRITFC) habitat monitoring program in the Grande Ronde River basin in Northeast Oregon (White et al. 2018). Predictive models for shade and temperature can be used to elucidate the impacts of land management and climate change on aquatic habitats and better understand our capacity to improve salmon population viability through restoration actions (Justice et al. 2017). Such models are incorporated into NetMap, an ArcGIS-compatible toolkit that provides comprehensive environmental analysis capabilities relevant to forestry, fisheries, restoration, riparian management and climate change assessments at scales ranging from individual stream reaches to entire watersheds (NetMap 2019). CRITFC recently invested in development of an updated NetMap dataset for the upper Grande Ronde River basin and Wallowa River basin incorporating high resolution LiDAR data and local stream channel measurements as inputs. With the objective of validating and potentially improving the accuracy of the NetMap shade and thermal loading calculations, we analyzed the relationship between field-based measurements of shade in streams from the upper Grande Ronde River basin and remotely-sensed estimates of tree stand height (m) and basal area (m^2/Ha) from the LEMMA dataset (Landscape Ecology, Modeling, Mapping & Analysis; https://lemma.forestry.oregonstate.edu/publications).

Methods

Shade, defined here as the fraction of total solar radiation that was blocked or absorbed by vegetation or other obstructions during summer (July – September), was measured at 143 randomly selected sites in the upper Grande Ronde River and its tributaries using a Solmetric SunEye device as part of the Columbia Habitat Monitoring Program (CHaMP). Eleven shade measurements were collected at each site spaced approximately two bankfull widths apart along the stream. Within-site shade measurements were then averaged together to compute a single average shade value for each site. CHaMP sites ranged in length from 120-600 meters and were roughly 20 times the bankfull width. Shade measurements collected between 2011 and 2016 were filtered to select a single visit from each site that was closest to 2012, the year that LEMMA imagery was collected.

Estimates of basal area (i.e., the summation of tree trunk cross sectional area) and stand height from LEMMA were provided at a 30m pixel resolution. These data were overlaid with the CHaMP survey extent polygons (i.e., the area surveyed by CHaMP crews using total stations) and the average basal area and stand height within each survey extent were computed using zonal statistics in ArcGIS 10.6. Survey extents were intended to capture stream channels and adjacent riparian areas and ranged in area from 0.001 to 0.44 km² (mean = 0.01 km²). Bankfull channel width as measured from CHaMP topographic surveys was also included in our analysis to account for the potential reduced ability of riparian vegetation to provide shade as channel widths increase.

We first examined pairwise plots of LEMMA and CHaMP data (Figure 21) and computed Pearson correlation coefficients (Table 8) to assess the degree of correlation among variables. We then built a set of eight candidate general linear models to determine which covariates explained the greatest amount of variation in stream shade (Table 9). We compared models using Akaike's Information Criterion corrected for small sample size (AICc) to arrive at the most parsimonious model (i.e., the model that adequately explains the variation in the response variable with the fewest parameters possible; Burnham and Anderson 2002). The models represented a limited set of biologically plausible *a priori* hypotheses regarding the factors influencing shade (Table 9). To avoid violating the assumption of independence, we selected explanatory variables for each model that were not correlated (Pearson's correlation coefficient < 0.10) (except for Model 8). Although Model 8 included highly correlated explanatory variables (stand height and basal area), it was added to the candidate model set to compare with a published model from Groom et al. (2011), which is used by the NetMap tools to estimate shade/thermal loading (NetMap 2019). We tested model assumptions using standard diagnostic plots and the Shapiro-Wilk test for normality.

Candidate linear models for Shade (y_i) with $i = 1, \ldots, n$ observations and k explanatory variables (x_i) can be expressed as:

$$y_i = \beta_0 + \beta_1 x_{i,1} + \beta_2 x_{i,2} + \cdots + \beta_k x_{i,k} + \varepsilon_i,$$

where β_k are the model coefficients and ε_i are the residuals, which are assumed to be normally distributed with a mean of 0 and variance of σ^2 ($\varepsilon_i \sim N(0, \sigma^2)$.

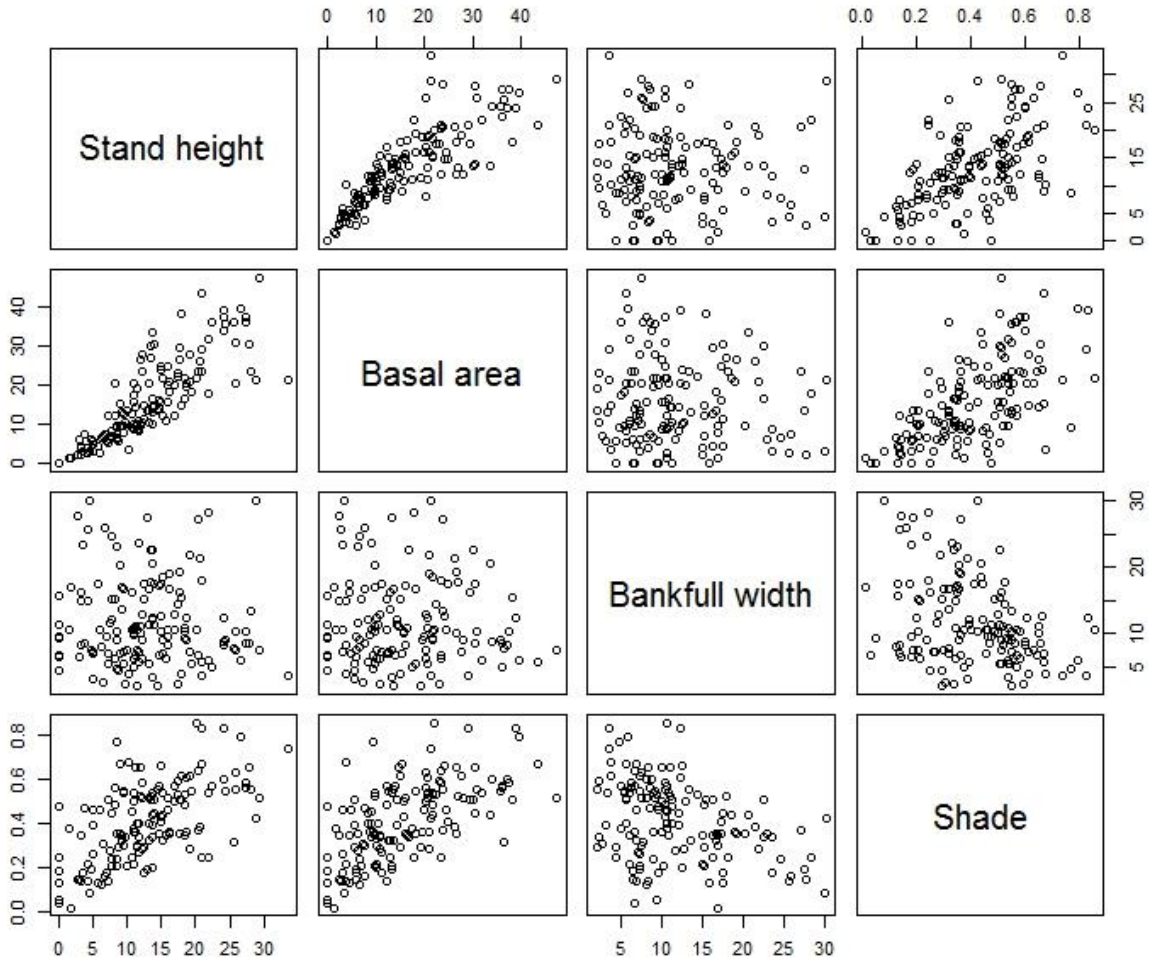

Figure 21. Exploratory pairwise scatterplots of raw data used to identify potential correlations among variables.

Table 8. Pearson correlation matrix for variables used in shade analysis.

	Stand height	Basal area	Bankfull width	Shade
Stand height	1.000	0.845	-0.045	0.591
Basal area	0.845	1.000	-0.054	0.606
Bankfull width	-0.045	-0.054	1.000	-0.368
Shade	0.591	0.606	-0.368	1.000

Table 9. Candidate set of models used to analyze factors influencing stream shade.

Model #	Explanatory variables
1	Basal area + Bankfull width + Basal area * Bankfull width
2	Stand height + Bankfull width + Stand height * Bankfull width
3	Basal area + Bankfull width
4	Stand height + bankfull width
5	Basal area
6	Stand height
7	Bankfull width
8	Basal area + Stand height + Basal area * Stand height

Results

The best fitting model for shade (*SHD*) among the set of candidate models examined was Model 3, which included basal area and bankfull width as additive explanatory variables (Table 10). The combination of basal area and bankfull width explained approximately 47% of the variation in shade, with both explanatory variables being highly significant at the $\alpha = 0.05$ level ($p < 0.0001$). Shade was positively related to basal area and negatively related to bankfull width (Table 11; Figure 22). Diagnostic plots and the Shapiro-Wilk test for normality indicated that model assumptions were reasonably satisfied. This model can be expressed as:

$$\widehat{SHD} = 0.363297 + 0.009741 * BA - 0.00914 * BW.$$

Model 3 had moderate relative support as the best fitting model in the candidate set with an AICc difference of 2.2 between it and the next best fitting model (AICc weight = 0.64; Table 10). The next best model (Model 1), which included basal area, bankfull width, and an interaction between bankfull width and basal area as explanatory variables, also had some empirical support for consideration as the best fitting model (AICc weight = 0.22). However, the interaction effect was not statistically significant ($p = 0.98$), and consequently, we did not consider Model 1 a good fitting model. None of the other models showed strong empirical support for inclusion as the best fitting model (ΔAICc > 3.8; Burnham and Anderson 2002).

Model 8, which included the same model structure as the top model for shade described in Groom et al. (2011), had virtually no empirical support as the best fitting model (ΔAICc = 22.8; AICc weight = 0; Table 10). The combination of basal area, stand height, and the interaction between basal area and stand height explained approximately 39% of the variation in shade. The interaction effect was not statistically significant ($p = 0.14$) but basal area and stand height were both statistically significant ($p < 0.01$; Table 12). Both basal area and stand height were positively correlated to shade.

Table 10. Model selection summary table comparing model fits based on Akaike's Information Criteria (AICc) and adjusted R^2.

Model #	Explanatory variables	K	LogLik	AICc	ΔAICc	AICc wt	Adj R^2
3	*BA* + *BW*	4	91.182	-174.1	0.0	0.638	0.472
1	*BA* + *BW* + *BA*BW*	5	91.182	-171.9	2.2	0.218	0.468
4	*SH* + *BW*	4	89.267	-170.2	3.8	0.094	0.458
2	*SH* + *BW* + *SH*BW*	5	89.721	-169.0	5.1	0.051	0.457
8	*BA* + *SH* + *BA*SH*	5	80.838	-151.2	22.8	0	0.386
5	*BA*	3	77.206	-148.2	25.8	0	0.363
6	*SH*	3	75.171	-144.2	29.9	0	0.344
7	*BW*	3	54.856	-103.5	70.5	0	0.129

Notes: *BA* = basal area (m^2/Ha), *SH* = stand height (m), *BW* = bankfull width (m), K = number of parameters, LogLik = log likelihood, AICc wt = AICc weight

Table 11. Model coefficients from the best-fitting model (Model 3).

Model parameter	Coefficient estimate	Std. Error	t value	p-value
(Intercept)	0.363297	0.028111	12.924	< 2e-16
Basal area (*BA*)	0.009741	0.001012	9.627	< 2e-16
Bankfull width (*BW*)	-0.00914	0.001663	-5.498	1.77E-07

Notes: Residual standard error = 0.1293 on 140 degrees of freedom. Adjusted R^2 = 0.4722. F-statistic = 64.52. Overall model p-value < 2.2e-16.

Table 12. Model coefficients from Model 8 for comparison with top model from Groom et al. (2011).

Model parameter	Coefficient estimate	Std. Error	t value	p-value
(Intercept)	0.1897505	0.033575	5.652	8.68E-08
Basal area	0.0096665	0.003094	3.124	0.00217
Stand height	0.0095876	0.003563	2.691	0.008
Basal area*Stand height	-0.0002106	0.000141	-1.493	0.13781

Notes: Residual standard error = 0.1394 on 139 degrees of freedom. Adjusted R^2 = 0.3856. F-statistic = 30.71. Overall model p-value < 2.702e-15.

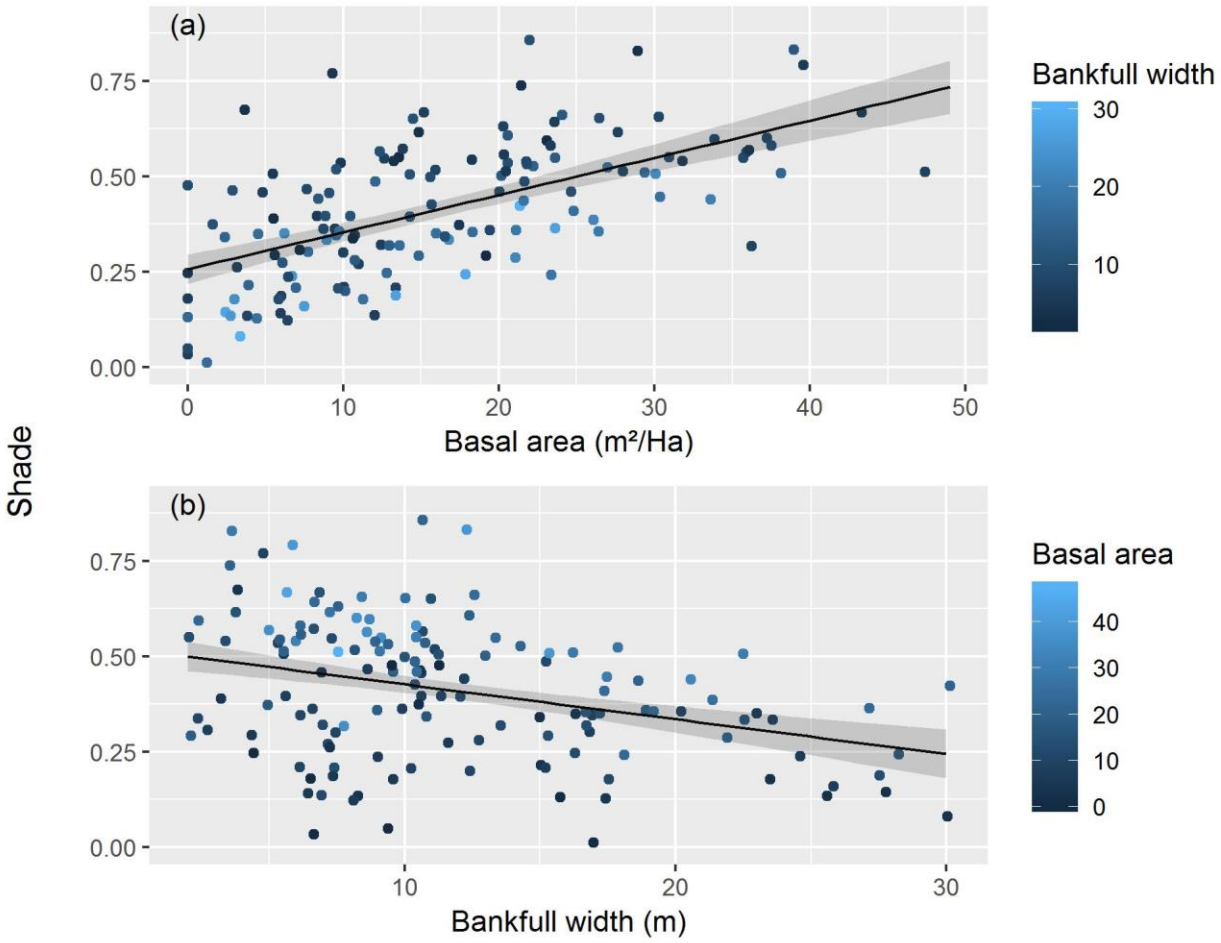

Figure 22. Fitted relationship between a) basal area (m²/Ha) and shade, and b) bankfull width (m) and shade from the best fitting model (i.e., model 3). Model fits (bold lines) and 95% confidence intervals (shaded ribbons) represent the predicted shade value across a range of each independent variable with the other independent variable held fixed at its average value.

Discussion

The observed relationship between shade in streams and remotely-sensed estimates of tree basal area and bankfull channel width may help to improve the accuracy of landscape scale models such as NetMap (NetMap 2019) or NorWeST (Isaak et al. 2017) which are commonly used to evaluate alternative land management or climate scenarios and their impact on aquatic habitats. Specifically, the model currently used in NetMap to estimate shade and thermal loading to streams is based on the work of Groom et al. (2011), which includes a positive effect of basal area and somewhat unintuitive negative effect of tree height (Shade = 1.795 + 0.031 * Basal area - 0.0625 * Tree height – 0.000468 * Basal area * Tree height; $R^2 = 0.69$, n = 33). The authors surmised that the negative relationship

between tree height and shade may be due to the negative correlation between tree height and crown ratio (the percentage of a tree's total height that has foliage). However, they also acknowledge that their findings differ from a similar modeling study by DeWalle (2010) which found a positive effect of both tree height and density on shade.

Empirical shade data collected in the Grande Ronde River basin does not appear to support the negative effect of tree height as described by Groom et al. (2011). Furthermore, basal area and tree height are highly correlated, and therefore should not be included together as explanatory variables in a predictive model to avoid violating the assumption of independence. Inclusion of correlated explanatory variables can lead to spurious conclusions regarding the independent effect of each explanatory variable. While basal area and channel width do not perfectly capture all physical attributes that may influence shade and thermal loading to streams (e.g., aspect, hillside topography, tree height), we maintain the model presented here represents a parsimonious and empirically-based representation of the key drivers of stream shading and will be useful for large scale modeling of land management scenarios and their impacts on stream shading and water temperature.

References

Burnham, K. P., and D. R. Anderson. 2002. Model selection and multimodel inference, a practical information-theoretic approach. Second edition. Springer-Verlag New York, Inc., New York, NY.

DeWalle, D. R. 2010. Modeling stream shade: riparian buffer height and density as important as buffer width. Journal of the American Water Resources Association 46(2):323–333.

Groom, J. D., L. Dent, L. J. Madsen, and J. Fleuret. 2011. Response of western Oregon (USA) stream temperatures to contemporary forest management. Forest Ecology and Management 262(8):1618–1629.

Isaak, D. J., S. J. Wenger, E. E. Peterson, J. M. Ver Hoef, D. E. Nagel, C. H. Luce, S. W. Hostetler, J. B. Dunham, B. B. Roper, S. P. Wollrab, G. L. Chandler, D. L. Horan, and S. Parkes-Payne. 2017. The NorWeST Summer Stream Temperature Model and Scenarios for the Western U.S.: A Crowd-Sourced Database and New Geospatial Tools Foster a User Community and Predict Broad Climate Warming of Rivers and Streams: STREAM CLIMATES IN THE WESTERN U.S. Water Resources Research 53(11):9181–9205.

NetMap. 2019. Version 3.1.9. Virtual watershed and analysis tools. TerrainWorks Inc. www.terrainworks.com.

White, S., C. Justice, L. Burns, D. Kelsey, D. Graves, and M. Kaylor. 2018. Assessing the status and trends of spring Chinook habitat in the upper Grande Ronde River and Catherine Creek. Page 142. Columbia River Inter-Tribal Fish Commission, BPA Project # 2009-004-00, Portland, Oregon.

Climate and Land Use Drivers of Salmonid Food Web Indicators

Introduction

Many regional fish habitat programs—including CRITFC and its member tribes—collect benthic macroinvertebrates as part of ongoing habitat monitoring, yet analyses are typically limited to evaluating standard water quality metrics such as indices of biotic integrity (IBIs) and other biodiversity indicators. However, BMI data can also be leveraged to provide information about the salmonid food base.

This report describes recent progress on the Columbia River Inter-Tribal Fish Commission (CRITFC) project, "Resilient Aquatic Foodwebs for Tribal Communities (RAFT)," jointly funded by the Bonneville Power Administration/Columbia Basin Accords and the Bureau of Indian Affairs' Tribal Resilience Program. The RAFT project aims to increase tribal capacity to mitigate climate change impacts to aquatic food webs that are important to river health, salmon, other native fish assemblages, and the tribal communities that depend on them. Climate change is expected to have acute and persistent effects on summertime streamflow and water temperature in tributaries that are the rearing grounds for salmon, a vital First Food for tribal communities (Quaempts et al. 2018). To date, climate vulnerability assessments typically account for anticipated shifts in fish habitat, abundance, and distribution based on thermal tolerance criteria, while overlooking ecosystem-level changes, e.g., impacts to food webs expected with climate change (Independent Scientific Advisory Board 2011). Meanwhile, many tribal, State, and Federal programs routinely collect aquatic macroinvertebrates as indicators of overall river health and water quality. These data have been under-utilized for describing the condition and resiliency of the food base for salmonids and other river life.

Since 2015, CRITFC has been translating routinely-collected aquatic macroinvertebrate data into metrics relevant to salmon food webs and aquatic ecosystems affected by a changing climate (Sullivan and White 2017). Under the RAFT project, the geographic scope of macroinvertebrate data collection will be increased throughout the Columbia River Basin through partnerships with the CRITFC member tribes (Yakama, Nez Perce, Umatilla and Warm Springs) and the Shoshone-Bannock Tribe. CRITFC will validate the new data using the established food web models and provide an analysis framework for climate vulnerability assessments for aquatic food webs. We anticipate that a vulnerability assessment of salmonid food webs will be useful for advancing tribal climate adaptation strategies (Halofsky, Peterson, and Marcinkowski 2015).

Here, we summarize recent progress on (1) developing and validating food web metrics from benthic macroinvertebrate data, (2) exploring relationships between food web metrics and land use, climate, and habitat variables, and (3) testing hypothesis about

climate and land use drivers of aquatic invertebrate distributions as they relate to available forage for salmonids.

Methods

Development of food web indices

In this report we summarize development of descriptive metrics of food webs (Cohen, Jonsson, and Carpenter 2003); and availability to food for salmonids based on life history characteristics, propensity to enter the water column, palatability to salmonids, and other characteristics (Rader 1997). Additional methods of benthic invertebrate sampling and analysis including targeted riffle sampling in the field, taxonomic identification and processing in the laboratory, and further details of metric development are found in Sullivan and White (2017). Invertebrate drift was additionally collected using standard methods described in CHaMP (2016). In summary, two adjacent drift nets were positioned in a riffle above the survey reach for approximately 2-4 hrs on the day of the CHaMP survey.

In order to calculate the suite of food web metrics desired, we utilized two published R packages with some modification: CHEDDAR (L. N. Hudson et al. 2013; L. Hudson, Reuman, and Emerson 2014) and FOODWEB (Perdomo, Thopmson, and Sunnucks, n.d.). Each community (sample) requires the total estimated number of individuals, their associated biomass and a matrix of food web linkages. Food web linkages are defined here as matrix of taxa (consumers) and the resources they consume (periphyton, other taxa, bacteria, etc.). Density and estimated biomass were derived from the data collected in the subsampling process.

The next of metrics were related to propensity to drift as originally described by Rader (1997). A total of 137 taxa were found in the project that were not contained in the original Rader (1997) manuscript designating life history and ecology traits related to drift propensity. Taxa missing drift attributes were evaluated using the same criteria as Rader (1997). A systematic approach was used to assign traits to each taxon. First, primary literature was consulted for attribute affinities. Secondly, if no literature was available, the most closely related taxon's values were used as a surrogate. Finally, if no literature or closely related taxa were available then empirical measurements were made, most commonly for 'drag index' and 'size' traits. Attributes were assigned and improved through a peer review process (Robert Wisseman, pers. comm.).

Rader's (1997) manuscript suggested the use of an "aquatic species composition" (ASC) score incorporating the expected or actual abundance of taxa for each site, weighted to account for each taxon's potential contribution to the salmonid prey base. We calculated

this and three additional scores, but for the purposes of this report we focus on an index accounting for the relative abundance of taxa abundance at sites:

$$ASC_{Rel} = \sum_{i=1}^{n} (St_i \cdot PRA_i)$$

where St_i is equal to the subtotal of the 11 drift traits of the i^{th} taxon, and PRA_i is the percent relative abundance of the i^{th} taxon in a given sample.

A hierarchical cluster analysis was performed on the trait scores assigned to these data to create guilds of drift availability. Three guild associations were classified using a Ward cluster analysis with a Euclidean distance measure (Ward 1963), and correspond to high, medium, and low drift availability. The dendrogram was cut off at 3 guilds to avoid overclassifying the drift propensity of any given taxa. The 93 low drift available taxa correspond to the taxa primarily occurring in depositional or hyporheic habitats that do not score several of the Rader (1997) metrics due to habitat associations. The low drift availability taxa are excluded from the ASC values as recommended by Rader (1997).

Climate, land use, and environmental data

For each site where benthic macroinvertebrates were collected, we matched climate, land use, habitat, and other environmental data to explore relationships and test hypotheses about drivers of invertebrate distributions. Spatially explicit predictions of current and future water temperature summaries are available through NorWeST Regional Database and Modeled Stream Temperatures site (Rocky Mountain Research Station, USFS, http://www.fs.fed.us/rm/boise/AWAE/projects/NorWeST.html). University of Washington's Variable Infiltration Capacity (VIC) Macroscale Hydrological Model Scenarios provide current and projected streamflow metrics (center of flow timing, mean annual and summer flows, and frequency of winter floods) under various climate scenarios (http://www.hydro.washington.edu/2860/). Land use metrics were derived from EPA's Stream-Catchment dataset (Hill et al. 2016) for road density and forest loss. We additionally developed a cattle grazing intensity map across the entire project area incorporating distance to water, terrain slope, land cover, and permitted animal unit months (AUMs), described in detail in (McCullough et al. 2016) (Figure 23). For each category of land use, we derived land use metrics for the entire watershed upstream of each site, in the watershed within a 100 m buffer, within the local catchment only, and within the local catchment and a 100 m buffer. Intrinsic variables such as elevation, watershed area, stream order, etc. were calculated for each site using specialized computer software (NetMap 2019) that incorporated 10 m DEMs and LiDAR data where available. Site-specific habitat conditions (large wood, pools, substrate, conductivity, etc.) in addition to invertebrate drift biomass were collected under the Columbia Habitat

Monitoring Program (CHaMP 2016), a program characterizing tributary spawning and rearing habitat of Columbia River salmonids. Juvenile Chinook salmon (*Oncorhynchus tshawytscha*) and steelhead-rainbow trout (*O. mykiss*) were enumerated using snorkel counts at each site as described in Justice et al. (2017) and expanded to abundance estimates using a correction factor developed from paired mark-recapture and snorkel survey data (Jonasson et al. 2015).

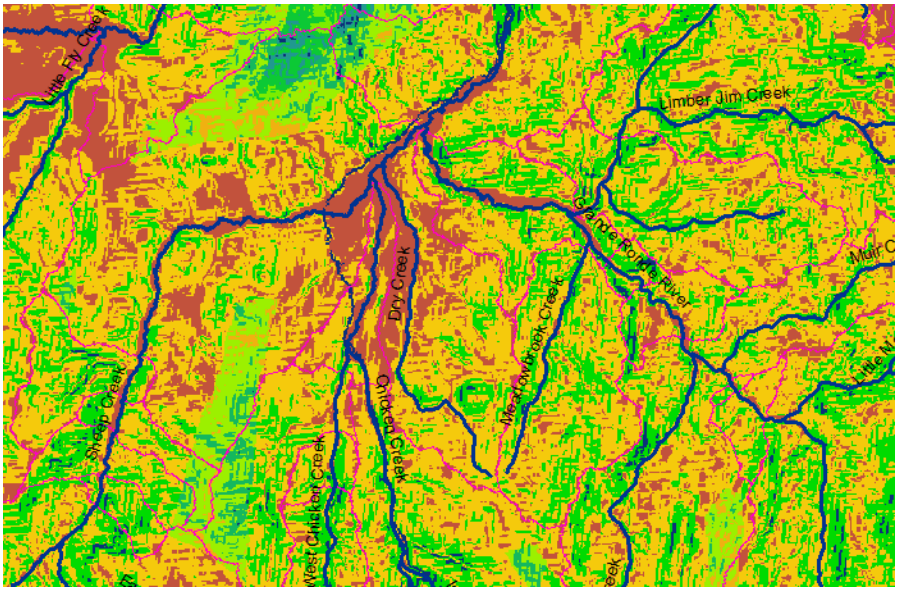

Figure 23. Grazing capacity raster for a selected portion of the upper Grande Ronde River. Grazing capacity increases as color scheme changes from green (low capacity) to red (high capacity) and is a function of distance to water, slope, and land cover. Information on allotted AUMs are combined with grazing capacity to arrive at our final metric of grazing intensity.

We used maximal information coefficients (MIC), a statistical tool for discovering linear and non-linear relationships in large datasets (Reshef et al. 2011) using the *minerva* package in R statistical software. Our intention was to explore links between standard and novel metrics derived from benthic macroinvertebrates against land use, climate, habitat, intrinsic, and fish variables.

Structural equation model

We tested hypotheses about climate and land use drivers on local habitat conditions and invertebrate distributions as relevant to salmonids (Figure 24) using structural equation modeling (SEM). The advantages of SEM for observational studies and differences from conventional univariate and multivariate approaches are reviewed in (J.B. Grace 2007). SEMs graphically relay complex hypotheses about how system components interrelate in a manner easily comprehended by stakeholders. Theoretical knowledge is typically used to develop models, which represent alternative hypotheses about processes leading to

observed patterns in the data. Overall, the approach is well suited to elucidating how different processes work in concert, how effects propagate through a system, and for evaluating the relative importance of different stimuli (Wu and Zumbo 2008; James B. Grace et al. 2010). We used the *piecewiseSEM* package (Lefcheck 2016) in R statistical software, which allowed us to first build individual linear regression models and then evaluate the combination of models in a SEM context.

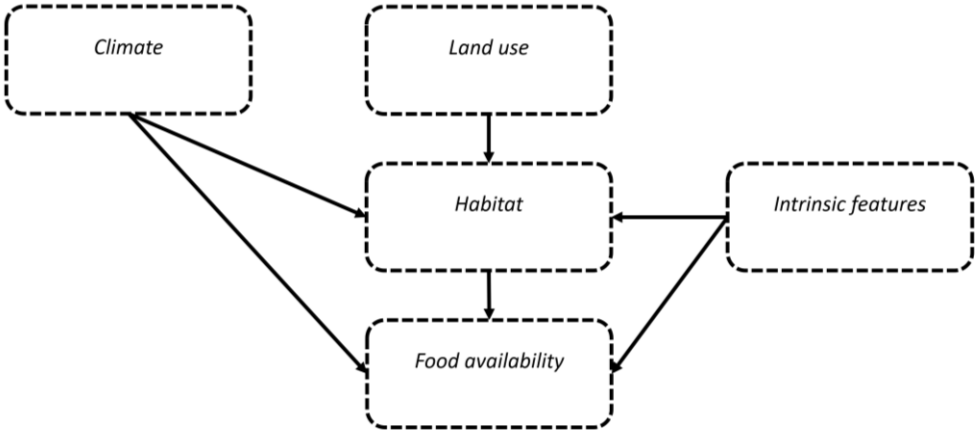

Figure 24. Conceptual framework used for structural equation model. Direction of arrows indicates hypothesized direction of influence.

Results and Discussion

Validation of food web indicators

For the purposes of this report, we focus on the propensity to drift metric because of its straightforward application to management through as a potential driver of fish distributions. However, we do compare relationships to other straightforward metrics like biomass of the benthic community to provide a contrast to the drift propensity metric. There appeared to be no relationship between benthic invertebrate biomass and invertebrate drift rates (Figure 25). Even at the lowest benthic biomass (~ 0e+03 mg m^{-2}) drift rates were found in their highest range (up to 4-5 mg m^{-3} day). Uncoupled relationships between benthic and drifting invertebrate biomass are likely the result of many factors, including density dependence and food limitation (Shearer et al. 2003), variations in discharge (Kennedy et al. 2014), and other poorly understood behavioral responses of invertebrates (Naman, Rosenfeld, and Richardson 2016). Propensity to drift metrics derived from the (Rader 1997) approach also failed to predict invertebrate drift rates in a linear manner, but performed better at delineating low vs. high values of drift propensity across the range of data (Figure 25). Furthermore, at the lowest drift propensity scores ($ASC_{Rel} < 4000$), invertebrate drift rates were quite low ($\leq$ 0.5 mg m^{-3}

day), indicating the drift propensity metric helped define a threshold value where higher or lower drift rates could be expected.

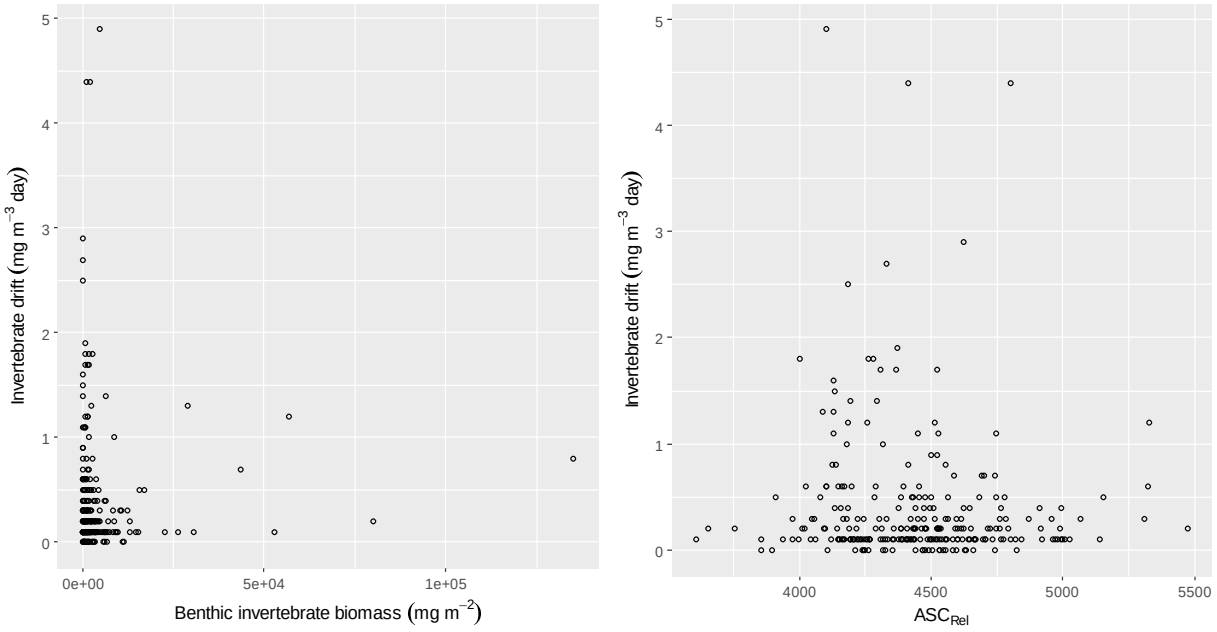

Figure 25. Relationships between benthic invertebrate biomass (left panel) and a selected drift propensity to metric (ASC_{Rel}) (right panel) and invertebrate drift rates for individual site visits.

Evaluation of drift frequency according to the propensity groups from cluster analysis (Figure 26) provided some insights into discrepancies between benthic and drift biomass. Drift frequency is the frequency of invertebrate taxa occurring in the drift when also present in the benthos. While most invertebrate taxa conformed to the model, some poor performers could be the cause of decoupling drift propensity metrics from drift rates in Figure 25. Specifically, *Neoplasta, Maruina, Deuterophlebia, Hemerodromia, and Stictotarsus* were rarely found in the drift when present in the benthos although they clustered in the high propensity group (C1). Further analysis of individual taxa frequencies and their traits could help refine the drift propensity metrics.

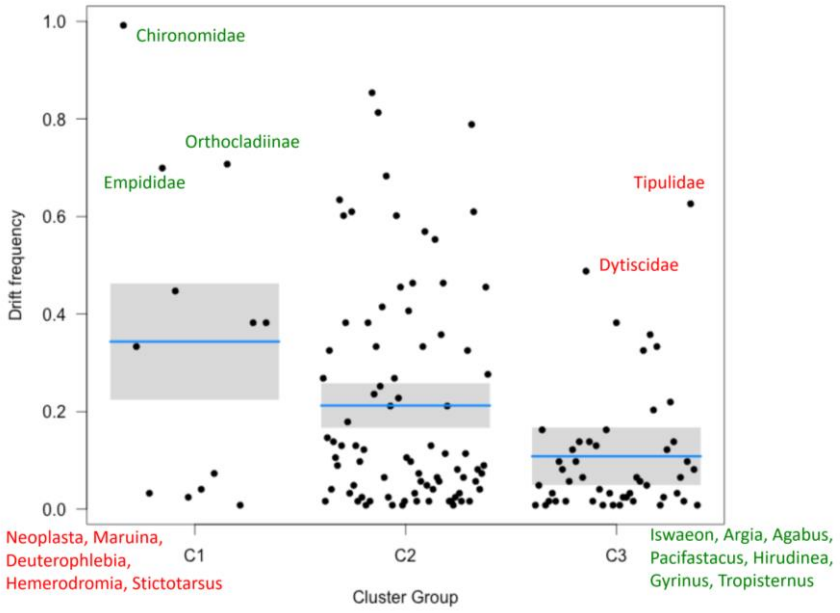

Figure 26. Frequency of invertebrate taxa occurring in the drift when present in the benthos. Invertebrates were grouped into high, medium, and low propensity to drift groups (C1, C2, and C3, respectively) based on cluster analysis of traits. Exceptionally well- or poor-performing taxa are indicated in green and red type, respectively. C3 taxa are excluded from *ASC* calculations.

We additionally evaluated whether juvenile Chinook salmon and *O. mykiss* density were associated with invertebrate drift rates or a drift propensity metric, ASC_{Rel} (Figure 27). Invertebrate drift did not appear to be positively associated with Chinook or *O. mykiss* density, with the highest fish densities occurring where drift biomass was lowest, and the lowest fish densities occurring where drift biomass was highest. On the contrary, the drift propensity metric—while not explaining all the variation in fish density, did appear associated with an upper limit to fish density, as illustrated by 98th quantile regression lines in Figure 27. At the lowest values of drift propensity (ASC_{Rel} < 3500), fish densities were in the range 0-2 fish m^{-1}; whereas at higher values of ASC_{Rel}, the upper envelope of fish densities increased to approximately 15 fish m^{-1}. We did not expect that a single variable (propensity to drift) would explain a large amount of variation in fish density, as stream fish respond to many abiotic, biotic, and stochastic factors (Jackson, Peres-Neto, and Olden 2001), rendering it difficult to predict their distributions. However, the drift propensity metric appears promising for establishing a relationship between fish and their prey distribution, and next steps involve teasing out the causes of additional variation.

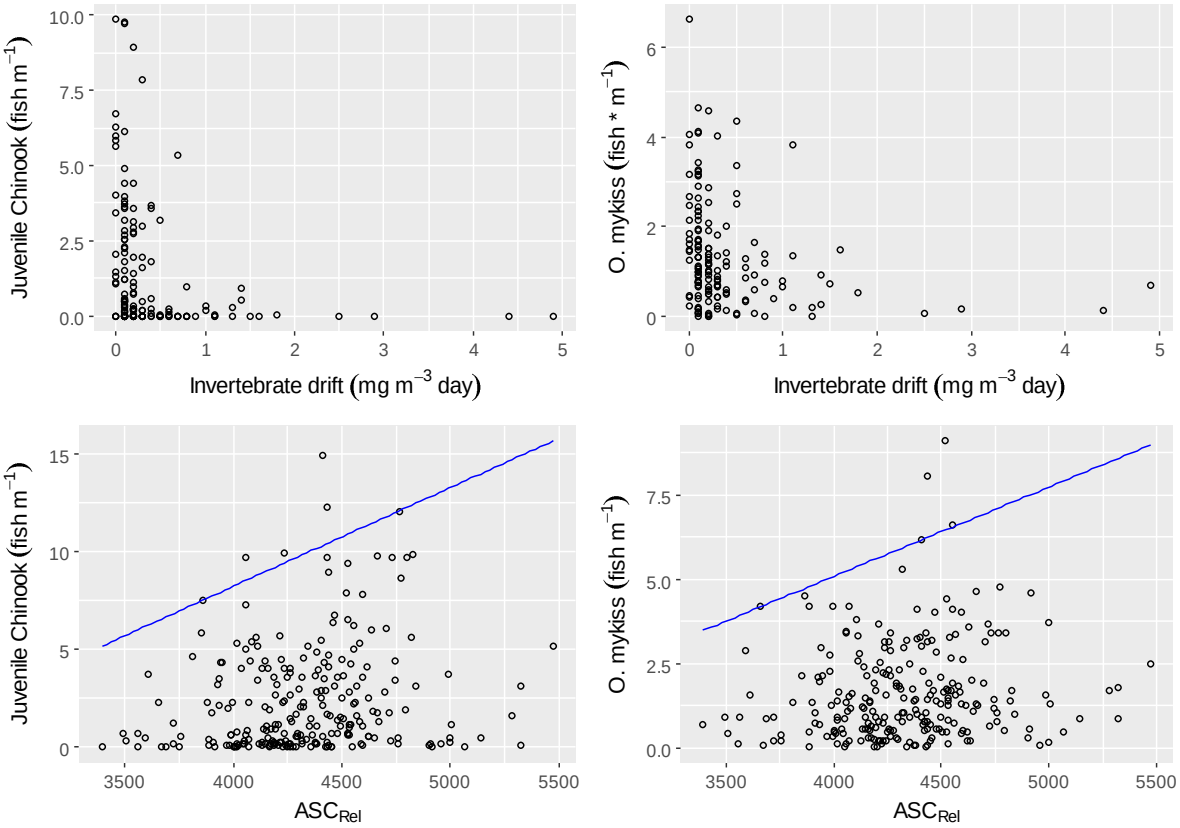

Figure 27. Juvenile Chinook salmon and *O. mykiss* density as a function of invertebrate drift rate (top panels) and a drift propensity metric (ASC_{Rel}) (bottom panels). The bottom two panels demark the 98th quantile regression line.

The only other explicit test of the Rader's (1997) model that we are aware of was conducted in the Feather River in California (Esteban and Marchetti 2004). Authors of that study found that Rader's model was correlated with stomach contents from fish diets, but not with invertebrate drift, and that trait rankings did not correlate with abundance in the drift. While results of the present study are not unequivocal, we find more promise in the development of a drift propensity metric.

Exploratory analysis of climate and land use drivers

The ASC_{Rel} drift propensity metric was distributed heterogeneously throughout the study area (Figure 28). Values of ASC_{Rel} were notably highest in upper portions of the Minam River (reference watershed) and North and South Fork Catherine Creek; and lowest in the middle reaches of the mainstem upper Grande Ronde River and Meadow Creek.

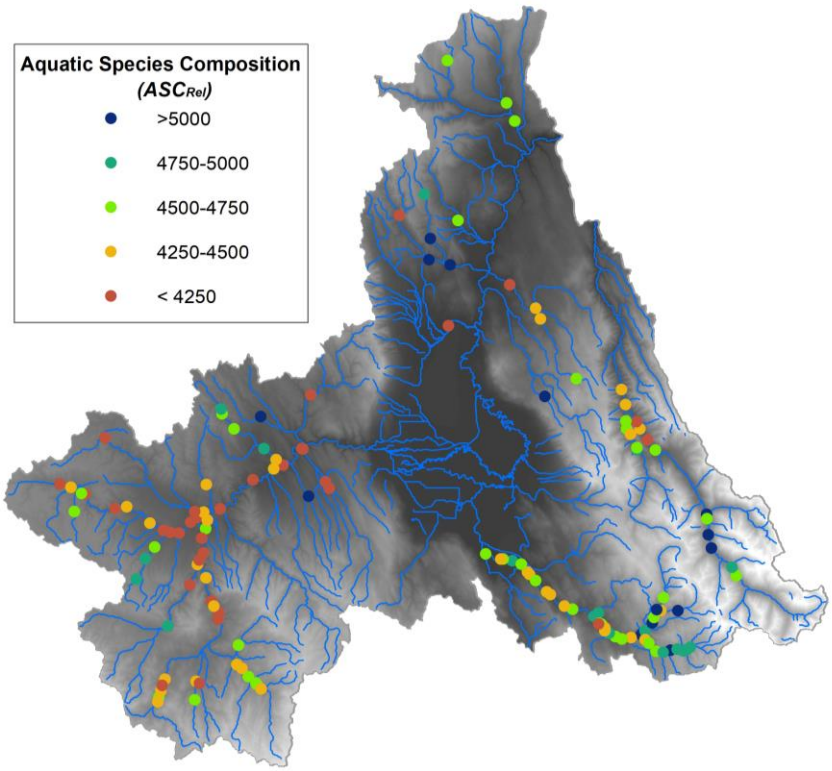

Figure 28. Distribution of drift propensity metric (ASC_{Rel}) values in upper Grande Ronde River, Catherine Creek, and Minam River. Lower ASC_{Rel} scores shown in red to yellow indicated benthic communities with a low propensity to drift; higher scores in green to blue indicate high propensity to drift.

The MIC analysis revealed that standard benthic macroinvertebrate indices were more responsive to climate, land use, intrinsic, and fish variables than were the new foodweb or drift propensity metrics (Table 13). In the case of all variables except fish metrics, stronger relationships with standard metrics were not surprising, since these metrics were honed to be responsive to environmental factors. We did expect stronger correlations between fish density and drift propensity scores, however, since those metrics were specifically designed to describe food availability and the distribution of fish. All metrics derived from benthic invertebrates were most strongly associated with climate variables, followed in descending order by intrinsic factors, land use, habitat conditions, and fish distribution. In the case of drift propensity metrics, ASC_{Rel} was the most sensitive to all environmental variables (i.e., climate, land use, intrinsic, and habitat). We therefore used ASC_{Rel} as the basis for a subsequent SEM analysis testing climate and land use drivers on food availability to salmonids.

Table 13. Maximal information coefficients (*MIC*) for relationships between standard benthic macroinvertebrate, foodweb, and drift propensity metrics and climate, intrinsic, land use, habitat and fish distribution (juvenile Chinook and *O. mykiss*). Values of *MIC* closer to 1 indicate stronger linear or nonlinear relationships between two variables.

Response category	*Response metric*	*Predictor category*	*Predictor metric*	*MIC*
Standard BMI	Weighted average temperature score	Climate	Mean Aug. water temperature	0.83
	No. fine sediment sensitive taxa	Intrinsic	Cumulative annual precipitation	0.70
	No. fine sediment sensitive taxa	Land use	Road density (watershed)	0.59
	No. temperature sensitive taxa	Habitat	Conductivity	0.46
	Weighted average fine sediment score	Chinook	Linear density juv. Chinook	0.36
	Weighted average fine sediment score	*O. mykiss*	Linear density *O. mykiss*	0.34
Foodweb	Proportion top level consumers	Climate	Mean Aug. water temp.	0.53
	Proportion top level consumers	Intrinsic	Cumulative annual precipitation	0.46
	Proportion top level consumers	Land use	Road density (catchment 100 m buffer)	0.45
	Proportion top level consumers	Habitat	Conductivity	0.42
	Average no. feeding links per taxa	Chinook	Linear density juv. Chinook	0.30
	Proportion of omnivores	*O. mykiss*	Linear density *O. mykiss*	0.29
Drift propensity	ASC_{Rel}	Climate	No. winter days exceeding 95^{th} percentile flows	0.47
	ASC_{Rel}	Intrinsic	Cumulative annual precipitation	0.43
	ASC_{Rel}	Land use	Road density (watershed)	0.41
	ASC_{Rel}	Habitat	Gradient	0.37
	ASC_{TotAdj}	Chinook	Linear density juv. Chinook	0.30
	ASC_{SubTot}	*O. mykiss*	Linear density *O. mykiss*	0.30

Structural equation model

Piecewise SEM was used to first test individual models predicting habitat conditions and drift propensity, and then models were combined to test relationships of the overall system (Figure 29). The habitat variable "Substrate D50" (mean b-axis diameter of substrate in mm) was a function of climate W95 (no. days winter flows exceed 95th percentile), land use AUMs/ha (cattle grazing in the upstream watershed), and the intrinsic factor Gradient (longitudinal gradient of the reach). Food availability to salmonids ASC_{Rel} was subsequently driven by W95, Substrate D50, and Gradient. These individual relationships are supported by widely understood mechanisms demonstrated in several other studies; however, because we evaluated relationships in a SEM context, novel insights about the system were revealed.

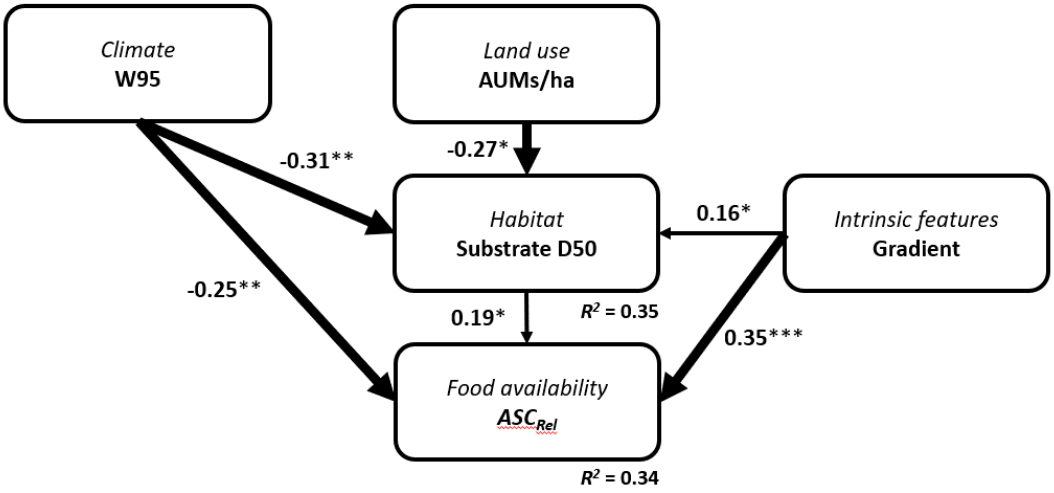

Figure 29. Structural equation model linking climate (no. days in winter exceeding 95th percentile streamflow) and land use (cattle grazing animal unit months per hectare) to habitat conditions (Substrate D50) and subsequently food availability (ASC_{Rel}). Direction and width of arrows indicates direction of hypothesized effect and relative strength of relationship, respectively. Values adjacent to arrows are standardized path coefficients. Significance values of coefficients are p < * 0.05, ** 0.01, and *** 0.001.

In a study conducted across the U.S. West (also using SEM), grazing was likewise associated with smaller substrate sizes, and increasing proportion of fine sediment negatively impacted benthic invertebrate biodiversity as measured by an observed/expected (O/E) score (Irvine et al. 2015). However, in that study the relationship between substrate and invertebrates was only marginally significant and explained a very low proportion of variation in invertebrate diversity (R^2 = 0.09) in sites with moderate precipitation comparable to those in our study. Irvine (2015) additionally found a significant relationship between climate-related factors (stream temperature) and invertebrate diversity but did not consider winter flooding as a driving variable. In exploratory analysis, we also found stream temperature negatively associated with

invertebrate distribution, but it was not a relevant variable in our model linking winter flows, cattle grazing, substrate, and drift propensity.

We found that of the two variables that can be influenced by management or policy decisions—land use and climate—the latter had a far greater relative influence on invertebrates. Using the rules of SEM path coefficients, the relative influence of land use on drift propensity is the product of standardized path coefficients leading from cattle grazing to substrate to invertebrates (-0.27 · 0.19 = -0.05). The relative influence of climate is the sum of the multiple pathways leading to invertebrates (-0.31 · 0.19 + -0.25 = -0.31). While improved cattle grazing strategies including decreasing AUMs may be an effective strategy for improving overall stream conditions, in context of our SEM improved management may not yield noticeable benefits to invertebrates, relative to the much stronger influence of climate change. Winter flooding is expected to increase substantially in the project area with climate change (Figure 30), which may have cascading negative impacts to stream habitat conditions and aquatic life.

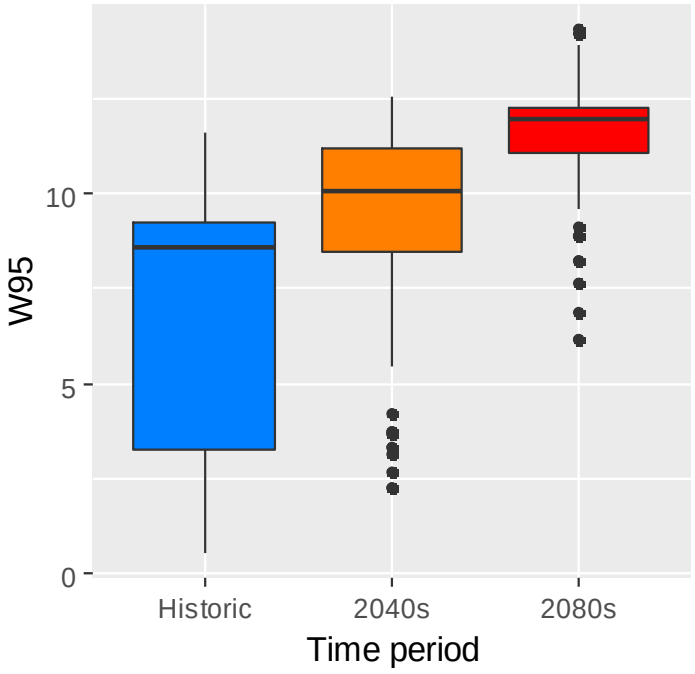

Figure 30. No. winter days exceeding 95th percentile streamflow (W95) at 136 habitat monitoring sites in the historic, 2040s, and 2080s time periods based on VIC model climate projections.

Future directions

These preliminary results point towards additional tasks to increase the utility of our approach in the upper Grande Ronde River and other Columbia River sub-basins:

- Additional refinement and validation of foodweb and drift propensity metrics, including analysis fish diets and taxon-specific conformance to models;
- Refinement of SEM to include linear mixed effects models with site as a random factor, and potentially watershed identity as a fixed factor;
- Exploration of additional land use variables identified in previous studies in the sub-basin (White et al. 2017) (e.g., forest loss and road density), climate factors (e.g., stream temperature, summer low-flows), and habitat conditions (e.g., pool and large wood frequency) as drivers of invertebrate communities;
- Projection of the likely impacts to invertebrate metrics from various management and policy scenarios related to climate change and land use; and
- Expansion of data collection, metric validation, and modeling into other Columbia River sub-basins, thereby increasing the generality of the approach.

References

CHaMP, (Columbia Habitat Monitoring Program). 2016. "Scientific Protocol for Salmonid Habitat Surveys within the Columbia Habitat Monitoring Program."

Cohen, Joel E, Tomas Jonsson, and Stephen R Carpenter. 2003. "Ecological Community Description Using the Food Web, Species Abundance, and Body Size." *PNAS* 100 (4): 1781–86.

Esteban, Elaine M., and Michael P. Marchetti. 2004. "What's on the Menu? Evaluating a Food Availability Model with Young-of-the-Year Chinook Salmon in the Feather River, California." *Transactions of the American Fisheries Society* 133 (3): 777–88. https://doi.org/10.1577/T03-115.1.

Grace, James B., T. Michael Anderson, Han Olff, and Samuel M. Scheiner. 2010. "On the Specification of Structural Equation Models for Ecological Systems." *Ecological Monographs* 80 (1): 67–87. https://doi.org/10.1890/09-0464.1.

Grace, J.B. 2007. "Structural Equation Modeling for Observational Studies." *The Journal of Wildlife Management* 72 (1): 14–22.

Halofsky, Jessica E, David L Peterson, and Kailey W Marcinkowski. 2015. "Climate Change Adaptation in United States Federal Natural Resource Science and Management Agencies: A Synthesis."

Hill, Ryan A., Marc H. Weber, Scott G. Leibowitz, Anthony R. Olsen, and Darren J. Thornbrugh. 2016. "The Stream-Catchment (StreamCat) Dataset: A Database of Watershed Metrics for the Conterminous United States." *JAWRA Journal of the American Water Resources Association* 52 (1): 120–28. https://doi.org/10.1111/1752-1688.12372.

Hudson, Lawrence N., Rob Emerson, Gareth B. Jenkins, Katrin Layer, Mark E. Ledger, Doris E. Pichler, Murray S A Thompson, Eoin J. O'Gorman, Guy Woodward, and Daniel C. Reuman. 2013. "Cheddar: Analysis and Visualisation of Ecological Communities in R." *Methods in Ecology and Evolution* 4: 99–104. https://doi.org/10.1111/2041-210X.12005.

Hudson, Lawrence, Daniel Reuman, and Rob Emerson. 2014. "Cheddar: Analysis and Visualisation of Ecological Communities in R."

Independent Scientific Advisory Board. 2011. "Columbia River Food Webs: Developing a Broader Scientific Foundation for Fish and Wildlife Restoration." Portland, Oregon.

Irvine, Kathryn M., Scott W. Miller, Robert K. Al-Chokhachy, Eric K. Archer, Brett B. Roper, and Jeffrey L. Kershner. 2015. "Empirical Evaluation of the Conceptual Model Underpinning a Regional Aquatic Long-Term Monitoring Program Using Causal Modelling." *Ecological Indicators* 50 (March): 8–23. https://doi.org/10.1016/j.ecolind.2014.10.011.

Jackson, D.A., P.R. Peres-Neto, and J.D. Olden. 2001. "What Controls Who Is Where in Freshwater Fish Communities -- the Roles of Biotic, Abiotic, and Spatial Factors." *Canadian Journal of Fisheries and Aquatic Sciences* 58 (1): 157–70. https://doi.org/10.1139/f00-239.

Jonasson, Brian C, Edwin R. Sedell, Shelley K. Tattam, Alan B Garner, Christopher D Horn, Kasey L. Bliesner, Joshua W Dowdy, et al. 2015. "Investigations into the Life History of Naturally Produced Spring Chinook Salmon and Summer Steelhead in the Grande Ronde River Subbasin." La Grande, Oregon.

Justice, Casey, Seth M. White, Dale A. McCullough, David S. Graves, and Monica R. Blanchard. 2017. "Can Stream and Riparian Restoration Offset Climate Change Impacts to Salmon Populations?" *Journal of Environmental Management* 188: 212–27. https://doi.org/10.1016/j.jenvman.2016.12.005.

Kennedy, Theodore A., Charles B. Yackulic, Wyatt F. Cross, Paul E. Grams, Michael D. Yard, and Adam J. Copp. 2014. "The Relation between Invertebrate Drift and Two Primary Controls, Discharge and Benthic Densities, in a Large Regulated River." *Freshwater Biology* 59 (3): 557–72. https://doi.org/10.1111/fwb.12285.

Lefcheck, Jonathan S. 2016. "PiecewiseSEM: Piecewise Structural Equation Modelling in R for Ecology, Evolution, and Systematics." Edited by Robert Freckleton. *Methods in Ecology and Evolution* 7 (5): 573–79. https://doi.org/10.1111/2041-210X.12512.

McCullough, D.A., S.M. White, C. Justice, M. Blanchard, R. Lessard, D. Kelsey, D. Graves, and J. Nowinski. 2016. "Assessing the Status and Trends of Spring Chinook Habitat in the Upper Grande Ronde River and Catherine Creek." Annual Report to Bonneville Power Administration. Portland, OR: Columbia River Inter-Tribal Fish Commission.

Naman, Sean M., Jordan S. Rosenfeld, and John S. Richardson. 2016. "Causes and Consequences of Invertebrate Drift in Running Waters: From Individuals to Populations and Trophic Fluxes." *Canadian Journal of Fisheries and Aquatic Sciences*, February, 1–14. https://doi.org/10.1139/cjfas-2015-0363.

NetMap. 2019. *Virtual Watershed and Analysis Tools*. TerrainWorks Inc. www.terrainworks.com.

Perdomo, G., R. Thopmson, and P. Sunnucks. n.d. “Food Web: An Open-Source Program for the Visualisation and Analysis of Compilations of Complex Food Webs.” *Environmental Modelling and Software*.

Quaempts, Eric J., Krista L. Jones, Scott J. O’Daniel, Timothy J. Beechie, and Geoffrey C. Poole. 2018. “Aligning Environmental Management with Ecosystem Resilience: A First Foods Example from the Confederated Tribes of the Umatilla Indian Reservation, Oregon, USA.” *Ecology and Society* 23 (2). https://doi.org/10.5751/ES-10080-230229.

Rader, Russell B. 1997. “A Functional Classification of the Drift: Traits That Influence Invertebrate Availability to Salmonids.” *Canadian Journal of Fisheries and Aquatic Sciences* 54 (6): 1211–34. https://doi.org/10.1139/f97-025.

Reshef, D. N., Y. A. Reshef, H. K. Finucane, S. R. Grossman, G. McVean, P. J. Turnbaugh, E. S. Lander, M. Mitzenmacher, and P. C. Sabeti. 2011. “Detecting Novel Associations in Large Data Sets.” *Science* 334 (6062): 1518–24. https://doi.org/10.1126/science.1205438.

Shearer, Karen A., John D. Stark, John W. Hayes, and Roger G. Young. 2003. “Relationships between Drifting and Benthic Invertebrates in Three New Zealand Rivers: Implications for Drift-feeding Fish.” *New Zealand Journal of Marine and Freshwater Research* 37 (4): 809–20. https://doi.org/10.1080/00288330.2003.9517210.

Sullivan, S.P., and S.M. White. 2017. “Methods Supporting the Development of Food Web Metrics from Benthic Macroinvertebrate Data.” Portland, OR: Columbia River Inter-Tribal Fish Commission. https://www.critfc.org/blog/reports/methods-supporting-the-development-of-food-web-metrics-from-benthic-macroinvertebrate-data/.

Ward, Joe H Jr. 1963. “Hierarchical Grouping to Optimize an Objective Function.” *Source Journal of the American Statistical Association* 58 (301): 236–44.

White, Seth M., Casey Justice, Denise A. Kelsey, Dale A. McCullough, and Tyanna Smith. 2017. “Legacies of Stream Channel Modification Revealed Using General Land Office Surveys, with Implications for Water Temperature and Aquatic Life.” *Elem Sci Anth* 5 (3): 1–18. https://doi.org/10.1525/elementa.192.

Wu, Amery D., and Bruno D. Zumbo. 2008. “Understanding and Using Mediators and Moderators.” *Social Indicators Research* 87 (3): 367. https://doi.org/10.1007/s11205-007-9143-1.

Fish-Habitat Modeling

Updates to Life Cycle Model for the Upper Grande Ronde River and Catherine Creek

The following is a brief summary of the life cycle mode report presented in Appendix B.

Introduction

During 2018 we worked with Eco Logical Research to update a life cycle model of Spring Chinook Salmon populations in the upper Grande Ronde River (UGR) and Catherine Creek (CC). The work presented here extended LCM development efforts previously initiated by the Columbia River Inter-Tribal Fish Commission (CRITFC) and included as part of the Independent Scientific Advisory Board's (ISAB) 2017 review of LCM efforts in the interior Columbia Basin (chapter 9.f in ISAB 2017). Ultimately, these efforts were intended to provide an analytical tool that can help guide long-term restoration and recovery strategies for two threatened Chinook Salmon populations under changing climatic conditions. This effort focused on two objectives that include: 1) Refinement of LCM parameters and functions to improve model accuracy and efficiency, and 2) leveraging the model to evaluate potential restoration strategies that might increase the viability of these populations under future time horizons that include climate change impacts.

Many of the additions to the 2018 LCM effort made use of novel unpublished population data from the Oregon Department of Fish and Wildlife that allowed us to update almost all life-stage transition parameters with the most up-to-date information. Some of these changes included:

1. Smolt-to-adult (SAR) return rates that are now specific to each population and origin (i.e. natural vs. hatchery).
2. A more realistic approach for modelling current hatchery supplementation operations within the UGR and CC.
3. Expanded incorporation of parameter variability allowing model stochasticity at all stage transitions within the LCM framework.
4. Updates to the model implementation that allow log-normal stochasticity on density-dependent predictions within a Beaverton-Holt framework.

This updated implementation of the LCM also included efficiency improvements that significantly decreased the duration necessary to run individual model scenarios. Doing so allowed us to increase the number of stochastic Monte Carlo iterations to 500 for each modelled management scenario.

The updated model was then used to evaluate simulated population dynamics and population extinction risk across restoration and climate scenarios described previously by Justice et al. (2017), as well as within a novel set of restoration scenarios that rely on structural equation models (SEM). Both of these approaches describe the potential impact that restoration actions may have on juvenile Chinook Salmon rearing capacity while also considering impending changes in stream temperature due to climate change. The updated LCM framework also allowed us to evaluate potential population responses (changes in population abundance and extinction risk) under restoration and climate scenarios with and without hatchery supplementation.

Simulation methods

We used the model to simulate trajectories for each population under each scenario (Table 14) over a 50 - year period (90 years minus a 40 year burn in) within 500 Monte Carlo model iterations. All model iterations were seeded with 10000 eggs and 1000 natural and hatchery origin smolt at LGD. Each scenario was run using the current hatchery supplementation scheme, as well as under a "cease supplementation" scenario in which hatchery supplementation is turned off in year 40.

We summarized the potential outcome of each scenario expressed as the median abundance of natural spawners over each 50 – year model iteration, and as the probability of quasi-extinction risk (pQER) for the population. A model run was considered at risk of quasi-extinction if at any point in the 50 - year simulation the spawning population remained below 50 for 4 consecutive years. pQER was calculated as the proportion of the 500 model iterations that the population reached the quasi extinction threshold at any point. pQER was only calculated for scenario simulations in which supplementation was discontinued as the hatchery supplementation programs ensures future viability of the populations.

To assess model sensitivity, we manipulated productivity parameters for all freshwater life-stages as well as smolt-to-adult survival. The analysis also included capacity but focused only on those stages in which density dependent survival was modelled within our restoration scenarios, namely egg-to-parr survival and adult survival on the spawning grounds. Starting with the base model for each population, we increased and decreased a single target parameter from -30% to +30% at 10% increments while holding all others constant. These values were chosen as they produced a realistic range of parameter rate changes that could be expected as a result of management actions and it allowed a normalized means to make comparisons of model sensitivity among parameters. At each increment the model was run for 500 iterations, over which pQER and the percent change in natural origin spawner abundance from the base parameter value was calculated. Again, because our broader aim is to provide results that are relevant to establishing viable populations with hatchery supplementation discontinued, we conducted the model sensitivity analysis with supplementation turned off at year 40.

Table 14. Scenarios modeled after Justice et al. (2017). For LCM inputs, each scenario is represented as a proportion increase or decrease in summer parr rearing and spawner capacity.

Scenario abbreviation	Description
Curr	Baseline model calibrated using 2010 temperature, climate, vegetation, and hydrologic conditions
Clim	Air temperature and streamflow set to 2080s climate projections.
ClimVeg	2080s climate projections and vegetation set to potential cover and height at 75 years.
ClimVegWid	2080s climate projections, vegetation set to potential cover and height at 75 years, and channel width set to historic conditions.

Summary of results and discussion

The model and analytical framework presented here provides novel insights concerning the dynamics of UGR and CC Chinook, and it is our intention that this work be used to guide future population management and prioritization of habitat restoration, as a well as providing a basis for future life cycle models for these populations. One of the major strengths of our LCM framework lies in efforts taken to model the dynamic interaction between the natural and hatchery component of each population, including the complexities and variability associated with the hatchery supplementation program. This modelling framework allowed us to evaluate the viability of each population according to alternative futures where the hatchery supplementation program has been discontinued.

Overall, our modelling results indicated minimal potential increases in adult Chinook Salmon abundance and low to moderate improvements in extinction risk from basin-wide restoration of riparian vegetation and channel width, owing largely to the overriding negative influence of climate change. For example, median natural spawner abundance in the upper Grande Ronde River was projected to increase from approximately 48 under current climate and stream habitat conditions to 89 (an 85% increase) for a 2080's future scenario (i.e., '*ClimVegWid'*) that included restored riparian and channel width conditions in combination with climate change (Table 15; Figure 31). Similarly, Catherine Creek natural spawners were projected to increase from 265 under the current scenario to 346 under the *ClimVegWid* scenario (a 31% increase; Figure 32). These projected increases in natural spawner abundance fall well below the minimum abundance target of 1000 identified in NOAA's NE Oregon Snake River recovery plan as necessary for long term persistence of these populations (NOAA 2014).

Our evaluation suggested that even with aggressive riparian and channel restoration, predicted climate change impacts to stream temperature regimes will result in relatively high extinction risk of Chinook Salmon within the UGR if hatchery supplementation is curtailed (Figure 33). Quasi extinction risk for the UGR population was predicted to

decrease from 0.97 under current population conditions (i.e., '*Curr*') to roughly 0.78 under the most aggressive restoration scenario (i.e., '*ClimVegWid*'). In contrast, our modelling suggests that even without hatchery supplementation, climate change will push CC Chinook toward a moderate extinction risk, and that restoration efforts could be invested to ensure the future long-term viability of this population. Catherine Creek has a relatively low extinction risk 0.032 under current conditions that would increase to roughly 0.12 in the face of climate change even when no restoration was implemented (i.e. 'Clim'; Table 15; Figure 33). With basin-wide riparian and channel restoration, extinction risk for the CC population could be reduced to less than 1% (Table 15). While we do not attempt to make broad management recommendations here, the hope is that these model outcomes can be used to optimize future investment in restoration and hatchery supplementation programs that support viable natural populations in these systems.

The relatively low projected population responses to habitat restoration actions in the face of climate change are in part related to the limited set of restoration actions and life stages evaluated in the model. For example, restoration scenarios which included water temperature reduction (via riparian restoration and channel narrowing), and pool habitat restoration (see SEM scenarios in the full model report) were assumed to affect population dynamics primarily by increasing summer parr capacity. However, it is likely that improvements in these habitat characteristics would also influence pre-spawn mortality of adult salmon as well as migration survival of smolts via improvements in growth of juveniles. In addition, other commonly applied restoration actions which target factors such as floodplain complexity and instream flow could have additional benefits that were not included in the model. Analysis of these factors are in progress and will likely be included in future iterations of the life cycle model.

Sensitivity analysis indicated that our LCM framework appeared more sensitivity to changes in productivity parameters than capacity (Figure 34 and Figure 35). Both populations appeared largely insensitive to changes in spawner capacity (availability of temperature-suitable habitat for adults during summer). This result may be an artifact of spawner capacity estimates used within the base model that are orders of magnitude above those on record for these populations. Manipulation of the survival parameter for adults on the spawning grounds had large impacts to the viability of each population, especially within the UGR model where current survival rates for spawners in the system are lower than that of CC. Sensitivity of the model populations to egg-to-parr survival and capacity followed a similar pattern, with proportional changes to survival rather than capacity having a larger effect on spawner returns and pQER.

Our sensitivity analysis also showed that both populations were most sensitive to increases and decreases in survival as smolt from LGD until their return as adults to the spawning grounds (i.e. the SAR). Sensitivity of our populations at this life stage is not surprising as the first - year survival input within our LCM framework (S1) are the lowest for any stage transition (0.04 and 0.07 for the UGR and CC, respectively). However, this

is not to say that increases or decreases to freshwater life-stages were completely drowned by the response of the populations to outmigration and ocean survival. Indeed, survival at other life-stage transitions, such as spawning grounds survival and winter survival of rearing presmolt also appear to impact the viability of each population over the range of values considered here.

Table 15. Median population size of natural origin spawning Chinook for 500 model iterations of restoration scenarios described by Justice et al. 2017. Also showing relative difference of each scenario to the current conditions ('Curr') in model runs at current hatchery supplementation and when supplementation is discontinued.

Pop	Scenario	Current Supplementation		Cease Supplementation		pQER
		Median natural spawners	Relative to Curr	Median natural spawners	Relative to Curr	
UGR	*Curr*	48	-	16	-	0.972
	Clim	24	-50%	5	-69%	1
	ClimVeg	72	50%	33	106%	0.872
	ClimVegWid	89	85%	42	163%	0.784
CC	*Curr*	265	-	186	-	0.032
	Clim	169	-36%	121	-35%	0.118
	ClimVeg	316	19%	223	20%	0.004
	ClimVegWid	346	31%	261	40%	0.01

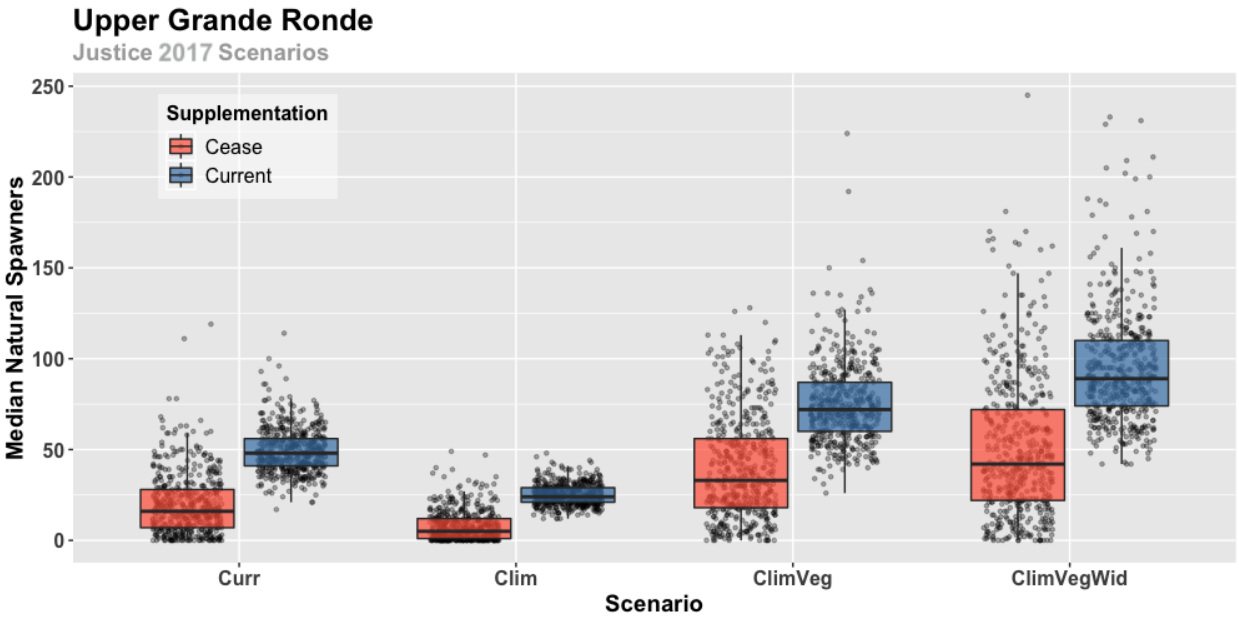

Figure 31. Boxplots showing the distribution of the median population size for upper Grande Ronde natural origin spawning Chinook for restoration and climate scenarios described by Justice et al. 2017.

Model runs at current supplementation and with supplementation discontinued are shown. Jittered points show the median value for each of 500 model runs.

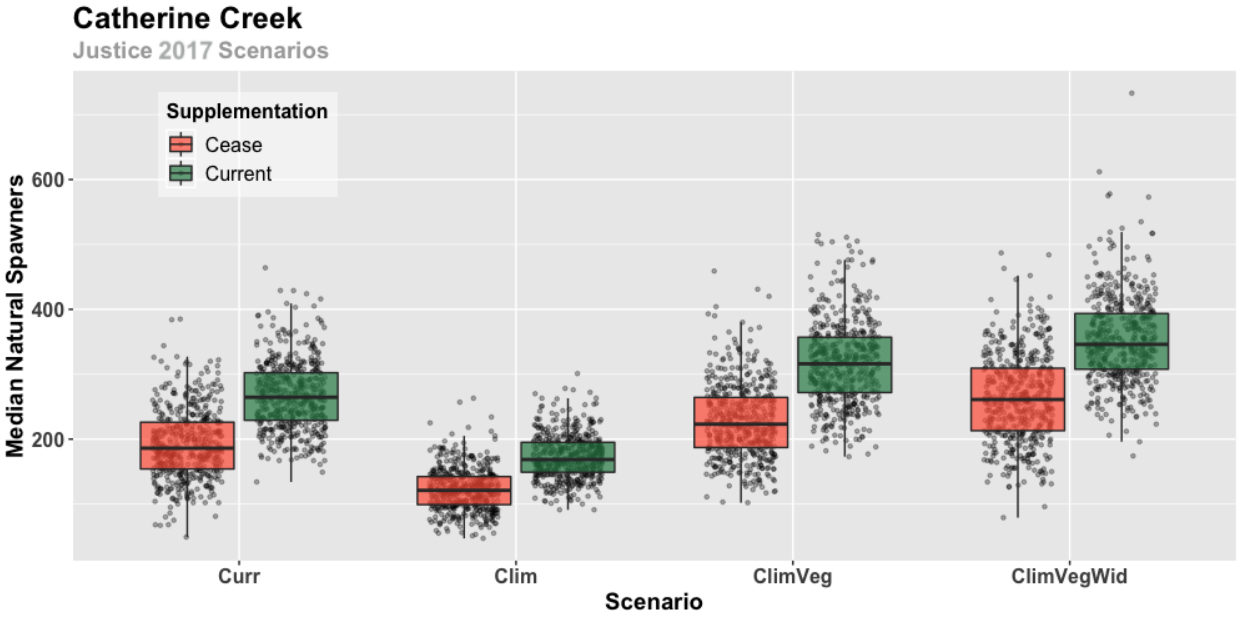

Figure 32. Boxplots showing the distribution of the median population size for Catherine Creek natural origin spawning Chinook for restoration and climate scenarios described by Justice et al. 2017. Model runs at current supplementation and with supplementation discontinued are shown. Jittered points show the median value for each of 500 model runs.

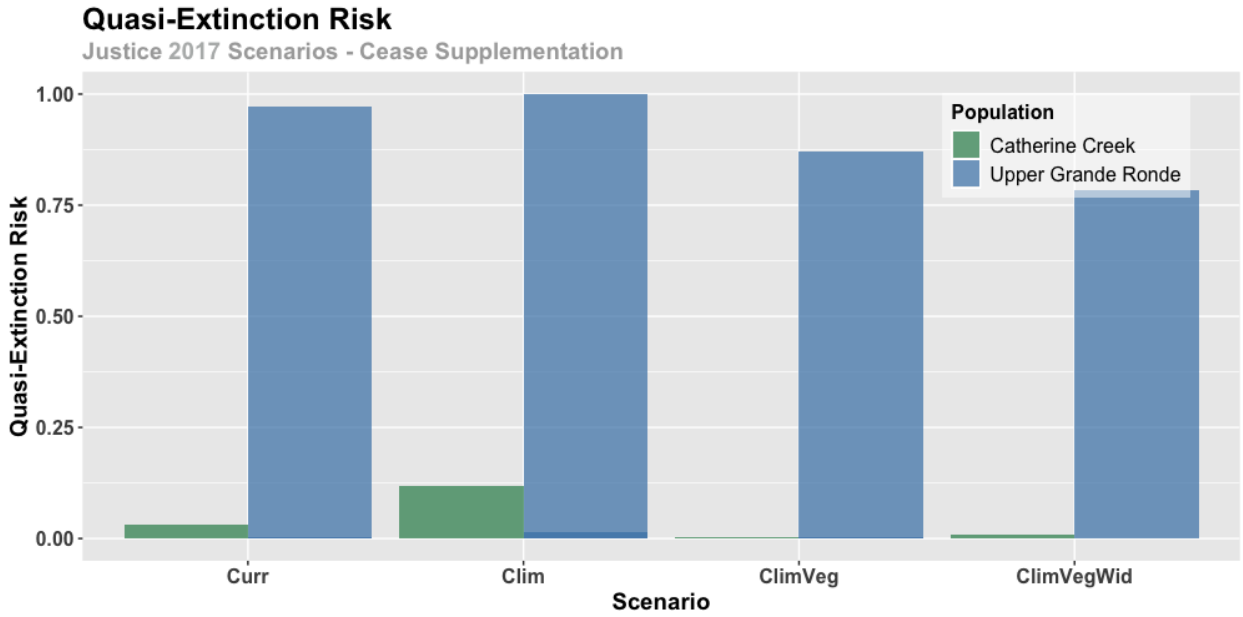

Figure 33. Quasi – Extinction Risk (pQER) under each restoration and climate scenario for the upper Grand Ronde and Catherine Creek Chinook populations for restoration and climate scenarios described by Justice et al. 2017.

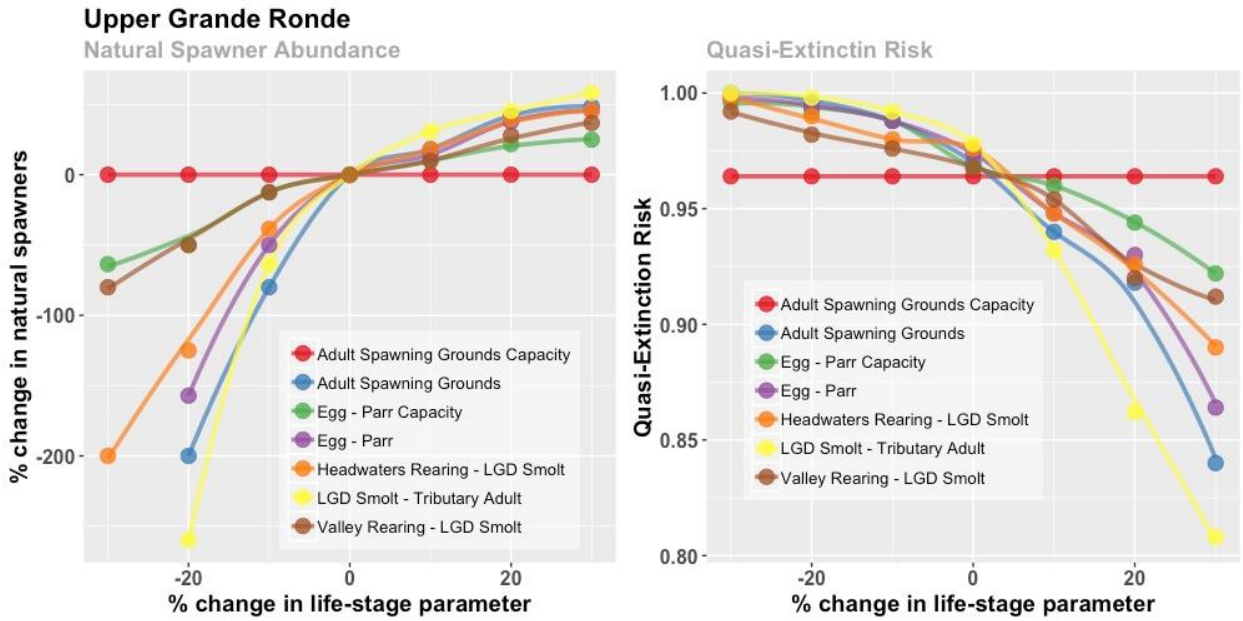

Figure 34. Results of the sensitivity analysis for the upper Grande Ronde. Left panel shows the percent change in natural spawners from the base model for simulations that manipulated life-stage survival and capacity from -30% to +30%. Right panel shows how changes to survival and capacity result in proportional changes in pQER. Note, that the % change in natural origin spawners at %-30 was removed for some life-stages as they greatly influenced presentation of the figure. Lines representing capacity are labelled as such within the legend with other lines representing productivity parameters.

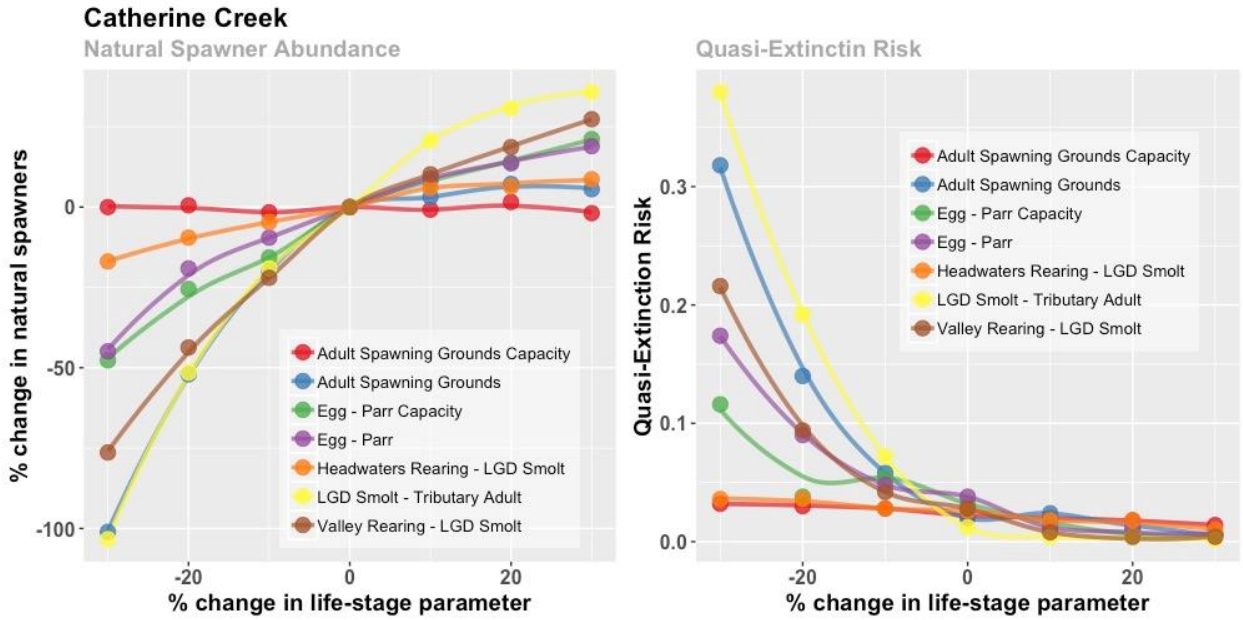

Figure 35. Results of the sensitivity analysis for Catherine Creek. Left panel shows the percent change in natural spawners from the base model for simulations that manipulated life-stage survival and capacity from -30% to +30%. Right panel shows how changes to survival and capacity result in proportional changes in pQER. Lines showing capacity are labelled as such within the legend with other lines representing productivity parameters.

References

Independent Scientific Advisory Board. 2017. Review of NOAA Fisheries' Interior Columbia Basin Life-Cycle Modeling. ISAB 2017-1. https://www.nwcouncil.org/media/7491311/isab-2017-1-noaalifecyclemodelreview22sep.pdf

Justice, C., White, S.M., McCullough, D.A., Graves, D.S., Blanchard, M.R., 2017. Can stream and riparian restoration offset climate change impacts to salmon populations? Journal of Environmental Management 188, 212-227.

NOAA. 2014. Draft ESA recovery plan for Northeast Oregon Snake River spring and summer Chinook salmon and Snake River steelhead populations. Page 529. National Oceanic and Atmospheric Administration.

Dissemination of Project Findings in 2018

Publications

Kaylor, MJ, A Argerich, SM White, B VerWey, I Arismendi. 2018. A cautionary tale for in situ fluorometric measurement of stream chlorophyll *a*: influences of light and periphyton biomass. *Freshwater Science* 37(2).

White, SM, D Graves, D Barton, and L Gephart. 2018. Conservation Planning for Climate Change Impacts to Benthic Macroinvertebrate Assemblages in the Columbia River Basin. Columbia River Inter-Tribal Fish Commission Technical Report 18-05, Portland, OR. 19p.

Draft publications

Kaylor, MJ; SM White; WC Saunders; and DR Warren. Linking spatial patterns of stream nutrient concentrations, stream metabolism, and juvenile salmonids in a river network. Target Journal: *Ecosphere*.

Kaylor, MJ; SM White; ER Sedell; and DR Warren. Juvenile salmonid responses to carcass additions along a thermal and species assemblage gradient. Target Journal: *Ecological Applications*.

Kaylor, MJ; SM White; ER Sedell; AM Sanders; and DR Warren. Carcass additions influence food webs through bottom-up and direct consumption pathways along a NE Oregon stream with varying fish species assemblages. Target Journal: *Freshwater Biology.*

White, SM; Justice, C; McCullough, D; Blanchard, M; and Sedell, T. Climate change meets the ghosts of land use past: Revisiting historical changes in salmon habitat in the Columbia River Basin. Target Journal: *Ecological Applications*.

White, SM, McHugh, P, Naman, S, Baxter, C, Bellmore, R, Naiman, R, and Danehy, R. What's in the toolbox? A primer of food web perspectives and methods for riverine fish conservation. Target Journal: *Fisheries.*

Presentations

Burns, LA. 2018. Using Drones for Habitat Monitoring. CRITFC Brownbag Seminar, Portland, OR.

Justice, C. 2018. Can stream and riparian restoration offset climate change impacts to salmon populations. USDA Fish and Watershed Program Manager's Meeting. Lincoln City, OR.

Justice, C. 2018. Can stream and riparian restoration offset climate change impacts to salmon populations. NOAA Interior Columbia Basin Office (ICBO) All Hands Workshop. McCall, ID.

Kaylor, MJ. 2018. Effects of carcass additions on stream food webs along a temperature and fish assemblage gradient in NE Oregon. Oregon American Fisheries Society Annual Meeting. Eugene, OR.

Kaylor, MJ. 2018. Salmonid and food web responses to salmon carcass additions along a stream temperature and fish assemblage gradient. Umeå University, Sweden.

Kaylor, MJ. 2018. Effects of carcass additions on stream food webs along a temperature and fish assemblage gradient in NE Oregon. State of the Science Meeting. La Grande, OR.

Kaylor, MJ. 2018. Effects of carcass additions on stream salmonids in a NE Oregon stream. CRITFC Brownbag Seminar, Portland, OR.

White, SM. 2018. Understanding rivers through metaphor. Presentation to Climate and Water seminar, Pacific Northwest College of Art (PNCA), Portland, OR.

White, SM. 2018. Fisheries research supporting tribal communities in the Columbia River basin. Palacký University, Olomouc, Czech Republic.

White, SM. 2018. Historical Ecology to inform river restoration planning in the face of climate change. US Forest Service-Eastern Oregon University Journal Club, La Grande, OR.

White, SM. 2018. Resilient rivers in the face of climate change. Ecosystem Resilience seminar, Pacific Northwest College of Art, Portland, OR.

Appendix A – Draft Habitat Protocol

Stream Habitat Monitoring Protocol

2018 Version

June 2018

A component of:

Monitoring Recovery Trends in Key Spring Chinook Habitat Variables

and Validation of Population Viability Indicators

(BPA Project No. 2009-004-00)

Prepared by: Casey Justice, Seth White, and Lauren Burns

Columbia River Inter-Tribal Fish Commission

Portland, OR

Table of Contents

Introduction

This document describes field methods for a salmonid stream habitat monitoring program currently being implemented in the Upper Grande Ronde River, Catherine Creek, and Minam River basins designed to evaluate the effectiveness of aggregate restoration actions in improving freshwater habitat conditions and viability of ESA-listed fish populations. After seven years (2011-2017) of intensive field sampling in these watersheds as part of the Columbia Habitat Monitoring Program (CHaMP), we have learned a great deal about limiting factors for salmon and steelhead populations and effective sampling methods for quantifying habitat conditions. However, many questions remain unanswered regarding long-term trends in habitat conditions, effectiveness of stream restoration actions, and about the accuracy of randomized site-level measurements for characterizing watershed-scale or restoration project-scale changes in fish habitat.

Following cancellation of the CHaMP program in spring of 2018, we have taken stock of lessons learned and refined our sampling protocol to improve efficiency and repeatability. In general, we intend to rely more heavily on available remotely sensed data (e.g., LiDAR, satellite imagery, NetMap tools) to characterize river and watershed conditions to the extent possible and to limit ground-based measurements to those that are most repeatable and relevant to salmon productivity. Most notably, we are incorporating aerial drone surveys into the protocol to eventually replace more time intensive Total Station topographic surveys and to expand our ability to accurately characterize riparian and floodplain conditions. In addition, we dramatically reduced the number of ground-based measurements compared with the CHaMP protocol, with emphasis on removing methods that are more subjective (e.g., drift invertebrates, visual estimation of fish cover and substrate size) and retaining methods that are more quantitative and repeatable (e.g., measurement of large woody debris, pebble counts, discharge). The 2018 field season is intended as a pilot study to test, refine, and validate new survey methods at a subset of previously surveyed CHaMP sites. Following 2018, our hope is to work with regional partners to further refine and implement a monitoring protocol that could be applied more rapidly and across larger spatial scales (10s of kilometers per year) and using additional sources of remotely-sensed information to answer critical questions regarding fish habitat.

Ground-based survey methods

Many of the methods described here were based directly on, or were modified from the CHaMP protocol (CHaMP 2016a). We acknowledge and thank all contributors to the CHaMP program for their efforts.

1.0 Survey workflow

This section describes an idealized workflow for a three-member survey crew. The specific workflow of an organization or crew may further depend upon the number of crew members and availability of sampling equipment. Auxiliary survey refers to ground-based measurements (e.g., large woody debris, pebble counts, discharge) that are independent from the topographic survey (total station and prism rod). The topographic survey workflow will vary depending on the complexity and size of stream as well as surveyor experience.

1) <u>Site scouting:</u>
    a. Locate and flag the bottom of site, top of site, active benchmarks, and water temperature logger location.

b. Survey active benchmarks and add additional ground control points as needed for the topographic and drone survey.

c. Download water temperature data and install a new logger if necessary.

d. Take notes as needed to aid in future surveys (i.e., good launch/landing area for drone, locations of difficult-to-find benchmarks, suggested survey strategy, landowner issues, etc.).

e. Complete scouting at all sites prior to conducting full surveys.

2) Reach layout:

a. Locate and establish the bottom of site.

b. For new sites, two people identify bankfull elevations, measure bankfull widths, and determine the width category. At revisits, width category will be predetermined.

c. Two members (auxiliary and rodman) lay out the site transects and identify/flag channel units. Meanwhile, the total station operator (gunner) establishes and surveys new benchmarks at new sites and locates and re-occupies benchmarks at revisits. When the rodman completes laying out the site, he/she returns to assist gunner with benchmarks and begins the topographic survey.

3) Auxiliary Survey:

a. After laying out the site, one crew member works downstream collecting transect level measurements (i.e., solar input, transect GPS coordinates).

b. Proceed upstream collecting all channel unit level information (i.e., large woody debris, pebble counts, channel unit GPS coordinates).

c. Measure discharge and conductivity as convenient.

d. After all other components of the auxiliary workflow are finished, complete the Land Use assessment form.

4) Topographic Survey:

a. After surveying benchmarks, traverse to the stream and survey points along the bottom of site cross-section (transect 1).

b. Work up one side of the stream collecting topographic points in the floodplain until there is no longer a line of site between the total station and prism.

c. Work back down along the same side of the stream collecting a combination of edge of water, top of bank, toe of bank, topographic points on the bank, and bankfull points.

d. Work upstream collecting in-channel features including thalweg, topographic, island/bar perimeters, and channel unit points. For larger streams, only sample half of the channel.

e. Work down along the opposite side of the stream collecting streambank points (see c).

f. Work up along the same side of the stream collecting topographic points in the floodplain.

g. Survey additional reach cross-sections at odd-numbered transects as they are encountered (transects 3, 5, 7, 9).

h. Review the survey on total station, fill in gaps as needed, check backsight, and traverse to new station location.

i. Repeat steps a-h until entire site is effectively surveyed. Finish by surveying points along the top of site cross-section (transect 11) and checking backsight.

2.0 Reach layout

Stream reaches (or sites) set the spatial boundaries for measurements of stream habitat and biota. Surveys will be conducted at 12-16 reaches that were previously surveyed using the CHaMP protocol (CHaMP 2016a), and consequently, reach boundaries have been predetermined. Reach lengths are approximately 20 times the average bankfull channel width (range 120 - 600 m).

2.1 Identifying bankfull elevation

Bankfull identification methods were adapted from CHaMP (2016a). Bankfull elevation is the location along the stream banks where the stream flow fills the channel to the top of the banks and water begins to overflow onto the floodplain (Leopold et al. 1964), an event that occurs approximately every 1.5 years. The portion of the stream channel that is at or below the bankfull elevation is termed the active channel. Numerous habitat metrics generated from the survey depend on accurate identification of the bankfull elevation.

Bankfull elevation is identified in the field using various physical indicators as defined by Harrelson et al. (1994). Indicators should be more distinguishable at unconstrained channel types where the tops of point bars, changes in substrate, and permanent vegetation may be the most reliable indicators. In constrained channels, especially those dominated by boulders and bedrock substrate, indicators may be more difficult to identify. Under these circumstances the crew may have to depend on stain lines, or move further up or downstream of a site to find reliable indicators.

Table 1. Indicators used to determine the bankfull elevation at a reach.

Indicator	Description
Change in slope	The change from a vertical bank to a horizontal surface is the best identifier of bankfull, especially in low-gradient meandering streams. Many banks have multiple breaks, so examine banks at several sections of the site for comparison. Slope breaks also mark the extent of stream terraces which are old floodplains above the active bankfull elevation. Terraces will generally have soil structure and perennial vegetation. Avoid confusing the elevation of the lower terrace with that of bankfull; they may be close in elevation.
Top of point bars	Point bars consist of bed material deposited on the inside of meander bends. The top elevation of point bars usually indicates the lowest possible bankfull stage. Multiple point bar elevations may be left from flows both above and below the bankfull elevation.
Change in Vegetation	Look for the lower limit of perennial vegetation on the bank or a sharp break in the density or type of vegetation. Often willow and alders form root lines near the bankfull elevation. The lower limit of mosses or lichens on rocks or banks, or a break from mosses to other plants may also help identify the bankfull elevation.

Indicator	Description
Change in Bank Materials	Look for changes in bank particle size, usually from coarse particles to a finer particle matrix (which is often associated with a change in slope).
Undercuts Banks	Look for bank sections where the perennial vegetation forms a dense root mat. Feel up beneath this root mat and estimate the upper extent of the undercut. This is usually slightly below bankfull stage. Undercut banks are best used as indicators in steep channels lacking floodplains.
Stain Lines	Look for water lines on rocks that indicate where rocks are frequently inundated. Stain lines are often left by lower, more frequent flows, so stain lines should only be used to assist in identifying bankfull along with another indicator or when no other indicators exist at a site.

2.2 Establishing reach transects

Some components of the habitat survey (e.g., channel cross-sections, solar input, and benthic macroinvertebrates) are conducted at systematically spaced transects, or straight lines extending across the stream channel perpendicular to the direction of stream flow. Transects are established at the beginning of the survey to delineate the boundaries of the survey reach and indicate locations for transect-based measurements.

Field procedures:

1) Navigate to the bottom of the reach using provided coordinates and driving/hiking directions. The bottom of the reach is usually marked with capped rebar on one of the adjacent stream banks. Reach photos, notes, and maps from previous surveys may be helpful in locating the bottom of the reach. Place flagging on the stream bank at the bottom of the reach to identify the location of the first transect. Write transect 1 (T1) on the flagging using a permanent marker.
2) Use the pre-determined average bankfull width category to determine the reach length and transect spacing (Table 2). Transect spacing is 2 times the bankfull width category.
3) Following the center of the main wetted channel (i.e., the channel containing the greatest amount of flow), stretch a measuring tape from transect 1 upstream a distance equal to the site width category. For repeatability purposes, all tape measurements are straight line distances (i.e., do not bend the tape around meander bends). By alternating positions with your field partner, measure one additional bankfull width distance upstream and then place flagging on the bank to identify the location of transect 2. Continue this procedure until all 11 transects have been established. If the channel is straight between transects, it is acceptable to measure the complete transect spacing distance instead of measuring in bankfull width increments.
4) If necessary, adjust the location of transect 11 to ensure that it lines up exactly with the previously established top of the reach. Look for capped rebar on the bank and examine previous site photos and notes to identify the correct location. If the transect location needs to be adjusted by a large amount (> 5% of the original reach length), then you may have made a mistake during transect layout and should double check your measurements.
5) Record the channel unit that each transect is in (see “Channel unit classification” below). If the transect intersects more than one channel unit, assign the transect to the unit with the largest proportion of the flow and make a note of the other channel units that the transect includes. If

the transect is located at the boundary between 2 channel units, assign the transect to the channel unit that it most represents (e.g., pool tail crests are generally more similar to the downstream fast water unit than to the pool itself).

6) Record GPS coordinates using a handheld GPS unit at each transect in the middle of the main wetted channel.

Table 2. Width category and reach lengths determined from the average bankfull width.

Average bankfull width (m)	Width category (m)	Site length (m)	Transect spacing (m)
≤ 6	6	120	12
> 6 and ≤ 8	8	160	16
> 8 and ≤ 10	10	200	20
> 10 and ≤ 12	12	240	24
> 12 and ≤ 14	14	280	28
> 14 and ≤ 16	16	320	32
> 16 and ≤ 18	18	360	36
> 18 and ≤ 20	20	400	40
> 20 and ≤ 22	22	440	44
> 22 and ≤ 24	24	480	48
> 24 and ≤ 26	26	520	52
> 26 and ≤ 28	28	560	56
> 30	30	600	60

2.3 Channel segments and side channels

Channel segment numbers are used to differentiate the main channel from side channels. Unique channel segment numbers are assigned to the main channel and all qualifying side channels.

The **main channel** is defined as the channel containing the largest amount of flow in the reach.

Qualifying side channels are defined as portions of the active channel (below bankfull elevation) that are separated from the main channel or other side channels by an island that is ≥ the bankfull elevation for a length ≥ the average bankfull width. If a channel is separated from another channel by a sediment deposit that is shorter than the average bankfull width or not meeting the height criteria (i.e., a bar), then the channel is considered part of the adjacent channel.

Non-qualifying side channels are distinguished from side channels by possessing one or more of the following characteristics:

i. The elevation of the streambed is above bankfull at any point.
ii. The channel lacks a continuously defined streambed or developed streambanks.
iii. The channel contains a substantial amount of terrestrial vegetation.

Non-qualifying side channels are not assigned a segment number and channel units within them are not delineated. However, if an off-channel unit occurs at the junction of a non-qualifying side channels and a larger channel, the off-channel unit is included in the survey and is considered part of the larger channel (see off-channel units below; Figure 1).

Field procedures:

1) While working upstream to lay out transects, assign segment numbers to the main channel and any qualifying side channels. Assign segment 1 (S1) to the main channel.
2) Designate the first qualifying side channel encountered (i.e., the furthest downstream) as segment 2 (S2). Designate additional qualifying side channels sequentially (S3, S4, S5, etc.) until all side channels have been uniquely numbered (Figure 1).

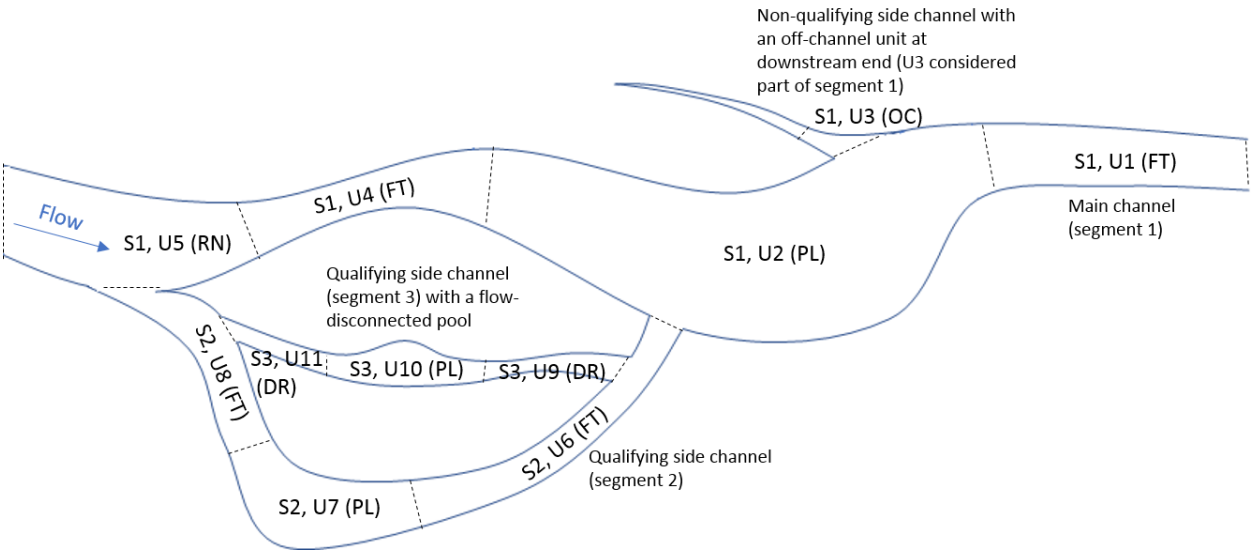

Figure 1. Example of a reach with correctly numbered channel segments and units. Channel segment numbers are preceded by a "S" (e.g., S1-S3) and channel unit numbers with a "U" (e.g., U1-U8).

2.4 Channel unit classification

Channel geomorphic units are relatively homogeneous areas of the channel with unique bedform shape, depth, velocity, and substrate characteristics. Habitat and biotic metrics such as large woody debris, substrate size and fish abundance are grouped by channel unit. Channel units within each survey reach are classified using a 2-tiered hierarchical classification system modified from Hawkins et al. (1993) (Figure 2). General channel unit characteristics are described in Table 3.

To consider a channel geomorphic feature as a separate channel unit, the maximum wetted length of the feature must be as long as the average wetted channel width in that segment. For example, a 3 m long pool in a side channel with an average wetted width of 2 m would qualify, but a pool of the same size in the main channel with an average wetted width of 8 m would not qualify. Exceptions to this rule include channel-spanning plunge pools, channel-spanning dammed pools, off-channel units, and special case units. Features that do not meet this minimum size criteria are lumped with the adjoining channel unit.

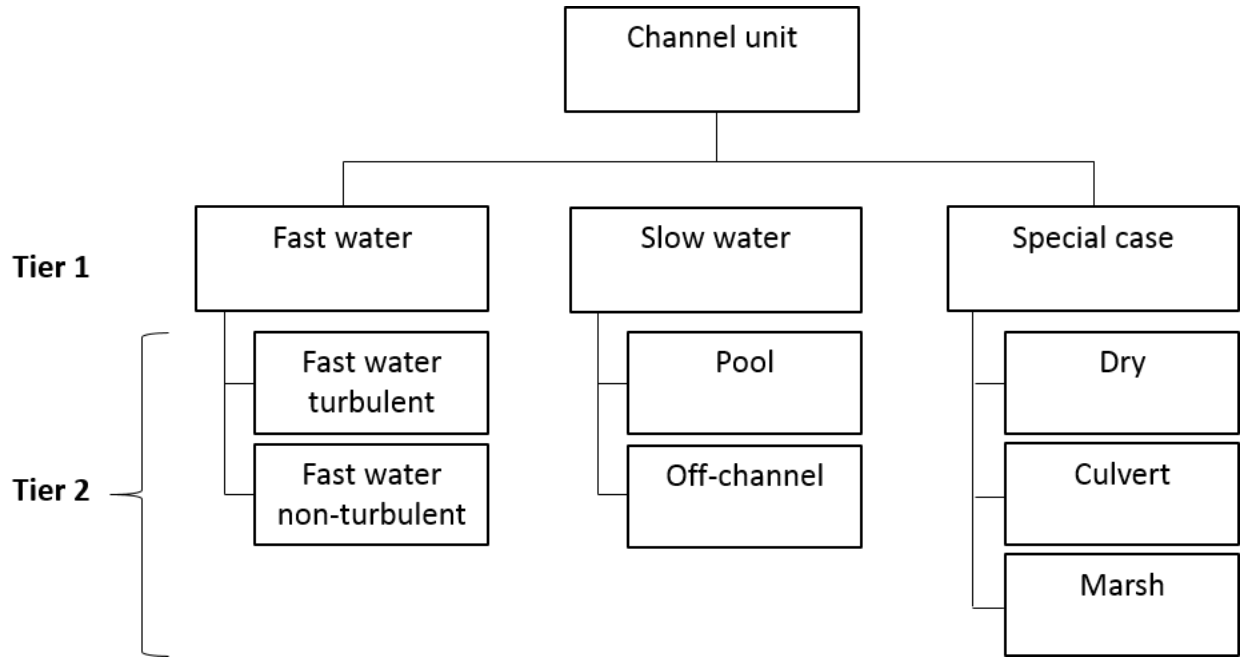

Figure 2. Hierarchical channel unit classification system modified from Hawkins et al. (1993).

Fast water units

Fast water turbulent (FT) channel units are high points in the bed profile that feature moderate to steep gradients, coarse substrate, and possess supercritical flow (i.e., hydraulic jumps sufficient to entrain air bubbles and create localized patches of white water). The bedform of these units generally lacks lateral and longitudinal concavity. Fast water turbulent units include a wide range of finer-scale channel unit types such as falls, cascades, chutes, rapids, and riffles, but we do not distinguish among these types for repeatability purposes.

Fast water non-turbulent (FNT) units, commonly called runs, feature low gradients (< 1 %), a generally uniform or planar bed profile and relatively smooth non-turbulent flow. Fast water non-turbulent units are distinguished from pools by their general lack of lateral and longitudinal concavity and often higher water velocity. These units are generally deeper than fast water turbulent units and often contain substrate ranging from sand to cobbles. Fast water non-turbulent units also include "sheets", which are common in bedrock-dominated streams and occur where shallow water flows uniformly over smooth bedrock of variable gradient.

Slow water units

Pools (PL) are low points in the bed profile that feature very low gradients (< 1 %), smooth non-turbulent flow, and possess both lateral and longitudinal concavity. A type of pool called scour pools are formed by scour that creates a depression in the streambed. A subtype of scour pool known as plunge pools are formed by bed scour resulting from the vertical fall of water over a channel-spanning obstruction such as woody debris, large substrate, or bedrock and are commonly shorter than they are long. Another type of pool called dammed pools have similar characteristics to scour pools except they are formed by impoundment of water upstream from an obstruction to flow (e.g., beaver dam, log jam, landslide). Owing to their characteristically slow water velocities, dam pools often have more surface fines than scour pools and fill with sediment at a more rapid rate. Dammed

pools are often wide at the downstream end, but not always very long. Although channel spanning plunge pools and dammed pools are not classified separately from other pools, it is important to be able to identify these pool types because they are exempted from the length criteria (i.e., they don't have to be longer than the average wetted channel width).

Off-channel (OC) units consist of low gradient (often 0%) alcoves and backwaters along channel margins that are connected to the main channel or side channels but have little (< 1%) to no flow through them. The thalweg never passes through off-channel units. The bedform profile in off-channel units is variable, but is often similar to pools. Substrate is generally dominated by finer sediment (silt to gravel) and organic matter. Off-channel units are often formed during high flows by eddy scour around obstructions on the channel margins or flow through side channels or floodplain depressions that are disconnected during low flow. Off-channel units are commonly found at the junction of non-qualifying side channels (Figure 1). In these cases, only the portion of the non-qualifying side channel that meets the physical characteristics of off-channel units described in Table 3 may be classified as off-channel. In these cases, off-channel units are assigned to the adjoining segment. No other portions of the non-qualifying side channel should be given a channel unit classification.

Special case units

Dry (DR) units are channel-spanning sections of the main channel or qualifying side channels that are dry at the time of the survey. Typical examples are riffles with subsurface flow or portions of side channels surrounding isolated pools. The length of the active channel that is dry must be greater than or equal to the active channel width in that segment to qualify as a separate dry channel unit. Additionally, if small puddles exist within a mostly dry channel but they are shorter or narrower than the active channel width in that segment, they are lumped with the surrounding dry channel unit.

Culvert (CV) units are sections of stream that pass through culverts. This classification does not apply to open-bottom culverts.

Marsh (MA) units are areas where the stream spreads out into a marshland and the streambed becomes indistinguishable from the surrounding wetland.

Field procedures:

1) Use the channel unit characteristics described above and in Table 3 to classify each channel unit while working upstream to lay out transects. Look for distinct changes in these features to determine unit boundaries.
2) Flag unit boundaries and assign a sequential number to each unit (U1, U2, U3, etc.). Also record the segment number that each unit belongs to (S1, U1). If a side channel is encountered during the reach layout, continue numbering channel units sequentially in the channel with the most flow until the upstream start of the side channel is located, then move to the downstream end of the side channel and proceed with numbering channel units in the side channel (Figure 1).
3) Record GPS coordinates at the downstream boundary of each channel unit in the middle of the wetted channel. For dry units, take a GPS reading at downstream boundary of the unit in the middle of the active channel.
4) Record whether the channel unit is flow-connected or not. Flow-connected channel units are connected by surface water (of any depth) to the downstream boundary of the reach. If there is any route that a small fish could swim (either upstream or downstream within the reach boundaries) to reach the downstream reach boundary, it is considered flow-connected.

Table 3. General channel unit characteristics.

Channel unit type						
Tier 1	**Tier 2**	**Gradient**	**Bedform profile**	**Substrate**	**Flow character**	**Formation**
Fast water	Fast water turbulent	> 1%	Topographic high points in the bed profile	Generally coarse substrate (cobbles and boulders)	Fast, turbulent flow with patches of white water	NA
	Fast water non-turbulent	< 1 %	Uniform depth, often deeper than faster water turbulent units, low complexity	Sand to cobbles	Generally slower water than fast water turbulent units but faster than pools, minimal surface turbulence	NA
Slow water	Pool	< 1 %	Laterally and longitudinally concave	Variable but generally smaller than fast water units	Slow water velocity, minimal surface turbulence	Formed by scour that creates a depression in the streambed (scour pool) or by impoundment of water upstream of an obstruction (dammed pool).
	Off-channel	0	Variable, but often laterally and longitudinally concave	Silt to gravel, organic matter common	Little to no flow, Thalweg does not pass through them.	Often formed during high flows by eddy scour around obstructions on the channel margins or flow through side channels or floodplain depressions that are disconnected during low flow.
Special case	Dry	variable	variable	variable	No flow, no surface water	NA
	Culvert	variable	Uniform depth	Sand to cobbles, corrugated metal, or concrete.	Variable, usually fast, turbulent flow	Culvert construction
	Marsh	0	No discernable streambed	Silt to gravel, organic matter common	Little to no flow, standing water	NA

3.0 Topographic survey

Surveys of stream channel and floodplain topography are conducted using methods described in CHaMP (2016a) and replicated here. The topographic survey is intended to provide the data needed to validate digital elevation models (DEMs) generated from the drone imagery. The topographic survey consists of using a surveying instrument (Total Station or Real Time Kinematic GPS (rtkGPS)) to collect a series of points and lines that capture topographic features within the stream channel and surrounding floodplain. Each point is attributed with a location (X, Y, and Z coordinates) and a description code. Points with the same description codes can also be connected to make lines. These points and lines are used to construct a DEM that represents a continuous topographic surface of the channel topography.

During the topographic survey, it is the responsibility of the person operating the prism rod to efficiently survey points and lines that accurately represent the channel's topography. The person operating the survey instrument captures these point locations during the survey. Table 4 provides descriptions of common terms used for topographic survey methods.

A stable, survey control network that can be reoccupied is the foundation for repeat topographic surveys and facilitating trend monitoring. The control network consists of a series of fixed points with known coordinates. The integrity of the control network through time depends on those fixed points being recoverable and re-occupiable with survey equipment (e.g., total station or rtkGPS). For example, for a total-station survey to take place in the coordinate system of the control network, the crew needs to be able to set up over a known fixed point and backsight to another known fixed point. If at least two inter-visible points do not exist, the total station survey cannot proceed without using more complicated surveying methods that are susceptible to large errors. There are many possible strategies one can employ to maintain the integrity of a survey control network (see Appendix I of the CHaMP (2016a) protocol). Total Station operating procedures are found in the Total Station Procedures Manual for the Columbia Habitat Monitoring Program (CHaMP 2016b).

The first priority of a survey crew at a new site is to properly establish benchmarks and then proceed with collecting topo data. The first priority of a survey crew at a revisit site is to reoccupy the original coordinate system, check benchmarks, and if necessary set new benchmarks and then proceed with collecting topo data.

Properly established benchmarks are integral to re-occupying a survey coordinate system at subsequent visits. Benchmarks will be surveyed repeatedly over many years, so it is imperative that benchmarks be established with the following criteria: stability, geometry, and inter-visibility (Figure 3). Stability refers to placing the benchmarks in locations that will be unaltered by natural processes or humans. Geometry refers to placing benchmarks in a large equilateral triangle as far apart as possible. Inter-visibility refers to the ability to see each benchmark location from the other 2 benchmark locations.

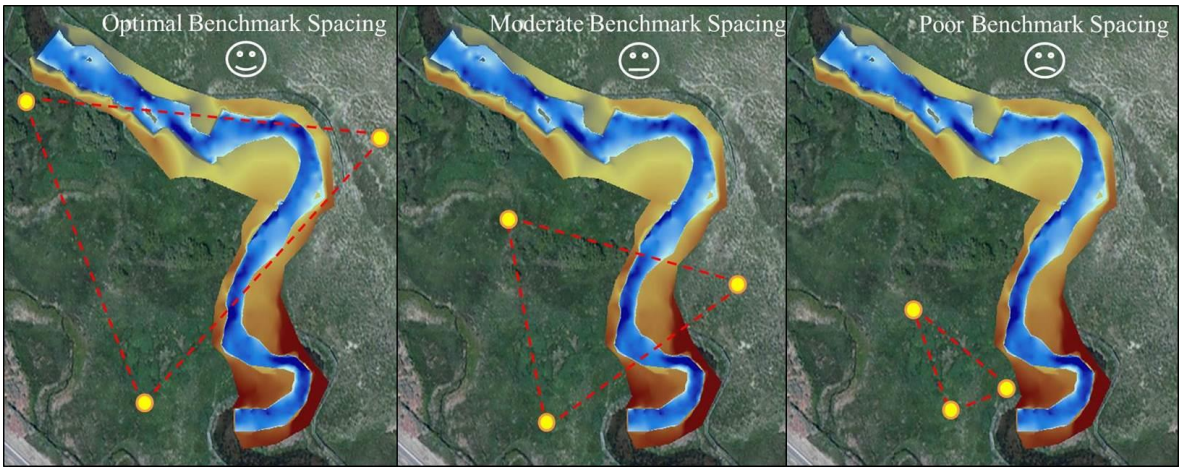

Figure 3. Examples of optimally, moderately, and poorly spaced benchmarks. Optimally placed benchmarks are as far apart as possible while still maintaining an equilateral triangle, are inter-visible, and extend the length of the site. Poorly placed benchmarks are close in proximity, in a non-equilateral triangle, and not inter-visible.

Table 4. Descriptions of commonly used terms for topographic survey methods.

Term	Description
Assumed Coordinate System	Fictional coordinate system of a survey established by attributing the first occupied point of a new site survey with the following coordinates: 3000 northing, 2000 easting, 1000 elevation. All new site surveys will be attributed an assumed coordinate system during the initial survey.
Backsight	Survey routine used to establish a basis for horizontal, vertical, and angular measurements within the surveying instrument. Backsight checks are used to assure the continued accuracy of a survey.
Benchmark	A permanent control point (typically capped rebar) used to establish new site surveys, and establish revisit site surveys. There is a minimum of 3 benchmarks established at each site.
Control File	File containing benchmarks and control points from previous surveys that are used to re-occupy the established coordinate system.
Control Point	Any permanent or temporary location (typically a nail and whiskers) used to set up or orient the surveying instrument. Includes any station setup, benchmark, and backsight locations.
Established Coordinate System	Spatially accurate coordinate system (Universal Transverse Mercator) established after the first survey of a site. All revisit site surveys must re-occupy the exact same established coordinate system as the first survey.
Foresight	A foresight is a control point that will be used for a future station setup location.
New Site Survey	The topographic survey of a new site where an established coordinate system has not been previously established. New benchmarks and control points must be established. The survey is conducted in an assumed coordinate system.
Re-occupy	To orient the surveying instrument into an established coordinate system for revisit site surveys using previously existing benchmarks and control points.
Resection	Survey routine used to re-occupy an established coordinate system by surveying at least 2 known benchmarks or control points from a centralized, previously unsurveyed point.

Term	Description
Revisit Site Survey	The topographic survey of a previously surveyed site where benchmarks and control points have been established. A Revisit Survey is conducted in a previously established coordinate system.
Stake Point	Survey routine used to check the accuracy of benchmark and control point locations when re-occupying an established coordinate system. Also used to re-locate the position of benchmarks and control points.
Traverse	Survey routine used to move the surveying instrument from one control point to the next. Done by 1) surveying a new control point (foresight) where instrument will be moved, 2) moving instrument to new location, and 3) backsighting to previous station setup location.

3.1 New site surveys

Field procedures:

1) Establish a minimum of 3 benchmarks with the following characteristics.
    a. Locations outside of the active stream channel.
    b. The ability to acquire a reasonable GPS signal.
        i. If using handheld GPS to obtain the benchmark coordinates, horizontal accuracy must be < 15m (< 5 is preferred).
        ii. If using RTK GPS to obtain benchmark coordinates, horizontal accuracy must be < 0.03 m and vertical accuracy must be < 0.015 m.
    c. Locations distributed as far apart as possible while still visible to one another. Attempt to distribute benchmarks as far along the entire length of a site as possible.
    d. Arrangement in an equilateral triangle. Ideally the stream will be contained within the equilateral triangle but this may not always be possible. If a stream has open space on one side, utilize it to the fullest extent. An equilateral triangle that extends the entire site length on one side of the stream is more ideal that a triangle that only spans ¼ the length of a site on both sides of the stream.
    e. Locations that can be re-occupied by a tripod. For example, do not place benchmarks too close to trees, fence posts, or other structures that would preclude proper set up of a total station.
2) Choose a benchmark or control point for the first station setup.
    a. Optimal locations for the first setup include:
        i. A vantage point that offers maximum line of sight to the channel for conducting the topographic survey, thereby minimizing the number of additional setups required for completing a survey.
        ii. Line of sight to all three benchmark locations.
        iii. Over a benchmark if both ‘a’ and ‘b’ are met.
    b. Control points refer to temporary or permanently monumented locations that are occupied by and/or used to orient the survey instrument during a survey.

i. Control points can be monumented by placing nail and whiskers in the ground, by etching a small “X” on a stable rock, or by establishing a piece of capped rebar. If the control point is one that is likely to persist until the next visit to the site (i.e., outside the active channel), consider using capped rebar.

ii. Control points are uniquely identified using the code “cp” and numbered sequentially in the order they are utilized during the survey (cp801, cp802, cp803 etc.). Benchmarks used as permanent control points are given the corresponding benchmark code (e.g., bm801, bm802, or bm803). The numbering convention corresponds to the year that the benchmark or control point was established (e.g., 600s for 2016, 700s for 2017, 800s for 2018).

c. After establishing an optimal location for the first station setup point, turn on, level, and measure the height of the instrument above the first occupied control point or benchmark.

3) Start a survey and establish the first station setup location on the instrument.

a. Open the survey template file on the total station. The template has preloaded codes that may be used during the survey (Table 4). Name the survey file using the following convention: SiteID-Date-Organization (e.g., CBW05583-007395-20160710-CRITFC). Use hyphens in place of underscores, spaces, or decimals when naming file; do not use spaces.

b. Navigate to the station setup menu of the survey instrument and initiate the setup routine. Choose to set up on a known point, and enter the appropriate code for the first setup point.

i. The first occupied point will always be labeled “cp801” unless it is established over a benchmark (whereas it would be labeled bm801, bm803, or bm803).

ii. The first occupied point of a new survey will always have the following coordinates: 3000 northing, 2000 easting, and 1000 elevation. These coordinates establish the first point in the assumed coordinate system (Table 4).

4) Establish a backsight and orient the survey instrument.

a. The orientation of the survey instrument is established by shooting to a backsight. The first backsight used during the initial setup of the instrument can be established over any of the permanently monumented benchmarks or control points. Establish a backsight over the benchmark/control point that is farthest from the occupied point.

b. Set up and level a tripod with tribrach and prism or survey rod with bipod and prism over the benchmark or control point used for backsighting.

c. Make sure that the total station is pointed at the backsight.

d. Check backsight and record error in the field notebook. Make sure the error is not greater than 0.030 m for horizontal error and 0.015 m for vertical error. Repeat procedures if backsight error is unacceptable. See Section 3.4 for backsight error troubleshooting steps.

5) Survey benchmarks and any visible control points.

a. Extra care should be taken to level the tripod or bipod and prism when shooting benchmark points as these points will be used to re-establish the location and orient the

survey instrument during future surveys of the site. Set the survey instrument to precise mode for these shots.

b. Begin survey following the methodology outlined in Section 3.5: Point Collection Methods.

3.2 Revisit site surveys

When revisiting a site, it is imperative to re-occupy the previously established coordinate system using the permanently monumented benchmarks. To re-occupy an established coordinate system during a site revisit, at least two known points must be inter-visible from each other or from a common point. The preferred revisit survey scenario involves setting up the survey instrument over a benchmark, backsighting to another benchmark, and conducting an accuracy check to the third benchmark. Make a concerted effort to clear vegetation or obstructions to make all benchmarks inter-visible from each other. Unforeseen factors may make it difficult or even impossible to locate benchmarks or see them from other benchmark locations. Therefore, you need to perform the appropriate station setup routine depending on the scenario encountered in the field. Utilize Figure 4 to determine the correct station setup routine for re-occupying an established coordinate system during a revisit site survey.

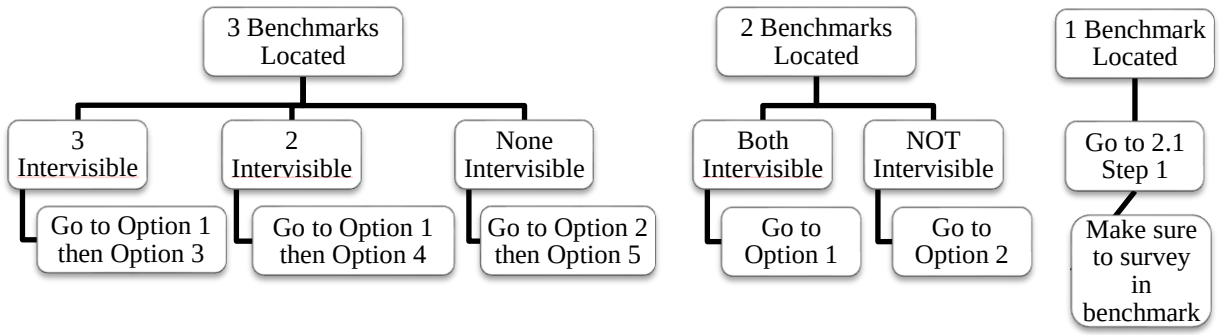

Figure 4. Revisit site scenarios used to determine the correct station setup routine after relocating benchmarks. Note that if no benchmarks are relocated, establish new benchmarks and proceed to Section 3.1.

Site Revisit Survey Options

Option 1: At least two benchmarks are inter-visible.

1) Start a revisit survey by establishing the first station setup.
    a. Set up surveying instrument over a benchmark that is visible from at least one other benchmark.
    b. Open the survey template file on the total station. The template has preloaded codes that may be used during the survey (Table 5). Name the survey file using the following convention: SiteID-Date-Organization (e.g., CBW05583-007395-20160710-CRITFC). Use hyphens in place of underscores, spaces, or decimals when naming files; do not use spaces.
    c. Import the site control file which contains previously established benchmarks and control points. The site control file will have the naming format "SiteID-Control-2018".
    d. Navigate to the station setup menu of the surveying instrument and initiate the setup routine. Choose to set up on a known point and select the appropriate point from the list (i.e., bm1).
2) Establish a backsight over a known point to orient the survey instrument.
    a. The orientation of the survey instrument is established by backsighting to a second benchmark. Set up and level a tripod with tribrach and prism or survey rod with bipod and prism over the benchmark used for backsighting. Select the appropriate backsight point from the menu (i.e., bm2).
    b. Make sure that the total station is pointed at the backsight.
    c. Check backsight and record error in the field notebook. Make sure the error is not greater than 0.050 m for horizontal error and 0.030 m for vertical error. Repeat procedure if backsight error is unacceptable. If survey crew is unable to establish revisit survey within error thresholds, see Section 3.4, Step 3 regarding revisit backsight checks.
    d. If necessary, establish additional benchmarks as described in Section 3.1, Step 1.
    e. If backsight errors are acceptable and three benchmarks are inter-visible, go to Option 3. If only 2 are inter-visible go to Option 4.

Option 2: At least two benchmarks exist but are NOT inter-visible.

1) Start a revisit survey by establishing the first station setup using the resection procedure.
    a. Locate a point that is visible from at least two other benchmarks and set up the surveying instrument.
    b. Open the survey template file on total station. The template has preloaded codes that may be used during the survey (Table 4). Name the survey file using the following convention: SiteID-Date-Organization (e.g., CBW05583-007395-20160710-CRITFC). Use hyphens in place of underscores, spaces, or decimals when naming files; do not use spaces.

c. Import the site control file which contains previously established benchmarks. The site control file will have the naming format “SiteID-Control-2018”.

2) Perform a resection following procedures outlined in Section 2.4 of the Total Station Procedures Manual (CHaMP 2016b).

   a. Make sure the error is not greater than 0.050 m for horizontal error and 0.030 m for vertical error. Start surveying. If three benchmarks exist but only two were used to resection, proceed to Option 4. If benchmarks cannot be resectioned within the error tolerance thresholds, begin surveying using procedures outlined in Section 3.1, Step 3. When establishing this new survey, make sure to pull in existing benchmarks from the previous survey. Keep the names consistent, retire the existing benchmarks and establish new ones.

   b. Be sure to survey all existing benchmarks and make sure that at least three benchmarks are inter-visible as described in Section 3.1, Step 1.

   c. If all three benchmarks were used during the resection, start surveying. If only two benchmarks were used during the resection, go to Option 5.

Option 3: Use Stake Point routine to survey third benchmark.

1) Complete Option 1.
2) From the first station setup location over the benchmark, use the Stake Points routine to “stake out” the third benchmark and evaluate the error results.
3) If the third benchmark is not within the error tolerance but the other benchmarks are, retire third benchmark and establish a new one.
4) Start surveying!

Option 4: Use Stake Point routine to survey third benchmark during the topographic survey.

1) Complete Option 1.
2) As the topographic survey is conducted you must find an opportunity to use the Stake Points function to survey the third benchmark.
3) If the third benchmark is not within the error tolerance but the other benchmarks are, retire third benchmark and establish a new one.
4) Start surveying!

Option 5: Use Stake Point routine to survey third benchmark.

1) Complete Option 2.
2) Immediately use the Stake Points procedures to survey the third benchmark or as the topographic survey is conducted you must find an opportunity to use the Stake Points function to survey the third benchmark.
3) Start surveying!

Table 5. List of codes used to identify unique points and lines in the topographic survey. Note that some codes are required for all CHaMP surveys.

Description Code	Name	Feature Type	Required	Definition
Water Surface Features				
lw	Left edge of water	Line or Point	Yes, Minimum of 50	Lines or points describing the elevation of the left wetted edge of the channel.
rw	Right edge of water	Line or Point	Yes, Minimum of 50	Lines or points describing the elevation of the right wetted edge of the channel.
mw	Mid-channel island	Line or Points	Yes, if island exists	Lines or points describing the wetted elevation of mid-channel qualifying islands.
br	Mid-channel bar	Line or Points	No	Lines or points describing the wetted elevation of mid-channel bars, large boulders, and non-qualifying islands.
ws	Water surface	Points	No	Points describing the water surface elevation above the stream bed at overhanging banks and mid-channel locations.
Channel Features				
bf	Bankfull	Line or Point	Yes, Minimum of 20	Lines or points describing the bankfull elevation.
bl	Breakline	Line	No	Other gradient breaklines as needed.
in	Inflow point	Point	Yes	Point at the upstream (top) end of the site indicating the inflow point of the thalweg.
out	Outflow point	Point	Yes	Point at the downstream (bottom) end of the site indicating the outflow point of the thalweg.
tb	Top of bank	Line	Yes	Lines describing the top of bank elevation.
to	Toe of bank	Line	Yes	Lines describing the toe of bank, or the line separating the active stream bed from the bank. Toe locations can be in and out of the water.
tp	Topography	Point	Yes	Points describing general channel topography.
u#	Channel unit	Point	Yes	Point describing channel unit perimeter within the wetted channel (named *u1*, *u2*, etc.).
wg	Thalweg	Line or Point	Yes, Minimum of 20	Lines or points describing the longitudinal thalweg profile.
Control Network				
cp#	Control point	Point	Yes	Control points used as station or backsight setup locations (*cp501*, *cp502*, etc.).
bm#	Benchmark	Point	Yes, Minimum of 3	Established benchmarks (*bm501*, *bm502*, etc.).
bos/tos	Control point	Point	No	Control points (rebar) used to define the bottom (*bos*) and top (*tos*) of site location markers.

3.3 Traversing

The traverse procedure is used to move the surveying instrument from one station setup location to the next and is required to propagate the coordinate system. This next station setup location is called a foresight and is typically a control point.

Field procedures:

1) Traverse to the next station setup location and move instrument.
    a. Check the backsight one last time and record error in the field notebook. Repeat procedures until the backsight error is within the acceptable limits. If error exceeds threshold, follow instructions outlined in Section 3.4.
    b. Assemble the second tripod or bipod over the control point that will be the foresight (i.e., cp802). Record the prism height above the point (rod height).
    c. From the current station setup location (cp801), survey in the new control point using the 'Traverse' routine.
    d. Moving forward: If you are using two tripods you will now have one tripod at the instrument and one tripod at the foresight. Remove the instrument from the tribrach, place it in the case, and move to the foresight. At the foresight, remove the prism from the tribrach and install the instrument (cp802). Check level bubbles and measure height of instrument. Install the prism on the tribrach at the previous station setup location (cp801). Check level bubbles and measure height of prism.
2) Occupying the second station setup location (Figure 6).
    a. With the instrument set up and leveled on the second station (cp802), the orientation of the survey instrument is established by shooting to the backsight (previous station setup location; cp801).
    b. Make sure that the total station is pointed at your previous station setup location (cp801) and conduct a backsight.
    c. Check backsight and record error in the field notebook. Make sure the error is not greater than 0.030 m for horizontal error and 0.015 m for vertical error. Repeat procedures if backsight error is unacceptable (see Section 3.4 for backsight error troubleshooting steps).

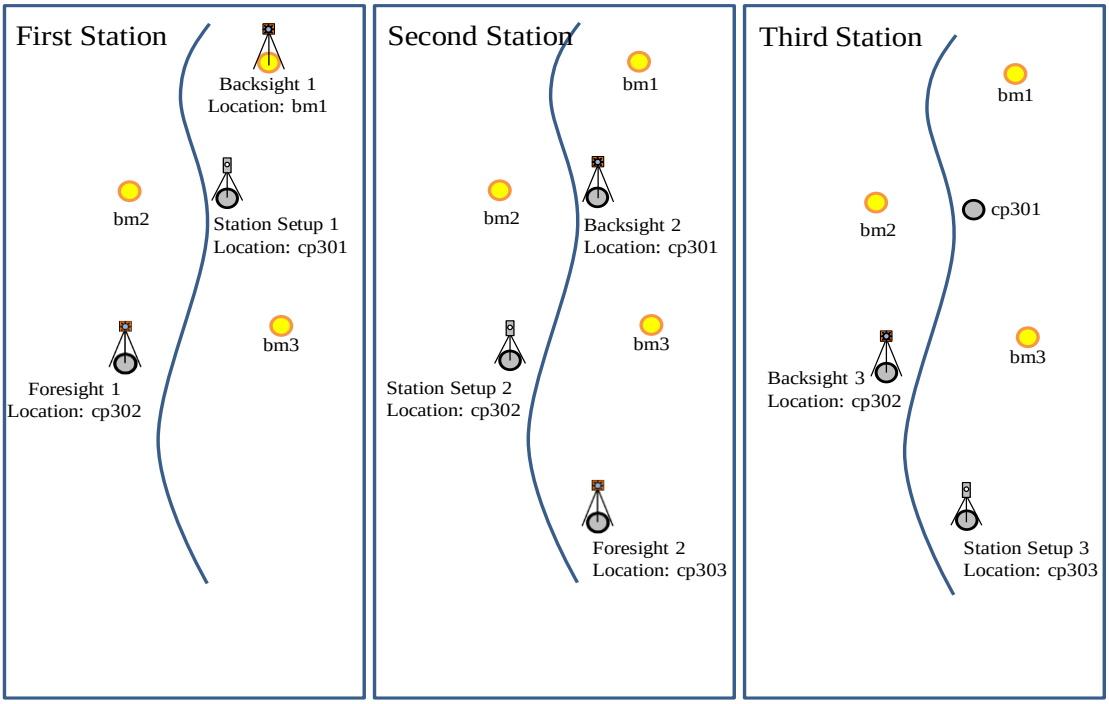

Figure 5. Illustration depicting station setup, backsight and foresight locations for the first station setup, after traversing to the second station setup, and after traversing to the third station setup.

3.4 Backsight checks

Horizontal, vertical, and angular errors can occur during surveying for many reasons. Therefore, it is important to periodically perform backsight checks to ensure that the survey is within allowable error constraints. Performing regular backsight checks also limits the total number of points that need to be resurveyed should a problem arise.

Field procedures:

1) Perform a backsight check:
    a. For every 50 to 100 points collected. Opportune times to perform a backsight check include when the rod person is taking a break and/or struggling through vegetation to position themselves for their next point.
    b. If the survey instrument or tripod legs have been bumped or knocked out of level. Make sure to check that the instrument is centered over point and re-level station before checking backsight.
    c. If the instrument has been exposed to a noticeable shift in temperature over the course of the survey (e.g., heating up in the sun).
    d. Before and after moving the survey instrument.
    e. Before closing the survey.
2) During a backsight check, if horizontal error exceeds 0.030 m or vertical error exceeds 0.015 m for new sites, conduct the following checks:

a. Re-measure the height of rod and the height of instrument and check that they were recorded correctly within survey instrument. Re-check backsight error.

b. If error remains unacceptable, re-level the survey instrument, conduct the setup or traverse routine again, and re-check the backsight error.

c. If error persists, double-check that the currently occupied point number and the backsight point number are entered correctly.

d. If backsight error is unresolved once the above checks have been conducted, move survey instrument back to the previous successfully occupied station setup location. Conduct setup routine and survey in a new control point. Move and set up survey instrument on the newly surveyed control point and check backsight error.

3) When establishing a revisit survey, if horizontal error exceeds 0.050 m or vertical error exceeds 0.030 m upon setup, conduct the following required checks in addition to those steps outlined above.

a. Check occupied point and backsight point coordinates. Compare the coordinates in the surveying instrument.

b. If possible, backsight to an alternate known point (benchmark or control point) and check error values.

c. If error persists once the above have been checked, set up instrument over an alternate known point (benchmark or control points) and check backsight errors using the other benchmark locations.

d. If unable to reduce error values once all above checks have been conducted, record error values in field notebook and begin survey using procedures outlined in Section 3.1, Step 3. When establishing this new survey, make sure to pull in existing benchmarks from the previous survey. Keep the names consistent, retire the existing benchmarks and establish new ones.

3.5 Point collection methods

The objective of the topographic survey is to capture X, Y, and Z coordinates as points and lines that collectively represent the topographic surface of the stream channel and floodplain. Many topographic surveys are time-limited, thus topographic points and lines must be collected efficiently and strategically to maximize the quality and utility of the DEM. The number of survey points collected is dependent on the size and complexity of the site. Complex topography should be represented with a higher density of points (approx. 1,000-1,200 points) compared to simpler planar topography (500-600 points). Larger sites may have more points overall but generally have less topographic complexity and a lower density of points.

Collect survey points at locations that represent changes in slope (inflection points). When capturing streambed topography, avoid capturing elements of bed roughness (e.g., substrate). Instead, focus effort on capturing the bedform of the channel. Extend survey points far enough into the floodplain so that the areal extent of the survey encompasses all large and small side channels in areas where lateral migration may occur.

Survey points and lines are attributed with a description code that is used to further represent features in the stream channel (Figure 6). Use the topographic descriptions in Table 5 to identify and code survey points and lines throughout the site.

Points: Points are used to capture changes in topography that are not captured by lines. Use points to capture non-linear features including general topographic features and channel unit boundaries.

Lines: Lines are connections between two or more survey points and are used to efficiently capture visible contours or breaks in the stream channel topography. Lines are best used where there are identifiable linear features such as the edges of water, and tops and toes of banks.

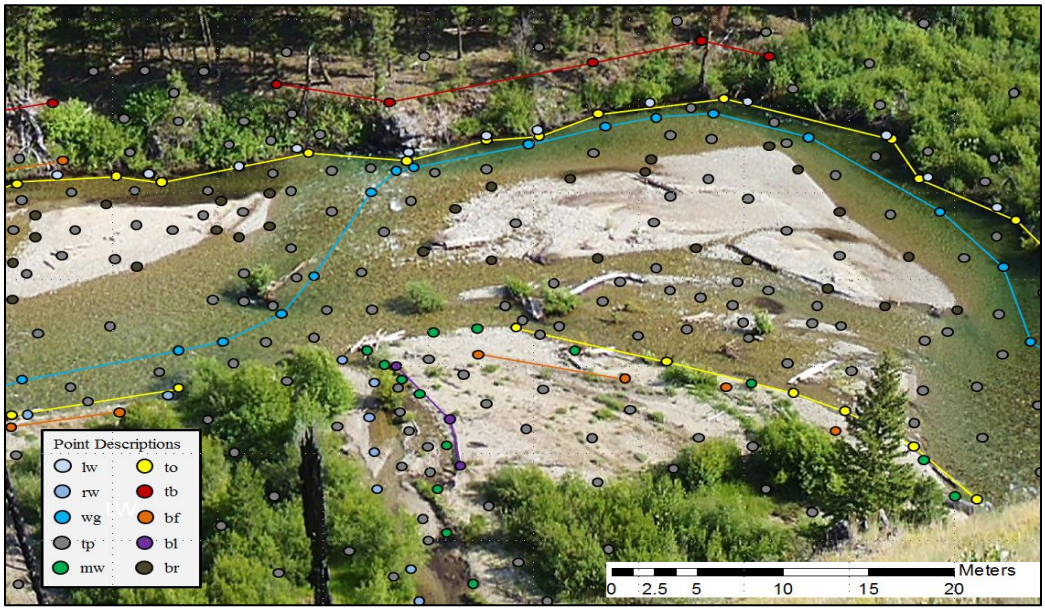

Figure 6. Representation of topographic points and descriptions used to capture the topography of the stream during surveys.

Channel cross-sections

Channel cross-sections are detailed measurements of the lateral profile of the stream channel and are used primarily to define the downstream and upstream extent of the topographic survey and to provide precise measurements of channel dimensions (e.g., mean bankfull width and depth). Cross-sections are surveyed at all odd-numbered transects (i.e., transects 1, 3, 5, 7, 9, and 11).

Field procedures:

1) Measure the bed elevation along the transect line perpendicular to the flow. The cross section should span the active channel and a portion of the floodplain, including notable features such as terraces, islands, or other features defining the constraints of the channel. Within the active channel, take measurements at regularly spaced intervals (approximately 15-20 points per channel width). Measure additional points representing slope breaks in the streambed or banks, bankfull elevation, water surface, and maximum depth. Place the rod firmly on the wetted bottom but don't dig it in. Avoid the tops of isolated boulders and logs (or shoot at close intervals to accurately measure very large boulders). If adjacent side channels are present, extend the cross-section laterally to include both the main channel and adjacent side channels.

2) The bottom of site cross-section at transect 1 must have a point indicating the outflow point at the thalweg coded *out*. This point should be offset by approximately 10 cm upstream of the cross-section line.

3) The top of site cross-section at transect 11 must have a point indicating the inflow point at the thalweg coded *in*. This point should be offset by approximately 10 cm downstream of the cross-section line.

4) Required point descriptions include inflow or outflow points (*in*, *out*) and left and right edge of water points (*lw*, *rw*). If bankfull, top of bank, and toe of bank (bf, tb, to) features exist at these cross-sections, it is important to collect these points with the proper description.

Water Surface Features – lw, rw, ws, mw, br

Wetted surface feature codes are used to represent the planform and elevation of the water surface.

Field procedures:

1) **Left and right wetted edge of the channel (*lw, rw).*** Left and right wetted edge features represent locations where the water surface elevation contacts the stream bank.

    a. Always survey *lw* and *rw* points on the furthest outside perimeter of the main channel or side channels. Use alternative codes to describe the edge of water for islands (*mw*) and bars (*br*) on the inside perimeter of the main channel and qualifying side channels.

    b. Survey *lw* and *rw* points as either lines or points. Lines make the survey processing easier to interpret and help to create better topographic surfaces.

    c. In streams that are flat and straight, fewer points will be needed to adequately represent the wetted channel edge (approximately 50 points per edge). Add more points to the edge of water for streams that feature a complex planform and water surface elevations. Complex edge of water areas should be collected using lines.

2) **Wetted edge of mid-channel islands (mw)**. Mid-wetted (*mw)* island points and lines are used to indicate water surface elevations surrounding qualifying mid-channel islands.

    a. Only survey *mw* points or lines at locations representing the wetted perimeter of qualifying islands (length ≥ average bankfull width and completely surrounded by water).

3) **Wetted edge of mid-channel bars (br)**. Bar (*br*) points and lines are used to indicate water surface elevations surrounding mid-channel bars, non-qualifying islands, and large boulders.

    a. Survey enough *br* points at the wetted edge of mid-channel bars and non-qualifying islands to provide a general representation of their wetted perimeter.

    b. Place topographic points (*tp)* on mid-channel bars and non-qualifying islands to represent the topography above and below the water surface elevation.

4) **Water surface (ws)**. Water surface points (*ws*) are used to represent locations where the water surface elevation is above the stream bed (Figure 7A).

    a. Survey *ws* points at locations where edge of water points (*lw/rw*) are not appropriate such as at overhanging banks. Also survey *ws* points at mid-channel locations where the lateral water surface elevation is not uniform (i.e., pitched riffles; Figure 7B).

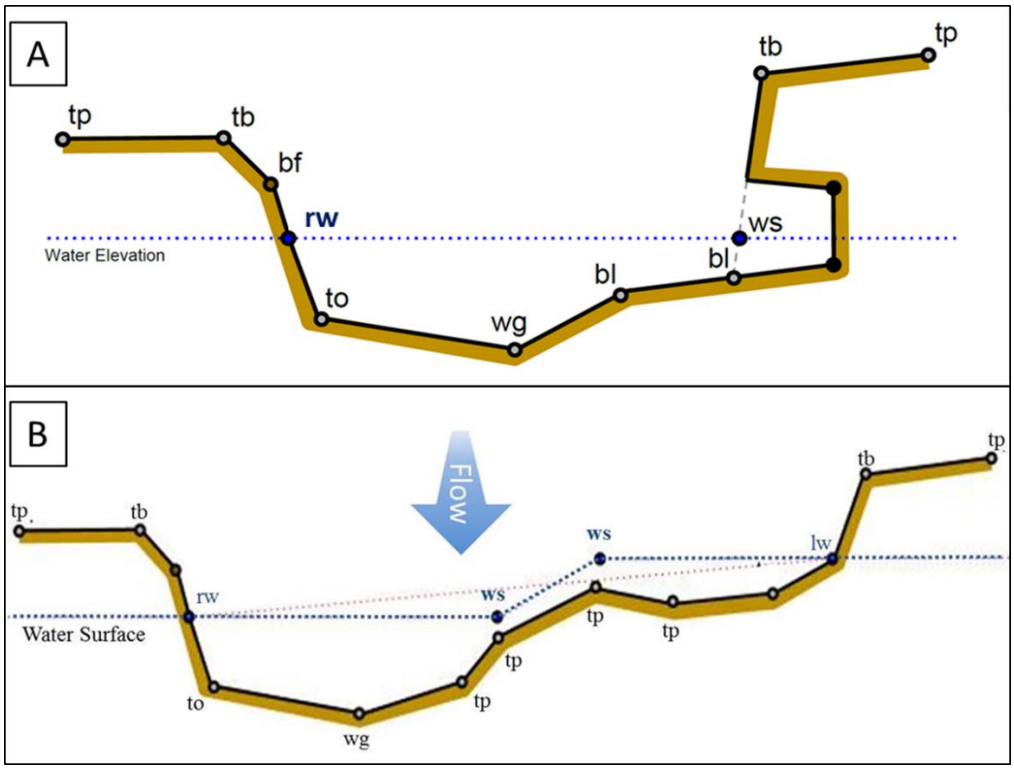

Figure 7. Channel cross-section indicating how water surface points (ws) are used to represent A) the water surface elevation at overhanging banks and B) mid-channel water surface gradient changes (i.e., pitched riffles).

Top and Toe of Bank Features – tb, to

Field procedures:

1) **Top of bank (*tb*).** Use top of bank lines to accurately represent convex gradient breaks that occur where steeper stream banks transition to flat floodplain-like features (Figure 8). In general, top of bank lines will run parallel to the channel but at times may run perpendicular to the channel on more complex banks.
2) **Toe of bank (*to*).** Use toe of bank lines to represent the bottom of the stream bank where the stream bed (typically courser substrate) and bank (typically finer substrate) meet. These concave gradient breaks occur where the stream bed transitions into a steeper stream bank.
    a. The toe of bank can be both inside and outside of the water.
    b. The toe of bank may not be present or clearly defined, such as along point bars with gradually sloping banks. In these cases, capture the general shape of the channel using topo points.

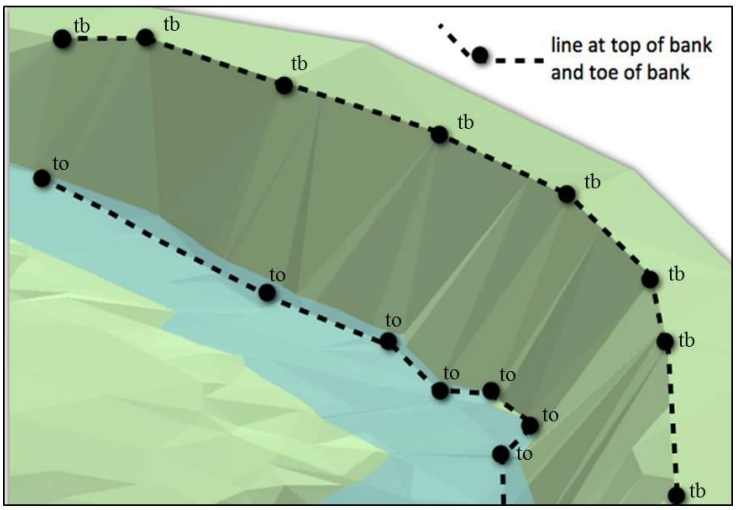

Figure 8. Channel view showing proper use of top of bank (tb) and toe of bank (to) lines.

Bankfull elevation - bf

Field procedures:

1) Survey bank features that are indicative of the bankfull elevation (Table 1). Bankfull features can be surveyed using points or lines.
    a. Use lines to survey bankfull features along consistent gradient breaks. These lines should be surveyed where stream banks transition to flat floodplain like bank features that are consistent with the bankfull elevation, and anywhere that the bankfull elevation represents a continuous linear feature in the landscape.
    b. Use points to survey bankfull features where the bankfull elevation is identifiable but does not appear as a continuous linear feature in the landscape.
2) A minimum of 20 bankfull points is required to be surveyed throughout the length of the reach at locations that have good bankfull indicators as described in Table 1.

Main Channel Thalweg - wg

The thalweg is the deepest point of the wetted channel with the most continuous flow. Longitudinal stream profiles along the thalweg are commonly used to calculate metrics such as residual pool depth, gradient, and bedform complexity.

Field procedures:

1) Survey thalweg (*wg*) points and lines at inflection points that accurately represent the thalweg profile (Figure 9). Take a minimum of 40 points throughout the site.
    a. Use lines to survey the thalweg profile on sections of channel when it is identifiable as a line running roughly parallel with the channel. Thalweg lines should extend the distance of the site in very small streams (usually 6 m wide or less) and contain enough points to capture inflection points in the thalweg (Figure 9).

b. In steeper streams dominated by fast water turbulent channel units and in some plane-bed streams, the thalweg profile will often be discontinuous. In these situations, survey the thalweg profile using a series of points.

2) Only label wg points and lines in the main channel. Use breaklines (bl) and/or topo points (tp) to capture the thalweg in side channels.

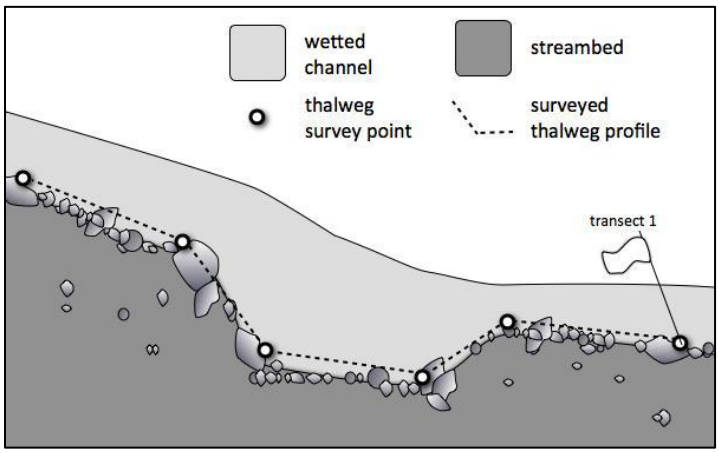

Figure 9. Longitudinal view of the stream channel showing the location of survey points that effectively capture inflection points in the thalweg profile.

Channel Unit Perimeter – u#

Channel unit perimeter points are surveyed to provide a representative outline of channel units. Channel units may be adequately represented by at least two points or up to as many as 8 points if they are larger and more complex.

Field procedures:

1) For each channel unit point, use a code that is consistent with the channel unit number being recorded (e.g., u1, u2, etc.).

2) In general, points describing the perimeter of channel units are surveyed at the edge of water (Figure 10). However, complex units may require additional channel unit vertices located in the wetted channel.

   a. In areas where multiple units converge in the wetted channel it will be necessary to survey additional perimeter points that represent the boundaries of each unit.

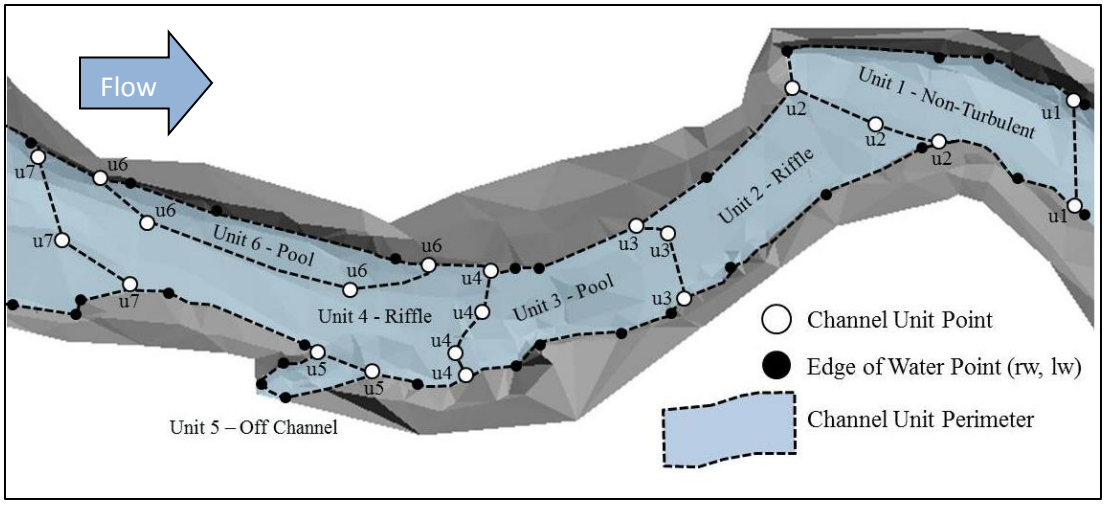

Figure 10. Channel unit perimeter and edge of water points. Figure from CHaMP (2016).

Topographic Points – tp

Topographic points represent features of the streambed or floodplain topography that do not follow a consistent line or fit any other definition listed in Table 5.

Field procedures:

1) Survey topographic points sparsely in areas that are topographically uniform, and densely in areas that are topographically complex.
2) Always capture the deepest portion of the stream, tail crest of pools, and maximum depth of pools using topographic points (if not already captured by thalweg points). The pool tail crest is defined as the highest point in the streambed profile at the downstream end of pools (i.e., hydraulic control) where the pool transitions into the next downstream channel unit (Figure 11).

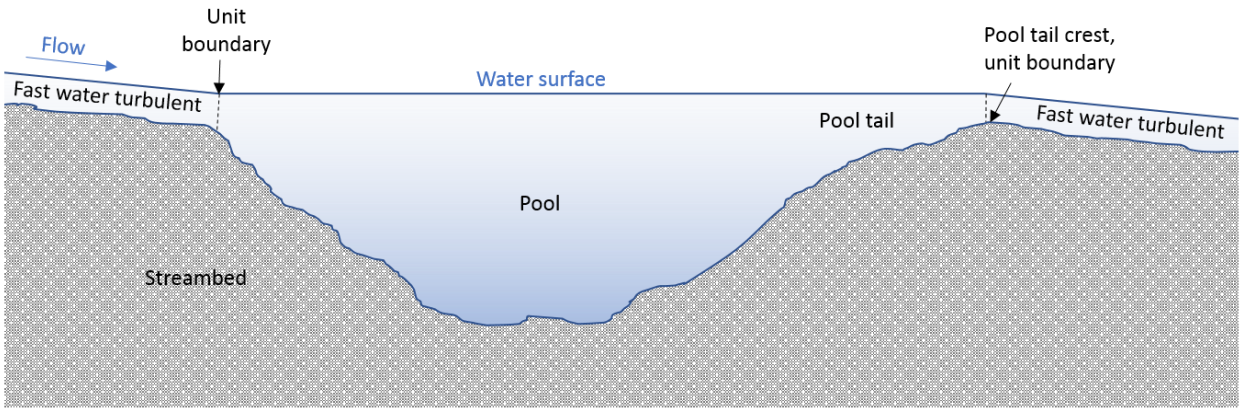

Figure 11. Longitudinal profile of a pool showing the location of the pool tail crest.

Breaklines - bl

1) Survey breaklines to represent linear features in the landscape along any consistent gradient breaks that are not represented by other line codes.

    a. Breaklines may run parallel or perpendicular to the channel, and are often used to represent obvious breaks in the channel including tops and bottoms of steep drops (e.g., falls), and artificial structures (e.g., bridge columns).

Side Channels and Islands

1) Side channels:

    a. All qualifying side channels will be encompassed in the topographic survey. If non-qualifying side-channels exist within the survey extent, minimally survey them to capture the general topography.

    b. Survey side channels using the same set of procedures and codes as the main channel when possible. Use breaklines and/or topo points (*tp*) to capture the thalweg of all side channels.

    c. Some small side channels are very brushy making surveying difficult. In these instances, at a minimum survey the thalweg as a breakline (*bl*) and edge of water (*lw/rw* and *mw*) lines throughout the side channel along with topo (tp) points on either bank. Survey additional codes (*tb*, *to*) to further define the side channel when possible.

    d. Other side channels can have little to no flow. In instances where a small side channel is only partially wet (island forms a peninsula), survey edge of water (*lw/rw*) points/lines along the wetted perimeter.

2) Islands:

    a. The wetted perimeter of qualifying mid-channel islands should be represented with the *mw* code. Collect bankfull, top of bank, toe of bank, and topographic points where appropriate to adequately represent the topography of the island.

    b. Survey the perimeter of all non-qualifying islands, bars, and large boulders with the *br* code.

    c. Survey channel unit perimeters in all side channels.

4.0 Auxiliary survey

4.1 Substrate size

Substrate particle size distribution of the streambed surface is measured using a Wolman pebble count procedure (Wolman 1954) within each primary channel unit type (fast water turbulent, fast water non-turbulent, and pool units). Pebbles are not measured in off-channel or special case units. A minimum of 100 particles are measured within each channel unit type. Pebble counts are conducted along 10 “pebble transects” (terminology used to avoid confusion with primary reach transects) distributed evenly across the available channel unit types. Ten pebbles are measured per pebble transect, resulting in 300 particles per reach. Particle size is measured along the intermediate or b-axis of each particle using a template or gravelometer with square holes corresponding to the Wentworth scale (Table 6).

Field procedures:

1) Pebble transect locations within the reach: Count the number of channel units of each type (excluding off-channel and special case units) and evenly distribute 10 pebble transects among the first 10 units of each type (working upstream). If there are fewer than 10 units of a given type, place additional pebble transects in the most downstream units.

2) Pebble transect locations within channel units:

    a. If there is only 1 transect allocated to a unit, place the transect at the midpoint of the unit. If there are multiple pebble transects in a unit, equally distribute them throughout the unit.

    b. Ensure that pebble transects are spaced no closer than the Dmax particle size (maximum particle dimension) within the sampling area to avoid double counting particles. If this is not possible due to limited sampling area, increase the number of particles measured per transect and decrease the number of pebble transects while maintaining a total count of 100 particles per channel unit type.

3) Visually divide each pebble transect into 10 equally spaced sample points running perpendicular to the stream channel and spanning the width of the bankfull channel (from toe of bank to toe of bank). Do not sample streambank particles. Ensure that sample points are spaced no closer than the Dmax particle size. If it is not possible to sample 10 particles while maintaining this particle spacing, reduce the number of particles per transect and increase the number of pebble transects. If there is insufficient sampling area within a given channel unit type to measure 100 particles while maintaining the prescribed spacing between pebble transects and sampling points, measure as many particles as possible.

4) Using a consistent pace between sample points, select a particle by averting your eyes and extending your finger straight down to the tip of your boot and picking up the first particle that you touch. Avoid changing your pace or trajectory to avoid large boulders, deep water, or other obstacles. Use a consistent location on your boot to minimize bias against smaller particles.

5) Use a gravelometer to classify the b-axis of each particle. Identify the largest square hole that the particle does not fit through—this corresponds to the low end of the size category for that particle. For example, if a particle fits through the 180 mm square but does not fit through the 128 mm square, the size category is > 128 – 180 (Table 6).

    a. For particles larger than 180 mm, use the gradations along the edge of the gravelometer or a depth rod to measure the b-axis. The edge of the gravelometer, which is 2 mm thick, can be used to identify particles less than 2 mm.

    b. If your finger touches a layer of fine sediment that completely covers larger rocks beneath, measure the fine sediment. Conversely, if your finger touches a rock that is covered by individual fine sediment particles, measure the underlying rock.

    c. Record “bedrock” when encountered at sample points.

    d. If particles are embedded and cannot be removed from the streambed, use the edge of the gravelometer or a depth rod to measure the b-axis of the exposed portion of the embedded particles.

    e. If particles are inaccessible due to deep water, use an underwater scope and visually estimate the size of the particle using the depth rod or your boot size for reference.

Table 6. Size gradation for sediment in the range of fines (sand, silt, clay) to boulders (Wentworth scale).

Particle size description		Particle size (mm) Minimum	Maximum
Bedrock		NA	NA
Boulder	mega	> 4096	NA
	very large	> 2896	4096
		> 2048	2896
	large	> 1448	2048
		> 1024	1448
	medium	> 724	1024
		> 512	724
	small	> 362	512
		> 256	362
Cobble	large	> 181	256
		> 128	181
	small	> 90.5	128
		> 64	90.5
Gravel	very coarse	> 45.3	64
		> 32	45.3
	coarse	> 22.6	32
		> 16	22.6
	medium	> 11.3	16
		> 8	11.3
	fine	> 5.66	8
		> 4	5.66
	very fine	> 2.83	4
		> 2	2.83
Fines (Sand, Silt, Clay)		< 2	2

4.2 Large woody debris

All large woody debris (LWD) meeting the minimum size criteria that is within, partially within, or suspended over the active channel is counted using methods adapted from the Oregon Department of Fish and Wildlife (ODFW) Aquatic Inventories Program (AIP; Moore et al. 2017). The minimum size requirement for wood to be counted is 15 cm diameter and 3 m in length as measured at 2m from the base of the stem (i.e., where the root wad meets the stem) or from the largest diameter of the main stem. Root wads < 3 m in length are an exception and all are counted. Live trees (including trees growing from dead nurse logs) are not counted as LWD.

Field procedures:

1) Count all LWD pieces including root wads and assign each to the channel unit that contains the largest volume of the piece. If the piece is not within the wetted perimeter of a channel unit, assign it to the nearest channel unit.

4.3 Solar input

Solar radiation entering the stream channel (termed solar access) is measured at all 11 transects throughout each reach using the Solmetric SunEye (model 210). To ensure accurate measurements, it is best to capture images during conditions of low sun angle (i.e., near dawn and dusk) or uniform overcast sky. Additionally, the SunEye should be held level and steady during operation to ensure that images are clear and accurate (Figure 12).

Field procedures:

1) Each SunEye image, or "skyline", is stored in a work session. Create a new work session for the reach using the reach id and date separated by an underscore (e.g., CBW05583-108010_20180715).
2) Measure solar input at the center of the main wetted channel at all 11 transects. If a mid-channel bar is present in the center of the wetted channel, conduct the solar reading over the bar. If an island is present in the center of the channel, conduct the solar reading over the center of the main channel.
3) Hold the SunEye 30 cm above the water surface (or dry bar) and orient the instrument so the heading is pointed south and the instrument is level. Stand on the north side of the instrument and ensure that you or other field crew are not blocking the sun path on the image viewer. Capture the image.
4) Review the image to ensure that it is not blurry and that no people or unintended objects are blocking the sun path. Retake the image if necessary. Delete all bad images.
5) Save each skyline image using the transect number that it corresponds to (T1, T2, T3, …, T11).

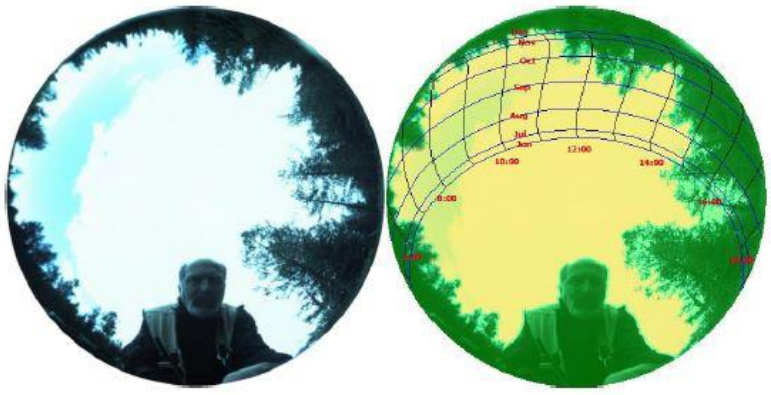

Figure 12. Example of a good quality skyline image showing a) the raw fisheye view, and b) the annual sun path view showing the time of year and day when the stream is exposed to sun (yellow) and shade (green).

4.4 Discharge

Discharge is measured at a single, carefully chosen cross-section within the survey reach boundaries using methods described in CHaMP (2016a). Ideal locations for discharge measurement include straight channels with approximately uniform depth and velocity. Fast water non-turbulent channel units with U-shaped channel cross-sections that are free of obstructions provide the best conditions for measuring discharge. Avoid areas with non-uniform cross sections, excessive surface turbulence, eddies, split channels, or very slow water velocity (e.g., pools). Ideally, average water depth should be above 15 cm and velocities above 0.15 m/s. It is acceptable to remove rocks and other obstructions to improve the cross-section before any measurements are made.

Field procedures:

1) Ensure that the velocity meter is charged, calibrated, and operational.
2) Identify cross-section location:
    a. Identify a cross-section location that meets the general criteria described above.
    b. If an appropriate cross-section location cannot be found within the reach, extend the search upstream or downstream of the site boundary, avoiding locations with different flow conditions due to tributaries or side channels.
    c. Avoid locating cross-sections in channels with less than 100% of the flow (i.e., adjacent side channels are present). If this situation is unavoidable, such as a braided channel, take separate cross-section measurements, one in the main channel and one in the side channel(s).
3) Set up cross-section and identify measurement locations:
    a. Stretch and secure a meter tape across the stream perpendicular to the flow with the "zero" end on the left bank.
    b. Divide the total wetted stream width into 15 to 20 equally spaced intervals (Figure 37). To determine interval width, divide the width by 15 or 20 and round up to a convenient number (e.g., nearest 0.05 m). Intervals should not be spaced less than 10 cm apart, even if this results in less than 15 intervals.
    c. Take the first depth and velocity measurement at the left edge of water. Conduct the second measurement one interval out from the left bank and continue measurements at each interval. The last depth and velocity measurement will be at the right edge of water.
4) Measure depth and velocity:
    a. Stand downstream of the velocity meter when taking measurements.
    b. Place the topset rod in the stream at the interval point and record the water depth. Set the topset rod to the correct height. This will raise or lower the velocity probe to 60% of the water depth at that interval. Position the velocity probe directly perpendicular to the stream channel and hold the topset rod vertically level. Wait for the progress on the velocity meter to go through a full 10 second cycle (i.e., fully through 0% to 100%). Record the velocity. Move to the next interval point and repeat the same procedure until depth and velocity measurements have been recorded for all intervals. If the depth is 0, record the velocity as 0. If velocity is negative (-), record the measured velocity.

c. Take the last depth and velocity measurement at the right edge of water. Verify that the tape distance of your final measurement recorded in the data logger is equal to the tape distance at the right edge of water.

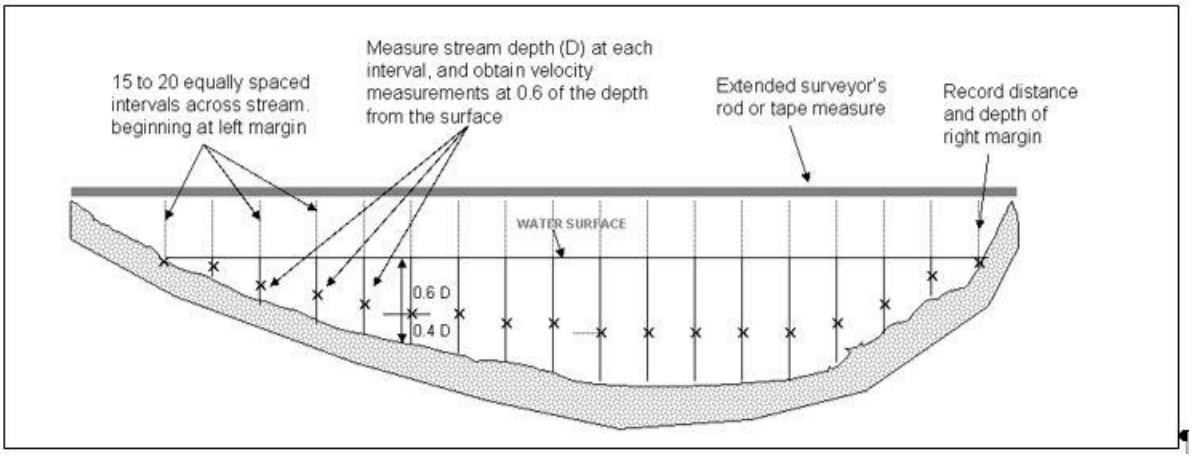

Figure 13. Cross-section of a streambed showing the locations of discharge measurements. Figure from CHaMP (2016a).

4.5 Conductivity

Stream conductivity (measured in micro-Siemens per centimeter or µS/cm) is a measure of the ionic content of water and has been linked to stream primary production and fish growth (Saunders et al. 2018).

Field procedures:

1) Before leaving for the field, ensure that the batteries in the conductivity meter are charged and the instrument is calibrated and operational.
2) Collect a sample of water from a well-mixed, flowing portion of the main stream channel within the boundaries of the survey reach.
3) Measure conductivity using the guidelines provided in the instrument instruction manual and record the reading in the data logger. Retake the measurement to ensure that the results do not fluctuate substantially.

4.6 Water temperature

Temperature monitoring methods were adapted from CHaMP (2016a). Year-round hourly water temperature is measured using Onset HOBO TibiT temperature data loggers at all survey reaches. Loggers were installed during previous site visits, so new logger deployments will not be necessary unless the loggers have been lost or damaged. Loggers should be downloaded and re-launched no later than July 15 to ensure that peak summer temperatures are captured. Temperature data should be downloaded again in the fall and before high spring flows.

If a new temperature logger is installed or a logger is moved, there are two acceptable options for logger installation (i.e., the epoxy method and the cable method). In both cases, the logger is placed in a PVC

housing unit to protect the loggers from solar radiation and damage during high flows. Housing units are drilled with multiple holes (1/4 – 1/2 in diameter) to ensure adequate exchange of flowing water.

Epoxy method: Search for a large rock or boulder that will be immobile during large floods and is easy for others to identify on subsequent site visits. Finding a good rock is the most important step to a successful logger installation. If a suitable rock is not available, consider placement using the cable method.

Optimal placement locations for the epoxy method include: 1) rocks, boulders, or structures that will not move or be disturbed at high flows, 2) boulders large enough that they protrude above the low flow water surface and wide enough that they can effectively shield the logger from moving rocks or debris during high flows, 3) areas downstream of large rocks in pockets of relatively calm water with smaller substrate sizes, and 4) a relatively flat downstream attachment surface that is deep enough to remain submerged in flowing water for the entire year.

Cable method: If there is not a suitable rock or boulder within or near (< 100 m) the site, identify a secure location such as the base of a tree or root wad to attach the logger using a steel cable Stainless steel cable ≥ 1/16 in diameter is recommended (galvanized cable will rust and break rapidly). It is also acceptable to attach the cable to a metal stake or rebar driven securely into the streambed (cement form stakes 2 – 2.5 ft long are recommended). A 1-2 oz weight is attached to the cable to ensure the logger and housing unit remain submerged.

Optimal placement locations for the cable method include: 1) areas with sufficient stream flow that will maintain year-round flow, but outside of strong currents, 2) areas that will not allow the logger to get hung up in vegetation or left on the bank at high flows, 3) areas away from seeps or steep banks on the side of stream to avoid groundwater influences, 4) camouflaged or inconspicuous areas at sites with high public use.

Suitable locations for attaching loggers may be relatively rare within low-gradient, meadow reaches. In these instances, examine potential placement locations no more than 100 m upstream or downstream of the site and away from tributary influences.

<u>Office procedures before leaving for the field:</u>

1) Check the accuracy of all temperature loggers using an “ice bucket” method prior to installing in the field (Dunham et al. 2005). Accuracy should not exceed ± 0.2 °C.
2) Ensure the laptop computer battery is fully charged and the date and time are correct.
3) Open the HOBOware software and check that it is set to standard international (SI) units (this ensures that temperature is recorded in degrees Celsius, not Fahrenheit).
4) Connect the HOBO shuttle to the laptop using a USB cable and check the battery level on the HOBO shuttle. Replace if necessary.
5) Sync the shuttle with the laptop. This ensures that any temperature loggers launched with the shuttle are programmed with the correct date and time. **Critical note: the shuttle must be re-synced with the laptop any time the shuttle batteries are replaced prior to launching or downloading any temperature loggers.**

<u>Field procedures:</u>

1) Installing new loggers:
    a. Identify a suitable logger location and installation method using the guidance above.

b. Record the logger serial number.

c. Connect the shuttle to the laptop computer, attach the logger to the shuttle and squeeze the black plastic lever on the shuttle coupler to establish a connection with the logger. Once connected, launch the logger. Set the start date and time for the next hour (on the hour) of the current day and set the logging interval to 1 hour. Ensure that the launch was successful (see message at the bottom of the HOBOware screen), then disconnect the logger.

d. Attach the logger to the inside of a PVC housing unit using plastic zip ties and install the logger.

e. Record GPS coordinates at the logger location (Preferred format UTM, NAD83).

f. Record the stream bank (facing downstream) that the logger is nearest to and the distance from the stream bank. If cable is attached to a tree on the bank, record the distance from bank as 0.

g. Record the attachment method ("Cabled to tree/roots", "Cabled to stake", or "Epoxy").

h. Record the condition of the logger as "In flowing water".

i. Record the action taken with the logger as "Installed new logger" and the date/time the action was taken.

j. Write a detailed description of the logger location. The description should include distance from the nearest transect or reach boundary and any other pertinent information for relocating the logger. The more detail the better. For example: Logger attached to grey, rectangular boulder 1 m in diameter near river left (~1.5 m from bank), 5 m upstream from transect 5.

k. Attach flagging to a nearby tree or other object to mark the location of the logger and take a photo of the logger location. Include enough of the surrounding environment to relocate the logger.

2) Previously installed loggers:

a. Use existing GPS coordinates, photographs, and site maps to locate the previously installed logger. If the logger location is found but the logger is missing, search downstream for the missing logger. If it cannot be found, install a new logger using the criteria outlined above.

b. Remove the logger from the housing unit and confirm that the correct logger serial number was recorded when originally installed. Avoid removing the logger from the water when it will be recording one of its hourly temperature measurements (on the hour). Rubber gloves, large pliers, or an oil filter wrench may be helpful for unscrewing housings that are difficult to open.

c. Attach the logger to the shuttle and squeeze the black plastic lever on the shuttle coupler to download the data. If working properly, the indicator light on the shuttle will blink orange during data transfer, and then blink green when the transfer is complete. If the light blinks red (indicating an error), clean the optical sensor on the logger and the shuttle connection surface and try again. If the data transfer fails after multiple tries, replace the logger and notify a project leader.

d. Attach the shuttle to the laptop computer, download the data, and briefly review the temperature data from the previous season. Look for erroneous spikes in temperature (> 30 °C), lack of variability (i.e., flat line), errors with the date/time (e.g., dates that don't vary or make sense), or other odd patterns in the data. Also check to ensure there is sufficient battery life in the logger. Replace the logger if the data looks erroneous or the battery is low.

e. After downloading the logger, note whether the red light on the logger is blinking (indicating that it is launched and operational). If there is no blinking light, attempt to relaunch the logger (Step 1c). If there is still no blinking light, replace the logger and notify a project leader.

f. Record the condition of the logger (i.e., "Buried", "Out of water", "In flowing water", "In non-flowing water", or "Missing"). Loggers that are partially out of water are designated as out of water.

g. Record the action taken with the logger (i.e., "Left in place", "Moved", "Removed", "Missing and replaced", or "Missing and didn't replace") and the date/time the action was taken. Move the sensor if it is in non-flowing water, out of water, or buried in sediment. Replace missing loggers with a new one unless otherwise instructed by a project leader. If a logger is removed and replaced with a new logger, the logger that is removed is assigned the action "Removed", and the replacement logger is assigned the action "Installed new logger".

h. Verify and update the logger location information as needed such as stream bank, distance from bank, attachment method, location description, and GPS coordinates. Only record new GPS coordinates if the logger was moved or if the original coordinates were erroneous. Take a new photo of the sensor only if the previous photo is no longer representative of the logger location or the photo is not stored in the temperature data entry application.

4.7 Reach Type

Channel-reach morphology, following the guidelines of Montgomery & Buffington (1997), is visually assessed at each sample reach. Reaches are defined as cascade, step pool, plane bed, pool riffle, dune ripple, or forced pool riffle (no colluvial or bedrock reaches are expected within spring Chinook salmon extent). Reaches can be rapidly identified into categories based on their general appearance, planform morphology, and longitudinal profile (Figure 14), as well as other diagnostic characteristics (Table 7). In cases where individual reaches encompass more than one type of reach morphology classify the reach based on the dominant morphology type. Classify the reach type only after walking the entire site; ideally after laying out channel units.

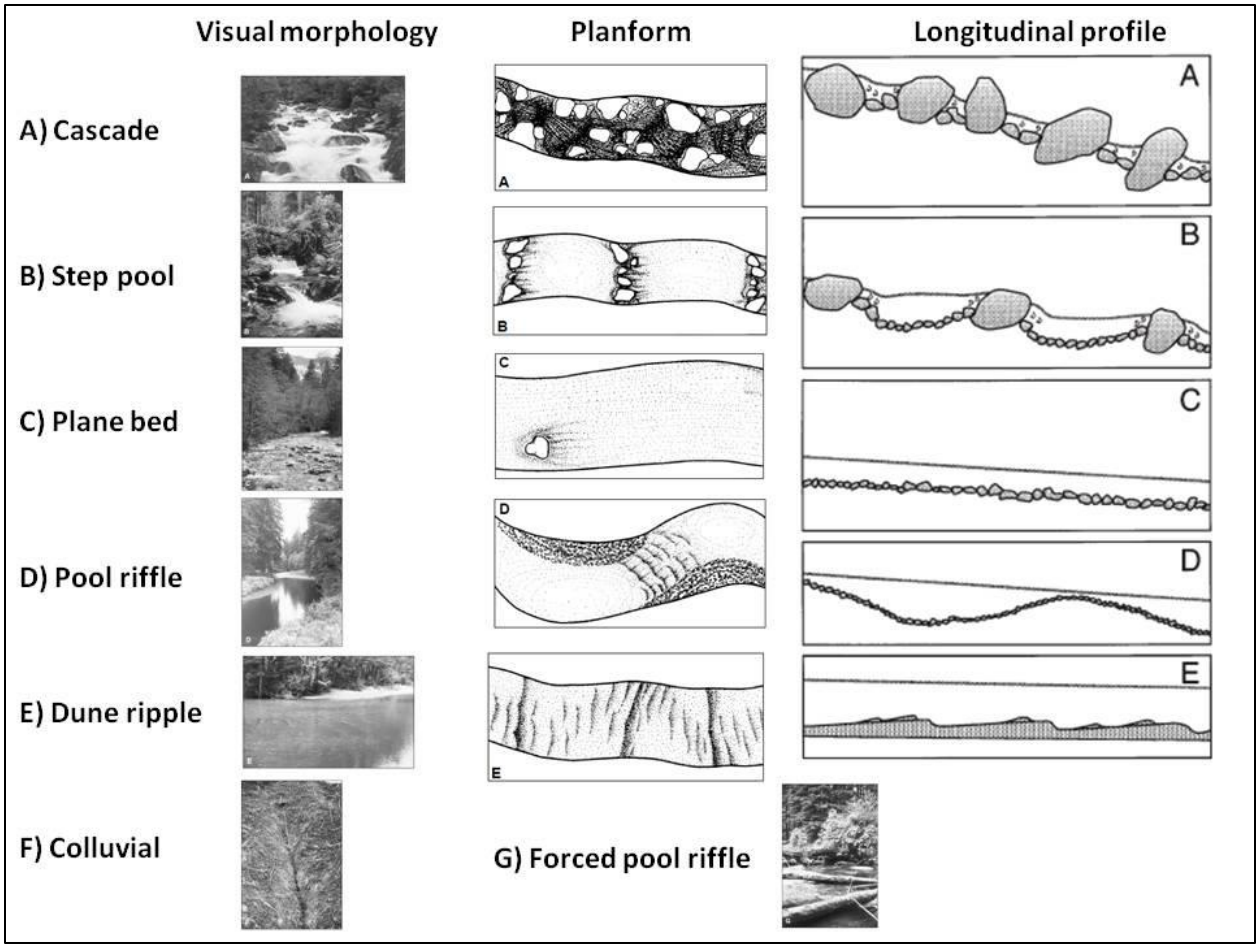

Figure 14. Visual morphology, planform, and longitudal profiles of Montgomery & Buffington's (1997) channel-reach types.

Table 7. Diagnostic features of channel-reach types, from Montgomery and Buffington (1997).

	Dune ripple	Pool riffle	Plane bed	Step pool	Cascade	Bedrock	Colluvial
Typical bed material	Sand	Gravel	Gravel-cobble	Cobble-boulder	Boulder	Rock	Variable
Bedform pattern	Multilayered	Laterally oscillatory	Featureless	Vertically oscillatory	Random	Irregular	Variable
Dominant roughness elements	Sinuosity, bedforms (dunes, ripples, bars) grains, banks	Bedforms (bars, pools), grains, sinuosity, banks	Grains, banks	Bedforms (steps, pools), grains, banks	Grains, banks	Boundaries (bed and banks)	Grains
Dominant sediment sources	Fluvial, bank failure	Fluvial, bank failure	Fluvial, bank failure, debris flows	Fluvial, hillslope, debris flows	Fluvial, hillslope, debris flows	Fluvial, hillslope, debris flows	Hillslope, debris flows
Sediment storage elements	Overbank, bedforms	Overbank, bedforms	Overbank	Bedforms	Lee and stoss sides of flow obstructions	Pockets	Bed
Typical confinement	Unconfined	Unconfined	Variable	Confined	Confined	Confined	Confined
Typical pool spacing (channel widths)	5 to 7	5 to 7	None	1 to 4	<1	Variable	Unknown

4.8 Land Use

A qualitive assessment of land use and human disturbance is performed for activities that can be detected while present at the reach. To describe the degree of human disturbance and to identify potential reference reaches, semi-quantitative levels of human land use will be scored based off the

Oregon DEQ Watershed Assessment's checklist and the National Rivers and Streams Assessment (USEPA 2013). Categories of land use are agriculture & urban, rangeland, roads, silviculture, and miscellaneous (mining, recreational, etc.). Human activities are rated on a Likert scale within each land use category depending on presence of land use by type and proximity to the stream channel. The dominant land use type is documented, and best professional judgment is used to determine whether the reach is suitable as a reference condition.

Field procedures:

1) Before leaving for the field, ensure that paper datasheets for land use are available in the event of a failed electronic data logger.
2) Conduct the Land Use assessment after the quantitative habitat survey so that the observer has detailed knowledge of reach conditions. The Land Use assessment is meant to be rapid and in most cases, should require maximum 10 minutes to complete.
3) Rate each land use activity within each category (Agriculture-Urban, Rangeland, Roads, Silviculture, Miscellaneous, and Natural Disturbance) according to proximity of the activity to bank (Table 8).

Table 8. Proximity scores for human land use rankings.

Land use activity	Proximity score
Activity absent at reach	0
Activity present at reach but > 10 m from bank	1
Activity present within 10 meters of bank	3
Activity present on stream bank (or channel)	5

4) Document the dominant land use for the reach as Forest, Agriculture, Range, Urban, or Suburban/Town.
5) Use best professional judgement to rate reach conditions as Ideal, Good, Marginal, Sub-marginal, Poor, or Very poor according to criteria in Table 9.

Table 9. Best professional judgement grade.

Rating	Grade
Ideal reach conditions. **Wilderness** area with **virtually no human disturbance**.	A
Good reach conditions. **Some human disturbance but not extensive**.	B
Marginal reach conditions. Human disturbance present, but **best available reference for basin/region**.	C
Sub-marginal reach conditions. **Considerable human disturbance** present.	D
Poor reach conditions. **Considerable human disturbance present with significant negative impact on stream conditions**.	E
Very poor reach conditions. **Completely unraveled stream conditions**.	F

Drone survey methods

The unmanned aerial vehicle survey (UAV) is intended to test the application of structure-from-motion (SfM) and image classification techniques to obtain remotely sensed topography and habitat features relevant to salmonids. The UAV survey consists of a minimum of one, but potentially multiple pre-planned flights to collect visible and multispectral imagery sets that will be used for subsequent analysis. Following designated flight parameters, the UAV collects imagery at pre-defined waypoints.

A portion of this work is designed to better understand the minimum number of ground control points (GCPs) necessary to minimize location error and accurately register the map spatially. For the purposes of this initial work, GCPs consist of at least ten fixed points evenly distributed throughout the sampling area that are both visible in imagery from overhead and at locations that exemplify the topographic variability throughout the site. GCPs should be pre-established as benchmarks or precisely measured using professional survey grade equipment (e.g., total station or rtkGPS) before the UAV flight.

During the flight the pilot-in-command (PIC) takes sole responsibility for the UAV operation but may employ the help of additional crew members to serve as visual observers, monitoring the status and progress of the UAV. The PIC must possess a valid Part 107 license and comply with all Federal Aviation Administration (FAA) regulations including registering the UAV and displaying the FAA Certificate of Registration serial number in visible sight on the UAV. Special care should be taken to ensure the safety of equipment, personnel, and surrounding area (people and landscape) and that the PIC is proficiently prepared for flight - these may include health, environmental pressures, and site related hazards. Proper flight planning is a multistep process that should be completed by the crew supervisor or PIC prior to flight and can begin days prior to or the morning of the flight.

<u>Field procedures:</u>

1) Before leaving for the field, begin competing the pre-flight checklist.
    a. The PIC should identify potential flight restrictions involving undesirable weather or airspace restrictions prior to leaving wifi or cell service.
    b. If no hazards are identified and if necessary, the PIC should proceed with notifying air traffic control (ATC) or local dispatch of the flight plan.
    c. Equipment including software should be checked and maintained as they may limit the ability of the UAV to launch (e.g., software updates, battery levels, compass calibration).
    d. Cache background maps in the flight planning software on the tablet.
2) At the survey location the PIC should conduct an initial assessment by walking the length of the reach to familiarize themselves with potential challenges and hazards.
    a. Identity the tallest objects within the flight area and use a laser rangefinder collect a minimum of five measurements of these potential hazards throughout the reach (e.g., trees, hillsides, cliffsides, powerlines). These measurements will be the basis of the chosen flight altitude.
    b. Make a final decision based on the overall reach assessment whether it is safe or suitable to fly.
3) If not already identified, locate a minimum of ten locations for ground control targets/GCPs.

a. Secure the center of the target with a nail and whisker that will be used to survey in each location. Using a combination of stakes, rocks, and/or logs, secure the four corners of the target while also trying to create a smoothed ground surface.

b. Flag each location with the CP# to use when surveying in each point.

4) Identify take-off and landing location(s).
5) Populate or review the pre-planned flight in DJI Groundstation Pro and set or check camera parameters using DJI Go for the following parameters:
    a. Altitude: > tallest obstacle measured, typically between 80 – 120 m.
    b. Image overlap: frontlap = 80%, sidelap = 70%
    c. Course angle: dependent on time of day, bank heights, riparian obstructions, and stream orientation
6) Unload UAS and prepare for launch.
7) Start flight
    a. Continue to monitor the location of the UAV both visually in the air and in the app to ensure it is adhering to the flight plan.
    b. If present, check radio connection between PIC and visual observer(s).
    c. Continue to monitor the status of the UAV
        i. Connection between the controller and UAV
        ii. Battery levels
        iii. Course
        iv. Imagery – exposure and clarity
8) Land the UAV
9) Review photos ensuring the desired extent was captured including all ground control targets and determine whether a secondary flight is needed to collect additional imagery.
10) If not returning for additional flights or surveying work collect all ground control targets, nails and whiskers, and flagging.

References

CHaMP (Columbia Habitat Monitoring Program). 2016a. Scientific protocol for salmonid habitat surveys within the Columbia Habitat Monitoring Program.

CHaMP (Columbia Habitat Monitoring Program). 2016b. Total station procedures for the Columbia Habitat Monitoring Program; Topcon DS-205, Magnet 2.5.1. Page 100.

Dunham, J., G. Chandler, B. Rieman, and D. Martin. 2005. Measuring stream temperature with digital data loggers: a user's guide. Page 15. USDA Forest Service, Rocky Mountain Research Station, General Technical Report RMRS-GTR-150WWW, Fort Collins, CO.

Harrelson, C. C., C. L. Rawlins, and J. P. Potyondy. 1994. Stream channel reference sites: an illustrated guide to field technique. Page 61. U.S. Department of Agriculture, Forest Service, Rocky Mountain Forest and Range Experiment Station, General Technical Report GTR-RM-245, Fort Collins, CO.

Hawkins, C. P., J. L. Kershner, P. A. Bisson, M. D. Bryant, L. M. Decker, S. V. Gregory, D. A. McCullough, C. K. Overton, G. H. Reeves, R. J. Steedman, and M. K. Young. 1993. A hierarchical approach to classifying stream habitat features. Fisheries 18(6):3–12.

Leopold, L. B., M. G. Wolman, and J. P. Miller. 1964. Fluvial processes in geomorphology. Dover Publications, Inc., New York.

Moore, K., K. Jones, J. Dambacher, and C. Stein. 2017. Aquatic Inventories Project: methods for stream habitat surveys. Page 89. Oregon Department of Fish and Wildlife, Version 27.1, Corvallis, OR.

Saunders, W. C., N. Bouwes, P. McHugh, and C. E. Jordan. 2018. A network model for primary production highlights linkages between salmonid populations and autochthonous resources. Ecosphere 9(3):e02131.

USEPA. 2013. National Rivers and Streams Assessment 2013-2014: Field Operations Manual – Wadeable. EPA-841-B-12-009b. U.S. Environmental Protection Agency, Office of Water. Washington, DC.

Wolman, M. G. 1954. A method of sampling coarse river-bed material. Transaction of the American Geophysical Union 35:951–956.

Appendix B – Life Cycle Model

LIFE - CYCLE MODEL FOR UPPER GRANDE RONDE AND CATHERINE CREEK SPRING CHINOOK

EVALUATION OF HABITAT RESTORATION AND POPULATION RECOVERY STRATEGIES

DECEMBER 2018

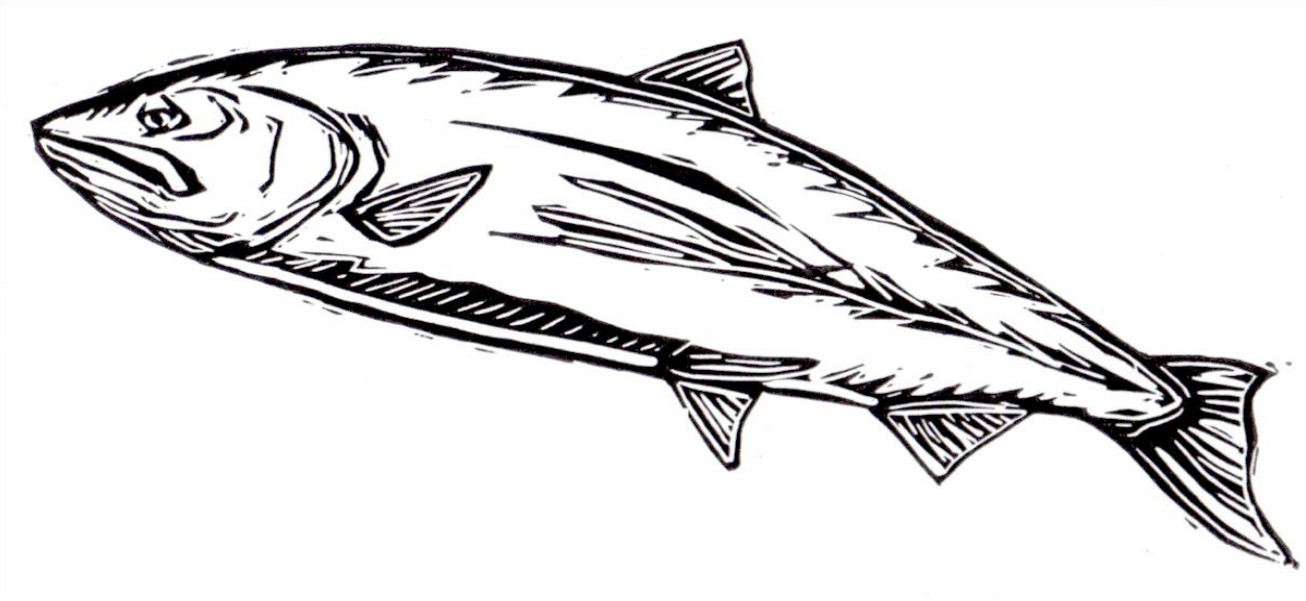

ECO LOGICAL RESEARCH

NICK WEBER & NICK BOUWES

BEND OR AND PROVIDENCE UT

THE COLUMBIA RIVER INTER-TRIBAL FISH COMMISSION

CASEY JUSTICE & SETH WHITE

PORTLAND OR

SUMMARY

The following describes continued progress toward assessment of Chinook salmon populations and habitat restoration opportunities within the upper Grande Ronde River (UGR) and Catherine Creek (CC) watersheds using a life-cycle modelling (LCM) framework. The work presented here extends LCM development efforts previously initiated by the Columbia River Inter-Tribal Fish Commission (CRITFC) and included as part of the Independent Scientific Advisory Board's (ISAB) 2017 review of LCM efforts in the interior Columbia Basin (chapter 9.f in ISAB 2017). Ultimately, these efforts are intended to provide an analytical tool that will guide long-term restoration and recovery strategies for two threatened Chinook Salmon populations under changing climatic conditions. This effort focuses on two objectives that include: 1) Refinement of LCM parameters and functions to improve model accuracy and efficiency, and 2) leveraging the model to evaluate potential restoration strategies that might increase the viability of these populations under future time horizons that include climate change impacts.

Many of the additions to the 2018 LCM effort make use of novel unpublished population data from the Oregon Department of Fish and Wildlife that allowed us to update almost all life-stage transition parameters with the most up-to-date information. Some of these changes include:

1. Smolt-to-adult (SAR) return rates that are now specific to each population and origin (i.e. natural vs. hatchery).
2. A more realistic approach for modelling current hatchery supplementation operations within the UGR and CC.
3. Expanded incorporation of parameter variability allowing model stochasticity at all stage transitions within the LCM framework.
4. Updates to the model implementation that allow log-normal stochasticity on density-dependent predictions within a Beaverton-Holt framework.

Our updated implementation of the LCM also includes efficiency improvements that significantly decreased the duration necessary to run individual model scenarios. Doing so allowed us to increase the number of stochastic Monte Carlo iterations to 500 for each modelled management scenario.

The updated model was then used to evaluate simulated population dynamics and population extinction risk across restoration and climate scenarios described previously by Justice et al. (2017), as well as within a novel set of restoration scenarios that rely on structural equation models (SEM). Both of these approaches describe the potential impact that restoration actions may have on juvenile Chinook Salmon rearing capacity while also considering impending changes in stream temperature due to climate change. The updated LCM framework also allowed us to evaluate potential population responses (changes in population abundance and extinction risk) under restoration and climate scenarios with and without hatchery supplementation.

ACKNOWLEDGEMENTS

This work was made possible by funding provided by the Bonneville Power Administration (BPA project # 2009-004-00). The life-cycle modelling approach was adapted from previous work by Rishi Sharma (Sharma and others, 2005), and a model implementation refined by the Integrated Status and Effectiveness Monitoring Program (ISEMP [Nahorniak and Armour 2017]).

Casey Justice and Seth White developed the analytical approaches used in the formulation of restoration and recovery scenarios and acquire data used in model parameter development. Nick Weber was responsible for development of the life-cycle modelling software environment, analytical approaches, and final report and figure generation. Nick Bouwes provided analytical oversight during all stages of the project. Pete McHugh and Carl Saunders also contributed to previous life-cycle modelling efforts that greatly informed the current analyses. Data used in the estimation of stage specific parameters was primarily supplied by the Oregon Department of Fish and Wildlife.

SUGGESTED CITATION

Weber, N., N. Bouwes, C. Justice, and S. White. 2018. *Life - Cycle Model for upper Grande Ronde and Catherine Creek Spring Chinook - Evaluation of Habitat Restoration and Population Recovery Strategies*. Prepared for the Bonneville Power Administration by Eco Logical Research and the Columbia Intertribal Fish Commission.

Table of Contents

List of Figures

LIST OF TABLES

LIFE CYCLE MODEL FRAMEWORK

Several populations of Snake River spring Chinook Salmon are listed under the ESA, including the Upper Grande Ronde and Catherine Creek populations. Both rivers are targeted as high-priority restoration areas in an effort to increase adult abundance to avoid extinction and eventually achieve recovery. To evaluate the benefits of different restoration strategies on long-term population dynamics, we developed a whole life-cycle model to evaluate life-stage specific benefits of restoration and potential changes to adult abundance, one of the primary responses for evaluating the status of ESA listed populations.

Our LCM framework is essentially a density-dependent, stage-structured stochastic projection model that has been adapted from modelling approaches described by Sharma et al. (2005) and implemented by the Integrated Status and Effectiveness Monitoring Program (Nahorniak and Armour 2017). The LCM uses a Beverton-Holt stock recruitment function to simulate the number of individuals surviving from one life-stage (N_i) to the next (N_{i+1}) (after Moussalli and Hilborn 1986) as defined by stage-specific capacity (c_i) and productivity (p,) parameters:

$$N_{i+1} = \frac{N_i}{\frac{1}{p_i} + \frac{1}{c_i} N_i}$$

Although the functional form of the model implies that density dependence occurs at all stage transitions, density-independent transitions are modeled by setting capacity to an infinitely large value and using empirical estimates of survival (S_i) as the productivity input (p_i). Otherwise, realized survival ($S_i = N_{i+1} / N_i$) is a function of both the capacity and productivity for each modelled life-stage of the population. Within the Beverton-Holt stock-recruit relationship, these parameters form the basis for modelling population responses to restoration and climatic scenarios evaluated for the upper Grande Ronde River and Catherine Creek Chinook populations (see Restoration and Climate Scenarios below).

IMPLEMENTATION ENVIRONMENT

The modelling framework is implemented within the R program for statistical analysis and graphics (R Core Team, 2014). All code and documentation needed to run and customize the model can be found at the following GitHub repository: https://github.com/webernick79/Life-Cycle-Model. The implementation was developed to allow a flexible framework for modelling organism life-cycles using a Beaverton-Holt function and is easily customized to allow an any number of alternative stage transitions. Additionally, the implementation also includes a life-history function that allows the user to specify variability and model stochasticity with respect to bivariate decisions (e.g., age specific maturation probability). Custom components have also been developed that allow easy scaling of parameters as well as routines for implementing and summarizing parameter sensitivity analyses.

MODEL STOCHASTICITY

Our implementation of the LCM framework enables the user to account for parameter and prediction uncertainty, thereby producing a stochastic model that is more reflective of temporal variation in natural processes. Variability can be explicitly specified for individual parameter inputs for p_i and c_i at each stage transition. Although variation around individual parameters is always specified as a standard deviation, the model accounts for different distributional assumptions with respect to parameter type. For example, the model generates values from a beta distribution when p_i values are < 1 (i.e. survival), and from a positive normal distribution for values of p_i >= 1 (i.e. fecundity) or c_i (capacity). In

our model of UGR and CC Chinook, stochasticity was modelled around Beaverton-Holt parameters for density-independent transitions, and/or where data was not available to fit a Beverton-Holt curve (i.e., parr-to-smolt, smolt-to-adult, spawner-to-egg [Appendix 2: Base Model Parameters]).

We used an alternative approach to model stochasticity among life-stage transitions where empirical stock-recruitment data was available and density-dependence was evident or biologically plausible (i.e., adult-to-spawner, egg-to-parr [Appendix 2: Base Model Parameters]). In these cases, the model generates prediction uncertainty based on the residual error associated with a Beaverton-Holt curve fit to available stage-specific data (see example below for Egg to Parr Survival). In this scenario, model parameters for p_i and c_i remain static among model iterations, and uncertainty is modelled on the prediction of N_{i+1} assuming a log-normally distributed residual error. Hilborn and Walters (1992) recommend using a log-normal residual error distribution for stock-recruitment relationships unless there is evidence to the contrary. Model parameters and associated residual error terms are estimated by fitting the log-transformed form of the Beaverton-Holt function to the stage-specific abundance data as suggested by Haddon (2001):

$$ln\left(\frac{N_{i+1}}{N_i}\right) = ln(a) - ln(b + N_i) + \varepsilon$$

where a is equivalent to the asymptotic limit or capacity (c_i) and a/b describes the initial steepness of the curve at low values of N_i or productivity (p_i) within the density dependent relationship, and error (ε) is assumed to be normally distributed with a mean of zero and variance equal to the sum of residual square for error:

$$\varepsilon = N(0, \sigma^2)$$

The LCM then uses the un-transformed form of the Beverton-Holt function to make predictions of N_{i+1} with log-normal residual error following:

$$N_{i+1} = \frac{N_i}{\frac{1}{p_i} + \frac{1}{c_i} N_i} e^{\varepsilon}$$

The model also utilizes a custom function that allows the user to specify variability around the probability associated with bivariate life-history transitions such as choice of life-history strategy (see Parr to Smolt at Lower Granite Dam below) or probability of maturation. In these cases, the mean and standard deviation of the observed data are used to randomly generate probabilities dependent (i.e. sum to 1) for bivariate outcomes using a beta distribution.

Base Model Parameters for the Upper Grande Ronde and Catherine Creek

In many LCM applications, population stage specific abundance information as well as capacity and productivity parameters are difficult to obtain, as these variables and parameters are rarely estimated as part of routine monitoring programs. However, a combination of entities has been closely monitoring the upper Grande Ronde River (UGR) and Catherine Creek (CC) Chinook populations allowing for estimation of population specific parameters for many life-stages. For over two decades (*ca.* 1993 to present) the Oregon Department of Fish and Wildlife (ODFW), and more recently the Columbia River Inter-Tribal Fish Commission (CRITFC), and other parties have been collecting data needed to estimate spawner, parr, and smolt abundance and/or survival each year. Below, we describe in greater detail the data and assumptions used to parameterize a base LCM used in subsequent modelling investigations of restoration and climate scenario impacts for the UGR and CC Chinook populations. A more concise overview of the parameters used in our LCM parameterization can be found in Appendix 2: Base Model Parameters, however the following discussion is intended to provide a greater understanding of model underpinnings and assist in future efforts to refine and apply this LCM to novel management scenarios.

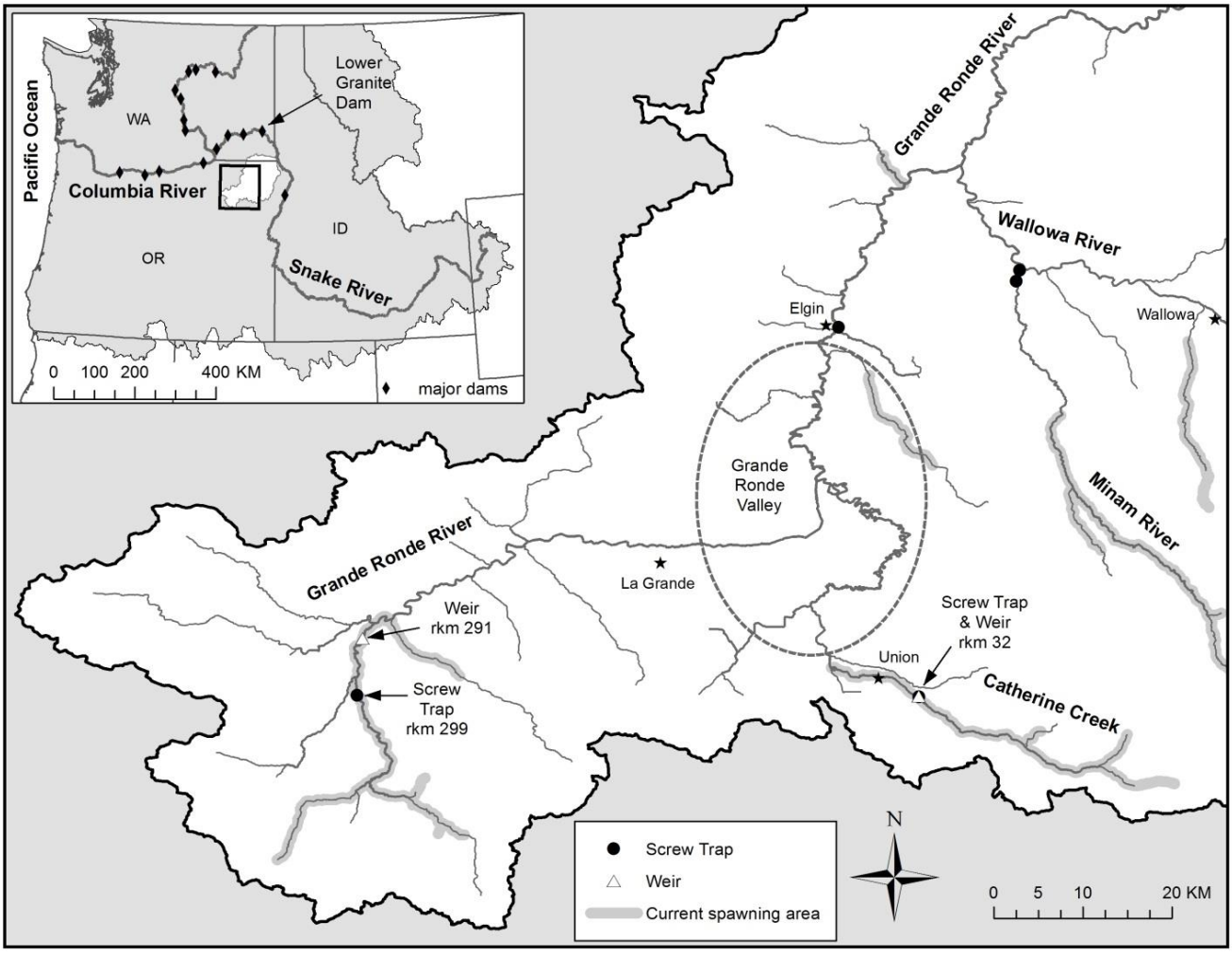

Figure 1. Overview of the Upper Grande Ronde River and Catherine Creek showing major points of accounting relevant to development of the LCM framework including adult weirs, juvenile screw traps, current spawning ground extent, valley rearing location, and Lower Granite Dam.

Model Spatiotemporal Structure

Our LCM framework is structured around data collection efforts within the domain of UGR and CC Chinook Salmon (Figure 1, Figure 6) life-histories where population abundance and survival estimates have been possible. Many of these estimates are a product of field mark-recapture surveys, screw trap operation, and adult weirs operated by ODFW. These efforts include estimates of total parr abundance for each population at a point in late summer, and a subsequent estimate of juvenile abundances exhibiting each of two dominate rearing and migration strategies (i.e. headwaters or valley rearing). PIT-tagging in each tributary also yield annual estimates of total smolts reaching Lower Granite Dam. Additionally, the model uses the best available data to approximate hatchery smolt supplementation abundance and their distinct survival to Lower Granite Dam (LGD). From LGD, our framework accounts for age specific maturation and survival probabilities of natural and hatchery origin smolt to the ocean and back to enumeration of adults at tributary weirs operated on both the UGR and CC. At the adult weir, we model broodstock retention schemas that support hatchery programs specific to each population and their impact on the total population of natural and hatchery origin adults passed to the spawning grounds. Finally, the model invokes a density-dependent survival of adults on the spawning grounds that is informed by redd and carcass surveys that estimate spawner abundances for each population.

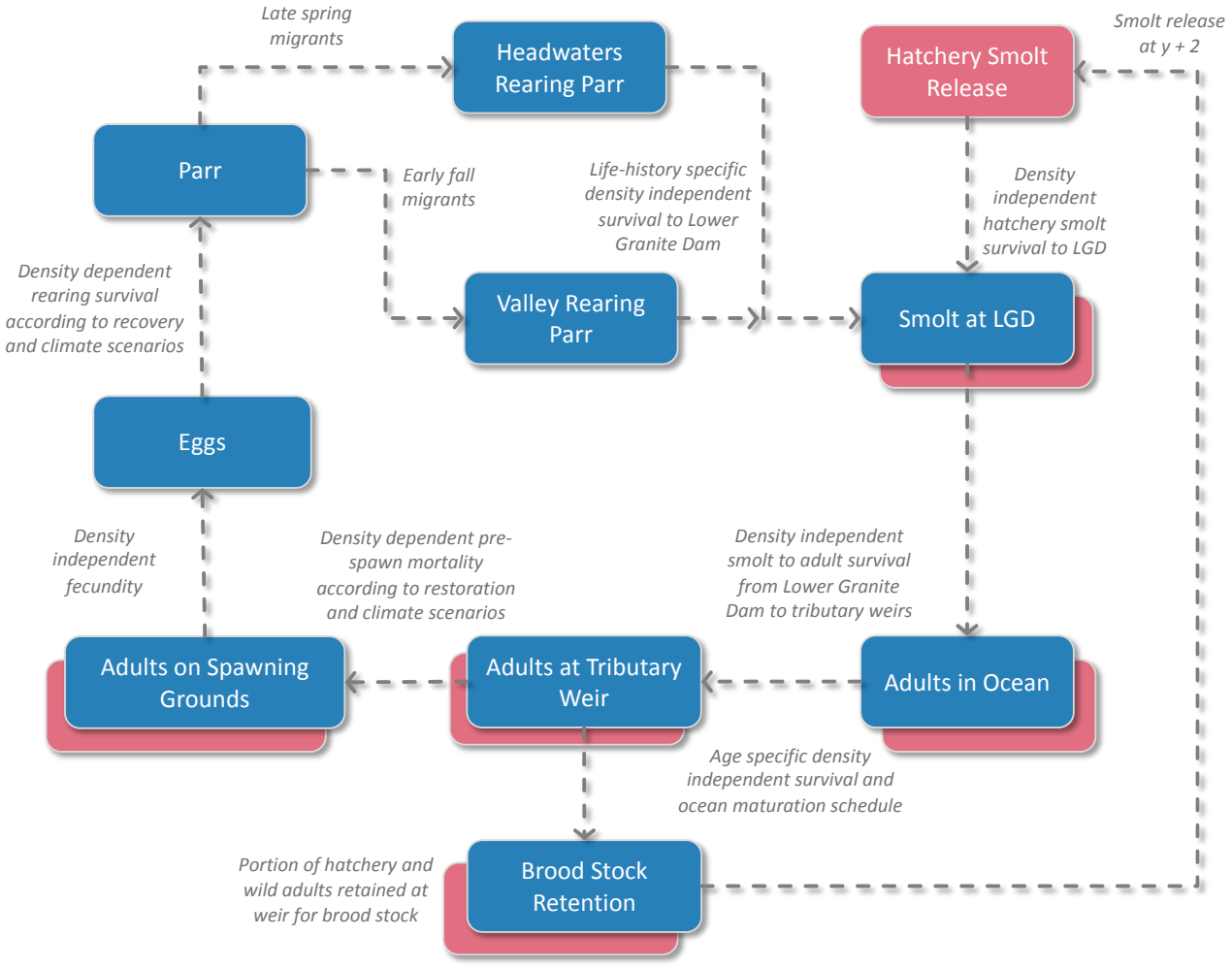

Figure 2. Conceptual diagram of the life cycle model (LCM) structure. Stacked boxes represent stages in which the model tracks natural and hatchery origin Chinook. All naturally spawned Chinook are considered of natural origin.

Egg to Parr Survival

The conversion of eggs to parr has particular importance within our LCM as the restoration and climate scenarios (discussed below) primarily affect juvenile rearing habitat and parr rearing capacity. We modelled this life-stage transition as a density – dependent survival probability using base estimates of p_i and c_i derived by fitting a Beaverton-Holt model to available abundance data (Table 1, Figure 3).

Table 1. Estimated abundances of eggs and late summer parr used in the derivation of Beaverton-Holt parameters for egg to parr survival.

Upper Grande Ronde			Catherine Creek	
Brood year	Eggs (N_i)	Summer parr (N_{i+1})	Eggs (N_i)	Summer parr (N_{i+1})
1992	747045	77467	-	-
1993	626369	125620	492284	42334
1994	-	-	53634	10437
1995	-	-	65127	9325
1996	-	-	65127	14878
1997	-	-	137916	38204
1998	-	-	174311	40393
1999	-	-	155156	41091
2000	-	-	93860	40463
2001	-	-	683834	71273
2002	-	-	762369	153078
2003	-	-	766200	151047
2004	-	-	390762	57927
2005	-	-	256677	74225
2006	101522	17113	459720	66043
2007	149409	36297	312227	46474
2008	181973	70212	385016	103336
2009	3913367	227463	367776	24732
2010	1656908	56714	1750767	116382
2011	739383	87176	2130036	77210
2012	605298	23768	1233582	75419
2014	2352234	58770	1890599	65947
2015	2045754	97513	919440	52011

Annual estimates of eggs were based on a conversion of total spawners (from unpublished ODFW spawning surveys) to eggs using fecundity values reported by Van Dyke (2008) for Catherine Creek female spawner to egg equivalence and assuming a 50:50 sex-ratio for spawning adults. Parr abundances were taken from unpublished estimates gleaned from annual mark-recapture electrofishing surveys conducted by ODFW within rearing habitat in each system during late summer and prior to the fall presmolt outmigration exhibited by a portion of the population (see Parr to Smolt at Lower Granite Dam below).

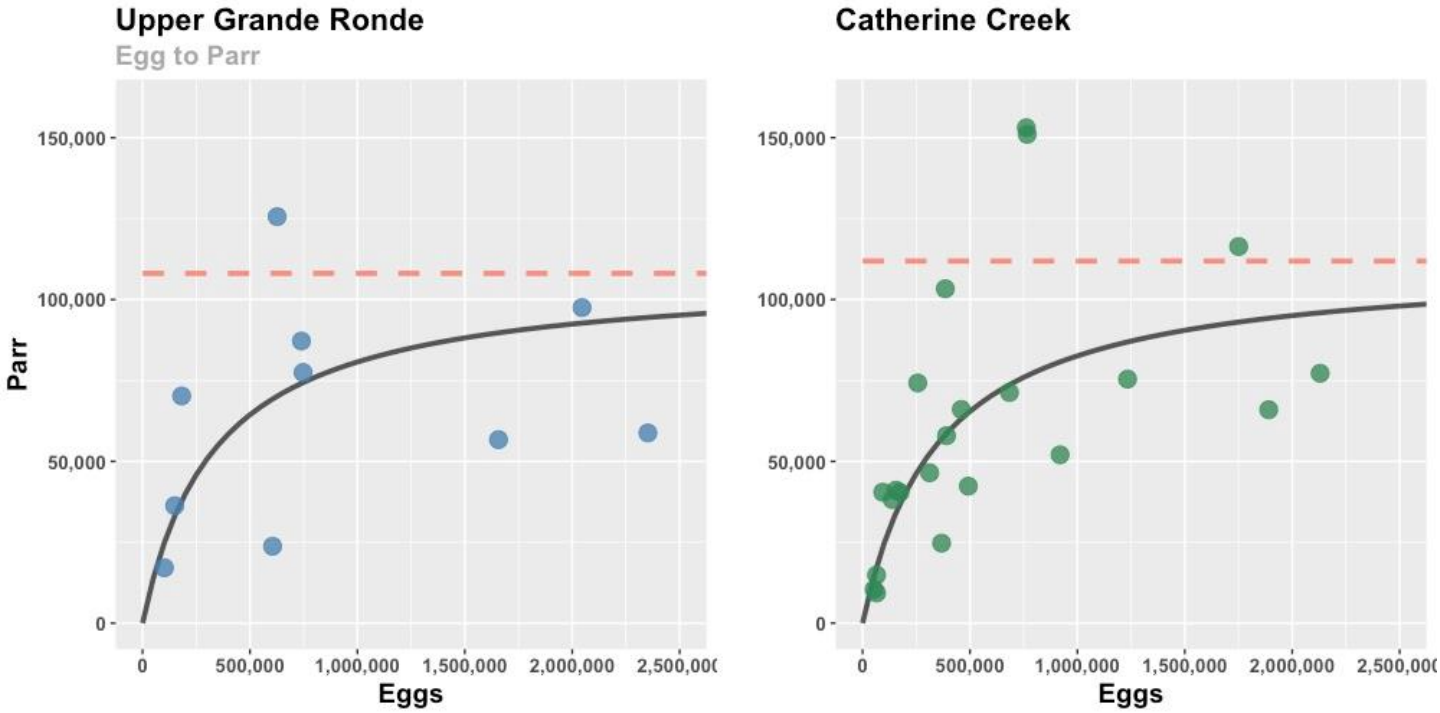

FIGURE 3. BEAVERTON-HOLT FUNCTION FIT TO AVAILABLE ESTIMATES OF EGGS AND SUMMER PARR FOR UPPER GRANDE RONDE AND CATHERINE CREEK CHINOOK. MODEL FITS WERE USED TO GENERATE ESTIMATES OF SURVIVAL AND CAPACITY (DASHED RED LINE) USED IN THE BASE LCM FRAMEWORK.

PARR TO SMOLT AT LOWER GRANITE DAM

In both the UGR and CC watersheds, spawning primarily occurs in headwater and tributary reaches of the Grande Ronde stream network (Figure 1). During the fall of their first year Chinook parr will exhibit one of two distinct rearing life-histories. These include headwaters rearing presmolts that will remain and overwinter within headwaters and tributary reaches prior to smolting the following spring, and valley rearing presmolts that exhibit a fall downstream migration where they winter within valley reaches of the Grande Ronde River. We model the survival of parr from late summer to smolt passing Lower Granite Dam the following year as a density independent survival rate that accounts for different survival rates among these two life-history strategies.

This component of our LCM framework relies on survival and abundance estimates generated by ODFW that are based on mark-resight data gleaned from PIT-tag capture surveys of parr and presmolts, screwtrap operations, and detections of smolt throughout the Columbia hydrosystem (Table 1, Figure 4). Specifically, we rely on survival estimated for three release groups to generate our estimates of parr to LGD smolt survival:

1. *Parr to smolt at LGD* – Cormack-Jolly-Seber (CJS) survival estimate generated from late summer (late July - August) PIT-tag and capture surveys of parr in the headwaters and subsequent detections of individuals throughout the hydrosystem.
2. *Headwaters rearing presmolt to smolt at LGD* – CJS survival estimate generated from late fall/winter (mid November – mid December) PIT-tag capture surveys of presmolt in the headwaters and subsequent detection of individuals throughout the hydrosystem as smolt.
3. *Valley rearing presmolt to smolt at LGD* – CJS survival estimate generated from fall (October – mid November) PIT-tagging of presmolt captured at screw traps as they migrate to valley rearing locations and subsequent detection throughout the hydrosystem as smolt.

TABLE 2. CORMACK JOLLY SEBER ESTIMATES OF SURVIVAL USED TO GENERATE LIFE-HISTORY SPECIFIC SURVIVAL PROBABILITIES FOR PARR THAT EXHIBIT HEADWATERS AND VALLEY REARING LIFE-HISTORIES PRIOR TO SMOLTING AND ARRIVAL AT LOWER GRANITE DAM.

Migratory year	Probability of survival to Lower Granite Dam by tagging group					
	Catherine Creek			Upper Grande Ronde Survival		
	Summer parr	Valley rearing	Headwaters rearing	Summer parr	Valley rearing	Headwaters rearing
1995	0.15	0.24	0.28	0.17	0.23	0.15
1996	0.28	0.36	0.31			
1997	0.18	0.37	0.08			
1998	0.21	0.24	0.28		0.29	0.11
1999	0.16	0.20	0.29		0.27	0.12
2000	0.15	0.21	0.14		0.34	0.13
2001	0.09	0.13	0.08			
2002	0.11	0.15	0.20		0.31	
2003	0.08	0.12	0.15		0.18	
2004	0.07	0.13	0.18		0.16	0.30
2005	0.06	0.12	0.11		0.14	0.21
2006	0.06	0.07	0.13		0.17	0.08
2007	0.04	0.20	0.09		0.24	0.17
2008	0.08	0.15	0.14	0.26	0.34	0.36
2009	0.15	0.27	0.11			
2010	0.11	0.18	0.18	0.24	0.21	0.13
2011	0.13	0.16	0.17	0.13	0.23	0.12
2012	0.12	0.19	0.10	0.08	0.20	0.04
2013	0.05	0.10	0.11	0.10	0.18	0.06
2014	0.09	0.14	0.12	0.10	0.20	0.07
2015	0.06		0.04	0.16	0.09	0.07
2016	0.03	0.06	0.08	0.08	0.12	0.05
2017	0.09	0.15	0.17	0.09	0.17	0.05

One challenge in integrating life-history specific survival rates within our LCM is that survival estimates from late summer parr tagging to fall cannot be generated for each life-history due to insufficient resight of tagged individuals at screw traps in each system. Rather than directly incorporating empirical estimates of parr to presmolt survival into the LCM we developed a correction factor for parr to smolt survival to LGD based on available Cormack-Jolly-Seber estimates of survival for both life-history strategies with the following assumptions:

1. Estimates of survival from late summer parr until fish reach LGD accurately reflect survival rates of all fish in the population. That is, without accounting for life history strategy, all fish experience an average survival rate, and the average of survival rates for each life history strategy is equal to the mean pooled survival for the population as late summer parr to smolts at LGD.
2. Headwaters rearing presmolts experience the same survival rate as valley rearing fish during the short period of time between when fall tagging occurs at the screw trap and fall/winter sampling occurs within the headwaters.

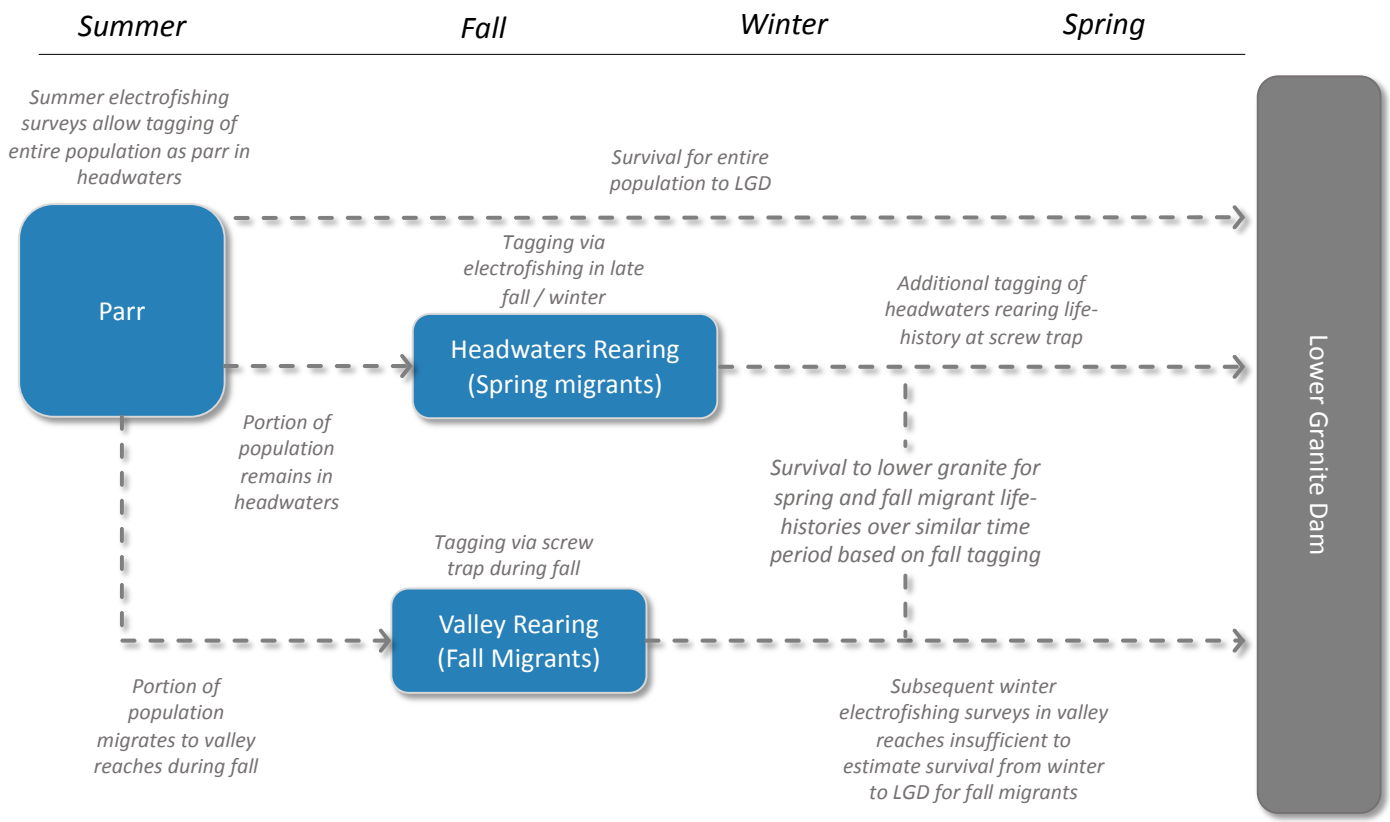

FIGURE 4. VISUAL REPRESENTATION OF JUVENILE LIFE-HISTORIES AND HOW FALL PIT-TAGGING OF HEADWATERS REARING PRESMOLTS VIA ELECTROFISHING AND VALLEY REARING PRESMOLT AT SCREW TRAPS CAN BE USED TO ESTIMATE SURVIVAL TO LOWER GRANITE DAM OVER ROUGHLY EQUIVALENT TIME INTERVALS THUS ACCOUNTING FOR EACH REARING STRATEGY.

Acknowledging these assumptions, we calculated a correction factor that accounts for the different survival rates of each life-history based on the ratio of survival for headwaters rearing presmolts tagged during fall/winter sampling and valley rearing presmolts tagged in the fall at the screwtrap. The ratio was used to adjust the model input of parr survival to smolt at LGD with respect to each life-history (Table 3).

TABLE 3. ESTIMATES OF TOTAL PARR SURVIVAL AND LIFE-HISTORY SPECIFIC SURVIVAL FOR PARR EXHIBITING FALL MIGRANT (VALLEY REARING) AND WINTER RESIDENT (HEADWATERS REARING) LIFE-HISTORIES. SURVIVAL ESTIMATES ARE BASED ON CJS ESTIMATES OF SURVIVAL FROM ODFW PIT-TAG SURVEYS AND WERE USED TO DEVELOP SURVIVAL CORRECTIONS FOR PARR TO SMOLT SURVIVAL FOR THE BASE MODEL.

Population	Mean survival				Correction factor		Survival estimate	
	Summer parr	Valley rearing	Headwaters rearing	Life-history mean	Valley	Headwaters	Valley	Headwaters
CC	0.11	0.18	0.15	0.16	1.10	0.94	0.12	0.10
UGR	0.14	0.21	0.13	0.17	1.25	0.77	0.18	0.11

HATCHERY SUPPLEMENTATION

The UGR and CC spring Chinook populations are presently supplemented by a target annual release of *ca*. 250K (UGR) and 150K (CC) hatchery-reared smolts released into acclimation ponds near the spawning grounds in both systems. Adults returning from supplementation releases are meant to home to the spawning grounds and spawn naturally with

natural-origin fish. To support an integrated hatchery program, a fraction of natural-origin fish returning to spawn in the wild are retained for spawning in the hatchery. Adult trap weirs situated in both streams are used to manage three aspects of escapement under the supplementation goals: (i) the proportion of the total natural-origin returns retained for the hatchery ($P_{NOS\text{-}R}$) (ii) the proportion of natural spawners of hatchery origin (P_{HOS}), and (iii) the proportion of hatchery broodstock/egg-take of natural origin (P_{NOB}). These supplementation efforts have a strong influence on abundance dynamics in both the UGR and CC populations. Thus, we attempted to implement a broodstock retention and supplementation scheme that approximates this management strategy within the LCM.

A more complete description of the LCM implementation of the broodstock retention program can be found in Appendix 1: Broodstock Retention Approach. But in brief, we developed a target brood retention for each system of 170 and 103 adults for the UGR and CC respectively based on an adult-to-smolt equivalence (assuming a 50:50 sex ratio) of 1,470 smolts per adult (M. McLean, CTUIR, pers. comm.). Based on these retention targets we used unpublished annual records of smolt supplementation release abundances to derive a mean adult-to-smolt conversion factor and standard deviation that were incorporated into the LCM and more accurately represent the natural variability exhibited by the supplementation program on each system. To better approximate the dynamics of current hatchery supplementation management we only used available supplementation release data from years following release year 2001 (brood year 1999) to develop inputs for the LCM (Table 4).

TABLE 4. ANNUAL SMOLT RELEASE ABUNDANCE USED TO PARAMETERIZE THE HATCHERY SUPPLEMENTATION PROGRAM WITHIN THE LCM. SMOLT TO ADULT EQUIVALENCE ASSUMES A TARGET BROOD RETENTION OF 103 ADULTS IN CC AND 170 ADULTS IN THE UGR.

	Catherine Creek		Upper Grande Ronde	
Release year	Total release	Smolt equivalence	Total release	Smolt equivalence
2001	136820	1328	2560*	
2002	180340	1751	151444*	
2003	129684	1259	237036	1394
2004	161868	1572	144919	852
2005	189581	1841	105369	620
2006	68820	668	18901*	
2007	71270	692	139423	820
2008	116882	1135	259932	1529
2009	138842	1348	146552	862
2010	144353	1401	232350	1367
2011	155475	1509	242382	1426
2012	161373	1567	285737	1681
2013			290572	1709

* Indicates years that were omitted from calculation of a mean smolt release equivalent as they did not reflect the current supplementation scheme that includes both the captive and integrative broodstock program.

HATCHERY SMOLT SURVIVAL TO LGD

Hatchery origin smolts experience a shortened survival period from the time of their release until they reach LGD and are released at a larger size relative to natural-origin smolts and were thus modelled separately from their natural counterpart (McCullough et al. 2014). Survival was estimated from PIT-tagged hatchery smolts using a Cormack-Jolly-Seber model implemented in program MARK as described in Appendix K of McCullough et al. (2014). Survival rates of hatchery smolts from release to LGD were then used to predict the number of hatchery smolts at LGD, a metric needed

to estimate smolt-to-adult return rates (SAR) for hatchery fish (Table 5). Hatchery smolt abundance information was taken from Feldhaus et al. (2017).

TABLE 5. ANNUAL ABUNDANCE OF HATCHERY SMOLTS RELEASED AND ESTIMATED HATCHERY SMOLT ABUNDANCE AT LOWER GRANITE DAM USED TO PARAMETERIZE HATCHERY SMOLT SURVIVAL TO LGD.

	Catherine Creek			Upper Grande Ronde		
Migration Year	Smolts released	Smolts at LGD	Survival to LGD	Smolts released	Smolts at LGD	Survival to LGD
2000	37982	16661	0.44	1508	594	0.39
2001	136820	85795	0.63	2559	1302	0.51
2002	180340	146802	0.81	151443	62782	0.41
2003	129684	88599	0.68	237036	105990	0.45
2004	161868	57837	0.36	144919	50891	0.35
2005	189581	61982	0.33	105369	18932	0.18
2006	68820	36135	0.53	18977	12333	0.65
2007	71270	42284	0.59	139423	76982	0.55
2008	116882	88587	0.76	259932	107662	0.41
2009	138842	88687	0.64	146552	73319	0.50
2010	144353	92712	0.64	232349	131046	0.56
2011	155475	97394	0.63	242385	101902	0.42
2012	161373	89539	0.55	285738	132372	0.46

NATURAL AND HATCHERY ORIGIN SMOLT TO ADULT RETURN RATES

Our LCM uses smolt-to-adult return rate (SAR) data to parameterize the marine survival and maturation schedules specific to each population and origin (i.e., natural vs. hatchery). The SAR is taken from unpublished estimates compiled by ODFW of smolt abundance at LGD and estimated abundance and age structure of adults returning to the weir traps within each system. Thus, within our modelling framework, ocean life-stages begin for smolt at LGD and end at weirs in proximity to the spawning grounds within each system (Figure 1).

TABLE 6. NATURAL ORIGIN SARS BASED ON ESTIMATES OF SMOLT AT LGD AND ADULT RETURNS TO THE SPAWNING GROUNDS ON EACH SYSTEM. ANNUAL RETURNING AGE STRUCTURE WAS OBTAINED VIA NOAAS SALMON POPULATION SUMMARY (SPS) DATABASE SYSTEM.

	Catherine Creek						Upper Grande Ronde					
				Return age structure						Return age structure		
Brood year	SAR	Smolt at LGD	Adults at weir	Age-3	Age-4	Age-5	SAR	Smolt at LGD	Adults at weir	Age-3	Age-4	Age-5
1992							0.008	11155	92	0%	91%	9%
1993	0.025	6519	163	7%	7%	85%	0.006	21732	127	0%	7%	93%
1994	0.007	2891	21	0%	39%	61%						
1995	0.058	1641	96	11%	90%	0%						
1996	0.027	3139	85	3%	95%	2%	0.018	3162	56	3%	95%	2%
1997	0.072	6131	441	6%	82%	12%	0.014	7337	100	4%	83%	13%
1998	0.070	6099	428	0%	21%	79%	0.039	7436	292	0%	27%	73%
1999	0.023	3763	87	0%	98%	2%						
2000	0.009	5768	53	12%	77%	12%	0.012	4247	53	4%	96%	0%
2001	0.008	5427	46	6%	86%	8%	0.012	1666	20	0%	97%	3%
2002	0.013	11163	144	4%	73%	23%	0.033	1919	64	0%	73%	28%
2003	0.008	8714	68	1%	26%	74%	0.018	2082	37	1%	4%	95%
2004	0.033	3372	112	5%	78%	16%	0.005	13156	71	12%	89%	0%
2005	0.035	3204	113	8%	75%	18%	0.017	5680	98	5%	76%	19%
2006	0.116	5375	625	9%	90%	1%	0.033	4518	150	11%	82%	7%
2007	0.079	7071	557	10%	55%	35%						
2008	0.043	11168	475	7%	84%	9%	0.031	10498	329	22%	65%	13%
2009	0.082	3238	267	28%	56%	16%	0.036	9314	335	11%	69%	19%
2010	0.052	13916	726	5%	93%	2%	0.032	26758	849	6%	88%	6%
2011	0.076	3938	300	17%	67%	16%	0.066	5979	396	22%	72%	5%

Using population specific age structure information from NOAA's Salmon Population Summary (SPS) database (https://www.webapps.nwfsc.noaa.gov/apex/f?p=261:HOME::::::) we decomposed the natural origin SAR return estimates into ocean age specific survival (S1, S2, S3) and maturation probabilities (m1, m2, and m3) that could yield an overall SAR and returning adult age structure on par with the observed data (Table 6). While the observed return-at-age pattern is a function of non-identifiable parameters, the approach used here places constraints on survival and maturation probabilities by age that allow parameter estimation (see McHugh et al. 2017 for an example and rationale). Also note that our model assumes a single SAR representative of an 'average' outmigrant experience and makes no attempt to parse transported vs. in – river individuals; thus, the assumption is the data for 1993-2011 brood years are a reasonable average of future mainstem/ocean conditions. We used an analogous set of hatchery smolt and adult return data (Table 7) to adjust our model for differences in hatchery and natural origin SARs. This was done by scaling the overall SAR for hatchery origin fish based on the ratio of the mean for hatchery and natural SARs for all available data (Table 8).

TABLE 7. HATCHERY ORIGIN SARS BASED ON ESTIMATES OF SMOLT AT LGD AND ADULT RETURNS TO THE SPAWNING GROUNDS ON EACH SYSTEM.

	Catherine Creek			Upper Grande Ronde		
Brood year	SAR	Smolt at LGD	Adults at weir	SAR	Smolt at LGD	Adults at weir
1998	0.025	16661	419	0.008	594	5
1999	0.003	85795	245	0.008	1302	11
2000	0.005	146802	673	0.010	62782	626
2001	0.002	88599	190	0.004	105990	462
2002	0.005	57837	269	0.003	50891	169
2003	0.003	61982	162	0.002	18932	41
2004	0.005	36135	193	0.007	12333	82
2005	0.006	42284	263	0.011	76982	877
2006	0.016	88587	1417	0.027	107662	2856
2007	0.009	88687	763	0.013	73319	976
2008	0.013	92712	1237	0.010	131046	1279
2009	0.003	97394	318	0.006	101902	577
2010	0.008	89539	705	0.010	132372	1346

TABLE 8. RATIO OF NATURAL AND HATCHERY SAR USED TO MODEL HATCHERY SPECIFIC SAR SURVIVAL PROBABILITIES WITHIN THE LCM.

	Mean SAR		
Population	Natural	Hatchery	Correction factor
CC	0.044	0.008	0.17
UGR	0.024	0.009	0.39

SPAWNING GROUNDS SURVIVAL AND CAPACITY

Spawner capacity is used to define the upper limit of the density-dependent pre-spawn survival function for adult fish on the spawning grounds given restoration and climate change scenarios (see Restoration and Climate Scenarios below). For our model, spawning grounds survival refers to the survival rate of adults passed above adult weirs to spawner abundance during late summer. Spawner capacity estimates capitalize on extensive field survey information and associated habitat suitability index (HSI) models to produce a spatially explicit depiction of spawning habitat quality and quantity.

TABLE 9. UNPUBLISHED ESTIMATES FROM ODFW OF ADULT CHINOOK ON THE SPAWNING GROUNDS AND NUMBER OF SPAWNERS IN LATE SUMMER USED TO DEVELOP BASE CASE PARAMETERS FOR THE LCM.

Catherine Creek				Upper Grande Ronde			
Brood year	Spawning grounds	Spawners	Survival	Brood year	Spawning grounds	Spawners	Survival
1987	699	684	0.98	1987	804	707	0.88
1988	727	691	0.95	1988	554	554	1.00
1997	82	72	0.88	1989	3	3	1.00
1998	101	91	0.90	1992	443	394	0.89
1999	88	81	0.92	1998	88	84	0.95
2000	61	54	0.89	2003	185	165	0.89
2001	556	513	0.92	2004	634	586	0.92
2002	462	432	0.94	2009	555	127	0.23
2003	487	424	0.87	2010	2339	2094	0.90
2004	216	216	1.00	2011	1559	1359	0.87
2005	152	146	0.96	2012	718	392	0.55
2006	283	253	0.89	2013	1084	395	0.36
2007	174	174	1.00	2014	1918	1388	0.72
2008	219	219	1.00	2015	1841	1144	0.62
2009	293	281	0.96	2016	239	151	0.63
2010	999	973	0.97	2017	155	99	0.64
2011	1725	1657	0.96				
2012	716	667	0.93				
2013	514	489	0.95				
2014	1101	1059	0.96				
2015	522	514	0.98				
2016	420	364	0.87				
2017	139	139	1.00				

The HSI model relies on habitat information collected by CRITFC and ODFW using the Columbia Habitat Monitoring Protocol (CHaMP 2015) throughout the UGR and CC historic Chinook spawning network. The HSI model uses depth and velocity results from Delft3D hydraulic model runs, as well as geo-referenced field observations of substrate size (i.e., gravel, cobble, etc.) to compute a spawning HSI score for every 10-cm raster cell within each surveyed reach (see Wheaton et al. 2017 for a more in-depth discussion of the HSI approach). HSI scores were then translated into a reach-scale estimate of available spawning habitat, weighted by habitat suitability (i.e. weighted usable area, WUA). The total spawning capacity for a reach was than estimated by dividing the WUA by the average territory size for a spawning Chinook (estimated here as 3.2m^2 for CC and the UGR).

Habitat Suitability Index estimates of reach-scale spawner capacity (estimated as redds) were available for a total of 186 CHaMP survey visits (CC = 81, UGR = 105) that occurred between 2011 and 2015. To obtain an estimate of total spawner capacity for each population domain, reach scale estimates were first divided by survey reach length as a measure of redd density per linear stream distance. Total redd capacity was then estimated by linear extrapolation of mean redd density within strata that correspond to position in the stream network (upper, lower, and valley sections) and channel

size (i.e. tributaries vs mainstem). Finally, capacity estimates for each strata were summed as an estimate of base model spawner capacity for each population (CC = 25,653, UGR = 28,397 [Appendix 2: Base Model Parameters]).

We used an approach similar to those described for egg to parr survival and capacity (see Egg to Parr Survival above) to estimate a survival parameter for use in the base LCM. This involved fitting a Beaverton-Holt function to abundance data at each stage with the capacity parameter fixed to our capacity estimate from the HSI model. This model was fit to unpublished ODFW estimates of annual adults on the spawning grounds to estimates of total spawners obtained through redd and carcass survey data. Fitting the Beaverton-Holt model to the data also yielded an estimate of error that was used to model variability in predicted spawner abundances.

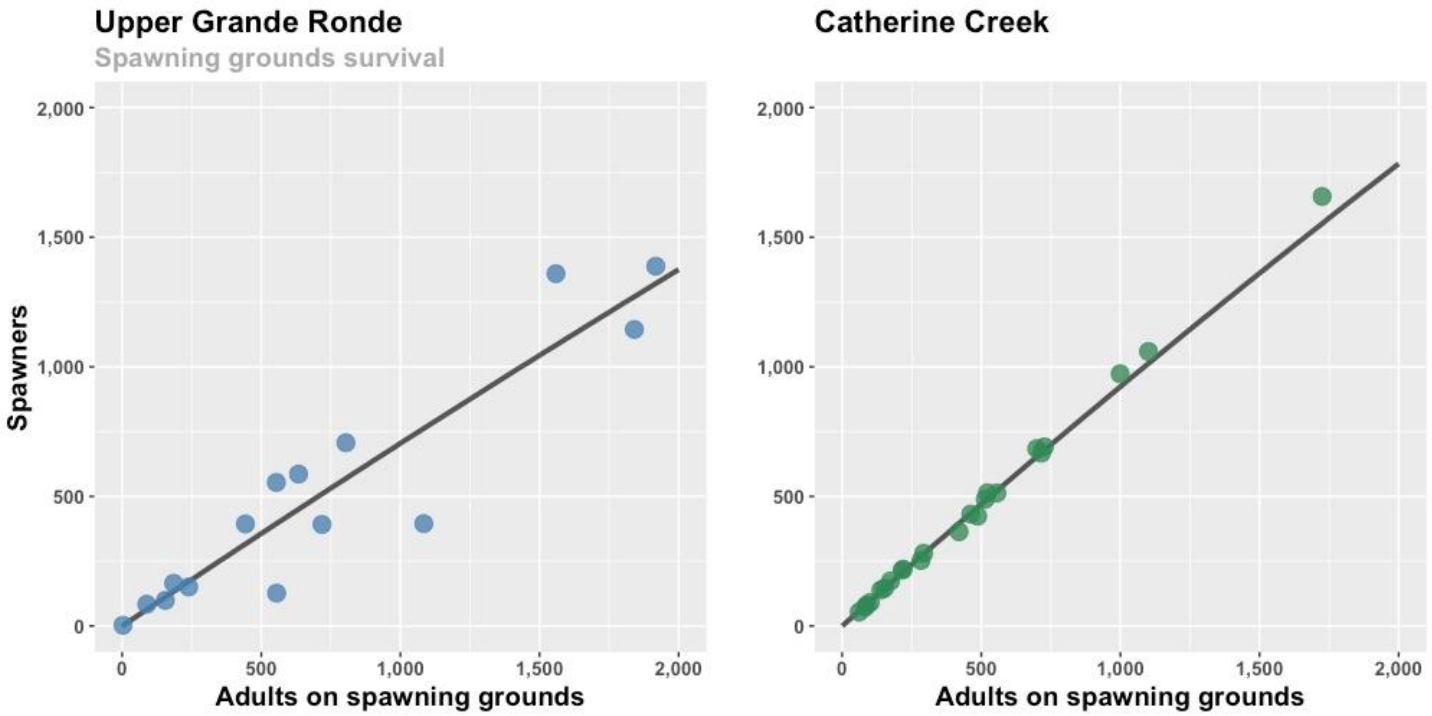

FIGURE 5. BEAVERTON-HOLT MODEL FIT TO ODFW ESTIMATES OF ADULTS PASSED ABOVE ADULT WEIRS AND TOTAL SPAWNING ADULTS IN EACH SYSTEM. NOTE, THAT CARRYING CAPACITY IS NOT SHOWN, AND CURVES APPEAR STRONGLY LINEAR DUE TO SPAWNER CAPACITY ESTIMATES FROM THE HSI MODEL BEING WELL ABOVE THOSE COMMONLY OBSERVED.

Spawner Fecundity

Female fecundity for both populations was modelled as 3831 eggs per female based on available estimates provided by Van Dyke (2008) for Catherine Creek chinook.

Table 10. Estimates of eggs per. female for Catherine Creek chinook from Van Dyke (2008).

Year	Fecundity (eggs per. female)
1997	3782
1998	4066
1999	3742
2000	3872
2001	3801
2002	3754
2003	3868
2004	3742
2005	3852

Base Model Validation

Several measures were taken to describe the accuracy of our LCM framework in reproducing UGR and CC population dynamics. This effort relied on an initial visual evaluation of model behavior and progressed to comparisons of modelled freshwater population abundances across life-stages to available data.

Base Model Behavior

We use initial model runs to visualize the behavior of the base model parameters developed for the Upper Grande Ronde and Catherine Creek Chinook Salmon populations. These model runs consisted of 500 iterations of a 150-year model seeded with 10,000 eggs and 5000 natural and hatchery origin smolt. To demonstrate the behavior of each population with and without supplementation we discontinued the supplementation component of each population at year 100.

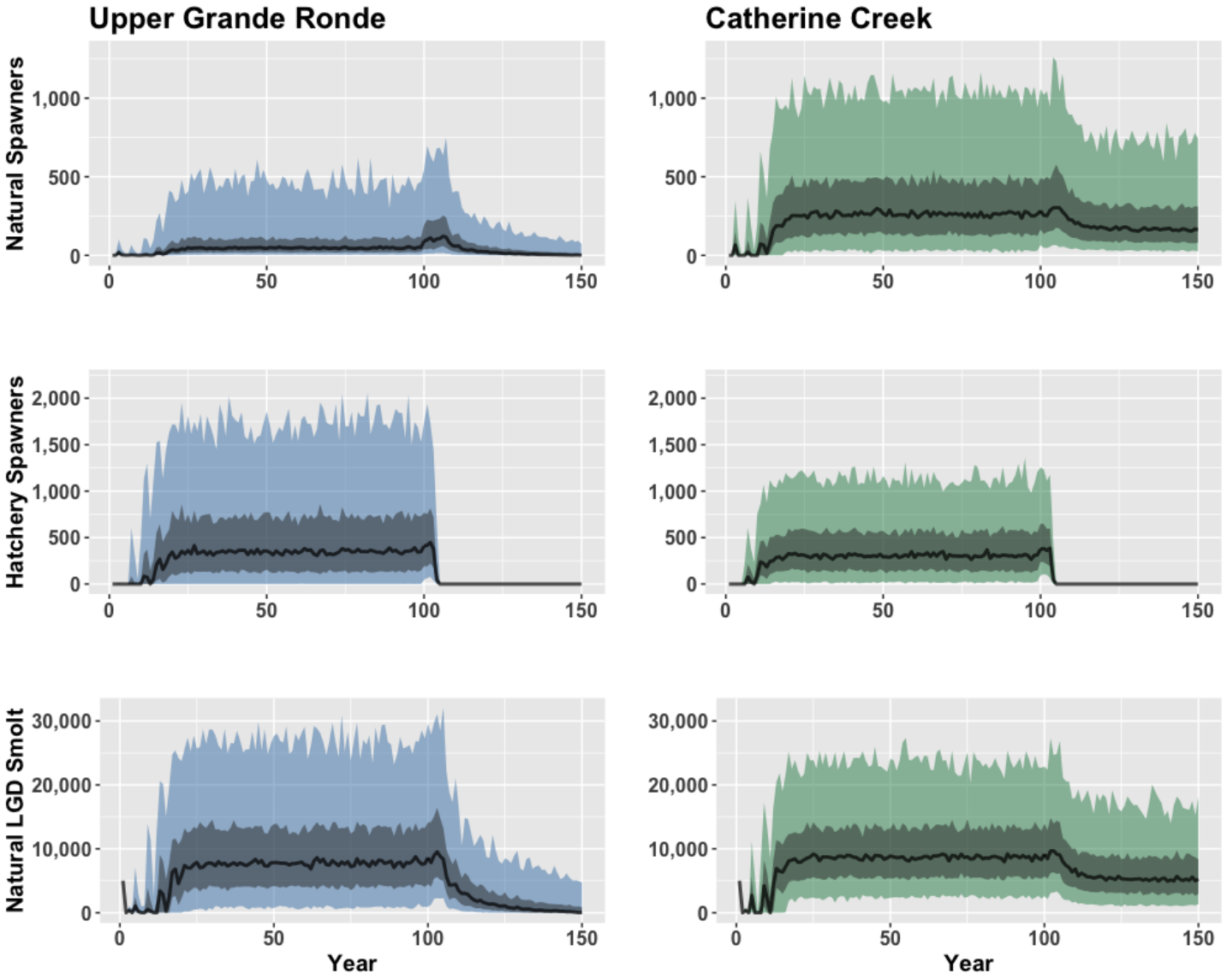

FIGURE 6. VISUAL DEPICTION OF MODEL SIMULATION BEHAVIOR SHOWING MAJOR LIFE-STAGE ABUNDANCE FOR 500 ITERATIONS OF A 150 YEAR MODEL. COLORED REGIONS REPRESENT THE 5TH AND 95TH, GREY REGIONS REPRESENT 25TH AND 75TH, AND BLACK LINES REPRESENT THE MEDIAN POPULATION ABUNDANCE. VISUALIZATIONS ALSO DEMONSTRATES THE IMPACT THAT CEASING HATCHERY SUPPLEMENTATION IN YEAR 100 HAS ON THE TRAJECTORY OF EACH POPULATION.

A visual evaluation of base model behavior (Figure 6Figure 1) showed that populations reach semi-stable equilibrium after approximately 30 years. Thus, we treated the first 40 years of each model run as a burn-in period during model validation and evaluation of restoration and climate change impacts. Modelled population abundances also increase slightly when the hatchery supplementation program is discontinued due to an initial increase of adults reaching the spawning grounds. However, the model suggests that the Upper Grande Ronde would quickly trend toward extinction without hatchery supplementation, while Catherine Creek would reach a new although slightly depressed stable population equilibrium.

MODELLED VS OBSERVED DATA

As part of our model validation process we compared available population abundance observations for late-summer parr, hatchery and natural origin smolt reaching LGD, and hatchery and natural origin adults returning to the spawning grounds (i.e. returning to adult weirs) with the predicted distribution of population abundances for these stages. To

develop a modelled dataset for use in validation we sampled the population abundance for each life-stage at year 50 from 500 iterations of a 100 - year run of the base model. Because our base model was parameterized using population data at a point when the hatchery supplementation program on the UGR and CC was being implemented (i.e., brood year 1998 to current), model predictions were only compared to observed data during this time period.

TABLE 11. COMPARISON OF THE MEDIAN POPULATION SIZE FROM OUR MODEL VALIDATION DATASET AND OBSERVED POPULATION ESTIMATES SHOWING THE DIFFERENCE AND RELATIVE DIFFERENCE ACROSS LIFE STAGES AND AMONG NATURAL AND HATCHERY COMPONENTS OF EACH POPULATION.

				Median abundance			
Pop.	Origin	Stage	Location	Observed	Modelled	Obs. - Mod.	Difference
UGR	Natural	Parr	Spawning grounds	58770	61767	2997	5%
		Smolt	Lower Granite Dam	9314	7669	-1645	-18%
		Adult	Returns to spawning grounds	240	143	-97	-40%
	Hatchery	Smolt	Release on spawning grounds	232350	199646	-32705	-14%
		Smolt	Lower Granite Dam	101902	84371	-17532	-17%
		Adult	Returns to spawning grounds	976	565	-412	-42%
CC	Natural	Parr	Spawning grounds	66043	80360	14317	22%
		Smolt	Lower Granite Dam	4657	8819	4162	89%
		Adult	Returns to spawning grounds	388	301	-87	-22%
	Hatchery	Smolt	Release on spawning grounds	141598	131057	-10541	-7%
		Smolt	Lower Granite Dam	88687	74808	-13880	-16%
		Adult	Returns to spawning grounds	705	435	-271	-38%

We assessed the agreement between observed population abundance estimates and model predictions visually in a series of boxplots (Figure 7, Figure 8) that also show raw observed and modelled population observations. We also evaluated the agreement between observed and modelled data in a regression between the median observed and median modelled value of abundance across life-stages (Figure 9, Table 11).

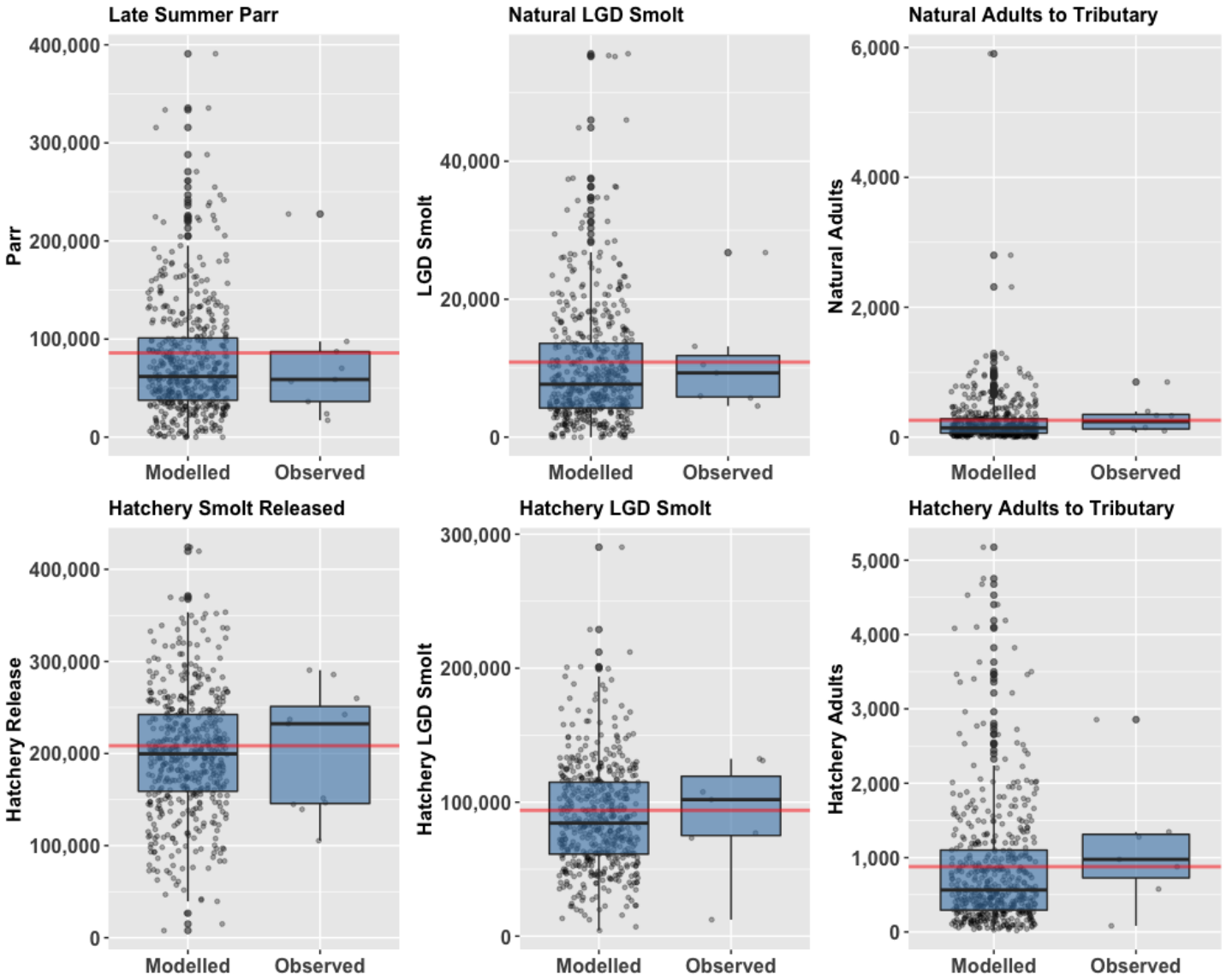

FIGURE 7. VISUAL VALIDATION OF MODEL PERFORMANCE FOR THE UPPER GRANDE RONDE. FIGURES CONTRAST THE DISTRIBUTION OF POPULATION ABUNDANCES FOR LIFE-STAGES AS MODEL PREDICTIONS AND OBSERVED ESTIMATES. THE MODELLED DATA IS BASED ON THE POPULATION ABUNDANCE AT YEAR 50 FROM 500 ITERATIONS OF A BASE MODEL SCENARIO. THE RED LINE SHOWS THE MODEL PREDICTED POPULATION ABUNDANCE AT EACH LIFE-STAGE WHEN MODEL STOCHASTICITY HAS BEEN TURNED OFF (I.E. DETERMINISTIC MODEL PREDICTION).

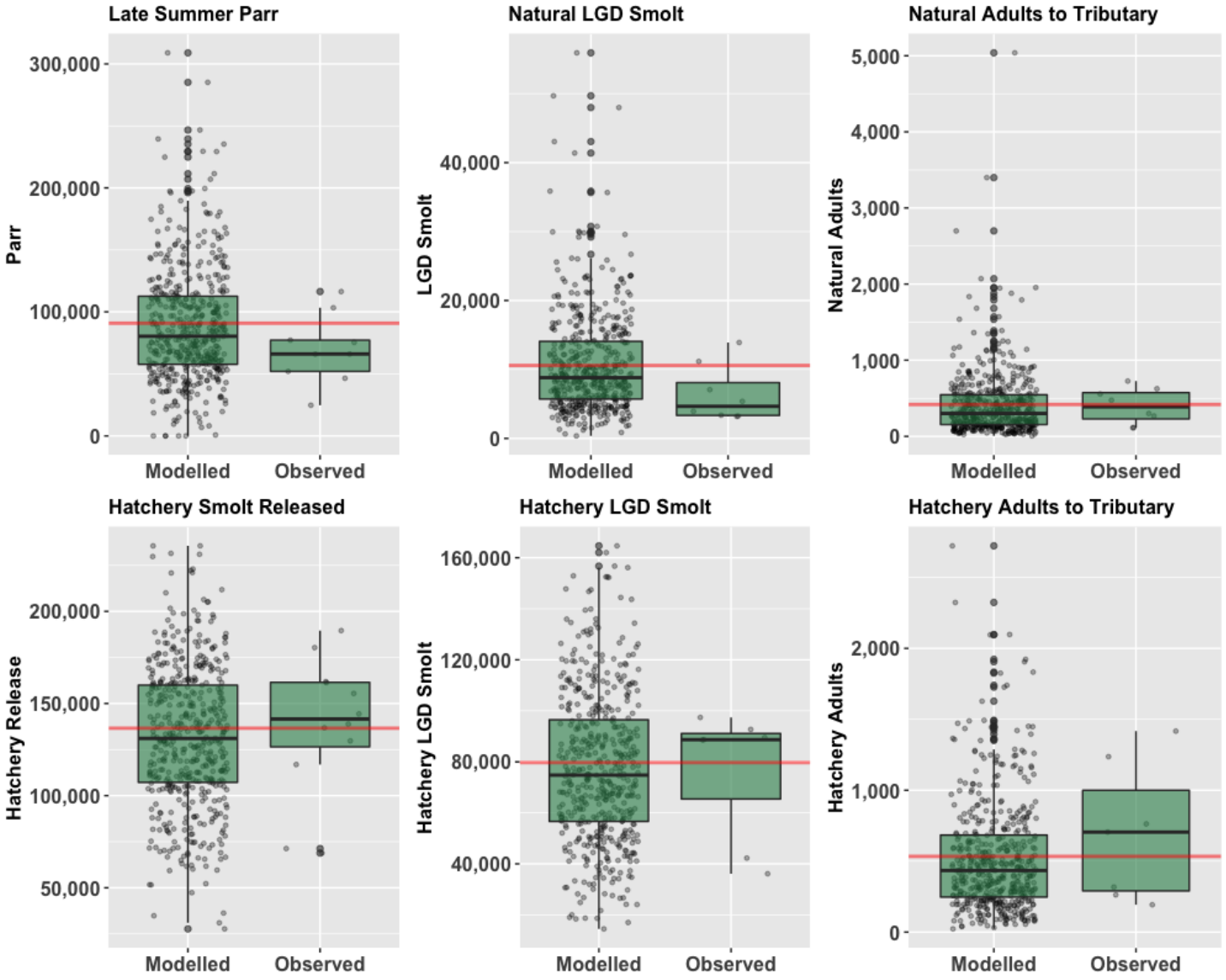

FIGURE 8. VISUAL VALIDATION OF MODEL PERFORMANCE FOR CATHERINE CREEK. FIGURES CONTRAST THE DISTRIBUTION OF POPULATION ABUNDANCES FOR LIFE-STAGES AS MODEL PREDICTIONS AND OBSERVED ESTIMATES. THE MODELLED DATA IS BASED ON THE POPULATION ABUNDANCE AT YEAR 50 FROM 500 ITERATIONS OF A BASE MODEL SCENARIO. THE RED LINE SHOWS THE MODEL PREDICTED POPULATION ABUNDANCE AT EACH LIFE-STAGE WHEN MODEL STOCHASTICITY HAS BEEN TURNED OFF (I.E. DETERMINISTIC MODEL PREDICTION).

Our validation procedures suggested a high correspondence between observed population abundance estimates and those predicted among life-stages by our base model. This statement holds particularly well when evaluating the median values of model - based predictions and observed estimates regardless of population and origin. However, visual validation of raw model predictions does suggest that population abundances within our model occupy a broader range than have been observed for these populations in the years on record. However, one must consider that the observed data available is sparse at best and based on roughly a decade of data collection and population estimation. In contrast, we used 500 individual 100 year model iterations to produce our validation datasets, and given the large variability built into our model framework it is not surprising that our modelled populations occupy a larger space of potential trajectories.

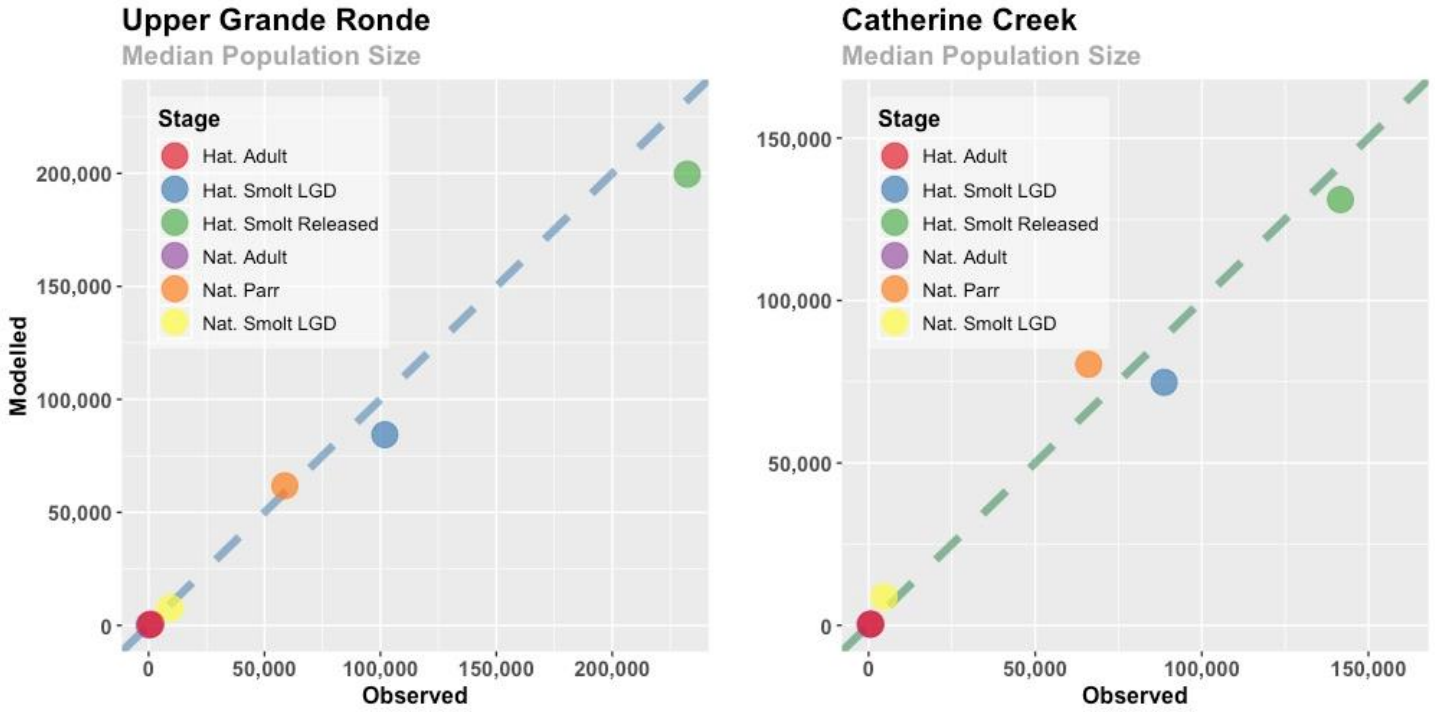

FIGURE 9. VISUAL VALIDATION OF MODEL ACCURACY BETWEEN OBSERVED AND MODEL PREDICTED POPULATION ABUNDANCES FOR NATURALLY (NAT.) AND HATCHERY (HAT.) REARED COMPONENTS OF THE POPULATION.

RESTORATION AND CLIMATE SCENARIOS

Following validation of the base model parameterization (hereafter 'Curr' for current condition), the LCM modelling framework was used to investigate Chinook population performance in the UGR and CC according to an array of restoration and climatic scenarios (Table 12, Table 14). These scenarios are based on two separate modelling frameworks developed by CRITFC that consider how future climate and restoration trajectories may impact the availability of juvenile rearing and adult spawning grounds habitat within the UGR and CC. More specific information on these restoration and climate modelling frameworks evaluated here can be found within Justice et al. (2017 [hereafter 'Justice Scenarios']), and in unpublished reports describing a Structural Equation Modelling (hereafter 'SEM Scenarios') approach that relates changes to instream habitat in the form of increased pool density to the capacity of juvenile Chinook in each system.

JUSTICE SCENARIOS

Restoration and climate modelling presented in work by Justice et al. (2017) evaluates the impacts of alternative temperature/habitat futures that include the effects of global warming manifested as increased streamflow and

hydrological change in the presence of habitat restoration (i.e., Table 12, scenarios 'Clim', 'ClimVeg', 'ClimVegWid'). These alternative futures are expressed in terms of proportional changes to freshwater rearing capacity from the base model, which are invoked within our LCM at the egg to parr stage transition.

TABLE 12. SCENARIOS MODELED AFTER JUSTICE ET AL. (2017). FOR LCM INPUTS, EACH SCENARIO IS REPRESENTED AS A PROPORTION INCREASE OR DECREASE IN SUMMER PARR REARING AND SPAWNER CAPACITY.

Scenario abbreviation	Description
Curr	Baseline model calibrated using 2010 temperature, climate, vegetation, and hydrologic conditions
Clim	Air temperature and streamflow set to 2080s climate projections.
ClimVeg	2080s climate projections and vegetation set to potential cover and height at 75 years.
ClimVegWid	2080s climate projections, vegetation set to potential cover and height at 75 years, and channel width set to historic conditions.

We also extended the Justice et al. alternative temperature futures to include impacts to prespawn habitat suitable for survival of adult Chinook on the spawning grounds during summer. This was done by proportionally adjusting spawner capacity (from the base model) based on the relative change in spawning habitat availability. Under each scenario, spawning habitat was considered unsuitable if modelled daily August mean temperature (available from Norwest 2080's stream temperature dataset: https://www.fs.fed.us/rm/boise/AWAE/projects/NorWeST.html) exceeded an upper threshold of 17.2 °C considered lethal for adult Chinook. This threshold was based on the observation that 95% of the salmon redds in the upper Grande Ronde River occurred in areas with water temperatures below 17.2 °C (Tom Cooney, NOAA, pers. comm.).

TABLE 13. PROPORTIONAL INCREASE/DECREASE AND ABSOLUTE CAPACITY ESTIMATES USED UNDER EACH RESTORATION AND CLIMATE SCENARIO FOR THE UPPER GRANDE RONDE (UGR) AND CATHERINE CREEK (CC) CHINOOK POPULATIONS UNDER THE JUSTICE ET AL. (2017) HABITAT FRAMEWORK.

		Parr capacity		Spawner capacity	
Population	Scenario abbreviation	% change	input	% change	input
UGR	Curr	0%	108087	0%	28397
	Clim	-53%	50801	-60%	11491
	ClimVeg	63%	176181	0%	28484
	ClimVegWid	114%	231306	10%	31264
CC	Curr	0%	111897	0%	25653
	Clim	-36%	71614	-36%	16399
	ClimVeg	20%	134276	-1%	25523
	ClimVegWid	37%	226992	1%	25955

SEM SCENARIOS

Similar to the Justice scenarios, the SEM scenarios consider future restoration and climatic conditions for the UGR and CC and associated impacts to the quantity and quality of juvenile rearing and adult summer habitat (Table 14). Again,

these scenarios account for climate change in the absence of restoration ('Clim') as well as when restoration results in increased riparian vegetation ('ClimVeg75') and/or creation of pool habitat ('ClimPools', 'ClimPoolsVeg'). As with the Justice scenarios, the availability of habitat with summer temperatures suitable for survival of pre-spawn adult Chinook were also modelled as proportional changes in spawner capacity. Also, because our primary management question is whether the proposed restoration actions can decrease extinction risk for these we only evaluate the SEM scenarios when the supplementation has been discontinued in year 40.

TABLE 14. STRUCTURAL EQUATION MODELING SCENARIOS. FOR LCM INPUTS, EACH SCENARIO IS REPRESENTED AS A PROPORTION INCREASE OR DECREASE IN SUMMER PARR REARING AND SPAWNER CAPACITY.

Scenario Abbreviation	Description
Curr	Baseline model calibrated using 2010 temperature, climate, vegetation, and hydrologic conditions
Clim	Air temperature and streamflow set to 2080s climate projections.
ClimPool	Air temperature and streamflow set to 2080s climate projections and restoration resulting in increase in pool habitat.
ClimVeg	2080s climate projections and vegetation set to potential cover and height at 75 years.
ClimPoolVeg	2080s climate projections, vegetation set to potential cover and height at 75 years, and restoration resulting in increase in pool habitat.

TABLE 15. PROPORTIONAL INCREASE/DECREASE AND ABSOLUTE CAPACITY ESTIMATES USED UNDER EACH RESTORATION AND CLIMATE SCENARIO FOR THE UPPER GRANDE RONDE (UGR) AND CATHERINE CREEK (CC) CHINOOK POPULATIONS UNDER THE STRUCTURAL EQUATION MODELLING SCENARIOS.

		Parr capacity		Spawner capacity	
Population	Scenario abbreviation	% change	input	% change	input
UGR	Curr	0%	108087	0%	28397
	Clim	-58%	45397	-60%	11491
	ClimPool	-53%	50801	-60%	11491
	ClimVeg75	3%	111654	0%	28484
	ClimPoolsVeg	13%	122138	0%	28484
CC	Curr	0%	111897	0%	25653
	Clim	-39%	68257	-36%	16399
	ClimPool	7%	120177	-36%	16399
	ClimVeg75	-3%	108876	-1%	25523
	ClimPoolsVeg	58%	176797	-1%	25523

LCM SIMULATION METHODS

We used the model to simulate trajectories for each population under each scenario over a 50 - year period (90 years minus a 40 year burn in) within 500 Monte Carlo model iterations. All model iterations were seeded with 10000 eggs and 1000 natural and hatchery origin smolt at LGD. Each scenario was run using the current hatchery supplementation

scheme, as well as under a “cease supplementation” scenario in which hatchery supplementation is turned off in year 40.

We summarized the potential outcome of each scenario expressed as the median abundance of natural spawners over each 50 – year model iteration, and as the probability of quasi-extinction risk (pQER) for the population. A model run was considered at risk of quasi-extinction if at any point in the 50 - year simulation the spawning population remained below 50 for 4 consecutive years. pQER was calculated as the proportion of the 500 model iterations that the population reached the quasi extinction threshold at any point. pQER was only calculated for scenario simulations in which supplementation was discontinued as the hatchery supplementation programs ensures future viability of the populations.

LCM Scenario Results and Discussion

Several significant changes to the LCM framework introduced here (as opposed to chapter 9.f in ISAB 2017) increases the realism and utility of the model to assess recovery potential for upper Grande Ronde River and Catherine Creek Chinook Salmon in a LCM context. Specifically, accounting for spawner capacity in addition to parr improves the model’s ability to represent the impact of each restoration and climatic scenario on total life-cycle productivity. Further, accounting for life-history dependent presmolt survival probabilities, natural and hatchery origin SAR rates, and more accurately representing the supplementation scheme and survival of hatchery smolts all contribute to a model that better reflects the population and management dynamics within these systems. Changes made to the variance structure of stochastic model components should also improve our confidence in the LCM’s ability to forecast future trajectories for the UGR and CC Chinook populations, and estimate probabilities associated with future population viability under different restoration and management scenarios.

Outcomes for the Justice and SEM restoration and climate scenarios are presented in Figures 10 – 15 and Tables 14 – 15 and demonstrate a number of considerations relevant to future recovery and restoration planning in these systems. For both populations, proportional changes in parr and spawner carrying capacity reflected in the Justice and SEM scenarios translated into increased natural spawner abundances on a rank order basis. However, the magnitude of the population response did not increase/decrease on a one-to-one basis to the capacity changes under each scenario. Productivity responses (i.e. increase/decrease) were generally more pronounced within the UGR, which may be due to several factors. Within the UGR, current temperature regimes throughout much of the spawning and rearing network are commonly very near the upper temperature threshold for Chinook. Additionally, returns of natural origin spawners to the UGR have been much lower than those observed within CC, and these low values are more sensitive to proportional changes in productivity.

Running the restoration and climate change scenarios with and without supplementation also has the potential to inform future management for these systems. For example, even under the base (i.e., ‘Curr’) population conditions, our model suggests that CC has a relatively low extinction risk 0.032 that would increase to roughly 0.12 in the face of climate change even when no restoration was implemented (i.e. ‘Clim’). On the other hand, our simulation results suggest that extinction risk is certain for the UGR in the absence of supplementation, and that under the most aggressive restoration scenario (i.e. ‘ClimVegWid’) extinction risk could be lowered to roughly 0.78. While we do not attempt to make broad management recommendations here, the hope is that these model outcomes can be used to optimize future investment in restoration and hatchery supplementation programs that support viable natural populations in these systems.

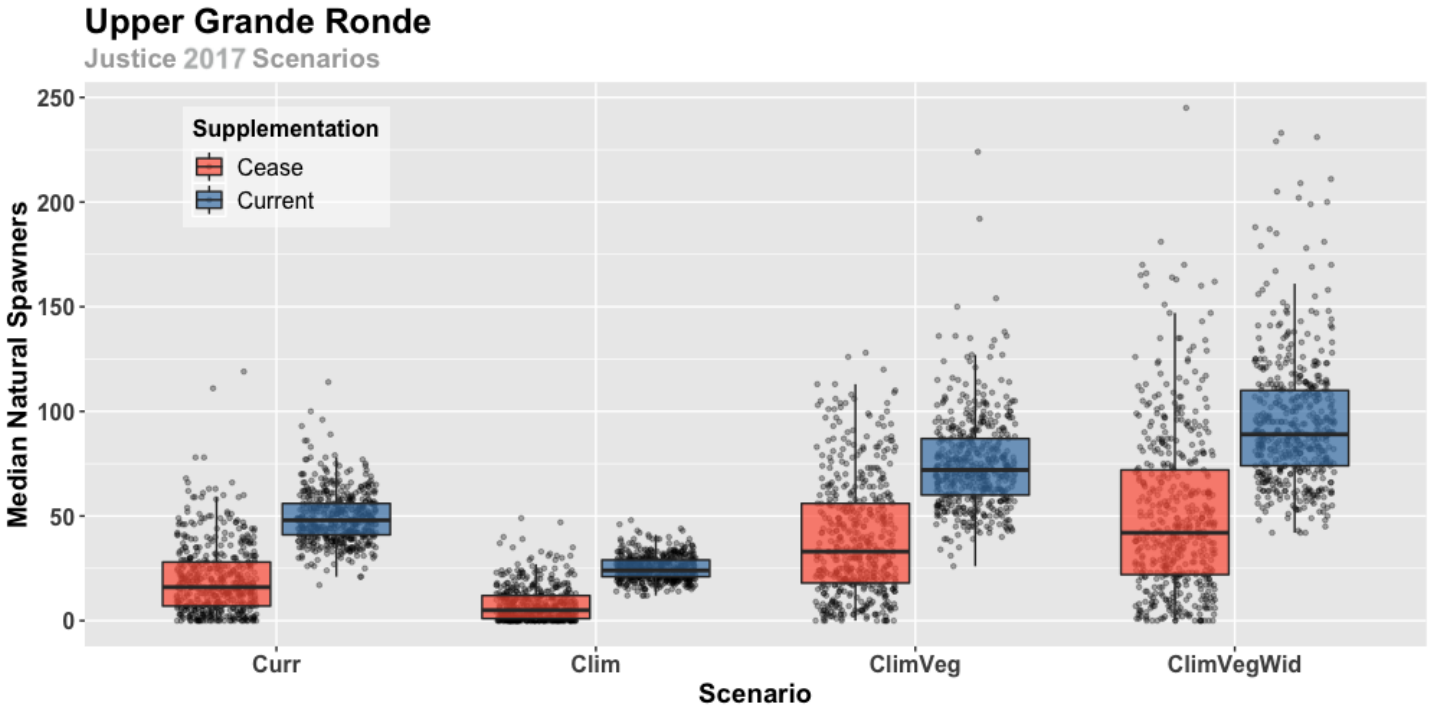

FIGURE 10. BOXPLOTS SHOWING THE DISTRIBUTION OF THE MEDIAN POPULATION SIZE FOR UPPER GRANDE RONDE NATURAL ORIGIN SPAWNING CHINOOK FOR RESTORATION AND CLIMATE SCENARIOS DESCRIBED BY JUSTICE ET AL. 2017. MODEL RUNS AT CURRENT SUPPLEMENTATION AND WITH SUPPLEMENTATION DISCONTINUED ARE SHOWN. JITTERED POINTS SHOW THE MEDIAN VALUE FOR EACH OF 500 MODEL RUNS.

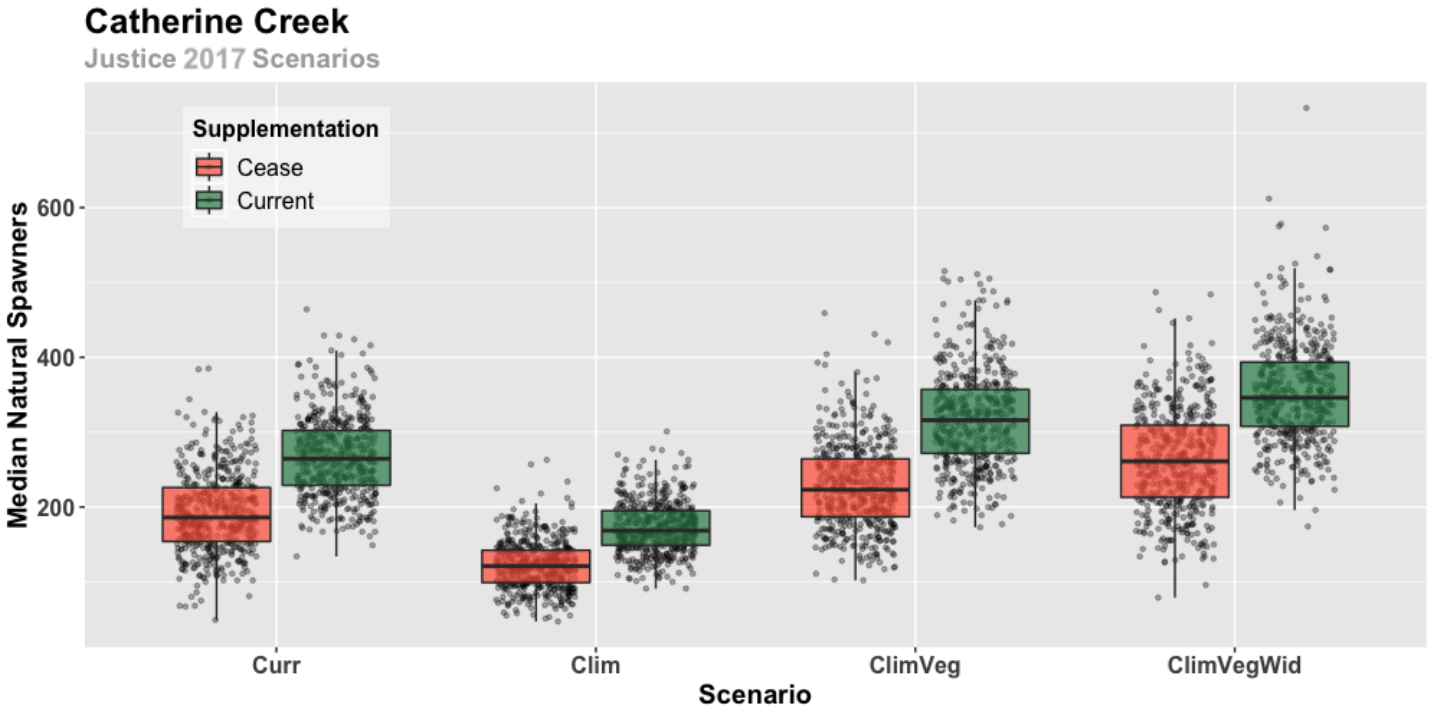

FIGURE 11. BOXPLOTS SHOWING THE DISTRIBUTION OF THE MEDIAN POPULATION SIZE FOR CATHERINE CREEK NATURAL ORIGIN SPAWNING CHINOOK FOR RESTORATION AND CLIMATE SCENARIOS DESCRIBED BY JUSTICE ET AL. 2017. MODEL RUNS AT CURRENT SUPPLEMENTATION AND WITH SUPPLEMENTATION DISCONTINUED ARE SHOWN. JITTERED POINTS SHOW THE MEDIAN VALUE FOR EACH OF 500 MODEL RUNS.

TABLE 16. MEDIAN POPULATION SIZE OF NATURAL ORIGIN SPAWNING CHINOOK FOR 500 MODEL ITERATIONS OF RESTORATION SCENARIOS DESCRIBED BY JUSTICE ET AL. 2017. ALSO SHOWING RELATIVE DIFFERENCE OF EACH SCENARIO TO THE CURRENT CONDITIONS ('CURR') IN MODEL RUNS AT CURRENT HATCHERY SUPPLEMENTATION AND WHEN SUPPLEMENTATION IS DISCONTINUED.

Pop	Scenario	Current Supplementation		Cease Supplementation		pQER
		Median natural spawners	Relative to Curr	Median natural spawners	Relative to Curr	
UGR	Curr	48	-	16	-	0.972
	Clim	24	-50%	5	-69%	1
	ClimVeg	72	50%	33	106%	0.872
	ClimVegWid	89	85%	42	163%	0.784
CC	Curr	265	-	186	-	0.032
	Clim	169	-36%	121	-35%	0.118
	ClimVeg	316	19%	223	20%	0.004
	ClimVegWid	346	31%	261	40%	0.01

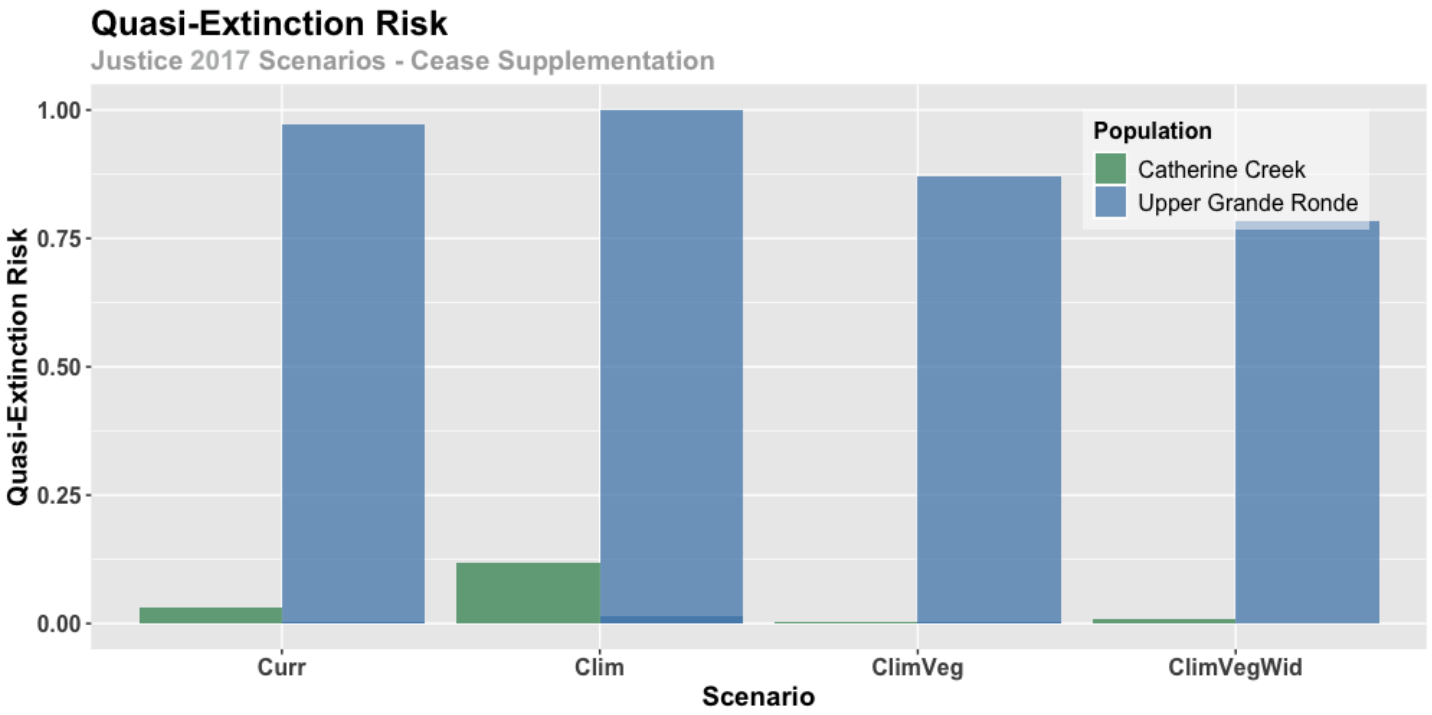

FIGURE 12. QUASI – EXTINCTION RISK (PQER) UNDER EACH RESTORATION AND CLIMATE SCENARIO FOR THE UPPER GRAND RONDE AND CATHERINE CREEK CHINOOK POPULATIONS FOR RESTORATION AND CLIMATE SCENARIOS DESCRIBED BY JUSTICE ET AL. 2017.

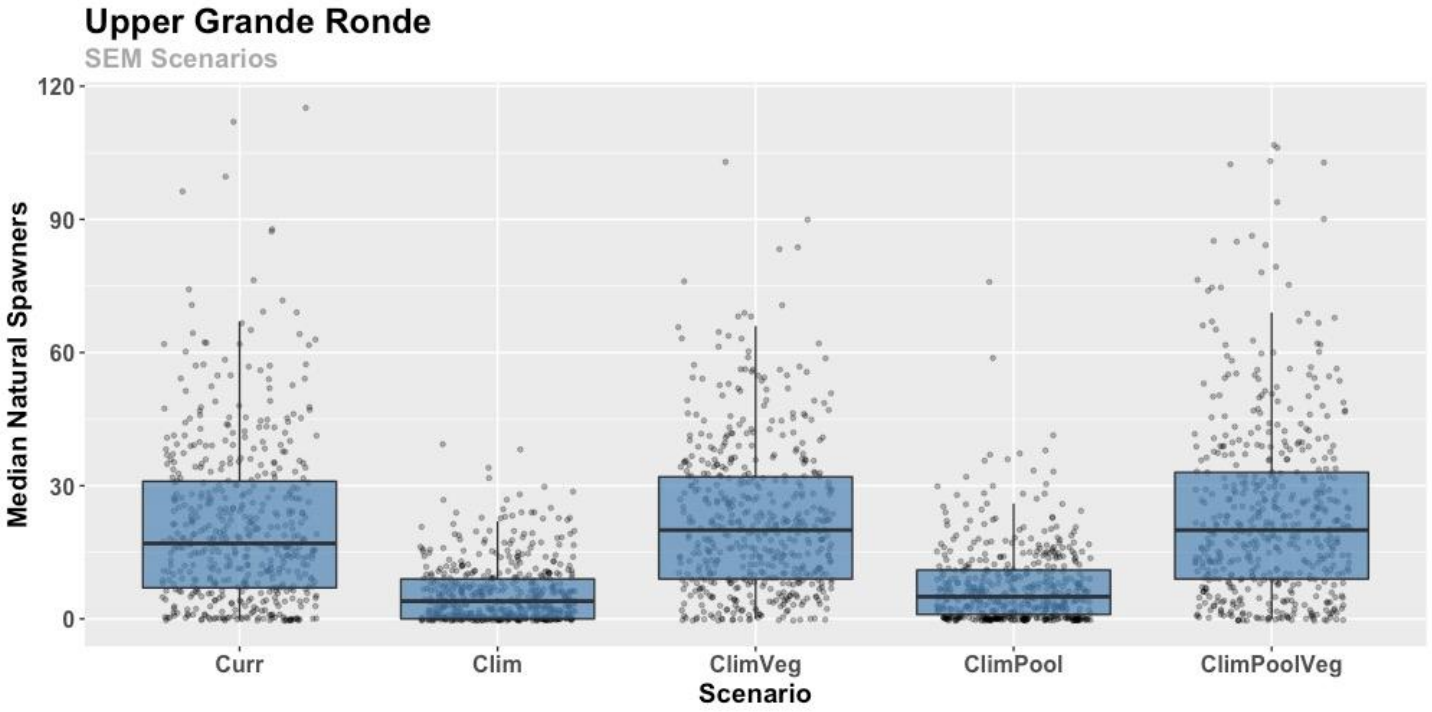

FIGURE 13. MEDIAN POPULATION SIZE OF UPPER GRANDE RONDE NATURAL ORIGIN SPAWNING CHINOOK BASED ON RESTORATION AND CLIMATE SCENARIOS DESCRIBED BY THE STRUCTURAL EQUATION MODEL RELATIONSHIPS. MEDIAN POPULATION SIZE IS FROM 500 MODEL SIMULATIONS AND ASSUMES DISCONTINUATION OF HATCHERY SUPPLEMENTATION.

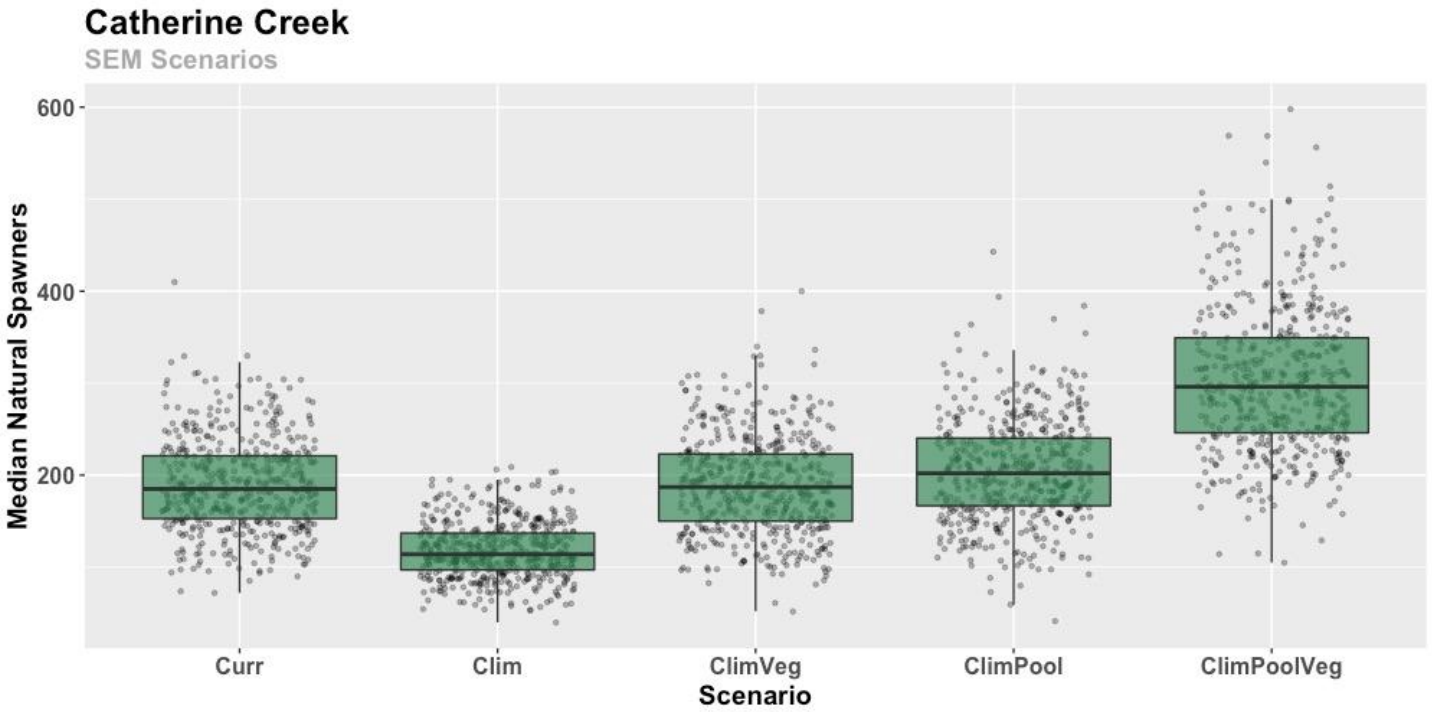

FIGURE 14. MEDIAN POPULATION SIZE OF CATHERINE CREEK NATURAL ORIGIN SPAWNING CHINOOK BASED ON RESTORATION AND CLIMATE SCENARIOS DESCRIBED BY THE STRUCTURAL EQUATION MODEL RELATIONSHIPS. MEDIAN POPULATION SIZE IS FROM 500 MODEL SIMULATIONS AND ASSUMES DISCONTINUATION OF HATCHERY SUPPLEMENTATION.

TABLE 17. MEDIAN POPULATION SIZE OF NATURAL ORIGIN SPAWNING CHINOOK FOR 500 MODEL ITERATIONS OF RESTORATION SCENARIOS DESCRIBED BY THE SEM SCENARIOS. ALSO SHOWING RELATIVE DIFFERENCE OF EACH SCENARIO TO THE CURRENT CONDITIONS ('CURR') AND QUASI EXTINCTION RISK (PQER).

		Cease Supplementation		
Population	Scenario	Median Natural Spawners	Relative to Curr	QER
UGR	Curr	17	-	0.968
	Clim	4	-76%	1
	ClimVeg	20	18%	0.982
	ClimPool	5	-71%	0.998
	ClimPoolVeg	20	18%	0.952
CC	Curr	185	-	0.028
	Clim	114	-38%	0.15
	ClimVeg	187	1%	0.04
	ClimPool	202	9%	0.022
	ClimPoolVeg	296	60%	0.002

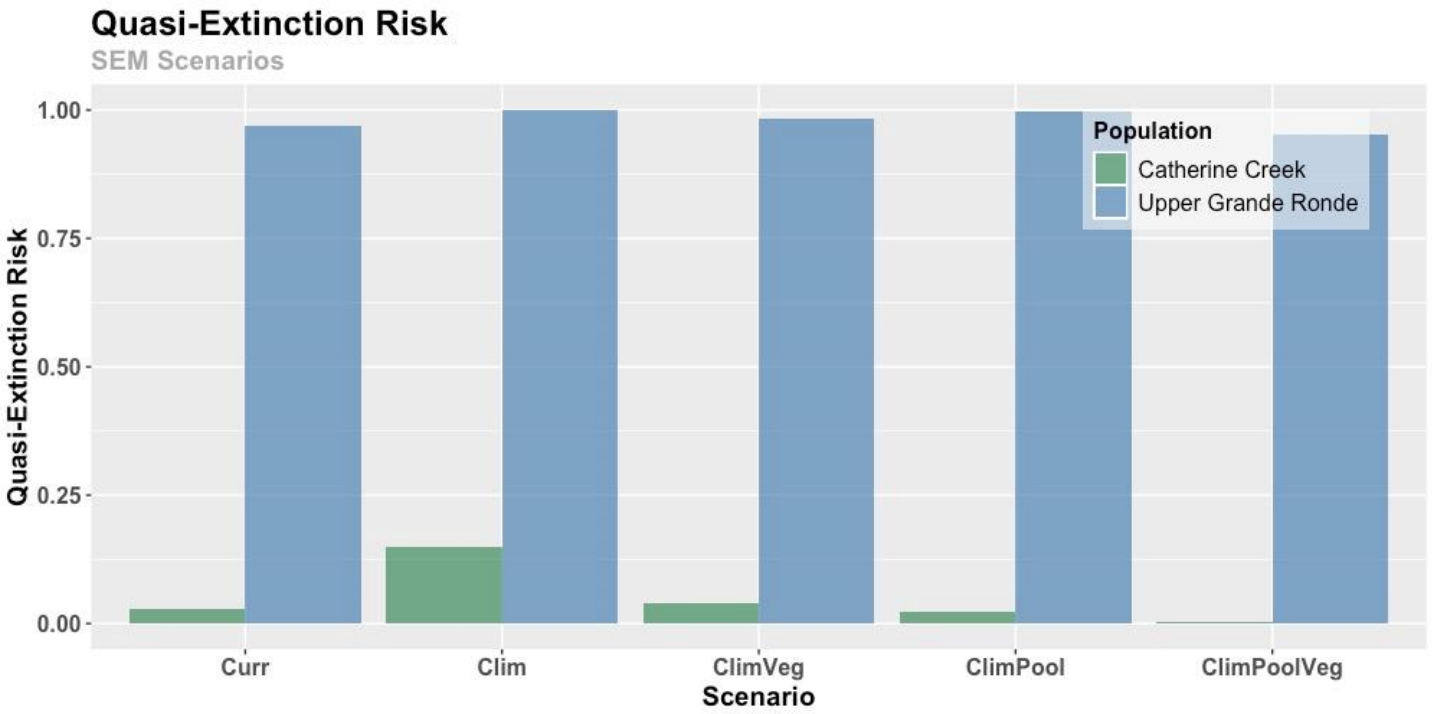

FIGURE 15. QUASI EXTINCTION RISK BASED ON RESTORATION AND CLIMATE SCENARIOS FROM THE STRUCTURAL EQUATION MODEL ANALYSIS FOR THE UPPER GRANDE RONDE AND CATHERINE CREEK CHINOOK POPULATIONS.

MODEL SENSITIVITY

As an extension to our modelling of future population trajectories under restoration and climatic conditions, we also conducted a sensitivity analysis for our LCM framework for both the UGR and CC base LCM parameterizations. This extension is included here for a number of reasons. First, our modelling scenarios only focused on manipulating capacity, and we sought to contrast model performance by comparing manipulations of capacity to increases and decreases directly to productivity (i.e. survival). Second, all of our LCM scenarios manipulated capacity simultaneously at two life-stages which did not allow us to attribute population responses to an individual life-stage. Additionally, modelling scenarios manipulated parameters at just two stage transitions (i.e. egg to parr and spawning grounds survival), and we wanted to contrast the sensitivity of the model over a broader scope within our populations.

For our sensitivity analysis we manipulated productivity parameters for all freshwater life-stages as well as smolt-to-adult survival. The analysis also included capacity but focused only on those stages in which density dependent survival was modelled within our restoration scenarios, namely egg-to-parr survival and adult survival on the spawning grounds. Starting with the base model for each population, we increased and decreased a single target parameter from -30% to +30% at 10% increments while holding all others constant (Table 18). These values were chosen as they produced a realistic range of parameter rate changes that could be expected as a result of management actions and it allowed a normalized means to make comparisons of model sensitivity among parameters. At each increment the model was run for 500 iterations, over which pQER and the percent change in natural origin spawner abundance from the base parameter value was calculated. Again, because our broader aim is to provide results that are relevant to establishing viable populations with hatchery supplementation discontinued, we conducted the model sensitivity analysis with supplementation turned off at year 40. We present the results of our sensitivity analysis visually in a series of plots that compare the proportional increase or decrease in natural spawners and pQER from the base model for each population (Figure 16, Figure 17).

TABLE 18. BASE (I.E. CURR) MODEL PARAMETER VALUES FOR CAPACITY AND PRODUCTIVITY ACROSS LIFE-STAGES INCLUDED IN THE SENSITIVITY ANALYSIS. ALSO SHOWING ACTUAL VALUES USED FOR EACH LIFE-STAGE IN SENSITIVITY SIMULATIONS FROM -30% TO %30.

Population	Parameter	Life Stage	Base Value	Sensitivity analysis values						
				-30%	-20%	-10%	0%	10%	20%	30%
CC	p_i	Adult Spawning Grounds	0.96	0.67	0.77	0.86	0.96	1.00	1.00	1.00
	p_i	Egg - Parr	0.32	0.22	0.26	0.29	0.32	0.35	0.38	0.42
	p_i	Headwaters Rearing - LGD Smolt	0.10	0.07	0.08	0.09	0.10	0.11	0.12	0.13
	p_i	Valley Rearing - LGD Smolt	0.12	0.08	0.10	0.11	0.12	0.13	0.14	0.16
	p_i	LGD Smolt - Tributary Adult Age 1	0.060	0.042	0.048	0.054	0.060	0.066	0.072	0.078
	p_i	Ocean Age 1 - Tributary Adult Age 2	0.66	0.46	0.53	0.59	0.66	0.73	0.79	0.86
	p_i	Ocean Age 2 - Tributary Adult Age 3	0.61	0.43	0.49	0.55	0.61	0.67	0.73	0.79
	c_i	Egg - Parr Capacity	111897	78328	89518	100707	111897	123087	134276	145466
	c_i	Adult Spawning Grounds Capacity	25653	17957	20522	23088	25653	28218	30784	33349
UGR	p_i	Adult Spawning Grounds	0.73	0.51	0.58	0.66	0.73	0.80	0.88	0.95
	p_i	Egg - Parr	0.32	0.22	0.26	0.29	0.32	0.35	0.38	0.42
	p_i	Headwaters Rearing - LGD Smolt	0.11	0.08	0.09	0.10	0.11	0.12	0.13	0.14
	p_i	Valley Rearing - LGD Smolt	0.18	0.13	0.14	0.16	0.18	0.20	0.22	0.23
	p_i	LGD Smolt - Tributary Adult Age 1	0.04	0.03	0.03	0.04	0.04	0.04	0.05	0.05
	p_i	Ocean Age 1 - Tributary Adult Age 2	0.63	0.44	0.50	0.57	0.63	0.69	0.76	0.82
	p_i	Ocean Age 2 - Tributary Adult Age 3	0.52	0.36	0.42	0.47	0.52	0.57	0.62	0.68
	c_i	Egg - Parr Capacity	108087	75661	86470	97278	108087	118896	129704	140513
	c_i	Adult Spawning Grounds Capacity	28387	19871	22710	25548	28387	31226	34064	36903

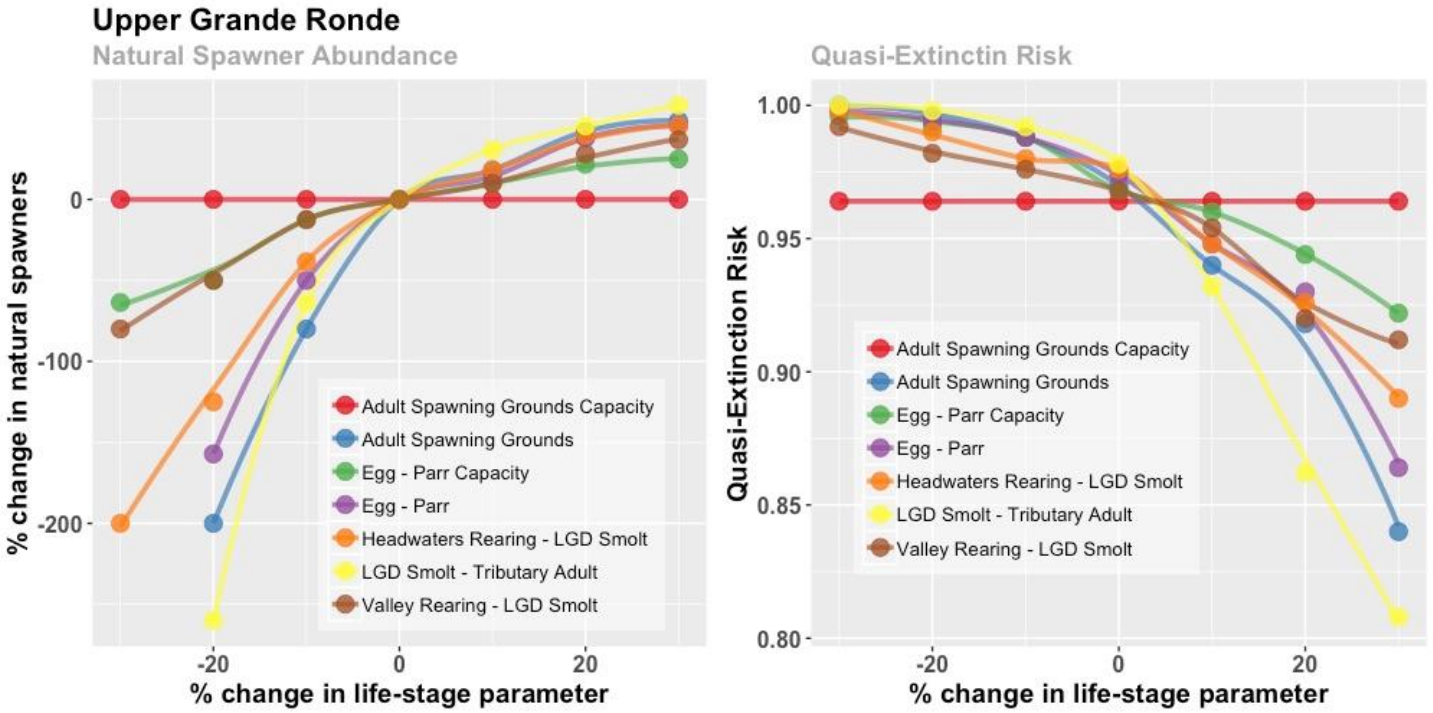

FIGURE 16. RESULTS OF THE SENSITIVITY ANALYSIS FOR THE UPPER GRANDE RONDE. LEFT PANEL SHOWS THE PERCENT CHANGE IN NATURAL SPAWNERS FROM THE BASE MODEL FOR SIMULATIONS THAT MANIPULATED LIFE-STAGE SURVIVAL AND CAPACITY FROM -30% TO +30%. RIGHT PANEL SHOWS HOW CHANGES TO SURVIVAL AND CAPACITY RESULT IN PROPORTIONAL CHANGES IN PQER. NOTE, THAT THE % CHANGE IN NATURAL ORIGIN SPAWNERS AT %-30 WAS REMOVED FOR SOME LIFE-STAGES AS THEY GREATLY INFLUENCED PRESENTATION OF THE FIGURE. LINES REPRESENTING CAPACITY ARE LABELLED AS SUCH WITHIN THE LEGEND WITH OTHER LINES REPRESENTING PRODUCTIVITY PARAMETERS.

Although our sensitivity analysis was based on proportional shifts among parameters, accurate interpretation of sensitivity results should be interpreted relative to the absolute parameter values used in this analysis. However, we do believe that the sensitivity exercise presented here demonstrates important model dynamics and may also have relevance to optimization of future management and restoration of the UGR and CC Chinook populations and habitat.

Based on this analysis, our LCM framework appears more sensitivity to changes in survival parameters rather than capacity. Both populations appeared largely insensitive to changes in spawner capacity (availability of temperature-suitable habitat for adults during summer). This result may be an artifact of spawner capacity estimates used within the base model that are orders of magnitude above those on record for these populations. Manipulation of the survival parameter for adults on the spawning grounds had large impacts to the viability of each population, especially within the UGR model where current survival rates for spawners in the system are lower than that of CC. Sensitivity of the model populations of egg-to-parr survival and capacity followed a similar pattern, with proportional changes to survival rather than capacity having a larger effect on spawner returns and pQER.

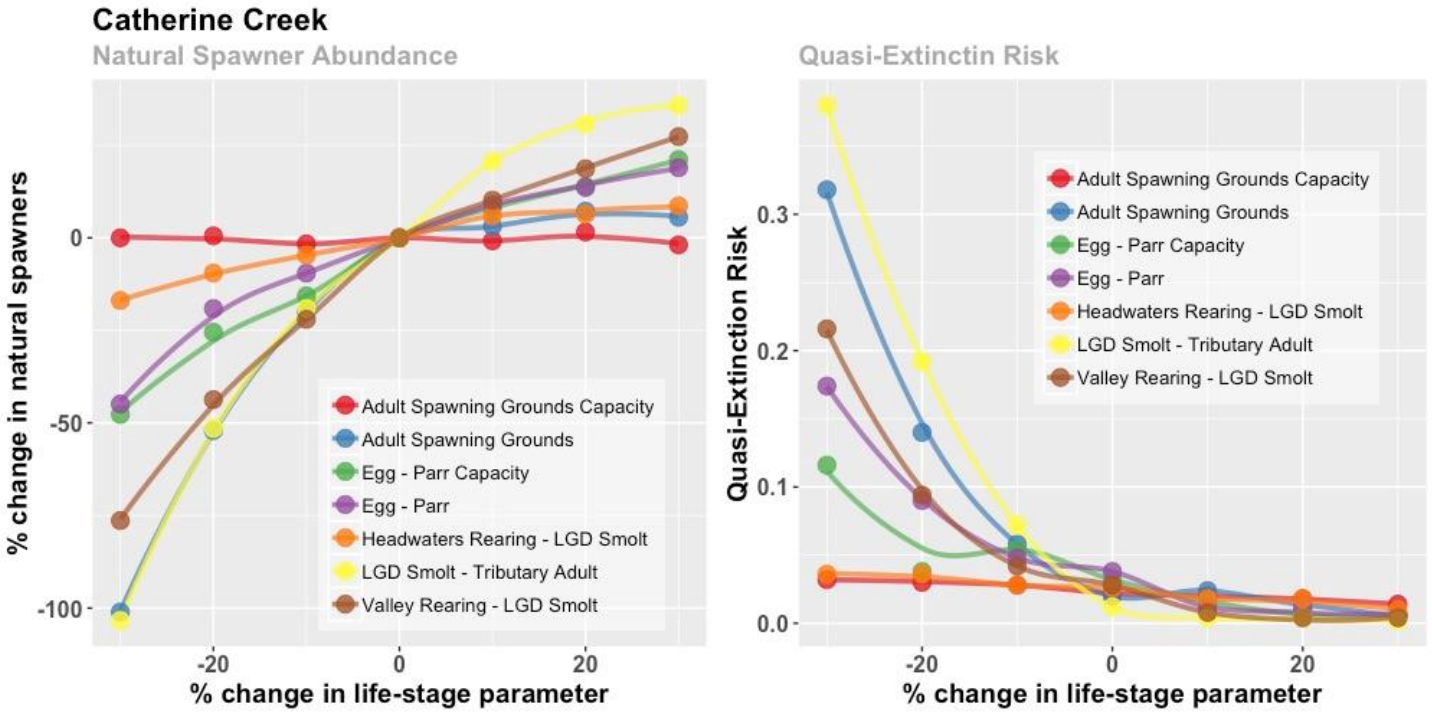

FIGURE 17. RESULTS OF THE SENSITIVITY ANALYSIS FOR CATHERINE CREEK. LEFT PANEL SHOWS THE PERCENT CHANGE IN NATURAL SPAWNERS FROM THE BASE MODEL FOR SIMULATIONS THAT MANIPULATED LIFE-STAGE SURVIVAL AND CAPACITY FROM -30% TO +30%. RIGHT PANEL SHOWS HOW CHANGES TO SURVIVAL AND CAPACITY RESULT IN PROPORTIONAL CHANGES IN PQER. LINES SHOWING CAPACITY ARE LABELLED AS SUCH WITHIN THE LEGEND WITH OTHER LINES REPRESENTING PRODUCTIVITY PARAMETERS.

Our sensitivity analysis also showed that both populations were most sensitive to increases and decreases in survival as smolt from LGD until their return as adults to the spawning grounds (i.e. the SAR). Sensitivity of our populations at this life stage is not surprising as the first - year survival input within our LCM framework (S1) are the lowest for any stage transition (0.04 and 0.07 for the UGR and CC, respectively). However, this is not to say that increases or decreases to freshwater life-stages were completely drowned by the response of the populations to outmigration and ocean survival. Indeed, survival at other life-stage transitions, such as spawning grounds survival and winter survival of rearing presmolt also appear to impact the viability of each population over the range of values considered here.

Manipulation of the presmolt survival parameters for each life-history strategy provided additional insight that may inform prioritization of restoration actions within these systems. For example, the sensitivity analysis suggested that within CC, improvements in headwaters rearing presmolt survival would result in almost no gain in adult returns, while the same improvement for valley rearing presmolt could potentially increase adult returns by greater than 25%. This type of result demonstrates the utility of an LCM and how a sensitivity analysis can be used to direct investments in habitat restoration that targets a specific life-stage.

DISCUSSION AND FUTURE ANALYTICAL CONSIDERATIONS

The model and analytical framework presented here provides novel insights concerning the dynamics of UGR and CC Chinook, and it is our intention that this work be used to guide future population management and prioritization of habitat restoration, as a well as providing a basis for future life cycle models for these populations. One of the major strengths of our LCM framework lies in efforts taken to model the dynamic interaction between the natural and hatchery component of each population, including the complexities and variability associated with the hatchery supplementation program. Indeed, our model validation suggests that our base model parameterization could accurately represent each of these components of the UGR and CC Chinook populations. This modelling framework allowed us to evaluate the viability of each population according to alternative futures where the hatchery supplementation program has been discontinued.

With this framework in place, we evaluated the future viability of each population according to two modelling approaches (i.e. Justice and SEM) that link future restoration and climate impacts to freshwater habitat quantity and quality. Our evaluation suggested that without aggressive riparian and channel restoration, predicted climate change impacts to stream temperature regimes will result in almost certain extinction of Chinook within the UGR if hatchery supplementation is curtailed. In contrast, our modelling suggests that even without hatchery supplementation, climate change will push CC Chinook toward a moderate extinction risk, and that restoration efforts could be invested to ensure the future long-term viability of this population.

While the LCM results and sensitivity analysis we present here stand alone as being informative to future management of these populations, we believe the real strength of this work resides in the development of a flexible modelling framework and set of base model parameters that can be applied to future management questions and future analysis of population trajectories. To this end, we offer a number of suggestions for further refinement of the LCM that might increase the effectiveness of these efforts:

Link habitat change to survival – Currently, the Justice and SEM scenarios that we evaluated rely on models describing the relationship between climate and habitat restoration impacts to capacity during freshwater life-stages. In reality, these habitat changes would also likely directly influence survival rates. Incorporating this interaction within future LCM scenario analyses may be informative to evaluate the effectiveness of alternative management decisions. This may be especially true for populations such as the UGR and CC which may be under-seeded due to poor hydrosystem and ocean survival.

Adult capacity on the spawning grounds – Within the current framework, estimated spawner capacities are obtained via a habitat suitability index (HSI) approach that relies on a standard redd size and the distribution of suitable substrate and velocity characteristics. Although these estimates (CC = 25,653, UGR = 28,397) may theoretically reflect a total spawner capacity based on available spawning habitat, they are an order of magnitude greater than the range of adults observed on the spawning grounds in either system (see Table 6 and Table 7). This disparity may suggest that these systems are largely under-seeded and that survival on the spawning grounds is indeed density independent. Alternatively, the disparity may indicate that the HSI model does not capture habitat characteristics that would limit over-summer adult survival. Nevertheless, the model framework, which allows for manipulation of both spawner productivity (i.e., pre-spawn survival) and capacity, provides model users the flexibility to adjust these parameters according to density dependent or independent processes as new estimates become available.

Parameter resolution within the SAR – Our current base model implements survival through the hydrosystem and ocean at a course resolution spanning from the passage of smolt at LGD until their return as adults to the spawning grounds in each tributary (i.e., CC and UGR). Although we do use age specific survival and maturation probabilities within our

model, adding additional stage transitions at key points within the outmigration and return as adults would allow the model to account for future changes to passage management and/or potential scenarios based on ocean survival.

Presmolt survival to LGD – Currently, recapture information following the parr life-stage occurs at time intervals that do not allow direct estimation of overwinter survival of presmolt rearing in headwater or valley reaches. Because of this, our LCM models presmolt survival from Summer parr to smolts at LGD adjusted for each life-history using a correction factor (see Parr to Smolt at Lower Granite Dam). Future LCM effort could emphasize the development of a more direct estimation approach, or acquisition of data that would allow a direct estimate of overwinter survival for parr exhibiting each rearing life-history strategy (i.e. headwaters or valley rearing) exclusive of survival during outmigration to LGD. This would allow the modelling framework to more directly assess the impacts that management and restoration of freshwater rearing habitat may have on the viability the UGR and CC chinook populations.

APPENDIX 1: BROODSTOCK RETENTION APPROACH

The supplementation program currently operated as part of Chinook management on the UGR and CC strongly influences the dynamics of these populations. We took the following measures in order to best represent this management strategy within the LCM framework. In order to implement the supplementation scheme, we made several simplifying assumptions that allowed us to model a mixed hatchery-natural broodstock population similar to the programs currently implemented within the UGR and CC:

1. All hatchery-reared fish are produced from supplementation fish captured in the wild and reared according to conventional hatchery practices; thus, no captive broodstock component was modelled due to its largely discontinued status and potential life history differences.
2. To model a feedback between total adult returns and adults eligible for retention as broodstock we assumed a target brood retention for each system of 170 and 103 adults for the UGR and CC respectively based on an adult-to-smolt equivalence (assuming a 50:50 sex ratio) of 1,470 smolts per adult (M. McLean, CTUIR, pers. comm.).

CATHERINE CREEK

In CC, the adult trapping operations span the entire run and management of hatchery and natural fish on the spawning grounds and as broodstock follows a 'sliding scale' framework (Carmichael et al. 2011). Under this framework target levels for the proportion of natural and hatchery origin spawners, and the proportion of natural origin broodstock vary across three levels of run size (Table 19).

TABLE 19. SLIDING SCALE FRAMEWORK USED IN MANAGEMENT OF THE INTEGRATED HATCHERY PROGRAM FOR CATHERINE CREEK SUPPLEMENTATION (ADAPTED FROM CARMICHAEL ET AL. 2011).

Total run size (H & N)	Max. % natural retained as broodstock	% hatchery above weir	Min. % natural origin broodstock
< 250	40%	-	-
251 - 500	20%	< 70%	> 20%
> 500	< 20%	< 50%	> 30%

While this rule set is straightforward, there are cases for which it is impossible to meet all constraints simultaneously, which made implementing it within the LCM code somewhat complicated. Consider a case in which returns fall between 250 and 500 but are almost exclusively of hatchery origin. In this case, it's quite likely that egg take needs will not be met if weir management strictly follows the sliding scale natural origin broodstock constraints; nor is it clear what passage goals (to spawning grounds) should be in cases for which returns exceed the upper abundance threshold but are composed predominantly of hatchery origin returns. Thus, we chose to implement a simplified interpretation of the CC sliding scale in which the ruleset specifying the proportion of natural origin spawners will always be met (if possible given the run size), and the remaining target for broodstock retention will be made up of hatchery origin adults. Under our interpretation, no attempt was made to constrain the modeled supplementation program based on the stated hatchery constraints set for the composition of the run above the weir as doing so introduced additional coding complications (i.e., due to exceptions and circular dependencies), and was virtually impossible to meet under the current modelled population demographics.

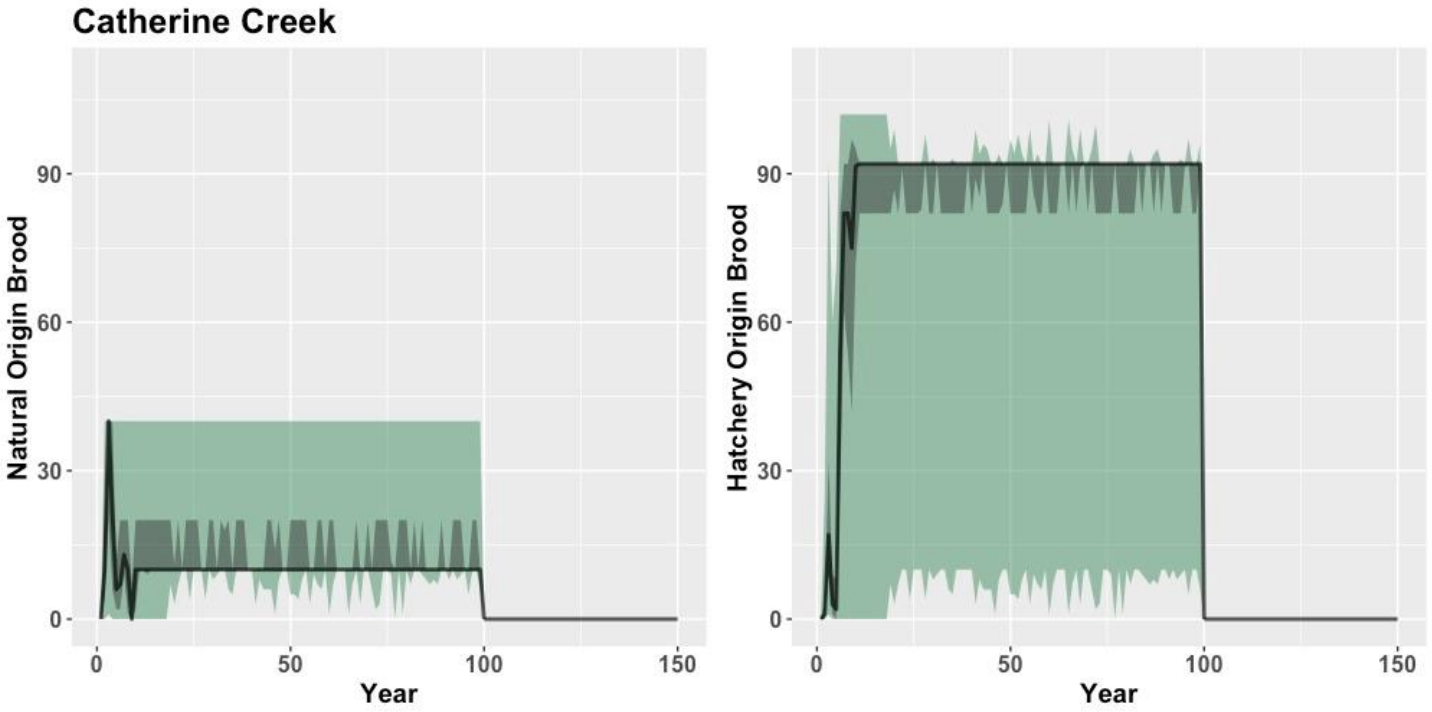

FIGURE 18. BROODSTOCK RETENTION FOR CATHERINE CREEK SUPPLEMENTATION MANAGEMENT DISCONTINUED IN YEAR 100. BLACK LINE SHOWS MEDIAN, GRAY SHADED REGION SHOWS 25TH AND 75TH PERCENTILES, AND GREEN SHADED REGION SHOWS MAXIMUM AND MINIMUM NUMBER OF NATURAL (LEFT) AND HATCHERY (RIGHT) ORIGIN ADULT CHINOOK RETAINED FOR BROODSTOCK.

UPPER GRANDE RONDE RIVER

In the Upper Grande Ronde (rule type = 5 in input files), the management of HOS/NOS on the spawning grounds and HOB/NOB at the hatchery is less formalized than in Catherine Creek, due to the fact that the weir is typically pulled before the majority of the run makes its way through to the spawning grounds and because its supplementation program is generally less restrictive. The main constraint imposed on weir/program management is that no more than 50% of the natural run can be retained for hatchery broodstock.

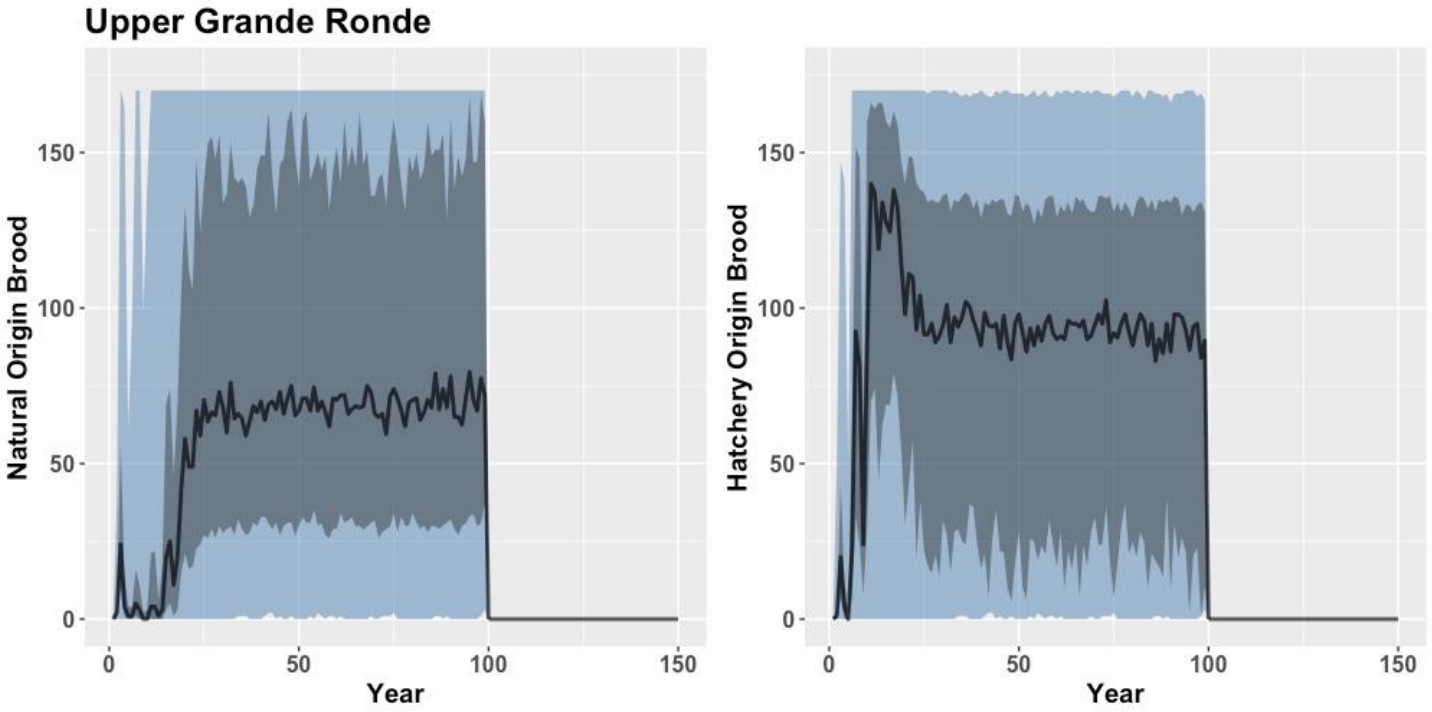

FIGURE 19. BROODSTOCK RETENTION FOR THE UPPER GRANDE RONDE SUPPLEMENTATION MANAGEMENT DISCONTINUED IN YEAR 100. BLACK LINE SHOWS MEDIAN, GRAY SHADED REGION SHOWS 25TH AND 75TH PERCENTILES, AND BLUE SHADED REGION SHOWS MAXIMUM AND MINIMUM NUMBER OF NATURAL (LEFT) AND HATCHERY (RIGHT) ORIGIN ADULT CHINOOK RETAINED FOR BROODSTOCK.

APPENDIX 2: BASE MODEL PARAMETERS

TABLE 20. SURVIVAL, FECUNDITY, LIFE-HISTORY, AND STOCHASTIC PARAMETERS USED IN THE BASE LCM FOR THE UGR AND CC POPULATIONS. STOCHASTIC PARAMETERS ARE EXPRESSED AS A STANDARD DEVIATIONS AND ALSO LIST THE DISTRIBUTION USED BY THE MODEL TO GENERATE PREDICTION OR PARAMETER UNCERTAINTY.

Life-stage(s)	Parameters	Value(s)	Stochasticity	Comments
Egg to parr	Density dependent survival from egg-to-parr	UGR = 0.32 CC = 0.32	Log-normal UGR = 0.54 CC = 0.41	Survival and capacity derived from Beaverton-Holt fit between annual estimate of eggs (converted from redds) and late summer parr. Stochastic component is a standard deviation calculated on the model fit (sse) to the log-transformed data.
	Parr capacity	UGR = 108,087 CC = 111,897		
Parr to smolt at LGD	Headwaters rearing presmolt	UGR = 0.72 CC =0.23	Beta UGR = 0.17 CC = 0.11	Probability of late summer parr life-history as fall migrant and valley rearing vs. spring migrant and headwater rearing based on ratio of population estimate. Stochasticity is modelled as beta distribution and is shared between each life-history.
	Valley rearing presmolt	UGR = 0.28 CC =0.77		
	Smolt survival to LGD headwaters rearing	UGR = 0.11 CC = 0.10	Beta UGR = 0.7 CC = 0.6	Density independent survival for parr to smolt at LGD specific to each life-history. Stochasticity modelled as beta distribution on survival.
	Valley rearing	UGR = 0.18 CC = 0.12		
Hatchery smolt release to smolt at LGD	Survival from release as smolt to smolt at LGD	UGR = 0.45 CC = 0.58	Beta UGR = 0.12 CC = 0.14	Density independent survival from release of hatchery smolts within each tributary to smolt at LGD.
LGD Smolt to adult at tributary weir (spawning grounds)	Ocean age maturation probability	Age 1, 2, 3 UGR = 0.03, 0.64, 1 CC = 0.05, 0.68, 1	Beta Age 1, 2, 3 UGR = 0.03, 0.31, 0 CC = 0.03, 0.28, 0	Probability of maturation at ocean age. Maturation schedule is shared among natural and hatchery origin Chinook.
	Annual survival rate by ocean age	Age 1, 2, 3 *Natural origin* UGR = 0.04, 0.63, 0.52 CC = 0.07, 0.66, 0.61 *Hatchery origin* UGR = 0.02, 0.24, 0.20 CC = 0.01, 0.11, 0.10	Beta Age 1, 2, 3 UGR = 0.03, 0.21, 0.27 CC = 0.04, 0.17, 0.16	Survival by ocean age. Note, decreased survival for hatchery origin fish is only applied in the year returning to spawn to account for a proportional difference in natural vs. hatchery SAR. Overall SAR for populations: UGR = 0.024, CC = 0.047.

Adult survival on spawning grounds (passage at weir to spawner)	Summer survival on the spawning grounds	UGR = 0.73 CC = 0.96	Log-normal UGR = 0.39 CC = 0.05	Density dependent survival of adults on the spawning grounds after being passed at the tributary weir and derived based on Beaverton-Holt model fit to ODFW estimates of abundance. Capacity is estimate from habitat data expanded to the population using habitat suitability index (HSI) modelling approach.
	Spawner capacity	UGR = 28397 CC = 25653		
Spawner to egg	Female spawner to egg fecundity	3831	Normal 102	Female spawner to egg fecundity assuming a 50:50 sex ratio for adult spawning Chinook. Estimate comes from CC data and is used for both populations.
Brood to hatchery smolt	Conversion of brood to smolt at release	UGR = 1226 CC = 1339	Normal UGR = 398 CC = 366	Based on ODFW smolt supplementation records and is composite of integrated and captive brood.

REFERENCES

Carmichael and coauthors. 2011. Catherine Creek spring Chinook salmon hatchery progam review. Oregon Department of Fish and Wildlife report to Lower Snake Comp. Program. https://www.fws.gov/lsnakecomplan/Reports/ODFW/Eval/CatherineCreekSpringChinookSalmonHatcheryReviewFINAL.pdf

CHaMP (Columbia Habitat Monitoring Program). 2015, May 15. Scientific Protocol for Salmonid Habitat Surveys within the Columbia Habitat Monitoring Program. Prepared by the Columbia Habitat Monitoring Program. https://www.champmonitoring.org.

Feldhaus, J. W., T. L. Hoffnagele, D. L. Eddy, and K. N. Ressel. 2017. Lower Snake River compensation plan: Oregon spring Chinook Salmon evaluation studies 2014 annual progress report. Page 68. Oregon Department of Fish and Wildlife, Salem, OR.

Hadden, M. 2011. Modelling and Quantitative Methods in Fisheries. Second Edition. CRC Press. Boca Raton, FL.

Independent Scientific Advisory Board. 2017. Review of NOAA Fisheries' Interior Columbia Basin Life-Cycle Modeling. ISAB 2017-1. https://www.nwcouncil.org/media/7491311/isab-2017-1-noaalifecyclemodelreview22sep.pdf

Justice, C., White, S.M., McCullough, D.A., Graves, D.S., Blanchard, M.R., 2017. Can stream and riparian restoration offset climate change impacts to salmon populations? Journal of Environmental Management 188, 212-227.

Justice, C. 2013. Factors influencing body size and survival of juvenile Chinook salmon migrants in the Upper Grande Ronde River basin. Technical Report. Columbia River Inter-Tribal Fish Commission

McHugh, P., and coauthors. 2017. Linking models across scales to assess the viability and restoration potential of a threatened population of steelhead (Oncorhynchus mykiss) in the Middle Fork John Day River, Oregon, USA. Ecological Modelling 355.

Moussalli, E., and R. Hilborn. 1986. Optimal Stock Size and Harvest Rate in Multistage Life-History Models. Canadian Journal of Fisheries and Aquatic Sciences 43(1):135-141.

Nahorniak, M., and M. Armour. 2017. ISEMP Watershed Model. https://github.com/SouthForkResearch/CHaMP-ISEMP-Life-Cycle-Model/wiki

R Core Team, 2014. R: A language and environment for statistical computing. R Foundation for Statistical Computing, Vienna, Austria.

Sharma, R., A. B. Cooper, and R. Hilborn. 2005. A quantitative framework for the analysis of habitat and hatchery practices on Pacific salmon. Ecological Modelling 183(2-3):231-250.

Wheaton, J. M., N. Bouwes, P. McHugh, C. Saunders, S. Bangen, P. Bailey, M. Nahorniak, E. Wall, and C. E. Jordan. 2017. Upscaling site-scale ecohydraulic models to inform salmonid population-level life cycle modeling and restoration actions - Lessons from the Columbia River Basin. Earth Surface Processes and Landforms 12(5):1510–25.